

# UC San Diego

## UC San Diego Electronic Theses and Dissertations

**Title**

The role of synaptogenic synaptic adhesion molecules in insulin secretion

**Permalink**

<https://escholarship.org/uc/item/23j2c4gm>

**Author**

Suckow, Arthur T.

**Publication Date**

2010

Peer reviewed|Thesis/dissertation

UNIVERSITY OF CALIFORNIA, SAN DIEGO

**The Role of Synaptogenic Synaptic Adhesion Molecules in Insulin Secretion**

A dissertation submitted in partial satisfaction of the requirements for the degree

Doctor of Philosophy

in

Biomedical Sciences

by

Arthur T. Suckow

Committee in charge:

Professor Steven D. Chessler, Chair  
Professor Alberto Hayek  
Professor Palmer W. Taylor  
Professor Wylie Vale  
Professor Geert W. Schmid-Schoenbein

2010

Copyright

Arthur T. Suckow, 2010

All rights reserved.

The dissertation of Arthur T. Suckow is approved, and it is acceptable in quality and form  
for publication on microfilm and electronically:

---

---

---

---

---

Chair

University of California, San Diego

2010

## DEDICATION

Dedicated to

Grandma Ginny, Mom and “Doc”.

## TABLE OF CONTENTS

SIGNATURE PAGE .....	iii
DEDICATION .....	iv
TABLE OF CONTENTS.....	v
LIST OF ABBREVIATIONS.....	xi
LIST OF FIGURES .....	xiii
LIST OF TABLES.....	xvi
ACKNOWLEDGMENTS .....	xvii
CURRICULUM VITA .....	xxi
ABSTRACT OF THE DISSERTATION .....	xxvi
CHAPTER 1: INTRODUCTION .....	1
A. The Neuronal Phenotype of Islet $\beta$ cells.....	1
B. Putative Roles for GABA in Islet $\beta$ cells.....	2
C. GAD-65, the Synaptic-Like Microvesicle and Diabetes .....	4
D. The Synapse as a Model towards a Better Understanding of $\beta$ -cell Development and Functional Differentiation.....	6
E. The Role of Neurexin/Neuroigin in Presynaptic Differentiation and Stimulus- Secretion Coupling .....	9
F. Objective of the Dissertation .....	11
CHAPTER 2: THE INHIBITORY PHENOTYPE OF THE ISLET $\beta$ -CELL: IDENTIFICATION AND CHARACTERIZATION OF A NOVEL ISOFORM OF THE VESICULAR GABA TRANSPORTER WITH GLUCOSE-REGULATED EXPRESSION IN RAT ISLETS .....	13

A. Abstract.....	13
B. Introduction.....	14
C. Materials and Methods.....	17
D. Results.....	25
1. <i>Synthesis and stability of VIAAT</i> .....	25
2. <i>The VIAAT gene contains an alternate start site of translation.</i> .....	27
3. <i>Two-dimensional gel analysis of V52 and V57</i> .....	29
4. <i>Differential regulation of V52 and V57 expression</i> .....	34
5. <i>VIAAT expression in INS-1 and islet <math>\beta</math> cells</i> .....	35
F. Discussion.....	40
G. Acknowledgements.....	44
CHAPTER 3: THE INHIBITORY PHENOTYPE OF THE ISLET $\beta$ -CELL: AN AP-3 DEPENDENT MECHANISM DRIVES SYNAPTIC-LIKE MICROVESICLE FORMATION IN PANCREATIC ISLET $\beta$ CELLS .....	46
A. Abstract.....	46
B. Introduction.....	47
C. Materials and Methods.....	49
D. Results.....	55
1. <i>Neuronal AP-3 Subunits are Expressed in Human Islets</i> .....	55
2. <i>B-Cell-Specific Expression of Neuronal AP-3B Subunits in Rat Islets</i> .....	56
3. <i>Resemblance of INS-1 <math>\beta</math>-cell SLMVs to PC-12 cell SLMVs</i> .....	56
4. <i>INS-1 and PC-12 SLMVs cosediment and share similar synaptic vesicle     markers</i> .....	63

5. <i>An AP-3 Dependent Pathway Drives SLMV Biogenesis in INS-1 <math>\beta</math>-Cells..</i>	65
E. Discussion .....	67
1. <i>Expression of AP-3B Subunits in Islets and Beta-Cells .....</i>	68
2. <i>AP-3-mediated SLMV Biogenesis in <math>\beta</math> Cells.....</i>	69
3. <i>Closing Remarks .....</i>	71
F. Acknowledgements .....	71
CHAPTER 4: THE INHIBITORY PHENOTYPE OF THE ISLET $\beta$ -CELL: EXPRESSION OF NEUREXIN, NEUROLIGIN, AND THEIR CYTOPLASMIC BINDING PARTNERS IN THE PANCREATIC BETA-CELLS AND THE INVOLVEMENT OF NEUROLIGIN IN INSULIN SECRETION .....	73
A. Abstract.....	73
B. Introduction.....	74
C. Materials and Methods.....	76
D. Results.....	87
1. <i>Expression of neurexin and neuroligin transcripts in islets and <math>\beta</math>-cell lines at levels comparable to brain.....</i>	87
2. <i>Expression of alternatively spliced neuroligin exons in human islets and INS-1 cells .....</i>	93
3. <i>Expression of an insert at splice site 4 in neurexin-1 transcripts .....</i>	95
4. <i>Expression of specific inhibitory and excitatory post-synaptic protein markers in <math>\beta</math> cells .....</i>	98
5. <i>Expression of neuroligin-2 protein in pancreatic islets .....</i>	99



6. Localization of the synaptogenic adhesion molecules neurexin, neuroligin and SynCAM in pancreatic islets .....	102
7. Overexpression of neuroligin family members increases insulin secretion .....	107
8. Neuroligin Knockdown Reduces Insulin Secretion in INS-1 Cells and Rat Islet Cells.....	110
E. Discussion .....	115
1. Neuroligin and neurexin gene expression in rat and human islets and INS-1 $\beta$ cells .....	115
2. Alternative splicing of neurexin and neuroligin in islets .....	117
3. Expression of gephyrin, but not PSD-95, in $\beta$ cells .....	118
4. $\beta$ cell-specific expression of neurexin and neuroligin .....	118
5. Involvement of neurexin and neuroligins in exocytosis and conclusion ...	120
G. Acknowledgements.....	121
CHAPTER 5: UTILIZATION OF THE INHIBITORY SYNAPTIC MACHINERY FOR REGULATION OF INSULIN SECRETION: IDENTIFICATION OF A NEUROLIGIN-DEPENDENT BUT NEUREXIN-INDEPENDENT MECHANISM FOR REGULATION OF INSULIN SECRETION FROM PANCREATIC BETA-CELLS. 122	
A. Introduction.....	122
B. Materials and Methods.....	125
C. Results.....	133
1. Neuroligin-2 is Expressed on the Surface of $\beta$ -Cells.....	133

2. <i>The Extracellular Domain of Neuroligin-2 Binds to the Surface of <math>\beta</math>-Cells.</i>	135
3. <i>Co-Culture of <math>\beta</math>-Cells with HEK Cells Expressing Full-Length Neuroligin-2 Markedly Enhances Glucose Stimulated Insulin Secretion</i>	138
4. <i>Soluble NL-2 Markedly Inhibits Glucose-Stimulated Insulin Secretion ...</i>	140
5. <i>Neuroligin-2 Interacts with <math>\alpha</math>-Neurexin in <math>\beta</math>-Cells.</i>	146
6. <i>Neuroligin Regulates Glucose-Stimulated Insulin Secretion Via a Neurexin-Independent Mechanism.</i>	151
D. Discussion	153
1. <i>Cell-Surface Expression of Neuroligin-2 and a Receptor on the Surface of <math>\beta</math>-Cells</i>	153
2. <i>The Involvement of Neuroligin-2 in the Regulation of Glucose-Stimulated Insulin Secretion</i>	155
3. <i>Neuroligin-2 Regulates Glucose-Stimulated Insulin Secretion Through a Neurexin-Independent Pathway</i>	157
4. <i>Closing Remarks</i>	158
E. Acknowledgements.	158
CHAPTER 6: CONCLUSIONS, OPEN QUESTIONS AND FUTURE STUDIES	159
A. Does GAD-65 Associate with AP-3 Generated Synaptic-Like Microvesicles in Islet $\beta$ Cells?	159
B. The Localization of Neuroligin and Neurexin in Islet $\beta$ Cells?	161

C. What is the Receptor through which Neuroligin Acts to Potentiate Insulin Secretion in the $\beta$ Cells? .....	163
E. Are $\beta$ -cell Neuroligin and Neurexin Necessary for the Differentiation and Maturation of the Stimulus-Coupling Machinery in $\beta$ cells? .....	166
F. Where is Neuroligin-1? .....	168
G. The Synptogenic Adhesion Molecules as Targets for $\beta$ Cell Imaging? .....	169
H. Therapeutic Applications? .....	171
REFERENCES .....	173

## LIST OF ABBREVIATIONS

AP	Adaptor protein
BFA	Brefeldin A
CNS	Central nervous system
DTSSP	3,3'-Dithiobis[sulfosuccinimidylpropionate]
GABA	$\gamma$ -aminobutyric acid
GAD	Glutamic acid decarboxylase
HBSS	Hanks balanced salt solution
HEK	Human embryonic kidney
Glu	Glucagon
GSIS	Glucose-stimulated insulin secretion
HRP	Horseradish peroxidase
IBMX	Isobutylmethylxanthine
Ins	Insulin
kDa	Kilodalton
mM	Millimolar
nM	Nanomolar
NCAM	Neural cell adhesion molecule
NL	Neurologin
NOD	Non-obese diabetic
NRXN	Neurexin
PBS	Phosphate Buffered Saline
PSD-95	Postsynaptic density protein-95

REST	RE1-silencing transcription factor/Neuron-restrictive silencer factor
SAM	Synaptic adhesion molecule
SDS	Sodium dodecyl sulfate
SLMV	Synaptic-like microvesicle
SNAP-25	Synaptosomal-associated protein-25
SNARE	Soluble NSF attachment protein receptors
SV	Synaptic vesicle
SynCAM	Synaptic cell adhesion molecule
V52	52 kilodalton VIAAT/VGAT isoform
V57	57 kilodalton VIAAT/VGAT isoform
V57'	Post-transcriptionally modified VIAAT/VGAT isoform
VAMP-2	Vesicle-associated membrane protein-2
VGAT	Vesicular GABA transporter
VGLUT	Vesicular glutamate transporter
VIAAT	Vesicular amino acid transporter
ZnT3	Zinc transporter 3

## LIST OF FIGURES

Figure 2.1. Synthesis and Stability of V57 and V52.....	26
Figure 2.2. VIAAT Synthesis from Mutated cDNA Templates. ....	28
Figure 2.3. Immunorecognition of V57 and V52 by Antibodies to the Amino and Carboxyl Termini of VIAAT. ....	30
Figure 2.4. 2-D Electrophoresis of VIAAT. ....	32
Figure 2.5. Effects of Glucose Concentration on Islet VIAAT Content.....	36
Figure 2.6. VIAAT Expression in the $\beta$ -Cell Line INS-1.....	37
Figure 2.7. Immunostaining of Rat and Human Pancreas Section with VIAAT Antibodies. ....	39
Figure 3.1. Expression of Neuronal AP-3 mRNA and Protein in INS-1 $\beta$ -cells and Pancreatic Islet Extracts.....	57
Figure 3.2. $\beta$ 3B is detected in the pancreatic islet $\beta$ cells.....	59
Figure 3.3. $\mu$ 3B is detected in pancreatic islet $\beta$ cells. ....	60
Figure 3.4. Detection of synaptic-like microvesicles (SLMV) in INS-1 cell homogenates by sucrose gradient sedimentation.....	62
Figure 3.5. $\beta$ -cell microvesicles are identical in size to PC-12 SLMVs and have matching cargo protein content.....	64
Figure 3.6. SLMV biogenesis in INS-1 $\beta$ cells is mediated by AP-3.....	66
Figure 4.1. Expression of neurexin and neuroligin mRNA in human pancreatic islets and rat and mouse $\beta$ -cell lines. ....	88

Figure 4.2. Abundance of neuroligin and neurexin transcripts in INS-1 $\beta$ cells and Rat Islets. ....	90
Figure 4.3. Neuroligin and neurexin mRNA expression in human islets. ....	91
Figure 4.4. Abundance of Neurexin and Neuroligin transcripts in INS-1 cells relative to rat brain. ....	92
Figure 4.5. Characterization of neuroligin splice variants in pancreatic $\beta$ cells. ....	94
Figure 4.6. Expression of an insert at splice site 4 in neurexin 1 islet transcripts. ....	97
Figure 4.7. Expression of gephyrin and CASK but not PSD-95 in islets and $\beta$ -cell lines. ....	100
Figure 4.8. Expression of neuroligin-2 in islets. ....	101
Figure 4.9. Localization of Neuroligin-1, Neuroligin-2 and SynCAM in Pancreatic Islets. ....	103
Figure 4.10. Neurexin-1 is not expressed in $\alpha$ -cells. ....	106
Figure 4.11. Overexpression and knockdown of neuroligin-2 alters insulin secretion in INS-1 cells. ....	108
Figure 4.12. Overexpression of Neuroligin-1, -3 and -4 increase insulin secretion at basal glucose levels. ....	109
Figure 4.13. Knockdown of neuroligin-2 in dissociated rat islets inhibits insulin secretion. ....	111
Figure 4.14. Insulin secretion from dispersed islet cells treated with low and high glucose. ....	114
Figure 5.1. Immunoblotting Analysis with Neuroligin-2 Antibodies Pre-incubated with Soluble Acetylcholinesterase or Soluble Neuroligin-2. ....	126

Figure 5.2. Endogenous Neuroligin-2 is Expressed on the Surface of INS-1E Cells....	134
Figure 5.3. Binding of Soluble Neuroligin-2 to the Surface of INS-1E, INS-1 and MIN-6 Cells. ....	136
Figure 5.4. Neuroligin-2 Binds to the Surface of INS-1E Cells with a Dissociation Constant of 15 nM. ....	139
Figure 5.5. Co-culture of MIN-6 Cells with HEK Cells Expressing Full-length Neuroligin-2 Markedly Enhances Insulin Secretion.....	141
Figure 5.6. Soluble Neuroligin-2 Inhibits Insulin Secretion from MIN-6 Cells.....	142
Figure 5.7. Soluble NL-2 Inhibits Glucose Stimulated Insulin Secretion from Rat Islets in a dose dependent fashion. ....	144
Figure 5.8. Dose-Response Curve for NL-2 Inhibition of Glucose-Stimulated Insulin Secretion from Rat Islets.....	147
Figure 5.9. NL-2 is Associated with $\alpha$ -Neurexin in MIN-6 $\beta$ Cells.....	149
Figure 5.10. Neuroligin Inhibits Glucose Stimulated Insulin Secretion via a Neurexin-Independent Mechanism.....	152



## LIST OF TABLES

Table 4.1. Primers for PCR Analysis.....	79
Table 4.2. Primers and Taqman Probes for Real Time PCR Analysis of INS-1 Cells and Rat Islets.....	80
Table 4.3. Primers for Real Time PCR Analysis of Human Islets. ....	81
Table 4.4. Primers for Splice Site Analysis of Neurexin and Neuroligin in INS-1 Cells and Human Islets.....	82
Table 4.5. Neuroligin-2 SiRNA Pool.....	85
Table 4.6. Neuroligin and Neurexin Splice Variants Detected.....	96

## ACKNOWLEDGMENTS

This work would not have been possible without the many friends, family and colleagues that supported me both emotionally and intellectually during my time at the University of California, San Diego. Through the many obstacles and unfortunate occurrences, you were always there to lift me up and provide the guidance to help me continue to succeed. I am eternally grateful to you all and would like to take this opportunity to acknowledge a few of you whose efforts will never be forgotten.

First and foremost, I want to thank my adviser, Dr. Steven Chessler, for providing an environment in which I could thrive. I learned so much about everything from you. Your patience is admirable and your kindness unfathomable. Thanks for putting up with me over the years, for hearing me out and for your encouragement and support for all of my many intellectual curiosities.

Secondly, I would like to thank my co-adviser, Dr. Palmer Taylor, for the hours he provided me each week during my first few years to present and discuss my research. His guidance was essential to my success here at UCSD. Dr. Taylor also provided me with reagents, tools and access to colleagues that greatly facilitated my work. Without him and this successful collaboration, it would have been impossible to compete with others working in the synaptogenic adhesion molecule field.

I would also like to thank my committee members, Dr. Alberto Hayek, Dr. Geert Schmid-Schoenbein and Dr. Wylie Vale, for their thoughtful intellectual contributions to this work. I would like to further acknowledge, Dr. Geert Schmid-Schoenbein, for believing in me and for providing me with an opportunity and a learning experience that most scientists only dream of.

I'd like to thank current and former Chessler lab members for technical support and camaraderie. Special thanks to Sonya Egodage for her extraordinary hard work and for putting up with me on a day to day basis. I'd also like to thank Megan Waldrop and Challise Cox for their assistance and for helping to keep the lab organized. Finally, Merrie Mosedale, I learned more from her than she'll ever know. Even though our friendship got off to a bumpy start, I always thought very highly of you and believe you are one of the brightest minds I have come across at UCSD, I know you will go on to do great things.

I thank members of the Taylor lab for all of their hard work and for providing me with the many reagent requests I have had over the years. I am especially indebted to Dr. Davide Comoletti, whom provided me with many constructs and aided me with several techniques, including protein purification. I'd also like to thank Helen Newlin, Jennifer Wilson and Megan Miller for helping me along the way and for listening during some of the more difficult and frustrating times.

Thank you to Dr. Joseph Cantor for all the great golf breaks, the stimulating lunch discussions and for challenging me along the way.

Thank you to Dr. Gary Laverty for believing in me, for the many beers we have shared together and for reading everything I sent you over the years. Without your help and guidance, I wouldn't be the scientist I am today. You are a great role model.

Thanks to Mom, "Doc" and Grandma for your support up to and through my graduate studies. Thanks for always providing me with the best, for allowing me to obtain the best high school, college and graduate school education out there, and for doing whatever you could to defray the financial stress associated with attending graduate

school and maintaining a household. I thank my mother for always listening to me, my father for instilling in me what it takes to be a winner and my grandmother for taking care of me since I was a baby and for teaching me to stand up for myself. I love you all an unbelievable amount, and because you were most integral to my ability to complete this dissertation, I have dedicated it to you. I'd also like to thank the not so lame sisters, Kristyn Suckow and Sharon Thimons, for their support along the way.

Much thanks to Challise Cox, for your kindness and loyalty. You are the greatest friend anyone could ever have. You kept me from breaking, at times carrying me through each day; I hope that one day I can give back all that you have given me.

Thanks to my two dogs, Preston and Stella, for teaching me about unconditional love and about what is truly important in this life. There is no better feeling than coming home to you guys every day. Thanks for watching over me patiently through it all.

Special thanks to my partner in crime, Jeff Rodgers, and my fellow UD alumna, Kristin Breen. I don't think it's a coincidence that we were brought together again through Vegas. Your advice and wisdom has taught me the true meaning of friendship, thanks for your support, understanding and encouragement over the last few years.

Thanks to my girlfriend, Denise Haley, who has patiently tolerated the long hours I have spent in the lab. I have had so much fun with you, and the distractions from work that you have provided have helped to carry me to the end.

Thanks to Kevin O'Reilly, a friend since childhood, for being by my side during the best and worst of times.

Thanks to Tim Scott, Dr. Bob Shopes and Dr. Keith Parowski for believing in me and for providing me the resources to accomplish something of which I am so proud.

You have been great mentors and I am forever grateful that, unlike so many others, you cared for me and looked out for what was ultimately in my best interest. I hope that one day I can help you as selflessly as you have helped me.

Finally, I'd like to thank the National Science Foundation for providing me with a graduate research fellowship and the Beckman Foundation for providing me with the foundation to complete my graduate work.

Chapter 2 is a reprint of the material as it appears in Suckow, A. T., Sweet, I. R., Van Yserloo, B., Rutledge, E. A., Hall, T. R., Waldrop, M. and Chessler, S. D. (2006). *Journal of Molecular Endocrinology*. The dissertation author was the primary investigator in the development and execution of the study, and the principal author of this paper.

A manuscript including chapter 3 has been submitted to *American Journal of Physiology: Endocrinology and Metabolism*. The dissertation author was the primary investigator in the development and execution of the study, and the principal author of this paper.

Chapter 4 is a reprint of the material as it appears in Suckow, A. T., Comoletti, D., Waldrop, M., Mosedale, M., Egodage, S., Taylor, P. and Chessler, S. D. (2008). *Endocrinology*. The dissertation author was the primary investigator in the development and execution of the study, and the principal author of this paper.

A manuscript including chapter 5 will be submitted in early 2010. The dissertation author was the primary investigator in the development and execution of the study, and the principal author of this paper.

## CURRICULUM VITA

### EDUCATION

- **Doctor of Philosophy in Biomedical Sciences.**
  - University of California, San Diego
  - August 2005-March 2010
  - Thesis Title: The Role of Synaptogenic Synaptic Adhesion Molecules in Insulin Secretion
  
- **Honors Bachelor of Science in Biology**
  - University of Delaware, Newark, DE
  - September 2000-May 2004
  - Concentration: Cell and Molecular Biology & Genetics
  - GPA: 3.94/4.0
  - Rank: 2<sup>nd</sup> in Class
  - Thesis Title: The Ocular Expression and Regulation of Junctional Adhesion Molecule-1.

## PROFESSIONAL EXPERIENCE

- **NSF Graduate Fellow**, University of California, San Diego, La Jolla, CA. August 2005-December 2009.
  - Identification of biomarkers for diagnosis/natural history of Type 1 Diabetes.
  - Investigate the role of synaptic adhesion molecules in insulin secretion.
  - Investigate the utility of synaptic adhesion molecules and/or ligands for imaging of pancreatic  $\beta$ -cells in collaboration with Pfizer.
  - Investigate the role of the machinery necessary for inhibitory neurotransmission (GABAergic) in pancreatic  $\beta$ -cells.
  - Mentored research technicians and undergraduate students.
  - Managed the daily activities/projects of research technicians
  - Set up collaborations that resulted in publications with groups at University of Washington, Pfizer, Emory University, University of Delaware and University of California, San Diego.
- **Teaching Assistant**, University of California, San Diego, La Jolla, CA. January 2006-June 2006.
  - Teach upper level biology students common laboratory techniques.
- **Lab Manager**, University of California, San Diego. La Jolla, CA. August 2004-August 2005.
  - Assist in the identification and characterization of molecules that play a role in the trafficking and pathogenic extravasation of autoantigens involved in Type I diabetes.
  - Assist in the development of a novel assay to predict diabetes before clinical onset.
- **Beckman Scholar**, University of Delaware. Newark, DE. December 2001-July 2004.
  - Investigate the role of JAM-1 in the maintenance and development of the corneal epithelium.
  - Investigate the role of JAM-1 in breast cancer metastasis.
- **Teaching Assistant**, University of Delaware. Newark, DE. February 2003-2004.
  - Tutor introductory biology courses and teach review sessions for upper level cell physiology courses.

## SCIENTIFIC PUBLICATIONS

- **Arthur T. Suckow**, Ian Sweet, Sonya Egodage, Davide Comoletti, Palmer Taylor and Steven Chessler. “Identification of a Neuroligin Dependent but Neurexin Independent Mechanism for Regulation of Insulin Secretion from Pancreatic Beta-Cells” 2009. *Manuscript in Preparation*.
- **Arthur T. Suckow**, Branch Craige, Victor Faundez and Steven D. Chessler. October 2009. “Identification of an AP-3 Mediated Pathway for Synaptic-Like Microvesicle Formation in  $\beta$ -cells” Manuscript submitted to *American Journal of Physiology: Endocrinology and Metabolism*.
- **Arthur T. Suckow**, Davide Comoletti, Megan A. Waldrop, Merrie Mosedale, Sonya Egodage, Palmer Taylor and Steven D. Chessler. 2008. *Endocrinology*. 6006-6017. “Expression of Neurexin, Neuroligin and their Cytoplasmic Binding Partners in the Pancreatic Beta-Cells and the Involvement of Neuroligin in Insulin Secretion”
- Meghna Naik, Tejal Naik, **Arthur T. Suckow**, Melinda K. Duncan and Ulhas P. Naik. “Attenuation of Junctional Adhesion Molecule-A is a Contributing Factor for Breast Cancer Cell Invasion” 2008. *Cancer Research*. 2194-2203.
- Megan A. Waldrop, **Arthur T. Suckow**, Santica M. Marcovina and Steven D. Chessler. “Release of GAD65 into the Circulation by Injured Pancreatic Islet  $\beta$ -Cells” 2007. *Endocrinology*. 4572-4578.
- Kang, LI, Wang, Y., **Arthur T. Suckow**, Czymmek, KJ, Cooke, VG, Naik, UP and Melinda K. Duncan. “Deletion of JAM-A Causes Morphological Defects in the Corneal Epithelium” 2007. *International Journal of Biochemistry and Cell Biology*. 576-585.
- **Arthur T. Suckow**, Ian R. Sweet, Brian Van Yserloo, Elizabeth A. Ruteledge, Tyler R. Hall, Megan Waldrop and Steven D. Chessler. “Identification and Characterization of a Novel Isoform of the Vesicular GABA Transporter with Glucose-regulated Expression in Rat Islets” 2006. *Journal of Molecular Endocrinology*. 187-199.
- Megan A. Waldrop, **Arthur T. Suckow**, Tyler R. Hall, Chris S. Hampe, Santica Marcovina and Steven D. Chessler. “A Highly Sensitive Immunoassay Resistant to Autoantibody Interference for Detection of the Diabetes-Associated Autoantigen GAD65 in Blood and Other Biological Samples” 2006. *Diabetes and Technology*. 207-218.



## AWARDS/HONORS

- **NSF Graduate Research Fellowship.**
- **Undergraduate Research Award** which is given to the senior who has shown exceptional ability in academics and research while at the University of Delaware as evidenced by publications or presentations at scientific meetings.
- **Beckman Scholars Award** which recognizes outstanding undergraduate students in chemistry and biological sciences research at select universities throughout the United States.
- **First Place Award** from the American Society for Biochemistry and Molecular Biology for excellence in scientific presentation at the ASBMB Undergraduate Poster Session at the Federation of American Societies for Experimental Biology Meetings in San Diego, CA. April 2003.
- **Richard M. Johnson, Jr. Memorial Award** which is given to the junior in biological sciences who best exemplifies the ideals of sound scholarship and intellectual leadership, actively pursues truth, and appreciates the significance of science to mankind. April 2003.
- **Undergraduate Travel Award** from the American Society for Biochemistry and Molecular Biology to allow for travel to the Federation of American Societies for Experimental Biology Meetings in San Diego, CA. April 2003.
- **Sigma Xi Student Research Award** from Thomas Jefferson University for excellence in scientific presentation. March 2003.
- **American Association for the Advancement of Science Honorary Member.** October 2003.
- **Delaware Academy of Science Award in Science and Biotechnology.** April 2003.
- 95<sup>th</sup> Percentile on the Standardized National ACS Organic Chemistry Final.

## SCIENTIFIC PRESENTATIONS

- **Arthur T. Suckow**, Ian Sweet and Steven D. Chessler. “Synaptic Adhesion Molecules—Neurexin, Neuroligin, and SynCAM—on the  $\beta$ -cell surface as Imaging Targets” Presented at Imaging the Pancreatic Beta Cell, 4<sup>th</sup> Workshop at NIDDK in Washington, D.C. April 2009.
- **Arthur T. Suckow**, Davide Comoletti, Megan Waldrop, Palmer Taylor and Steven D. Chessler. “Expression of the Synaptogenic Adhesion Molecules Neurexin, Neuroligin and SynCAM in Islet  $\beta$ -cells” Presented at the European Association for the Study of Diabetes Annual Meeting in Amsterdam, Netherlands. September 2007.
- **Arthur T. Suckow**, Branch Craige, William Cain, Victor Faundez and Steven D. Chessler. “Identification of a Novel Pathway for SLMV biogenesis in Islets” Presented at the Western Region Islet Study Group in San Diego, CA. October 2005.
- **Arthur T. Suckow**, Ulhas P. Naik, Bhareesh K. Chauhan, Ales Cvekl and Melinda K Duncan. “Ocular Expression and Regulation of Junctional Adhesion Molecule-1” Presented at the Federation of American Societies for Experimental Biology Meetings in Washington D.C. April 2004.
- **Arthur T. Suckow**, Ulhas P. Naik, Bhareesh K. Chauhan, Ales Cvekl and Melinda K Duncan. Thesis Defense at University of Delaware. April 2004. “Ocular Expression and Regulation of Junctional Adhesion Molecule-1”
- **Arthur T. Suckow**, Vesselina Cooke, Ulhas P. Naik, William Skarnes, Bhareesh K. Chauhan, Ales Cvekl and Melinda K Duncan. “Ocular Expression and Regulation of Junctional Adhesion Molecule-1” Presented at the Beckman Scholars Symposium at the Beckman Center in Orange County, California. July 2003.
- **Arthur T. Suckow**, Ulhas P. Naik, Bhareesh K. Chauhan, Ales Cvekl and Melinda K Duncan. “Ocular Expression of Junctional Adhesion Molecule-1” Presented at the Federation of American Societies for Experimental Biology Meetings in San Diego, CA. April 2003.

## ABSTRACT OF THE DISSERTATION

### **The Role of Synaptogenic Synaptic Adhesion Molecules in Insulin Secretion**

by

Arthur Thomas Suckow

Doctor of Philosophy in Biomedical Sciences

University of California, San Diego, 2010

Professor Steven D. Chessler, Chair

The insulin secreting pancreatic  $\beta$  cells, by virtue of their pattern of protein expression and the architecture of their secretory apparatus, share many features with neurons in the central nervous system (CNS). The work described throughout this dissertation arose from the observation that the  $\beta$  cells' expression of the machinery necessary for GABAergic neurotransmission makes the  $\beta$ -cell cellular "phenotype" very much resemble that of an inhibitory synapse. This observation led to the overarching hypothesis that key insights into the functional maturation of  $\beta$  cells could be derived

from existing knowledge of the development, differentiation and maintenance of GABAergic synapses in the CNS.

$\beta$  cells contain synaptic-like microvesicles of which the origin, trafficking and role are poorly understood. Here, I demonstrate that the biogenesis of these vesicles in  $\beta$  cells is driven by adaptor proteins that are important for the formation of vesicular GABA transporter-containing synaptic vesicles in the CNS. Additionally, high level expression of the vesicular GABA transporter is detected in both human and rat  $\beta$  cells, and a novel glucose-regulated variant of this protein is described. These findings suggest that  $\beta$ -cells and neurons share molecules and mechanisms important for mediating the neuron-specific GABAergic membrane trafficking pathways that underlie synaptic vesicle formation.

The synaptogenic adhesion molecules, neuroligin and neurexin, drive synapse formation *in vitro* and regulate the differentiation of nascent synapses into either glutamatergic or GABAergic fully mature nerve terminals. Here, the expression of those neuroligin and neurexin family members important for the maturation of GABAergic synapses, and the expression of their intracellular, GABAergic binding partners, is demonstrated in  $\beta$ -cells. Neuroligin expression is revealed to be important for glucose-stimulated insulin secretion and evidence is presented that it may drive the proper assembly of the insulin secretory apparatus. Neuroligin is found to affect insulin secretion through a neurexin-independent mechanism in rat  $\beta$ -cells.

Overall, these results indicate that knowledge of the pathways that guide GABAergic synapse formation and function will aid in our understanding of  $\beta$ -cell

development and functional differentiation, and may yield important targets for remedying some of the  $\beta$ -cell dysfunction that occurs during the pathogenesis of diabetes.

## CHAPTER 1: INTRODUCTION

The insulin secreting pancreatic  $\beta$  cells, by virtue of their pattern of protein expression and the architecture of their secretory apparatus, share many features with neurons in the central nervous system (CNS). For example, these cells express high levels of the major inhibitory neurotransmitter GABA and much of the machinery necessary for GABA secretion and signaling [1-5]. The work described throughout this dissertation arose from the observation that the  $\beta$ -cells' expression of the machinery necessary for GABAergic neurotransmission makes the  $\beta$ -cell cellular "phenotype" very much resemble that of an inhibitory synapse. This observation led to the overarching hypothesis that key insights into the functional maturation of  $\beta$  cells could be derived from existing knowledge of the development, differentiation and maintenance of GABAergic synapses in the CNS. The introduction that follows serves to familiarize the reader with aspects of both neuronal and islet biology relevant to this dissertation.

### A. The Neuronal Phenotype of Islet $\beta$ cells

Insulin-secreting, pancreatic islet  $\beta$  cells appear to have evolved from a neuronal precursor and to have retained exocytic mechanisms that, in neurons, are important for neurotransmitter release. Evidence linking the  $\beta$  cells to a neuronal ancestor includes the finding that in some non-vertebrate species, such as *Drosophila*, insulin is exclusively released from neurons in the brain. Ablation of these neurons results in the accumulation of sugar within a fly's circulation—a phenotype that is similar to that observed in human diabetic patients and that is consistent with these neurons being the functional equivalent

of mammalian  $\beta$  cells [6]. Further evidence of a common precursor comes from the observation that human neural progenitor cells can be differentiated into glucose-responsive, insulin-secreting cells [7]. Similarities between  $\beta$  cells and neurons can also be observed at the molecular level. The absence of the transcriptional repressor, RE1 (REST), in  $\beta$  cells is consistent with a neuronal phenotype [8]. REST is expressed in all tissues except mature neurons and acts to repress proteins that are important for normal synaptic function and particularly, those scaffolding and synaptic vesicle proteins important for exocytosis of neurotransmitter [9-11]. Many of these same proteins are expressed by  $\beta$  cells and are key components of the insulin secretory machinery [12-18]. Consistent with the  $\beta$  cell being dependent on neuronal traits for proper functioning, the forced expression of REST in islets and  $\beta$  cell lines limits the expression of this machinery and abolishes normal stimulus-secretion coupling [19, 20]. Taken collectively, these data suggest that  $\beta$  cells and neurons utilize similar developmental pathways and molecules to attain their fully differentiated state.

## B. Putative Roles for GABA in Islet $\beta$ cells

Consistent with their resemblance to neurons,  $\beta$ -cells express high levels of the major inhibitory neurotransmitter GABA and much of the machinery necessary for GABA synthesis, secretion and signaling [1, 5, 21]. In human and rat  $\beta$  cells, the synthesis of GABA from L-glutamic acid is catalyzed by GAD-65 and then transported into synaptic-like microvesicles by the vesicular GABA transporter (VGAT/VIAAT) through the use of a proton electrochemical gradient set up by vacuolar  $H^+$  ATPase [1,

22-24]. GABA is then stored in these vesicles, which are distinct and much smaller than the large dense-core vesicles that carry insulin, until it is exocytosed in a regulated manner after entry of calcium through L-type channels and subsequent depolarization of the  $\beta$ -cell membrane [24-28]. Secreted GABA most likely functions to regulate islet hormone secretion via an autocrine or paracrine signaling mechanism [1].

Evidence is mounting that GABA released by  $\beta$  cells acts in an autocrine manner via the metabotropic GABA<sub>B</sub> receptor (GABA<sub>B</sub>R) to inhibit insulin secretion. This receptor is a G-protein coupled receptor (GPCR) regulated by inhibitory G-proteins (G<sub>i</sub>). Incubation of MIN-6 cells or rat islets with baclofen, a GABA<sub>B</sub>R agonist, markedly inhibits glucose-stimulated insulin secretion [29, 30]. The effect of baclofen can be inhibited by inclusion of pertussis toxin—a molecule that prevents interaction of G<sub>i</sub> proteins with their GPCR receptors [29]. These results were consistent with an older study demonstrating that GABA and baclofen inhibit glucose-stimulated insulin secretion from isolated perfused pancreas [31]. Further evidence that GABA acts through GABA<sub>B</sub>Rs on  $\beta$  cells comes from mice lacking the gene for a key subunit of the GABA<sub>B</sub>R. Consistent with a role for GABA in the inhibition of insulin secretion, male GABA<sub>B</sub>R  $-/-$  mice exhibit markedly increased insulin secretion in response to a glucose overload and decreased serum sugar levels during glucose tolerance testing [32]. In contrast to isolated wildtype islets, baclofen treatment fails to inhibit glucose-stimulated insulin secretion from isolated GABA<sub>B</sub>R  $-/-$  islets [32]. The combination of these data suggests that secreted GABA is part of a feedback mechanism that acts to suppress insulin secretion through the GABA<sub>B</sub>R under conditions of high glucose.



GABA secreted by  $\beta$  cells can also act in a paracrine manner to inhibit glucagon release from  $\alpha$  cells during hyperglycemic conditions via the ionotropic GABA<sub>A</sub> receptor (GABA<sub>A</sub>R). This receptor is a Cl<sup>-</sup> ion channel that upon activation leads to the influx of Cl<sup>-</sup> ions and as a result, the hyperpolarization of the  $\alpha$  cell plasma membrane [33]. Consistent with the idea that GABA mediates the inhibition of glucagon secretion, treatment of isolated rat islets with the GABA<sub>A</sub>R antagonist, SR95531, completely prevented the inhibition of glucagon under hyperglycemic conditions [34]. It was further demonstrated that the GABA<sub>A</sub>R receptor was internalized by  $\alpha$  cells under conditions of normoglycemia and that insulin secreted by  $\beta$  cells during hyperglycemic conditions acts on  $\alpha$  cell insulin receptors to sensitize these cells to GABA by causing the phosphorylation and translocation of GABA<sub>A</sub>Rs to the  $\alpha$  cell plasma membrane through Akt-kinase mediated downstream signaling pathways [35]. These data explain how insulin and GABA work together to inhibit glucagon secretion and underscore the importance of GABA as an autocrine/paracrine mediator of the secretion of the hormones most important for maintenance of glucose homeostasis throughout the body.

### C. GAD-65, the Synaptic-Like Microvesicle and Diabetes

In autoimmune diseases of the nervous system, nerve terminal proteins are especially susceptible to autoimmune attack, and, in Type 1 diabetes, shared  $\beta$ -cell-nerve terminal proteins are major, early targets of autoimmunity [36-39]. GAD-65, a protein associated with GABAergic nerve terminals, is a major autoantigen in Type 1 diabetes [39-42]. Autoantibodies to this protein are present in 70-80% of newly diagnosed type 1

diabetics [43-45]. Because GAD-65 is associated with the cytoplasmic face of synaptic-like microvesicles and does not traffic to the plasma membrane, its role as an autoantigen suggests that in order to come into contact with the immune system during the development and pathogenesis of Type 1 diabetes it must be released from  $\beta$  cells [46-49]. Support for this idea comes from an assay I developed alongside Dr. Chessler that was later used to demonstrate that GAD-65 is released into the circulation in a rat model of autoimmune diabetes [50, 51]. Because an important characteristic of  $\beta$ -cell and nerve-terminal autoantigens is their tendency to be vesicle-associated proteins, increased knowledge of the trafficking of GAD-65 and the mechanism of its association with the  $\beta$ -cell synaptic-like microvesicles may provide new insights into its release from  $\beta$  cells and the pathogenesis of islet autoimmunity [38, 51-54].

The biogenesis of synaptic vesicles in neurons, the functional equivalent of synaptic-like microvesicles in  $\beta$  cells, is driven by heterotetrameric adaptor protein complexes. Four such complexes have been described (AP-1, AP-2, AP-3 and AP-4) and each is comprised of 4 subunits (called adaptins): a large  $\alpha$ ,  $\gamma$ ,  $\delta$  or  $\epsilon$ , a large  $\beta$ , a medium  $\mu$ , and a small  $\sigma$  subunit [55]. Synaptic vesicle biogenesis is primarily driven by AP-2 complexes via clathrin-mediated endocytosis from the plasma membrane; however, synaptic vesicle formation also occurs from endosomes by means of an AP-3-mediated mechanism [56, 57]. The AP-3-mediated pathway is of particular interest because the trafficking of the vesicular GABA transporter, a protein associated with GAD-65 positive synaptic vesicles in neurons and demonstrated to be a component of  $\beta$  cell synaptic-like microvesicles in chapter 2 of this dissertation, is impaired as a result of decreased GABAergic synaptic vesicle biogenesis in mice lacking the neuron-specific AP-3

subunits [58-60]. These findings, along with the well-documented similarities between  $\beta$  cells and GABAergic neurons, suggested that  $\beta$  cells would express neuronal AP-3 subunits and utilize them for the biogenesis of their synaptic-like microvesicles. This hypothesis is explored in chapter 3 of this dissertation.

#### D. The Synapse as a Model towards a Better Understanding of $\beta$ -cell Development and Functional Differentiation

The architecture of the  $\beta$ -cell secretory apparatus very much resembles that used by neurons for exocytosis of neurotransmitter.  $\beta$  cells express many of the scaffolding and synaptic vesicle proteins important for neurotransmitter release [12], several of which have also been implicated as key components of the insulin secretory machinery including SNAP-25 [16], VAMP-2 [15], Mint1 [18], ELKS [14], munc13 [61, 62], munc18 [17], syntaxin [63] and piccolo [13]. The striking resemblance between the neuronal and  $\beta$ -cell secretory machinery, along with the accumulation of the data described thus far highlighting the similarities between the  $\beta$  cells and the GABAergic neurons of the central nervous system, suggests that knowledge of the pathways that guide synapse formation and neurotransmitter release may aid in the understanding of  $\beta$ -cell development and functional differentiation.

The formation of synapses—highly specialized cell-cell contacts through which neurons communicate with each other—is thought to be mediated by synaptic adhesion molecules that tether the pre and post-synaptic membranes. Synaptic adhesion molecules on dendrites interact through both homophilic and heterophilic mechanisms with synaptic adhesion molecules on axons to recruit the machinery necessary for neurotransmitter

release to the synapse (pre-synaptic differentiation). Likewise, synaptic adhesion molecules on axons interact through both homophilic and heterophilic mechanisms to induce the clustering and alignment of neurotransmitter receptors on dendrites (post-synaptic differentiation) [64]. Several early studies implicated two protein families, neurexin and neuroligin, as the primary drivers of synapse formation [65, 66].

The neurexins are a family of transmembrane proteins that are encoded by 3 distinct genes. Each of these genes is subject to a high degree of alternative splicing and can be transcribed from two promoters, generating longer  $\alpha$  and shorter  $\beta$  forms [67]. Transcription of  $\alpha$  and  $\beta$  variants of each of the three neurexin genes results in the expression of 6 different neurexin transcripts:  $1\alpha$ ,  $1\beta$ ,  $2\alpha$ , etc. Their expression is restricted to axons (presynaptic) and they interact across the synaptic cleft with the neuroligins, which are localized to dendrites (post-synaptic). The neuroligins are also a family of transmembrane proteins; they are encoded by four distinct genes in humans and rodents, and are also subject to alternative splicing [68]. The expression of each of these protein families is thought to be restricted to the nervous system [68-70].

*In vitro* co-culture experiments initially implicated neurexin and neuroligin family members as key players in the process of synapse formation. Uniquely, when non-neuronal cell lines expressing members of these protein families are co-cultured with hippocampal neurons, synaptic densities form at points of contact between the non-neuronal cells and the hippocampal neurons [65, 66, 71]. The expression of neurexin on non-neuronal cells specifically induces postsynaptic differentiation, whereas the expression of neuroligin specifically induces presynaptic differentiation on contacting hippocampal neurons [65, 66]. Although these data and other follow up *in vitro* studies

provided compelling evidence that these protein families drove synapse formation, more recent *in vivo* data suggests that the neurexin and neuroligin protein families are not necessary for the initial formation of synapses, rather they are important for specifying whether a particular synaptic connection will differentiate and mature into either a glutamatergic (excitatory) or GABAergic (inhibitory) synapse. In studies analyzing the brains of mice lacking the genes for all 3 neuroligin family members or all 3 neurexin family members, little or no change in the structure or number of synapses were observed; however, significant deficits in both GABAergic and glutamatergic synaptic function were evident and these mice die of respiratory failure within 24 hours of birth [72, 73]. Interestingly, when mice lacking individual neuroligin genes are studied, neuroligin-1 deletion exclusively perturbs excitatory neurotransmission and neuroligin-2 deletion exclusively perturbs inhibitory neurotransmission [74]. These results are in accord with the differential expression patterns of neuroligins-1 and -2, where neuroligin-1 is detected primarily at excitatory synapses [75] and neuroligin-2 exclusively at inhibitory synapses [76] and also, with overexpression studies in cultured hippocampal neurons demonstrating that neuroligin-1 exclusively affects excitatory neurotransmission and neuroligin-2 exclusively affects inhibitory neurotransmission [74]. It is not clear whether specific neurexin genes or isoforms are differentially localized to either inhibitory or excitatory synapses as studies are ongoing and an analysis of the effects of deletion of individual neurexin genes on excitatory and inhibitory activity have yet to be published; however, co-culture experiments involving a particular splice variant of neurexin-1 suggest that it is more important for the differentiation of inhibitory synaptic contacts [77]. Collectively, these data implicate the neuroligin and neurexin gene

families as necessary for the differentiation and maturation of synapses to either a glutamatergic (excitatory) or GABAergic (inhibitory) phenotype.

The relevance of this detailed discussion of the role of neurexins and neuroligins in the formation of GABAergic synapses stems from the observation that the  $\beta$  cells' expression of the machinery necessary for GABAergic neurotransmission makes the  $\beta$ -cell cellular "phenotype" very much resemble that of an inhibitory synapse. This observation led to the hypothesis that those neuroligin and neurexin family members important for driving the functional differentiation of inhibitory synapses (e.g. neuroligin-2) would be expressed by  $\beta$  cells and may play a role in the differentiation and maturation of autocrine or paracrine GABAergic signaling mechanisms. This hypothesis is explored in chapter 4 of this dissertation. Because neurexin-neuroligin interactions drive the assembly of the synaptic exocytic machinery *in vitro* and are necessary for its proper functioning *in vivo* [65, 66, 72, 73], the hypothesis that neurexins and neuroligins might be important for the normal maturation and/or functioning of the highly-similar insulin secretory apparatus is also considered in this chapter and expanded upon in chapter 5. A more detailed rationale for this alternative hypothesis is presented in the next section.

#### E. The Role of Neurexin/Neuroligin in Presynaptic Differentiation and Stimulus-Secretion Coupling

The mechanism through which neuroligin and neurexin regulate synaptic function is not entirely clear. The *in vivo* neurexin and neuroligin data described thus far seem to exclude the possibility that the *trans*-interaction of these two proteins across the synapse is important for the initial contact between an axon and a dendrite, but do not exclude the

idea that the interaction of these proteins across the synapse drives the recruitment and proper assembly of the neurotransmitter release machinery on the axonal membrane after an initial contact is established by other synaptic adhesion molecules. Consistent with an *in vivo* role for neuroligin in presynaptic differentiation, mice lacking all 3 neuroligin genes have significant deficits in neurotransmitter release from both excitatory and inhibitory synapses, as well as defects in  $\text{Ca}^{2+}$ -triggered exocytosis from secretory granules in the pituitary gland [73, 78]. Further analysis of these mice suggested that neuroligins are required for the coupling of  $\text{Ca}^{2+}$  channels to the synaptic exocytic machinery [73, 78, 79]. It is possible that the interaction of neuroligin with neuroligin promotes the coupling of the exocytic machinery with  $\text{Ca}^{2+}$  channels. Evidence that neuroligin is involved *in vivo* in the regulation of presynaptic differentiation come from the findings that transgenic mice overexpressing neuroligin-2 express significantly higher levels of several key components of the exocytic machinery and that mice lacking all three neuroligin genes have significant deficits in several key components of the exocytic machinery [72, 80]. Additionally, the presynaptic active zones in neurons isolated from mice lacking the neuroligin-1 gene resemble those of immature neurons both structurally and functionally [81]. When combined with the *in vitro* data demonstrating the ability of neuroligin to induce the assembly of the secretory machinery through neuroligin interactions in co-culture studies, these *in vivo* data suggest that neuroligin promotes the assembly and maturation of the neurotransmitter release machinery by inducing the clustering of neuroligins on axons and as a result, the coupling of  $\text{Ca}^{2+}$  channels to the synaptic exocytic machinery.

It has been well-documented that cell-cell interactions between  $\beta$  cells are essential for functional stimulus-secretion coupling [82-87]. It may be that, as in pre-synaptic differentiation, interaction between proteins on two contacting  $\beta$  cells promotes the coupling of voltage gated  $\text{Ca}^{2+}$  channels to the secretory machinery—a process that is necessary for robust glucose-stimulated insulin secretion from  $\beta$  cells [88]. Because the architecture of the  $\beta$  cell insulin secretory apparatus very much resembles that used by neurons for exocytosis of neurotransmitter, these same proteins are critical for insulin secretion from the  $\beta$  cell and many of these proteins interact in complex with neuexin at the presynaptic active zone [89-95], it is intriguing to propose the hypothesis that assembly of the apparatus necessary for insulin release from  $\beta$  cells is, like assembly of the presynaptic active site, dependent on neuexin-neuroligin interactions. It is conceivable that the interaction of neuroligin on one  $\beta$  cell with neuexin on a contacting  $\beta$  cell promotes the coupling of voltage dependent  $\text{Ca}^{2+}$  channels with the exocytic machinery and facilitates the enhanced glucose-stimulated insulin secretion observed in contacting  $\beta$  cells. This hypothesis is explored in chapter 5 of this dissertation.

#### F. Objective of the Dissertation

The work described throughout this dissertation arose from the observation that the  $\beta$  cells' expression of the machinery necessary for GABAergic neurotransmission makes the  $\beta$ -cell cellular “phenotype” very much resemble that of an inhibitory synapse. The objective of my dissertation research, then, was to explore the hypothesis that key insights into the functional maturation of  $\beta$  cells could be derived from existing



knowledge of the development, differentiation and maintenance of GABAergic synapses in the CNS. Chapter 2 focuses on the expression and regulation of the vesicular GABA transporter in  $\beta$  cells. Chapter 3 addresses the hypothesis that the proteins that mediate the biogenesis of GABAergic synaptic vesicles in the central nervous system are expressed by  $\beta$  cells and that these proteins regulate the assembly of synaptic-like microvesicles. Chapter 4 investigates whether the proteins that regulate the differentiation of an immature synapse to a GABAergic state are expressed by  $\beta$  cells and attempts to elucidate whether these proteins might also be important for insulin secretion. Chapter 5 addresses whether the synaptic adhesion molecules important for recruiting the GABAergic synaptic release machinery to an inhibitory synapse might be important for regulating the assembly of the insulin secretory apparatus in  $\beta$  cells.

CHAPTER 2: THE INHIBITORY PHENOTYPE OF THE ISLET  $\beta$ -CELL:  
IDENTIFICATION AND CHARACTERIZATION OF A NOVEL ISOFORM OF THE  
VESICULAR GABA TRANSPORTER WITH GLUCOSE-REGULATED  
EXPRESSION IN RAT ISLETS

A. Abstract

Pancreatic islets are unique outside the nervous system in that they contain high levels of the inhibitory neurotransmitter  $\gamma$ -aminobutyric acid (GABA), synthesized by the enzyme glutamic acid decarboxylase (GAD). Since the role that GABA plays in the islet and the mechanisms whereby the two major GAD isoforms (GAD65 and GAD67) function as diabetes-associated autoantigens are unknown, continued characterization of the islet GAD-GABA system is important. We previously demonstrated that the GABA and glycine transporter VIAAT (vesicular inhibitory amino acid transporter, also known as VGAT) is present in rat islets. Here we identify a novel 52-kDa variant of VIAAT in rat islets: VIAAT-52 (V52). V52 is an amino-terminally truncated form of VIAAT (V57) that likely results from utilization of a downstream start site of translation. V57 and V52 display different patterns of post-translational modification and cellular expression. Our results indicate that islet content of V52, but not V57, is responsive to changes in glucose concentration and other extracellular conditions. VIAAT is expressed in the islet  $\alpha$  cells, but there have been conflicting findings regarding the presence of VIAAT in the  $\beta$  cells. Here we also provide additional evidence for the presence of VIAAT in islet  $\beta$  cells and show that the  $\beta$  cell line INS-1 expresses V57. V52 may be better adapted than V57 to

the unique rat  $\alpha$ -cell GAD-GABA system, which lacks GAD65 and in which VIAAT traffics to secretory granules rather than just to synaptic microvesicles.

## B. Introduction

A distinctive feature of pancreatic islets is that they synthesize and store  $\gamma$ -aminobutyric acid (GABA). Despite much work, though, the role of GABA in the endocrine pancreas remains unknown [22, 96]. In the central nervous system, GABA is the major inhibitory neurotransmitter. In the islets, it probably also functions as an intercellular signaling molecule, perhaps—as there is evidence to suggest—as a paracrine or autocrine regulator of insulin or glucagon secretion [22, 25, 29]. Recent evidence suggests that a second inhibitory neurotransmitter, glycine, also plays a role in islet function [2].

Characterization of the cellular GABA signaling machinery in islets will likely yield important insights into the role of GABA in islet function. The GABA system is also of great interest because the enzymes that catalyze the synthesis of GABA—GAD65 and GAD67, the two major isoforms of glutamic acid decarboxylase—are key autoantigens associated with human (in the case of GAD65) and NOD mouse (in the case of both GAD65 and GAD67) autoimmune diabetes [39, 97]. The interactions of GAD65 and GAD67 with other protein constituents of the islet GAD-GABA system may help mediate the intracellular trafficking of the two enzymes, their characteristic association with microvesicles, and, perhaps, therefore, their distinctive ability to function as autoantigens [38].

In the central nervous system, the vesicular inhibitory amino acid transporter (VIAAT) is a key component of the GABAergic and glycinergic signaling machinery. VIAAT is a transmembrane protein that utilizes a proton electrochemical gradient to transport GABA and glycine into synaptic vesicles where they are stored prior to release [98]. Because of the importance of characterizing the pancreatic islet GAD-GABA system, we previously investigated the distribution of VIAAT in rat islets. We found that the rat islet mantle (the islet periphery, where the  $\alpha$  cells are found) harbors a unique GAD-GABA signaling apparatus, characterized by the presence of GAD67, GABA and VIAAT but not GAD65 [99]. Lower levels of VIAAT were also detected VIAAT in the rat islet  $\beta$  cells, which contain GAD65 [99]. Hayashi et al. [100] subsequently confirmed the presence of VIAAT in the rat islet mantle, detecting none in the islet  $\beta$  cells. Unexpectedly, VIAAT was found to localize to the glucagon-containing secretory granules rather than to the synaptic-like microvesicles also present in islet  $\alpha$  cells. In contrast, Gammelsaeter et al. [2] identified VIAAT in both secretory granules and microvesicles in rat islet  $\alpha$  cells and also detected comparatively low levels in the  $\beta$  cells.

VIAAT is a 57.4 kDa protein (V57). A phosphorylated form (V57') that migrates more slowly by SDS-PAGE is observed in brain tissue extracts [101]. We found that islet extracts, in contrast to neural tissue, contain little or no V57' [99]. Unexpectedly, immunoblotting also revealed a second, more rapidly migrating form of the protein in islet and brain extracts. This form was predominant in islet cell extracts and has an apparent molecular weight of 52.5 kDa (V52). Hayashi et al.[100], using a novel antibody that may have a relatively lower affinity for V57, observed only an ~52 kDa

VIAAT band in rat islet extracts and  $\alpha$ TC6 cells, while both V57 and V52 were detected in brain. The ~52 kDa form of VIAAT is present in low abundance in rat and human brain tissue extracts and is detected, as well, in purified synaptic vesicles and rat pineal gland extracts [58, 99, 102, 103]. COS-7 and tsA201 cells transfected with different VIAAT cDNA constructs also express an ~52 kDa form of the protein along with the more-abundant 57 kDa form [102, 104]. Using rat and human brain extracts, we found that the 52.5 kDa VIAAT proteins from neural and islet cells comigrate by SDS-PAGE and are therefore most likely identical [99]. Similar data suggest that V52 from islet and brain extracts is identical to that synthesized after VIAAT cDNA is either transfected into tsA201 cells or introduced into reticulocyte lysates for *in vitro* transcription and translation [99, 102].

Because of the relatively low abundance of V52 in neural tissue as compared to islet cells, evidence pointing to the existence of a 52 kDa isoform of VIAAT has been previously overlooked. Here, we identify V52 as a novel variant of VIAAT truncated at the amino terminal end and differentially modified. We also show that V57 is present in INS-1 cells and use immunohistochemistry to provide further evidence of the presence of VIAAT in islet  $\beta$  cells. Herein, we also test the hypotheses 1) that V52 is formed by utilization of an alternate start site of translation and 2) that its level of expression is independent of that of V57 and responsive to glycemic conditions.

## C. Materials and Methods

### *Antibodies*

The antibody referred to as VT/510 is an affinity-purified antibody to the carboxyl terminus of VIAAT (Chemicon, Temecula, CA). VT/75 (Synaptic Systems, Göttingen, Germany) is an affinity-purified antibody to VIAAT residues 75-87. A monoclonal antibody raised against the same peptide (M-VT/75) was also purchased from Synaptic Systems. VT/75 and M-VT/75 are well-characterized and have been used extensively to detect VIAAT in neural and testicular tissue, to specifically identify inhibitory synapses and to immunopurify VIAAT-carrying microvesicles (see, for example: [105-108]. VT/17 was made to our specifications by Alpha Diagnostic, Inc. (San Antonio, TX) in rabbit hosts by coupling a peptide representing VIAAT residues 17-30 (CSNKSQAKVSGMFAR) to keyhole limpet hemocyanin. In preliminary immunoblotting experiments, VT/17 was found to recognize the 57 kDa VIAAT band in rat brain and islets but did not detect a 57 kDa protein in three tissues previously shown not to express VIAAT: rat kidney, liver and skeletal muscle [109]. Preimmune serum from the same rabbit used to generate VT/17 was retained for use as a negative control. VT/17 was not suitable for immunohistochemistry using either frozen or paraffin-embedded tissues. A monoclonal antibody to glyceraldehyde-3-phosphate dehydrogenase was from Chemicon and another to the amino terminus of GAD65 was a kind gift from Dr. Åke Lernmark [110]. Rat brain extract was purchased from Stressgen (Victoria, Canada).

### *In vitro expression of VIAAT*

Transcription and translation of VIAAT cDNA to produce radiolabeled VIAAT in rabbit reticulocyte lysates was carried out as described previously [99]. The Quickchange Site-Directed Mutagenesis Kit (Stratagene, La Jolla, CA) was used to introduce point mutations into the VIAAT cDNA. A T>C substitution at cDNA position 2 was used to generate mutation M1T, and M31L was created by changing A>C at position 91 and G>A at position 93. MIT-6xHis was made by utilizing PCR to introduce a 6xHis tag on the 3' end of VIAAT M1T: VIAAT M1T was amplified with the primers GACCAAGCTTGCCGCCAC (5') and TTAATGATGATGATGATGATGGTCCTCCGCGTTGGTT (3') and the resulting product then cloned into PCRII-Topo (Invitrogen). Full-length sequencing of all plasmid inserts confirmed that the constructs were as expected. 6xHis-tagged V52 was purified using His-Select Nickel Affinity gel (Sigma, St. Louis, MO). Purified protein was sent to the Harvard Microchemistry and Proteomics Facility (Cambridge, MA) for N-terminal sequencing after being prepared and blotted onto Sequi-Blot PVDF membrane (Bio-Rad Laboratories, Hercules, CA) as specified by the microsequencing facility.

### *Islet preparation*

Islets were isolated from the pancreata of diabetes-resistant (DR) BioBreeding (BB) rats [111] by digestion with Liberase (Roche Molecular Biochemicals, Indianapolis, IN) followed by Optiprep (Nycomed, Oslo, Norway) gradient purification as previously described [99]. Isolated islets were hand-picked in Hank's Balanced Salt Solution

(Invitrogen, Carlsbad, CA). They were then either rinsed with phosphate-buffered saline (PBS) and lysed or cultured in RPMI (Invitrogen) with 3, 10 or 20 mmol/l glucose and supplemented with 10% fetal bovine serum. Islets were lysed at 4°C in Novex NuPage sample buffer (Invitrogen) or SDS boiling buffer (5% SDS, 10% glycerol, 60 mmol/l Tris pH 6.8; 4 islets/ $\mu$ l) and the extracts either boiled for 4 min or heated for 7 min at 70°C. At the time of islet lysis, detergent buffers were supplemented with a protease inhibitor cocktail (P8340, Sigma, St. Louis, MO) and 1 mmol/l phenylmethylsulfonyl fluoride (PMSF). To test lysis in non-ionic detergent, islets were incubated for 30 min in a solution of 1% Nonidet P40 (NP-40) in PBS, and the nuclei and other debris pelleted by spinning for 10 min at 10,000 x g. Islets not immediately lysed were stored frozen at -80°C.

#### *INS-1 cells*

INS-1 cells were a kind gift from Christopher Rhodes (Pacific Northwest Research Institute, Seattle, WA). INS-1 cells from the Rhodes laboratory have been successfully used by that laboratory and others as a model of  $\beta$  cell biology in the publications cited here and others [112-115]. One of us (I. Sweet) has performed perfusion experiments using the INS-1 that we received and that were in the same passage number range as the cells used for the experiments described herein [116]. These perfusion experiments demonstrated appropriate responses to glucose and epinephrine and as well as sulfonylurea (glibenclamide) binding [116]. Using an insulin ELISA (Crystal Chem Inc, Downers Grove, IL), we have periodically evaluated glucose-



stimulated insulin secretion using static culture and similarly determined that the cells have maintained glucose-responsiveness (data shown herein and other data not shown). Immunohistochemistry reveals uniform insulin expression by this INS-1 line, with all cells expressing insulin (data shown herein and other data not shown).

INS-1 cells were cultured in medium with 11 mM glucose as described [117]. Cells extracts were prepared in the same manner as islet extracts. Protein content of cell and islet extracts was determined with the DC Protein Assay (Bio-Rad) to ensure that equal amounts of protein were loaded into gel lanes.

#### *Subcellular Fractionation*

INS-1 cells were fractionated using the method of Clift-O'Grady *et al.* [118]. Briefly, cells were pelleted at 800 x g for 5 minutes, resuspended in budding buffer (38 mM potassium glutamate, 38 mM potassium gluconate, 20 mM 4-morpholinepropanesulfonic acid pH 7.2, 5 mM reduced glutathione, 5 mM sodium carbonate, 2.5 mM magnesium sulfate) and pelleted again at 800 x g for 5 minutes. Cells were resuspended in budding buffer with protease inhibitors (Roche Molecular Biochemicals, Indianapolis, IN) and homogenized using a Balch-designed cell cracker (European Molecular Biology Laboratory). Trypan blue exclusion was used to ensure efficient homogenization. The resulting homogenate was sedimented in an SS34 rotor at 1000 x g for 5 minutes to obtain low speed supernatant (S1). S1 supernatants were then sedimented at 27,000 x g for 35 minutes to generate a high speed supernatant (S2) and pellet (P2). To verify exclusion of secretory granules from the S2 supernatant, the

supernatant was fractionated by velocity gradient centrifugation [118] and the fractions evaluated for chromogranin A content by western blot analysis. The S2 supernatant utilized for the experiments shown herein contained synaptophysin, a marker of synaptic-like microvesicles, and, as expected, lacked chromogranin A, which instead was found in P2 (A.S., unpublished observations). Tissue extract from BB (DR) rat brains and crude synaptic vesicle preparations were made as previously described [58].

### *Immunofluorescence*

Cells were seeded on 4-well chamber slides (BD Biosciences) coated with poly-L-lysine and allowed to grow for 48 hours. They were fixed in a 4% paraformaldehyde solution for one hour, washed twice in 1x phosphate buffered saline (PBS) and permeabilized and blocked with PBS containing 0.2% Triton-X-100 and 3% BSA for 1 hour. Cells were then incubated with a 1:200 dilution of mouse anti-insulin and of rabbit anti-VGAT antibody for 1 hour. After incubation, cells were washed three times with PBS and incubated with a 1:200 dilution of AlexaFluor568 anti-mouse IgG conjugate, a 1:200 dilution of AlexaFluor488 anti-rabbit IgG and a 1:1000 dilution of To-pro 3 (Molecular Probes; OR). Confocal microscopy was performed on an FV1000 confocal microscope configured with an Argon/Krypton laser (488- and 568-nm excitation lines) (Olympus; Melville, NY).

### *Insulin Secretion Assays*

Cells were grown on 12 well plates 48 hours prior to measuring insulin then washed 2 times with Krebs-Ringer bicarbonate buffer containing 0.2% BSA and 2.5 mM glucose. They were then incubated for 30 minutes in this buffer. After incubation, this solution was removed and replaced with Krebs-Ringer containing either 2.5 mM glucose or 25 mM glucose. Cells were incubated for 2 hours, the media was removed and insulin content was measured using a rat insulin ELISA kit (Crystal Chem).

### *Immunohistochemistry*

Paraffin-embedded rat and human pancreas tissue were deparafinized and blocked in a 1% bovine serum albumin/PBS solution for one hour at room temperature. Sections were incubated with a 1:200 dilution of primary antibody for one hour. They were washed twice in 1x PBS for 10 minutes and incubated in a 1:500 dilution of biotinylated goat anti-rabbit IgG followed by a 30-min incubation in a 1:200 dilution of alkaline phosphatase streptavidin. Vector Red (Vector Laboratories; Burlingame, CA) was used to visualize the binding of the primary antibodies. Sections were counterstained with hematoxylin (Fisher Scientific; Fairlawn, NJ) using standard methods.

### *Protein electrophoresis*

Proteins were run on NuPage gels (Invitrogen) and immunoblotted as previously described [99]. For quantitation, immunoblots were incubated with ECL-Plus chemiluminescent substrate (Amersham Biosciences, Piscataway, NJ) and directly

analyzed using a Molecular Dynamics Storm 840 imager and ImageQuant software (Amersham). Otherwise, blots were incubated with ECL substrate (Amersham) and the chemiluminescent signal captured by XAR film (Kodak, Rochester, NY).

Two-dimensional electrophoresis was performed according to the method of O'Farrell [119] by Kendrick Labs, Inc. (Madison, WI). To enhance the solubility of membrane proteins, islet samples were prepared in SDS boiling buffer [120]. No urea was added to the sample buffer, and samples were kept frozen at -80°C, avoiding any risk of carbamylation [121]. Isoelectric focusing was carried out in glass tubes using 2% pH 3.5-10 ampholines (Amersham). After equilibration, the tube gels were sealed to stacking gels on top of 8% acrylamide slab gels for SDS-polyacrylamide gel electrophoresis (PAGE). Two 2-dimensional gels were run in parallel: one with 200 µg islet extract, which was analyzed after western transfer to polyvinylidene fluoride membrane, and another with 10 µl of radiolabeled VIAAT spiked into 200 µg islet extract, which was analyzed by autoradiography (using a storage phosphor screen) and phosphorimaging with a Storm 840 imager. A tropomyosin marker was added to each sample, and molecular weight markers (Sigma) were also run in the second dimension. Tropomyosin yields a characteristic pattern of spots which was observed in all 2-D gels run. To allow precise alignment of the resulting images, the western blot and the gel used for autoradiography were both stained with Coomassie blue to allow visualization and alignment of islet and marker proteins. Alignment was performed electronically using scanned images.

*Statistical analysis*

Data are presented as means  $\pm$  SE. Differences between quantitative data sets were analyzed by one-way ANOVA.  $P < 0.05$  was considered significant.

## D. Results

### 1. *Synthesis and stability of VIAAT*

In vitro transcription and translation of VIAAT cDNA yields significant quantities of two proteins: V52 and V57. Parallel reactions with GAD67, GAD65, luciferase and *S. cerevisiae*  $\alpha$ -factor cDNAs, in contrast, yielded significant amounts only of the expected protein: the appearance of a prominent, lower molecular weight protein was unique to VIAAT [99] (and data not shown). To verify that V52 does not result from proteolytic degradation, the time-course of V52 and V57 synthesis was analyzed (Fig. 2.1A). In repeated experiments, we consistently found that V52 and V57 appeared simultaneously: accumulation of V52 was not preceded by accumulation of V57. Furthermore, the amount of V52 relative to V57 did not increase over time, as would be expected if V57 were gradually converted to V52.

We also investigated the relative stability of both proteins in islet cell extracts, both to test for evidence of proteolytic activity that converts V57 to V52 and also to ensure that V52 is not formed as an artefact of islet cell lysis. We lysed isolated islets in both ionic (SDS) and non-ionic (1% Nonidet P40) detergent solutions both with and without addition of protease inhibitors. Each type of lysis buffer performed equally well in extracting V52 and V57 from purified islets (data not shown). The lysates were incubated at 4°C or 37°C and aliquots were withdrawn at set time points. To determine whether there was an increase with time in the ratio of V52 to V57, which would be consistent with post-lysis conversion of V57 to the smaller isoform, the VIAAT content of the islet extract samples was examined by immunoblotting. One such experiment is depicted in Fig. 2.1B. A similar approach was used by Bedet et al. [101] to demonstrate

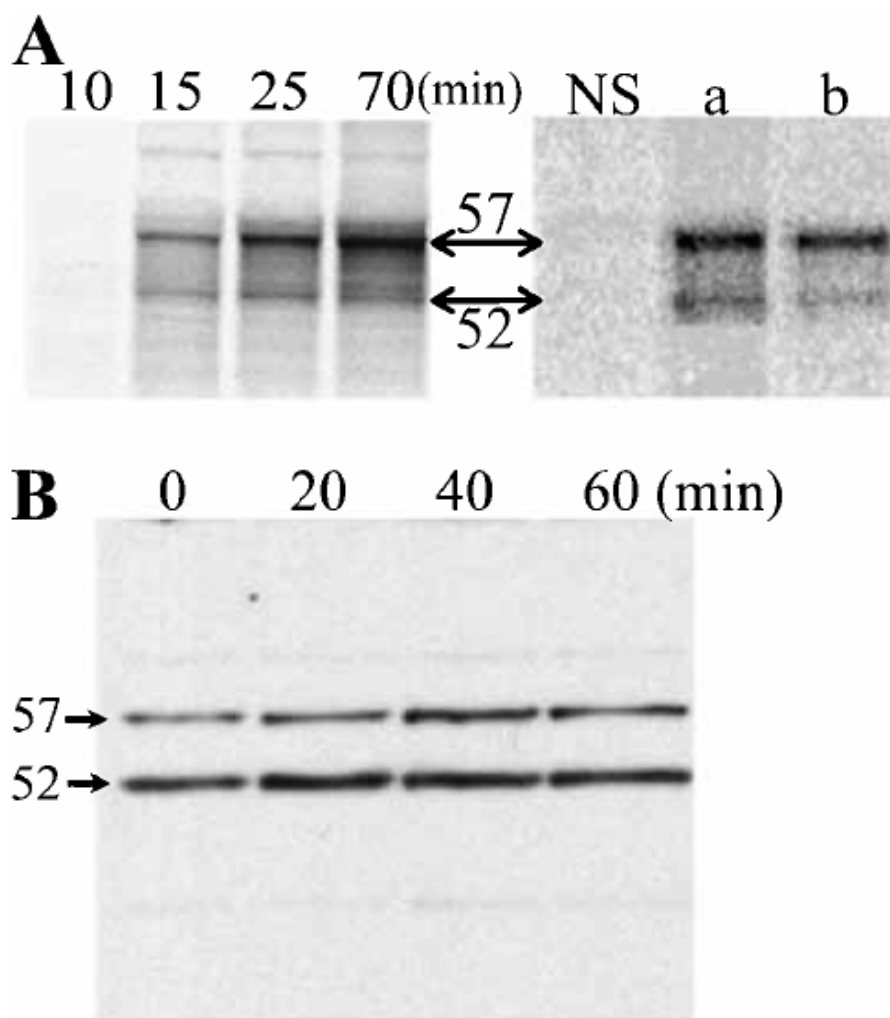


**Figure 2.1. Synthesis and Stability of V57 and V52.**

**A**, VIAAT cDNA was added to an in-vitro, reticulocyte lysate expression system containing  $^{35}\text{S}$ -met (time 0). Aliquots of the reaction mix were withdrawn at the times indicated above the lanes (left panel), and radiolabeled proteins were analyzed by SDS-PAGE and autoradiography. V52 and V57 appeared simultaneously 15 min after the addition of the VIAAT cDNA to the reticulocyte lysate, and there was no increase over time in the ratio of V52:V57. Immunoprecipitation of the reaction mixture after 70 min (right panel) with two different anti-VIAAT antibodies, VT/510 (lane "a") and VT/75 (lane "b"), verified that the bands running at 57 kDa and 52 kDa were isoforms of VIAAT. A control immunoprecipitation was also performed with normal rabbit serum (NS). **B**, Islet proteins were extracted in NP-40 lysis buffer without addition of protease inhibitors and incubated at 37°C for the amount of time indicated. V52 and V57 protein content was analyzed by immunoblotting with antibody VT/510. Both isoforms are stable in the lysis buffer. In experiments such as this with both non-ionic and ionic (SDS) detergent buffers and both with and without protease inhibitors, there was no evidence of conversion of V57 to V52.

that V57' (a phosphorylated form of V57) is gradually converted to V57 in brain extracts. In contrast, V57 was not converted into V52: there was no evidence of an increase in V52 content at the expense of V57 content during incubation at either 4°C or 37°C in either type of detergent lysis buffer. The same result was obtained when radiolabeled, in vitro-translated VIAAT was incubated in islet extracts and then analyzed by autoradiography (data not shown).

## *2. The VIAAT gene contains an alternate start site of translation.*

To test whether synthesis of V52 could be due to the utilization of an alternate, downstream start site of translation, we analyzed VIAAT protein expression after mutating the V57 initiator codon (V57-M1T). As shown in Fig. 2.2, V52 is preferentially translated after mutation of VIAAT codon 1.

The ATG codon encoding methionine residue 31 occurs in a region of high homology to the eukaryotic consensus sequence for translation initiation [122] and is thus a candidate for an alternate translation start site. While alteration of this downstream codon suppressed synthesis of V52, the degree of suppression was, for unclear reasons, inconsistent (Fig. 2.2 and data not shown). As expected, the M>L substitution at residue 31 did not affect synthesis of V57.

The formation of V52 by utilization of a downstream start site of translation and the recognition of this protein by an antibody to the carboxyl-terminus of VIAAT suggests that it is truncated at its amino-terminal end relative to V57. To confirm this, western blots of islet extracts were probed with an antibody to VIAAT residues 17-30



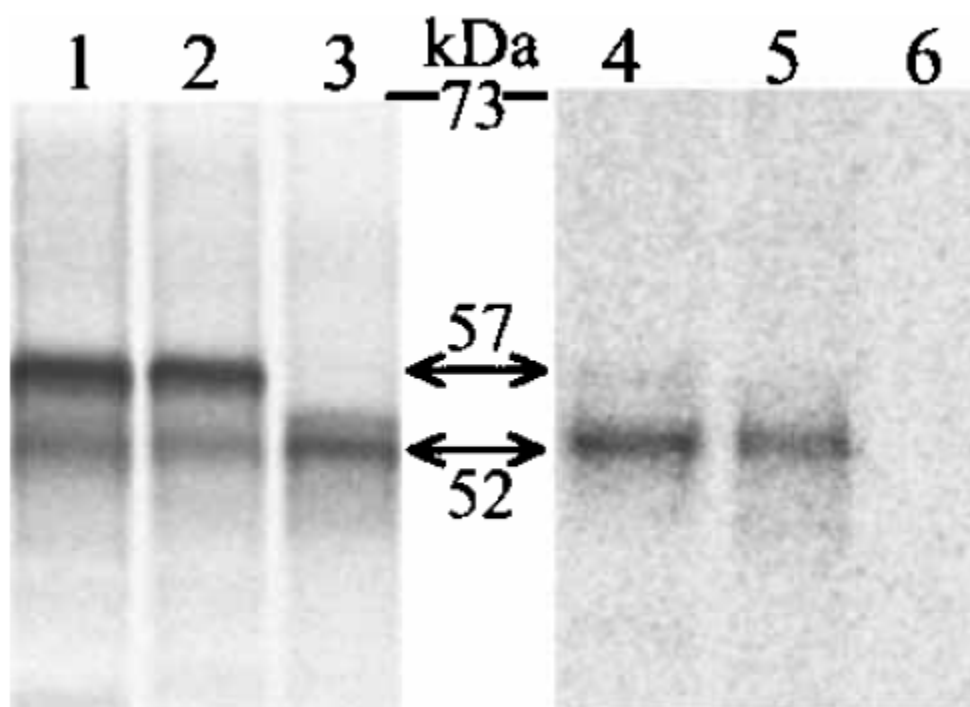


**Figure 2.2. VIAAT Synthesis from Mutated cDNA Templates.**

*Lanes 1-3*, VIAAT (lane 1), VIAAT M31L (lane 2) and VIAAT M1T (lane 3) were synthesized in rabbit reticulocyte lysates in the presence of  $^{35}\text{S}$ -met and analyzed by SDS-PAGE and autoradiography. As seen in lane 3, mutation of the initiator methionine (M1T) suppressed synthesis of V57 but not V52. *Lanes 4-6*, To ensure that an isoform of VIAAT was synthesized from the M1T template despite mutation of the initiator codon, the M1T reaction product was immunoprecipitated with two anti-VIAAT antibodies, VT/510 (lane 4) and VT/75 (lane 5). The 52 kDa protein yielded by the M1T template was recognized by both antibodies. Normal rabbit serum was used as a control for non-specific binding (lane 6).

(VT/17). Consistent with the hypothesis that the two VIAAT variants differ at their amino-terminal ends, VT/17 recognized V57 but not V52 (Fig. 2.3).

To isolate V52, we introduced a 6xHis tag on the carboxyl terminus of V57-M1T. V52-6xHis was preferentially translated from this construct and could be captured on nickel agarose beads (not shown). This confirmed that the carboxyl-terminus of VIAAT is intact in V52 (since the 6xHis tag remained functional). Captured V52-6xHis was sent for amino-terminal sequencing. Sequencing, however, was unsuccessful, perhaps due to N-terminal blockage, a common problem with eukaryotic proteins [123, 124].

### 3. *Two-dimensional gel analysis of V52 and V57*

In order to analyze the pattern of post-translational modification of islet VIAAT and to confirm the identity of *in vitro* synthesized V52, VIAAT was detected by immunoblotting rat islet proteins separated using two-dimensional non-equilibrium pH gradient electrophoresis (NEPHGE)/SDS-PAGE [119]. As seen in Fig. 2.4, islet V57 runs as a “train” of five to eight spots. This indicates that post-translational modifications result in multiple forms, but does not indicate the specific nature of the modifications. In contrast, islet V52 appears only as a single spot.

To verify that islet V52 and the reticulocyte lysate-derived V52 synthesized after mutation of codon 1 are the same, we asked whether they would comigrate during two-dimensional electrophoresis. Radiolabeled V52 was prepared in the reticulocyte lysate system, spiked into islet extract and loaded onto a 2-D gel. This gel was run in parallel with the gel used to create the immunoblot shown in Fig. 2.4. The spots yielded by the

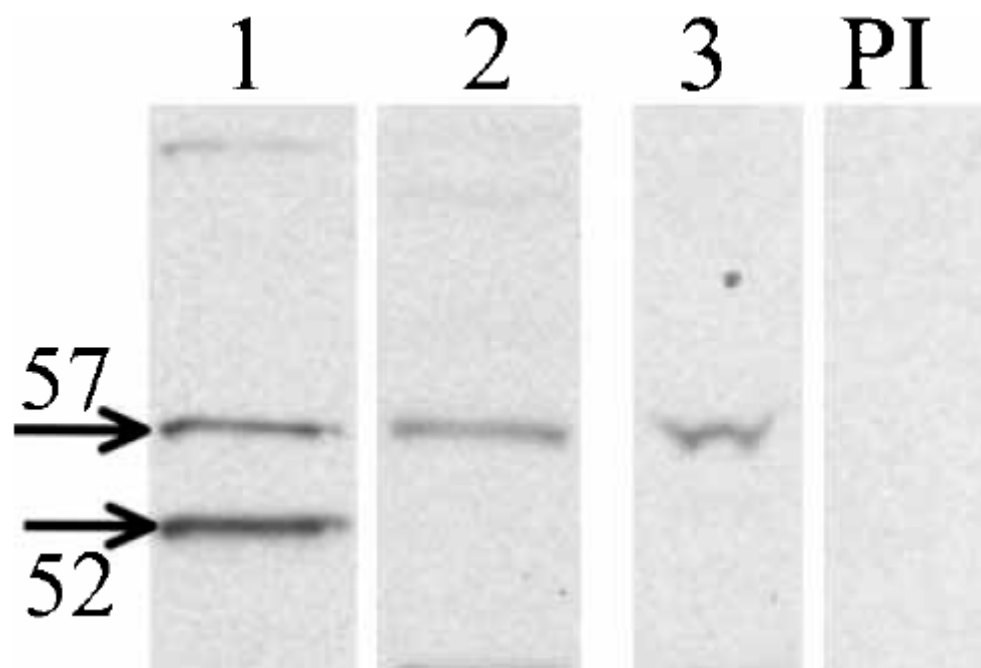


**Figure 2.3. Immunorecognition of V57 and V52 by Antibodies to the Amino and Carboxyl Termini of VIAAT.**

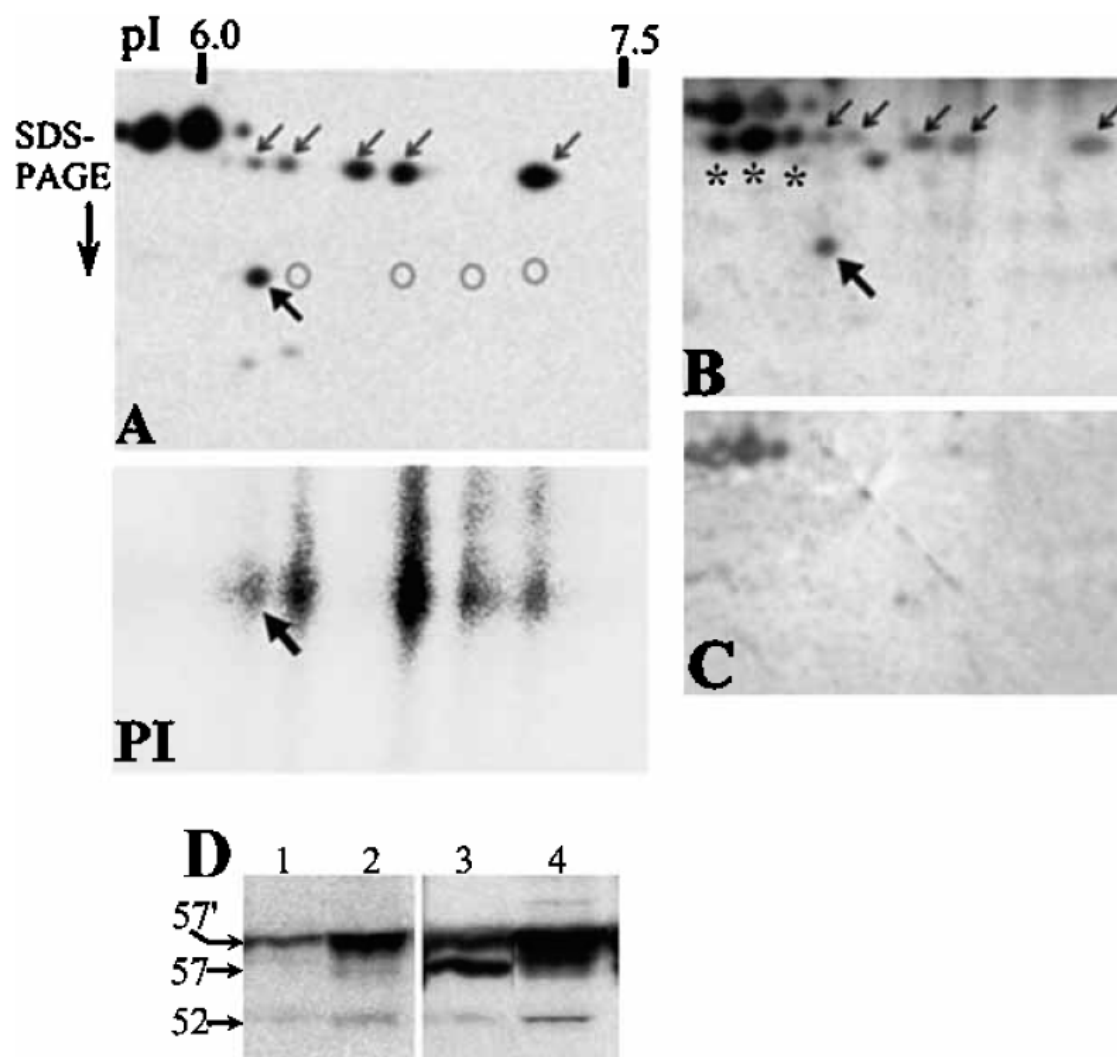
Lanes 1,2: A rat islet extract was immunoblotted with antibodies to the carboxyl terminus (VT/510, lane 1) and to the amino terminus (VT/17, lane 2) of VIAAT. Lanes 3,4, Immunoblots of a rat brain extract using antibody VT/17 (lane 3) and preimmune serum from the same rabbit (PI). VT/17 exhibits specific recognition of V57 but does not bind V52. Detection of V52 by the carboxyl-terminal antibody (VT/510; lane 1, lower band) but not the amino-terminal antibody (VT/17; lanes 2,3) shows that V52's lower molecular weight (compared to V57) is attributable to an amino-terminal truncation.

radiolabeled V52 (Fig. 4Pi) aligned with the immunoblot at the positions indicated (Fig. 2.4A). As shown in Fig. 2.4A, the pattern of modification undergone by V52 synthesized in rabbit reticulocyte lysates is similar to that of islet-derived V57, with the protein separating into five forms in the same pI range as V57. We previously observed that bands representing V52 protein derived from islet and brain extracts and from *in vitro* synthesis comigrate by SDS-PAGE [99]. In the present study, we find that reticulocyte-lysate derived V52, in the case of the form with the most acidic pI, precisely comigrates with rat islet V52 during two-dimensional electrophoresis, suggesting that they are identical (Fig. 2.4A). Though membrane proteins can be well resolved during NEPHGE/SDS-PAGE, variable protein loss is a common problem and likely explains what, in Fig. 2.4, appears to be a greater abundance of V57 than V52 [120, 125, 126].

The two-dimensional gel results show V57 to consist of a heterogeneous group of differentially modified VIAAT molecules (Fig. 2.4A and B). Some of this heterogeneity is also apparent on standard one-dimensional gels, with brain-derived V57 frequently seen to migrate as a doublet: V57 and V57' [99, 101]. We previously showed that this differential modification results in differential detection of V57 by antibodies, likely due to specific modifications masking targeted epitopes [99]. VT/510, for example, does not detect human brain V57 or V57' on western blots [99]. Differential recognition of differently modified forms of V57 is probably the reason why the pattern of V57 spots seen with VT/75 and VT/510 varies (Fig. 2.4A and B). Differing detection of V57 by different antibodies is also seen in Fig. 2.4D, with VT/75 preferentially binding more-slowly migrating forms in brain extracts (lanes 1,2) as compared with VT/510 (lanes 3,4).

### Figure 2.4. 2-D Electrophoresis of VIAAT.

Two NEPHGE/SDS-PAGE gels were run in parallel to analyze proteins from rat islets (by immunoblotting) and radiolabeled V52 synthesized *in vitro* using a VIAAT cDNA construct with a mutated initiator codon. **A**, Immunoblot analysis of the rat islet extract using antibody VT/510. V57 separated into a train of 5 spots (small arrows), indicating that there are at least 5 differentially modified forms of the protein. V52, in contrast, migrated as one spot (larger, bold arrow). **Pi**, *In vitro* synthesized, radiolabeled V52 was spiked into islet extract and run in parallel on a separate 2-D gel. It also separated into 5 differentially modified species. The phosphorimage (**Pi**) was aligned with the immunoblot (panel **A**) as described in Materials and Methods to allow direct comparison of the spots generated by *in vitro* synthesis with those derived from the islet extract. One of the five VIAAT species detected by phosphorimaging precisely comigrated with endogenous islet V52 (indicated by the bold arrow). The other four forms ran where indicated by the circles drawn on the immunoblot. **B**, The immunoblotted membrane was stripped and probed with a second anti-VIAAT antibody, VT/75. The spots depicted by the five small arrows and one large arrow comigrate with the spots shown in panel **A**. VT/75 also detected what are likely three additional V57 species (marked by asterisks) with more acidic pIs. **C**, The immunoblotted antibody was stripped and probed with normal rabbit serum. The 4 spots present in the upper left-hand corner of this panel and panels **A** and **B** likely represent non-specific antibody binding. **D**, Immunoblot of rat brain extract (lanes 1, 3) and rat brain synaptic vesicle preparation (lanes 2, 4) with VT/75 (lanes 1,2) and VT/510 (lanes 3,4). As in panels **A** and **B**, different patterns of recognition of V57 species can be seen depending on which antibody is used. For example, in lane 1, VT/75 can be seen to preferentially detect a more slowly-migrating form (V57').



#### 4. *Differential regulation of V52 and V57 expression*

Levels of VIAAT expression in the brain have been reported to be responsive to agonists and antagonists of presynaptic GABA<sub>B</sub> receptors, to ethanol and to antipsychotic medications [127-129]. Since, in the pancreatic islets, GAD65 and GAD67 expression and GABA release are subject to metabolic regulation, we hypothesized that islet VIAAT content may be similarly regulated [130-132]. We therefore investigated VIAAT expression after islet exposure to different glycemic conditions. Rat islets were equilibrated overnight in standard RPMI and then cultured for 20 hours in different glucose concentrations. Afterwards, islet VIAAT content was examined by immunoblot analysis (Fig. 2.5A). V57 content did not vary in response to media glucose concentration. V52 levels, however, increased in response to higher glucose levels. Consistent with past published results [130, 132], levels of GAD67—the form of GAD present, along with VIAAT, in the islet mantle—were also observed to increase (data not shown).

Unexpectedly, we noted that V52 levels decreased relative to V57 levels during the overnight period of equilibration in RPMI medium immediately following islet isolation. The extent of decline was variable, and V52 levels reached their nadir--15 to 30% of 4 hour culture levels--by 20 hours (Fig. 2.5B and data not shown). Elevated glucose concentrations significantly attenuated but did not prevent the fall in V52 content: after 4 hours, V52 content was 56% ( $\pm 7\%$ ) greater in islets cultured at 20 mmol/l glucose than in islets cultured in 3 mmol/l glucose, and, after 20 hours, V52 content was 41% ( $\pm 5\%$ ) greater at the higher glucose level ( $n=5$ ,  $p < 0.05$  for both; see Fig 2.5B). In

contrast, V57 and glyceraldehyde 3-phosphate dehydrogenase levels did not change (Fig. 2.5B). During the initial 20 hour period of equilibration in culture media after islet isolation, then, a higher glucose concentration resulted in less of a decline in V52 content (as in Fig. 2.5B). In these experiments performed immediately after islet isolation, the overall effect of glucose on V52 content was less than in experiments performed after the islets had been allowed to equilibrate in culture medium overnight (as in Fig. 2.5A). The initial fall in V52 content, then, was due to conditions other than just glycemic levels.

#### 5. *VIAAT expression in INS-1 and islet $\beta$ cells*

Conflicting results have been published concerning whether VIAAT is expressed in  $\beta$  cells [2, 99, 100]. Immunoblot analysis showed that the rat  $\beta$  cell line INS-1 expressed V57 but not V52, consistent with  $\beta$ -cell expression of at least one form of the transporter (Fig. 2.6A) [133].

Gammelsaeter et al. [2] presented evidence that VIAAT localizes to synaptic-like microvesicles (SLMVs) in  $\beta$  cells. To test whether VIAAT also associates with SLMVs in INS-1 cells, cells were fractionated as described in Materials and Methods to yield a high-speed supernatant S2 containing microvesicles and depleted of secretory granules and endosomes [118]. S2 contained VIAAT (Fig. 2.6A); this demonstrates its presence in SLMVs but does not exclude that it is also present in secretory granules [118, 134]. Detection of microvesicular proteins in P2 in addition to S2 is typical due to their passage through other, larger membranous compartments, such as endosomes, during sorting. Because of this, detection of VIAAT in P2, as seen, is not informative as to whether



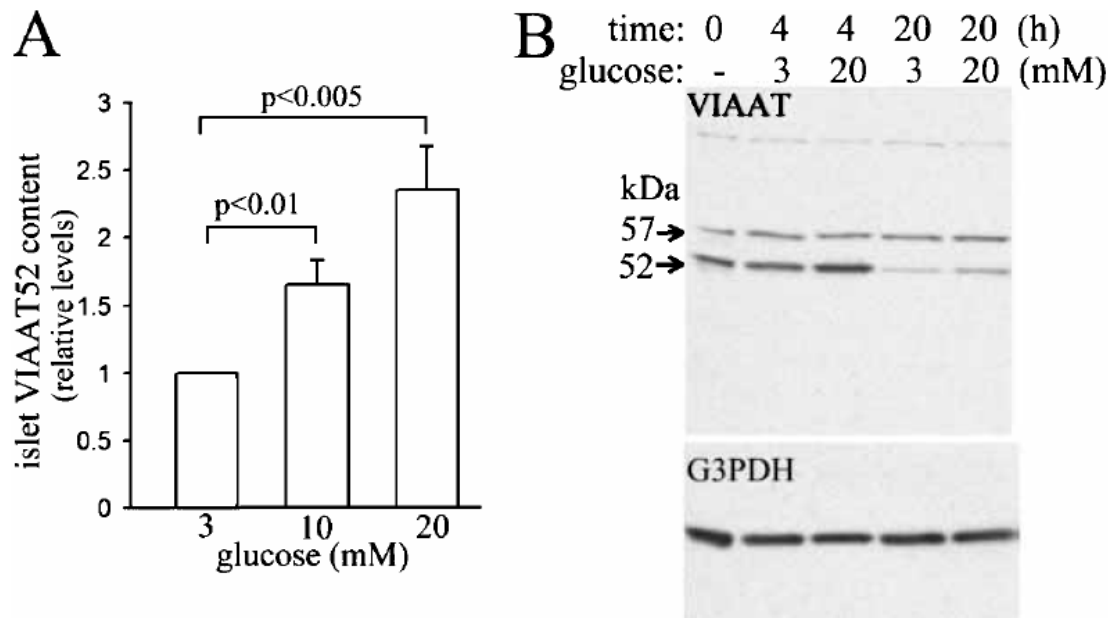


**Figure 2.5. Effects of Glucose Concentration on Islet VIAAT Content.**

**A**, Islets were isolated and allowed to equilibrate overnight in RPMI. Equal numbers of islets were then cultured separately at the glucose concentrations indicated, and V52 and V57 content was analyzed by immunoblotting with VT/510 and VT/75. Islet V57 content did not vary with glycemic conditions. V52 content varied as shown (levels shown are relative to V52 content at 3 mmol/l glucose;  $n=6$ ;  $p > 0.05$  for the difference between the 10 mmol/l and 20 mmol/l glucose datasets). **B**, We noted that islet V52 content decreased over 20 hours after newly-isolated islets were placed in culture. To test the effect of glucose on the decline in V52 levels during this initial 20 hour period, newly isolated islets were cultured for 4 or 20 hours after purification as indicated above each lane or lysed immediately after isolation (0 hours, left-most lane). The culture media contained either 3 or 20 mM glucose, as indicated. After 4 or 20 hours in culture media, the islets were harvested and lysed. VIAAT content in the resulting extracts was analyzed by immunoblotting. A representative experiment is shown. As previously noted, V52 content fell after the newly-purified islets had been in culture for 20 hours. Higher glucose concentrations attenuated this decrease. After 4 hours, V52 content was 56% ( $\pm 7\%$ ) greater in the islets cultured at 20 mmol/l glucose, and, after 20 hours, V52 content was 41 ( $\pm 5\%$ ) greater at the higher glucose level ( $n=5$ ,  $p < 0.05$  for both). In contrast to V52 content, content of V57 and glyceraldehyde 3-phosphate dehydrogenase (G3PDH) did not change significantly in response to removal of islets from the pancreatic to the tissue culture environments or in response to glycemic conditions. Note also that there was also no change in the protein apparent as a background band above the two VIAAT bands.

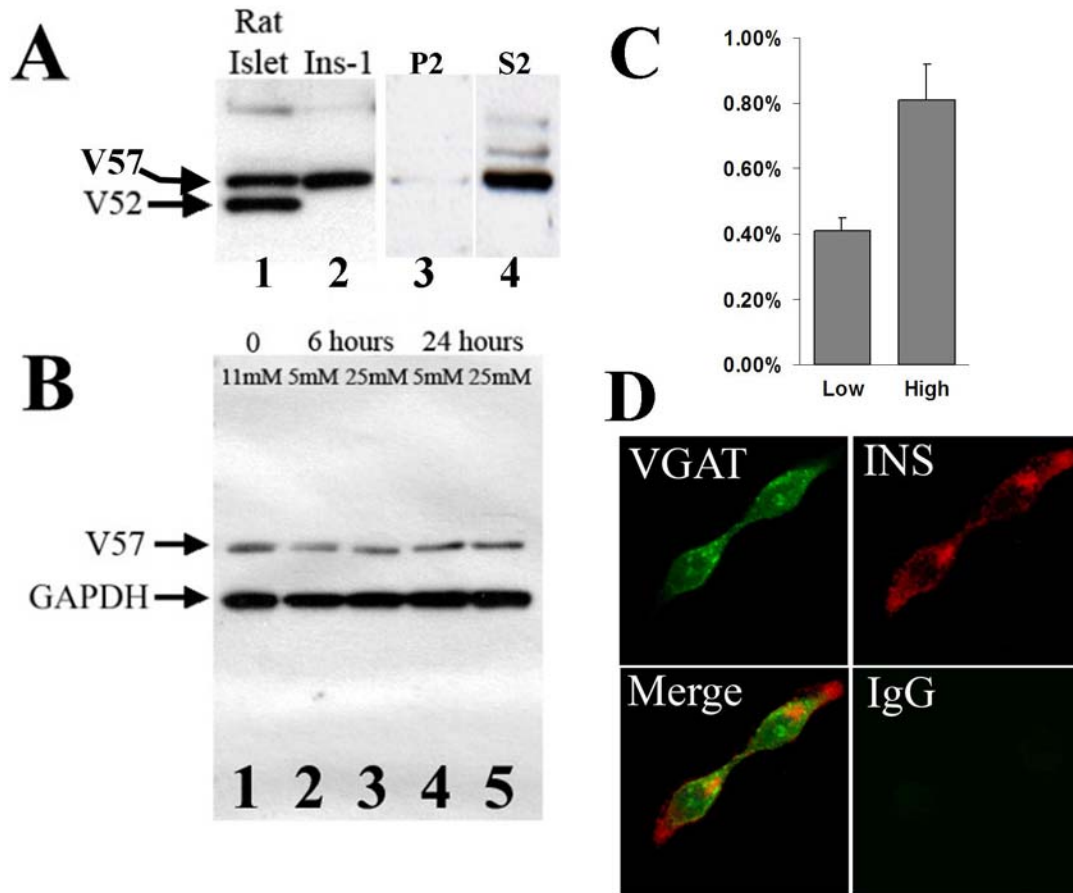


**Figure 2.6. VIAAT Expression in the  $\beta$ -Cell Line INS-1.**

**A**, Immunoblot of extracts prepared from rat islets (lane 1) and INS-1 cells (lane 2) using antibody VT/510. INS-1 cells express VIAAT, but only V57 and not V52. After INS-1 cell fractionation, V57 was detected in S2 (lane 4), consistent with its presence in synaptic-like microvesicles. VIAAT is also detected in P2 (lane 3) which contains the other membranous compartments, such as endosomes and secretory granules, separated from the microvesicles during the high-speed centrifugation. **B**, INS-1 cells were either maintained in 11 mM glucose (lane 1) or switched 6 hours (lanes 2, 3) or 24 hours (lanes 4, 5) before being harvested into medium with 5 mM (lanes 2, 4) or 25 mM (lanes 3, 5) glucose. Equal amounts of extracted proteins were analyzed by SDS-PAGE with antibody VT/510. V57 content did not change in response to changes in glucose concentration. As a control for protein loading, the blot was simultaneously probed with an antibody to glyceraldehyde-3-phosphate dehydrogenase (GAPDH). **C**, In parallel with the experiment shown in panel B, insulin secretion was assessed in INS-1 cells cultured in low glucose (2.5 mM) or high glucose (25 mM) for two hours. Secretion is shown as a percent of total cellular insulin content ( $n=12$ ,  $p<0.001$  for the difference between low and high glucose). **D**, INS-1 cells were immunostained for insulin (INS, red) and VIAAT (with VT/510; VGAT, green). The merged image shows that VIAAT and insulin do not colocalize. Control staining of INS-1 cells (panel labeled IgG) with non-immune IgG revealed no non-specific.

VIAAT is also present in secretory granules (Fig. 2.6A). V57 content in INS-1 cells did not change in response to glycemic conditions (Fig. 2.6B); this was in contrast to insulin secretion, which was tested in parallel (Fig. 2.6C). Immunofluorescent staining revealed that INS-1 cells uniformly expressed both insulin and VIAAT (Fig. 2.6D). Consistent with trafficking of the transporter to microvesicles in INS-1 cells, VIAAT and insulin did not colocalize (Fig. 2.6D). The intranuclear staining seen with VT/510 was likely an artifact of cell fixation such as has been previously described [135-137].

Antibody VT/510 previously yielded relatively weak staining of the rat islet core ( $\beta$ -cell region) compared to the mantle [99]. Because VT/75 displays a different pattern of recognition of the modified forms of V57 and because it has been proven to be an effective antibody for immunohistochemistry in a variety of settings (see, for example, [105-108], we used it to stain rat and human pancreas sections (Fig. 2.7). VT/75 made staining of the rat islet core readily apparent and enabled detection of VIAAT in human islets for the first time (Fig. 2.7A,C). These results were reproducible with M-VT/510, a monoclonal antibody made against the same peptide (for example, see Fig. 2.7D).

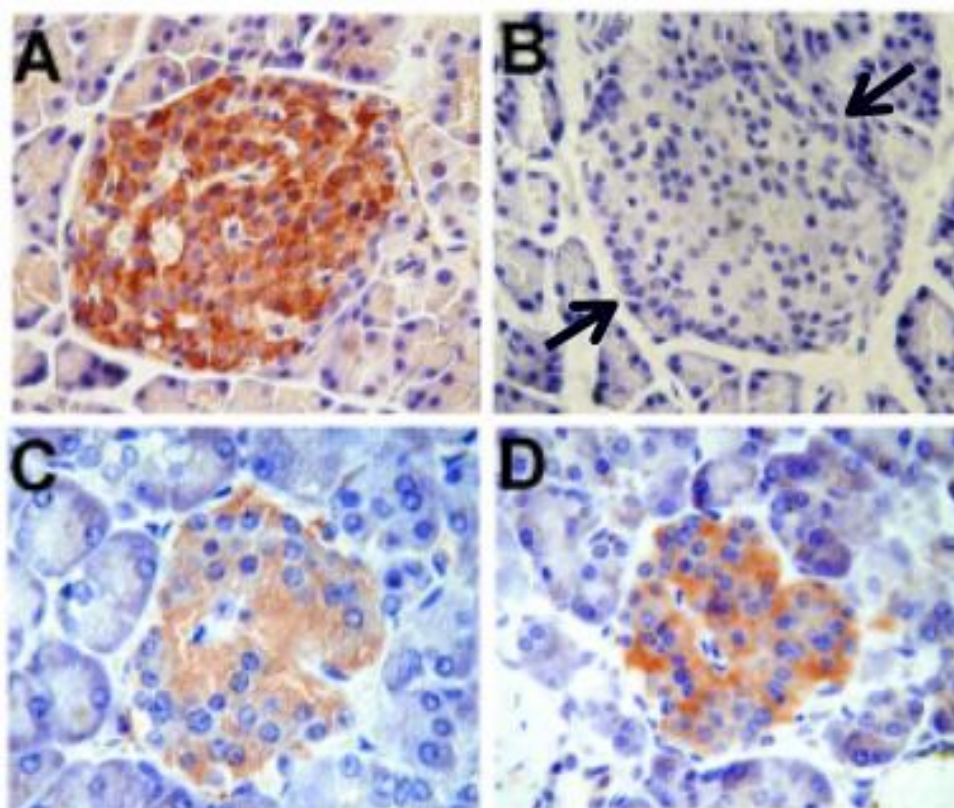


**Figure 2.7. Immunostaining of Rat and Human Pancreas Section with VIAAT Antibodies.**

**A, C,** VIAAT was detected in rat (**A**) and human (**C**) islets using antibody VT/75. In contrast to VT/510, which previously yielded weak staining of the islet core ( $\beta$  cell region), detection of VIAAT with VT/75 was readily apparent. These results were reproducible using a monoclonal antibody (M-VT/75) targeted to the same VIAAT peptide. **D,** for example, shows human tissue stained using M-VT/75. **B,** Non-immune rabbit IgG was used in the same concentration as VT/75 as a control for non-specific staining. A representative rat islet (between arrows) stained with control IgG is shown.

## F. Discussion

Islet cells likely evolved from an ancestral neuronal precursor and have inherited a diverse set of proteins that, in the central nervous system, provide the machinery for cell-to-cell signaling across synapses [6, 138, 139]. These proteins include GAD65, GAD67, GABA receptors, glutamate and glycine receptors and vesicular glutamate and GABA transporters [2, 96, 99, 100]. It is highly likely that, in the islet, these proteins are similarly constituents of intercellular signaling mechanisms. Continued characterization of the islet neurotransmitter signaling apparatus will be important for eventually understanding islet paracrine and autocrine signaling and the means by which islet function is coordinated at the cellular level.

Here, we have followed up on our prior work demonstrating that rat islets contain VIAAT, including a heretofore unidentified 52.5 kDa variant: V52. We have now identified V52 as an isoform of VIAAT that likely results from translation initiation at an alternate, downstream start site. V52 is subject to a different pattern of post-translational modifications than V57. Cellular V52 content is regulated independently of V57 content and is responsive to changes in glucose concentration. V52 content is affected as well by other, extracellular conditions, since basal levels changed during islet culture regardless of glycemic conditions. V57, we found, is subjected to a complex pattern of post-translational modifications. These modifications result in formation of a doublet, V57 and V57', seen on western blots, with V57' being most evident in brain extracts [101]. The true heterogeneity of post-translationally modified V57, however, is only apparent after two-dimensional electrophoresis which, we have shown, reveals approximately 5-8 differentially modified species.

It is clear that, in the rabbit reticulocyte lysate system, V52 is synthesized as a result of utilization of an alternate initiator codon. This mechanism for formation of multiple protein products from the same gene, while not common, has been observed with a variety of other eukaryotic genes (e.g., see refs.: [140-143]. Rat islet V52 and *in-vitro*-synthesized V52 comigrate by SDS-PAGE and by two-dimensional NEPHGE/SDS-PAGE, suggesting that they are identical and that they are thus formed by the same mechanism of downstream translational initiation. It is also possible that V52 is formed in islets by proteolytic cleavage during post-translational processing. In this case, the identical (or nearly identical) localization of an alternate initiation codon and a proteolytic cleavage site would have to be attributed to an unlikely coincidence. No evidence of a proteolytic activity that converts V57 to V52 was detected in rat islet extracts. Since antibody VT/17 binds only V57 while VT/75 binds both V52 and V57, the site of the amino-terminal truncation that results in V52 must lie between the binding sites of the two antibodies. These reside between VIAAT residues 17-30 for VT/17 and between residues 75-87 for VT/75.

In the central nervous system, VIAAT traffics to synaptic vesicles and may associate with GAD65 [58]. In islet  $\alpha$  cells, GAD65 is absent, and the trafficking pattern of VIAAT is different, as the protein ends up associated predominantly with secretory granules [100]. It is possible that—as a result of truncation of VIAAT's cytoplasmic amino-terminal domain—V52 is better adapted to the different pathway of intracellular sorting and protein complex formation that is perhaps followed by VIAAT in the islet  $\alpha$  cells. Here we show that in rat islet extracts, up to eight species of modified V57 but only one of V52 are detected by two-dimensional NEPHGE/SDS-PAGE. Further work is

needed to more fully characterize the sorting and posttranslational modification pathways of the two isoforms.

Ebihara et al. [144] have reported that mouse neurons synthesize a VIAAT splice variant with a unique carboxyl-terminal sequence. This splice variation, like the truncation that produces V52, affects the cytoplasmic region of the protein [109, 144]. While the mouse VIAAT coding region spans 3 exons, the exon structure of the rat VIAAT gene is identical to the human exon structure: the amino-terminal 130 residues are encoded by one exon and the remaining 395 residues by a second [99, 144]. In the absence of an exon-intron structure amenable to minor splice variations, as in the mouse, utilization of alternate initiator codons provides a different means for modification of the cytoplasmic region of VIAAT in rat and human cells. Others have presented evidence that protein expression can be regulated in this manner and have proposed mechanisms [140-143].

Immunohistochemistry with antibody VT/510 suggested that rat islet  $\beta$  cells contain VIAAT (Chessler *et al.*, 2002). Results published subsequently have been conflicting [2, 100]. The immunostaining results shown herein provide further evidence of  $\beta$  cell expression of VIAAT. We also found that INS-1 cells contain V57 but not V52. This result is consistent with the presence of VIAAT in the islet  $\beta$  cells and suggests that V52 may be limited to the  $\alpha$  cells. The mechanism whereby V52 expression is suppressed in INS-1 cells remains to be determined. Regulation may occur at the level of translation, as has been described with other proteins formed from alternative start sites or, alternatively, there may be increased turnover of V52 in INS-1 cells [141-143].

The islet GAD-GABA system is subject to metabolic regulation. Levels of GAD65 and GAD67 expression and of GABA release vary in response to glycemic conditions [130-132]. This suggests that GABA signaling may play a role in coordinating islet function to maintain euglycemia. Glycine likely plays a similar role [2]. Unlike neurons or islet  $\beta$  cells, rat  $\alpha$  cells contain only GAD67: GAD65 is absent. This unique feature of the islet GAD-GABA system has important implications, as it limits the means by which GABA signaling can be regulated. Unlike GAD65, which is highly regulated, both by association/dissociation with an essential cofactor and by phosphorylation, GAD67 activity is not actively regulated, and the enzyme is, in essence, constitutively active [39, 145]. We therefore hypothesized that regulation of  $\alpha$ -cell VIAAT content could provide an important means by which to regulate GABA release. Regulation of VIAAT levels would similarly be expected to modulate islet cell glycine release. Since GABA levels are markedly lower in rat  $\alpha$  cells than in  $\beta$  cells, regulation of glycinergic signaling may be particularly relevant to  $\alpha$  cell function [2].

Our results show that cellular V52 content increases with glucose concentration. Interestingly, the  $\alpha$ -cell content of vesicular glutamate transporter (VGLUT) is affected by glycemic conditions in the opposite direction [146]. Glutamate is an excitatory neurotransmitter and, like VIAAT,  $\alpha$ -cell VGLUT is secretory granule-associated [147]. It is possible, therefore, that as glucose concentrations rise,  $\alpha$  cells secrete relatively more GABA and glycine and less glutamate. Besides glycemic conditions, other metabolic or intercellular signals play an important role in determining  $\alpha$ -cell V52, but not V57, content, as levels of the smaller isoform dropped after islets were removed from their



native environment and placed in tissue culture. Regulation of cellular VIAAT content is not unique to islet cells, as neuronal VIAAT content responds markedly to agonists and antagonists of presynaptic GABA<sub>B</sub> receptors, ethanol and antipsychotic medications [127-129]

In summary, we have identified a novel isoform of VIAAT: V52, a variant of the transporter truncated within the cytoplasmic, amino-terminal domain. V52 is abundant in rat islets and is also synthesized in neurons and in cells transfected with VIAAT cDNA constructs. In reticulocyte lysates, VIAAT cDNA directs the synthesis of both V52 and V57 as a result of utilization of alternate start sites of translation, and islet V52 is likely formed by the same mechanism. Post-translationally, V52 traverses a different pathway of processing and, perhaps, sorting than V57. Islet-derived V57, unlike V52, displays a complex pattern of posttranslational modifications. By immunostaining pancreas sections, we confirmed prior reports that VIAAT is present in islet  $\beta$  cells and were able to detect the protein in both rat and human islets. We also found that the  $\beta$  cell line INS-1 expresses VIAAT, but only in the form of V57. Islet content of V52, but not of V57, increases in response to higher glucose concentrations. This is consistent with prior results indicating that the islet GAD-GABA system is responsive to metabolic stimuli. This sensitivity to metabolic stimuli, in turn, suggests that GABAergic and probably also glycinergic signaling helps coordinate the endocrine functioning of the islet.

#### G. Acknowledgements

Chapter 2 is a reprint of the material as it appears in Suckow, A. T., Sweet, I. R., Van Yserloo, B., Rutledge, E. A., Hall, T. R., Waldrop, M. and Chessler, S. D. (2006).

*Journal of Molecular Endocrinology*. The dissertation author was the primary investigator in the development and execution of the study, and the principal author of this paper.

# CHAPTER 3: THE INHIBITORY PHENOTYPE OF THE ISLET $\beta$ -CELL: AN AP-3 DEPENDENT MECHANISM DRIVES SYNAPTIC-LIKE MICROVESICLE FORMATION IN PANCREATIC ISLET $\beta$ CELLS

## A. Abstract

Pancreatic islet  $\beta$ -cells contain synaptic-like microvesicles (SLMVs). The origin, trafficking and role of these  $\beta$ -cell SLMVs are poorly understood. Synaptic vesicle (SV) biogenesis is mediated by cytosolic protein complexes called adaptors. Two different adaptor complexes drive SV formation: a ubiquitous AP-2 complex and the neuron-specific AP-3B complex. AP-3B modulates the composition of both glutamatergic and GABAergic SVs. Since  $\beta$ -cell maturation and exocytic function seem to parallel that of the inhibitory synapse and mice lacking neuronal AP-3B subunits have evident defects in GABAergic neurotransmission, we predicted that AP-3B-associated vesicles would be present in  $\beta$ -cells. Here, we test the hypotheses that the AP-3B subunits  $\beta$ 3B (Beta-NAP) and  $\mu$ 3B are expressed in islets and that SLMV biogenesis in  $\beta$ -cells is mediated by AP-3B. Another aim was to test whether the sedimentation properties of INS-1  $\beta$ -cell microvesicles are identical to those of bona fide SLMVs isolated from PC12 cells. Our results show that the two neuron-specific AP-3 subunits are expressed in  $\beta$ -cells, the first time these proteins have been found to be expressed outside the nervous system. Sucrose- and glycerol-gradient sedimentation indicates that  $\beta$ -cell SLMVs share the same sedimentation properties as PC12 SLMVs and contain SV marker proteins that sort specifically to AP-3B-associated vesicles in the brain. Brefeldin A, a drug that interferes

with AP-3-mediated SV biogenesis from endosomes, inhibited the delivery of AP-3 cargoes to  $\beta$ -cell SLMV. Our findings suggest that  $\beta$ -cells and neurons share molecules and mechanisms important for mediating the neuron-specific membrane trafficking pathways that underlie synaptic vesicle formation.

## B. Introduction

The pancreatic islet  $\beta$ -cells, by virtue of the architecture of their secretory apparatus and their pathway of differentiation, have much in common with neurons [6, 19, 148-150]. In neurons, specialized vesicles, the synaptic vesicles (SVs), store neurotransmitters in the presynaptic compartment.  $\beta$  cells contain synaptic-like microvesicles (SLMVs), small vesicles which are distinct from the insulin granules and that resemble SVs [28, 148].

The biogenesis and trafficking of the SLMVs in  $\beta$  cells is poorly understood. Since  $\beta$ -cell SLMVs carry the inhibitory neurotransmitter GABA, one benefit of their better characterization will be an increased knowledge of the  $\beta$ -cell GABAergic signaling machinery [1, 28, 35]. In autoimmune diseases of the nervous system, nerve terminal proteins are especially susceptible to autoimmune attack, and, in type 1 diabetes, shared  $\beta$ -cell-nerve terminal proteins are major, early targets of autoimmunity [36-39]. Since an important characteristic of both nerve-terminal and  $\beta$ -cell autoantigens is their tendency to be vesicle-associated proteins, increased knowledge of the  $\beta$ -cell SLMVs may provide new insights into the pathogenesis of islet autoimmunity [38, 51-54].

Outside the central nervous system (CNS), the pancreatic  $\beta$  cells are the only tissue with significant expression of the enzyme GAD65, which catalyzes the synthesis of

GABA [22]. GAD65 binds to the surface of SVs/SLMVs and is both a neural and  $\beta$ -cell autoantigen [39]. We previously determined that  $\beta$  cells also express the SV-associated vesicular GABA transporter VGAT (also referred to as VIAAT: vesicular inhibitory amino acid transporter) [5, 99]. Overall,  $\beta$  cells express all of the machinery necessary for GABA synthesis, secretion and signaling [1, 5, 22]. More recently, we found that  $\beta$  cells express cell-surface, synaptic cleft proteins critical for the maturation and continuing function of the inhibitory pre- and post-synaptic terminals [149]. If, as we believe, the  $\beta$ -cell secretory machinery develops and functions in a manner parallel to that of the inhibitory synapse, a pathway of SV biogenesis that regulates the composition of GABAergic nerve terminals in the central nervous system would be predicted to be operative in the  $\beta$ -cells as well.

Adaptor protein complexes are involved in the biogenesis and cargo selection of a variety of transport vesicles in the secretory and endocytic pathways [55]. Four adaptor complexes have been described (AP-1, AP-2, AP-3 and AP-4). Each is comprised of 4 subunits (called adaptins): a large  $\alpha$ ,  $\gamma$ ,  $\delta$  or  $\epsilon$ , a large  $\beta$ , a medium  $\mu$ , and a small  $\sigma$  subunit [55]. SV biogenesis is primarily driven by AP-2 complexes via clathrin-mediated endocytosis from the plasma membrane; however, SV formation also occurs at endosomes by means of an AP-3-mediated mechanism [56, 57]. Several subunits of the AP-3 complex are encoded by alternative genes. The  $\beta$ 3A,  $\mu$ 3A and  $\sigma$ 3 subunits are expressed ubiquitously and play a role in the biogenesis of lysosomes and other specialized secretory organelles. The  $\beta$ 3B subunit (also referred to as Beta-NAP or AP-3B2) and  $\mu$ 3B (AP-3M2), which are unique to the AP-3B adaptor protein complex, are

expressed exclusively in neural tissue and are important for the formation and function of a distinct subset of synaptic vesicles including GABAergic SVs [57, 59, 151].

Mice lacking  $\beta$ 3B and  $\mu$ 3B have phenotypes consistent with defective SV assembly, and impaired formation of GABAergic SVs may underlie the reduced levels of VGAT observed in the hippocampus of  $\mu$ 3B knockout mice [59, 60]. Because of the similarities between  $\beta$ -cells and neurons, most notably  $\beta$ -cell expression of VGAT and other synaptic proteins, we hypothesized that  $\beta$ -cells would express the neuronal AP-3B subunits and that AP-3B would participate in the biogenesis of SLMVs within  $\beta$ -cells.

Here, we demonstrate  $\beta$ -cell-specific expression of the neuronal AP-3 subunits. We show that INS-1  $\beta$ -cell SLMVs have identical sedimentation properties as PC12 SLMVs and that SLMV formation in INS-1  $\beta$ -cells is sensitive to brefeldin A, much like the formation of SLMVs by AP-3-dependent mechanisms in PC12 cells.  $\beta$ -cell SLMVs may be generated primarily from endosomes via the AP-3B mediated pathway. Further analysis of this pathway may yield new insights into the trafficking and role of GAD65 and GABA in the pancreatic islets and into the mechanisms that render  $\beta$ -cells susceptible to autoimmune targeting.

### C. Materials and Methods

#### *Antibodies*

The SV2 monoclonal antibody developed by K. M. Buckley was obtained from the Developmental Studies Hybridoma Bank (University of Iowa, Iowa City, IA) [152]. Synaptophysin (SY38) and vacuolar ATPase antibodies were purchased from Chemicon

(Temecula, CA) and Synaptic Systems (Göttingen, Germany), respectively.

Carboxypeptidase E, tubulin and  $\beta 3\beta$  antibodies (for western blotting) were purchased from BD Pharmingen (San Diego, CA). One of us (V.F.) has previously confirmed the specificity of the monoclonal  $\beta 3B$  antibody in immunoblot experiments using brain tissue lysates from  $\beta 3B$  knockout mice and control mice [60]. We also found that the monoclonal yields a band corresponding to  $\beta 3B$  in western blots with extracts from human brain but not human liver. A previously-characterized rabbit polyclonal anti- $\beta 3B$  antibody (used for immunostaining) was generously donated by Robert Darnell of The Rockefeller University [53]. In preliminary experiments, this polyclonal antibody also yielded a band at the expected molecular weight in western blots with protein extracts from brain and not with extracts from liver. Phosphatidylinositol 4-kinase type II alpha ( $PI4KII\alpha$ ) antibodies were described previously [153]. Rabbit antibodies against  $\mu 3B$  were made by injection of the peptides TVTSQMPKGVLN and YFGVCSEPVIKD after conjugation to Keyhole Limpet Hemocyanin (KLH). Antiserum was validated for affinity and specificity for  $\mu 3B$  by ELISA, immunoprecipitation of recombinant  $\mu 3B$  and western blotting. Recombinant  $\mu 3B$  was made by cloning the full-length mouse cDNA (IMAGE Consortium/Open Biosystems, Huntsville, AL) into the plasmid vector pTNT (Promega Madison, WI) and then performing in vitro transcription and translation in a reticulocyte lysate-based system (TnT SP6 Quick Coupled Transcription/Translation System, Promega) exactly as per the manufacturer's instructions.

### *RT-PCR*

Total RNA from human islets was prepared as previously described [149]. Gene-specific primers were designed over exon-exon boundaries to the neuronal AP-3 subunits  $\beta$ 3B (5'—AGCCAAGCTCTACCTGACCA—3' and 5'--TCCAAGACTGGAGCTGGTTT—3') and  $\mu$ 3B (5'—TGTCAGCTTCCATCCTTGTG—3' and 5'—TCCCACCGTTATTTCAAAGC—3') and PCR was performed using human islet and brain cDNA (OriGene Technologies, Rockville, MD). Amplification was performed with HotStarTaq enzyme. cDNA was denatured at 92°C, annealed at 60 °C and extended at 72 °C for 35 cycles. PCR products were analyzed by agarose gel electrophoresis and ethidium bromide staining. Controls with no template (no reverse transcriptase added to the reverse transcription reaction) were used to ensure that there was no genomic DNA contamination.

### *Cell Culture*

INS-1 cells (provided by the cell culture facility of the University of Washington Diabetes and Endocrinology Research Center, Seattle, WA) were cultured in RPMI 1640 medium supplemented with 10% fetal bovine serum, 50  $\mu$ M  $\beta$ -mercaptoethanol, 1 mM sodium pyruvate, 2 mM L-glutamine, 100 U/mL penicillin and 100 mg/mL streptomycin (Invitrogen, San Diego, CA) in a humidified 37° C chamber with 5% CO<sub>2</sub>. PC-12 cells were grown in DME H21 media supplemented with 10% horse serum, 5% fetal bovine serum, 100 U/mL penicillin and 100 mg/mL streptomycin in a humidified 37°C chamber with 10% CO<sub>2</sub>. Brefeldin A (Epicentre Biotechnologies, Madison, WI), when used, was



added to the tissue culture medium for 2 h at 10  $\mu$ g/ml (final concentration; stock solution: 5 mg/ml in methanol).

### *Subcellular Fractionation*

PC-12 and INS-1 cells were fractionated according to Clift-O'Grady *et al.* (1998). Briefly, cells were removed from culture dishes by rinsing with calcium- and magnesium-free phosphate buffered saline (PBS). They were pelleted at 800 x g for 5 minutes, resuspended in budding buffer (38 mM potassium glutamate, 38 mM potassium gluconate, 20 mM 4-morpholinepropanesulfonic acid pH 7.2, 5 mM reduced glutathione, 5 mM sodium carbonate, and 2.5 mM magnesium sulfate) and pelleted again at 800 x g for 5 minutes. Cells were resuspended in budding buffer with protease inhibitors (Roche Molecular Biochemicals; Indianapolis, IN) and homogenized using a Balch-designed cell cracker (European Molecular Biology Laboratory) pre-rinsed with budding buffer. INS-1 cells were passed 24 times through the cell cracker and PC-12 cells 16 times. Trypan blue exclusion was used to ensure efficient homogenization.

The resulting homogenate was sedimented in an SS34 rotor at 1000 x g for 5 minutes to obtain S1 supernatant. For sucrose sedimentation, S1 supernatants were loaded onto a 10-45% continuous sucrose gradient. Sucrose gradients were centrifuged for 2.5 h at 183,440 x  $g_{av}$ . For glycerol sedimentation, S1 supernatants were sedimented at 27,000 x g for 35 minutes to generate S2 supernatant. S2 supernatant was loaded onto a 5-25% glycerol gradient and spun in an SW55 rotor at 218,000 x g for 75 minutes. For both types of gradients, 400  $\mu$ L fractions were collected from the bottom and stored at -80° C.

### *Western Blot Analysis*

Human brain and human and rat liver protein extracts were obtained commercially (Biochain, Hayward, CA and ProSci, Poway, CA). INS-1 and human islet extracts (ICR Basic Science Islet Distribution Program, City of Hope, Duarte, CA) were prepared by homogenization in RIPA buffer (PBS, 1% NP-40, 0.5% sodium deoxycholate, 0.1% SDS, 45 µg/ml aprotinin, 100 µg/ml phenylmethylsulphonyl fluoride and 1mM sodium orthovanadate). Cell extracts were quantified using the Bio-Rad D<sub>c</sub> Protein Assay (Bio-Rad, Hercules, CA). Fractions and lysates diluted 1:4 with reducing sample buffer were electrophoresed on either 10% SDS-PAGE gels, 4-12% Bis-Tris NuPage gels or 3-8% Tris-Acetate NuPage gels according to the molecular weight of the protein of interest (Invitrogen). The protein was transferred to a PVDF membrane (Millipore, Billerica, MA) and blocked for 1 hour in 5% non-fat dry milk and TBS-Tween (20 mM Tris-HCl, 137 mM NaCl, 0.1% Tween-20, pH 7.4). The membrane was incubated in primary antibody at 4° C overnight and washed 3 times in TBS-tween for 10 minutes. It was then incubated with HRP-conjugated anti-mouse IgG or anti-rabbit IgG (Jackson Laboratories, Bar Harbor, ME) for one hour and washed 3 times in TBS-tween for 10 minutes. The membrane was immersed in ECL (Amersham Biosciences, Piscataway, NJ) for 5 minutes and exposed to x-ray film (Kodak, Rochester, NY).

### *Immunofluorescence*

Flash-frozen rat pancreas (Rockland Immunochemicals, Gilbertsville, PA) was fixed for 24 hours in Pen-Fix (Richard Allan Scientific, Kalamazoo, MI), embedded in paraffin, and sections were cut at 6 µm by the Moores Cancer Center histology core at the

University of California, San Diego. Tissue sections were deparaffinized in D-limonene (Fisher Scientific, Fairlawn, NJ), rehydrated through a graded ethanol series and antigen retrieval was performed on sections for 10 minutes in boiling 1x citrate buffer (10 mM sodium citrate, 0.05% Tween 20, pH 6.0). Sections were blocked in a 3% bovine serum albumin/1% goat or donkey serum/phosphate buffered saline solution for 1 hour and then incubated with primary antibody in the same solution for 1 hour. They were washed twice in PBS for 10 minutes each and then incubated with AlexaFlour conjugated anti-mouse and anti-rabbit IgG conjugates (Invitrogen). Sections were washed twice in PBS and mounted with coverslips. Images were captured using an Olympus FV1000 spectral confocal microscope configured with an Argon/Krypton laser (488- and 568-nm excitation lines) and either 40x or 60x oil immersion lenses. Controls included tissue stained either exclusively with secondary antibody or treated with preimmune serum followed by secondary antibody.

### *Immunohistochemistry*

Paraffin-embedded rat pancreas sections were treated as described above through the first wash step. Sections were then incubated with biotinylated anti-mouse or anti-rabbit IgG in blocking buffer for 1 hour and washed twice with PBS. They were then incubated for 30 minutes in a 1:200 dilution of alkaline phosphatase streptavidin (Vector Laboratories, Burlingame, CA, USA). Vector Red (Vector Laboratories) was used to visualize the binding of the primary antibodies. Sections were counterstained with hematoxylin (Fisher Scientific) using standard methods. Images were captured on a Nikon Optiphot microscope with a Nikon Coolpix 5400 using a 20x lens. Controls

included tissue treated with preimmune serum followed by secondary antibody or stained exclusively with secondary antibody.

## D. Results

### 1. *Neuronal AP-3 Subunits are Expressed in Human Islets*

An expressed sequence tag (EST) search suggested the expression of the neuronal AP-3 subunits,  $\beta 3B$  and  $\mu 3B$ , in human and mouse islets (data not shown). To confirm expression of these genes, primers for  $\beta 3B$  and  $\mu 3B$  were designed over exon-exon boundaries and PCR analysis was performed using human brain and islet cDNA. Amplicons of the expected size were detected in human islets and, as expected, in human brain (Fig. 3.1A).

To confirm  $\beta 3B$  protein expression in islets, western blot analysis was performed using a  $\beta 3B$ -specific monoclonal antibody. As expected,  $\beta 3B$  was detected in lysates from human, rat and mouse brain (Fig. 3.1B).  $\beta 3B$  protein was also detected in cell lysates from the insulin-secreting  $\beta$ -cell lines  $\beta$ -TC3, HIT-T15 and INS-1 and in tissue lysates from isolated human and rat islets (Fig. 3.1B) [154, 155]. Lysates from the dedifferentiated, glucagon- and insulin-producing mouse islet cell line  $\alpha$ TC6 also contained  $\beta 3B$  protein (not shown). The monoclonal antibody is specific for the neuronal protein: it does not yield a band with extracts from  $\beta 3B$  knockout mouse brain [60] or from human liver (not shown).

As with  $\beta 3B$  protein, INS-1 and  $\alpha$ TC6 cell lysates also contained  $\mu 3B$  protein (Fig. 3.1C). As expected,  $\mu 3B$  was not detected in liver extract (Fig. 3.1C) or, as will be

discussed later, in immunostained pancreatic exocrine tissue. The observed  $\mu$ 3B band precisely comigrated with  $\mu$ 3B synthesized de novo by in vitro translation, providing further confirmation of the specificity of the  $\mu$ 3B antibody (Fig. 3.1C).

## 2. *B-Cell-Specific Expression of Neuronal AP-3B Subunits in Rat Islets*

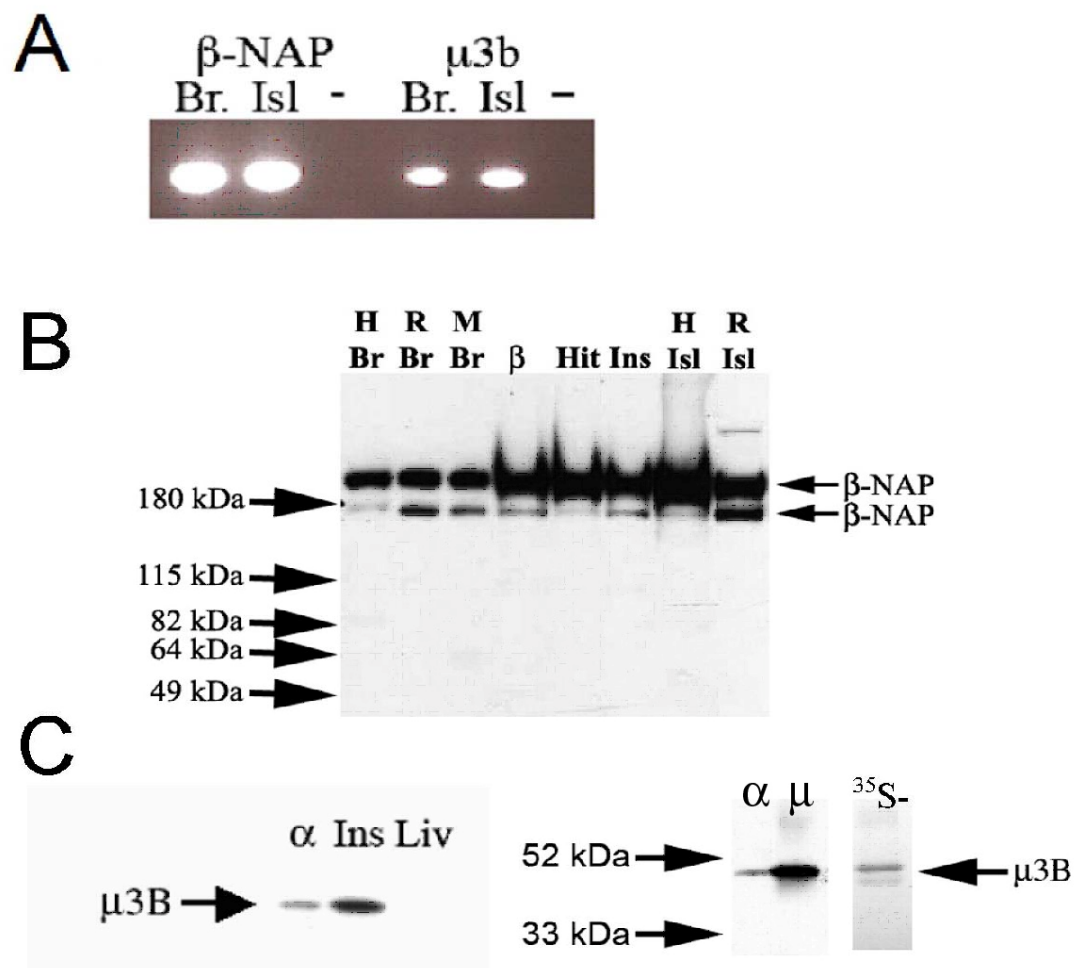
To determine the localization of the  $\beta$ 3B and  $\mu$ 3B proteins in islets, immunolocalization studies were performed on rat pancreas sections using antibodies to  $\beta$ 3B and  $\mu$ 3B.  $\beta$ 3B was detected exclusively in cells expressing insulin (i.e.,  $\beta$ -cells) but not in those expressing glucagon ( $\alpha$ -cells) (Fig. 3.2).  $\beta$ 3B was absent from the surrounding pancreatic exocrine tissue. Islet-specific expression of  $\beta$ 3B was also observed in mouse and human pancreas sections (not shown). A similar pattern of expression was observed for  $\mu$ 3B. Analysis of serial sections of rat pancreas revealed  $\mu$ 3B protein expression in  $\beta$ -cells but not in  $\alpha$ -cells (Fig. 3.3). As expected, there was no immunostaining of the exocrine pancreas. The latter result provides further confirmation that the  $\mu$ 3B polyclonal antibody does not cross-react with the ubiquitously-expressed  $\mu$ 3A isoform.

## 3. *Resemblance of INS-1 $\beta$ -cell SLMVs to PC-12 cell SLMVs*

The expression of AP-3B in  $\beta$ -cells, along with its role in the biogenesis of SV in neurons, led us to next ask whether AP-3B is important for the formation of SLMV in  $\beta$ -cells. A well-characterized  $\beta$ -cell line, INS-1, was chosen to test for AP-3B function

**Figure 3.1. Expression of Neuronal AP-3 mRNA and Protein in INS-1  $\beta$ -cells and Pancreatic Islet Extracts.**

(A) PCR analysis was performed to determine whether the neuronal AP-3 subunits  $\beta$ 3B ( $\beta$ -NAP) and  $\mu$ 3B are expressed in human islets (Isl). Human brain (Br) cDNA was used as a positive control. PCR products of the expected size were detected in brain and islets for both  $\beta$ 3B and  $\mu$ 3B. A negative control (-) in which no reverse transcriptase was added during the reverse transcription reaction (no RT Control) is shown to the right the brain and islet lanes. cDNA from human tissues (shown) and from rat tissues (not shown) yielded identical results. (B) To determine whether  $\beta$ 3B ( $\beta$ -NAP) protein is expressed in islets, western blot analysis was performed using a  $\beta$ 3B-specific monoclonal antibody. As expected,  $\beta$ 3B was detected in human (H), rat (R) and mouse (M) brain (Br).  $\beta$ 3B protein was also present in cell lysates from the insulin-secreting  $\beta$ -cell lines  $\beta$ TC3 ( $\beta$ ), HIT-T15 (Hit) and INS-1 (Ins), and in tissue lysates from human and rat islets (Isl).  $\beta$ 3B was also present in the dedifferentiated islet cell line  $\alpha$ TC6 and was (as expected) not detected in human liver or in brain from  $\beta$ 3B knockout mice ([60] and not shown). As observed previously, immunoblot detection of  $\beta$ 3B yielded two bands. It is not known why  $\beta$ 3B forms a doublet band. The distance migrated by molecular weight markers is indicated by arrows on the left. The prestained markers allow only approximate estimation of molecular weight and exhibit less accuracy at higher molecular weights. In general, in different experiments the  $\beta$ 3B bands were observed to run between molecular weight markers for  $\sim 115$  kDa and  $\sim 200$  kDa, consistent with the reported molecular weight of  $\sim 140$  kDa. (C) Left panel:  $\mu$ 3B was detected in  $\alpha$ TC6 cell lysate ( $\alpha$ ), INS-1 cell lysate (Ins) but not in rat liver lysate (Liv). Right panel:  $\mu$ 3B ( $\mu$ ) produced by in vitro transcription and translation (second lane) and analyzed by immunoblotting with the  $\mu$ 3B antibody ran at the expected  $M_r$  of  $\sim 47,000$  (location of molecular weight markers is indicated to the left). This band comigrated precisely with the band that was observed in  $\alpha$ TC6 cells ( $\alpha$ , first lane) and INS-1 cells.  $^{35}$ S-met was included in the in vitro translation reaction. Autoradiographic detection of the radiolabeled  $\mu$ 3B (lane on far right) yielded a band that precisely aligned with the band detected by immunoblot analysis. This confirms that the  $\mu$ 3B antibody detected  $\mu$ 3B synthesized de-novo in the in vitro transcription and translation reaction.



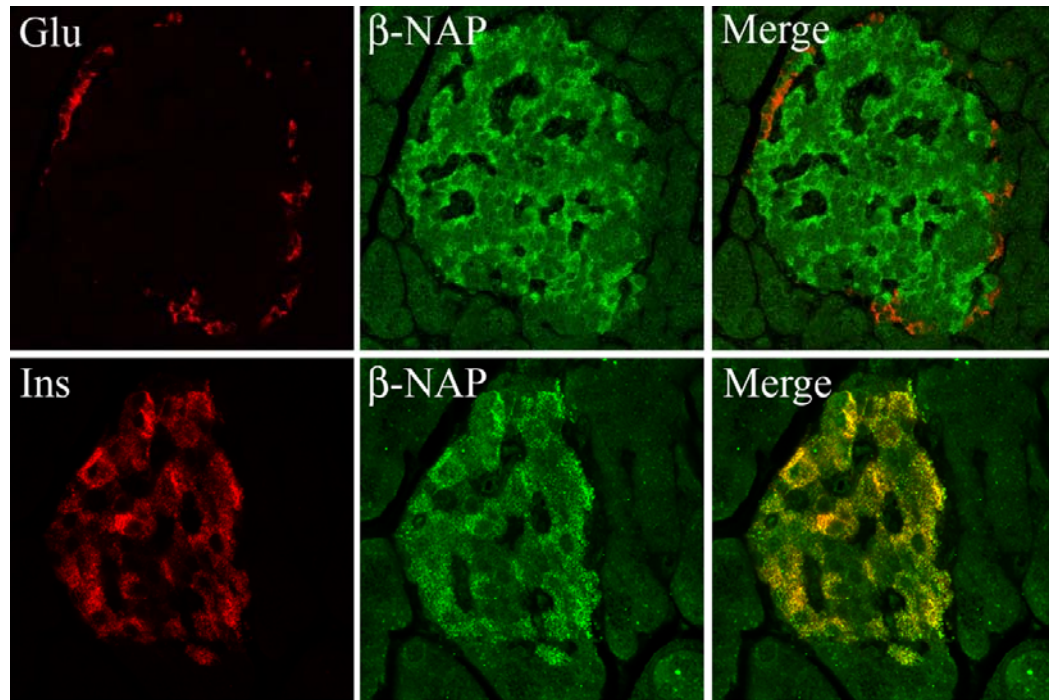


**Figure 3.2.  $\beta$ 3B is detected in the pancreatic islet  $\beta$  cells.**

Immunofluorescent localization was performed to determine the localization of  $\beta$ 3B ( $\beta$ -NAP, green) in rat pancreas sections. Tissues were co-stained for either insulin (INS, bottom row, red) or glucagon (Glu, top row, red).  $\beta$ 3B was detected in cells expressing insulin (colocalization yields orange-yellow in the merged images) but not in cells expressing glucagon. As expected,  $\beta$ 3B was also not present in the surrounding pancreatic exocrine tissue. Islet-specific expression of  $\beta$ 3B was also observed by immunostaining using the same antibody in mouse and human pancreas sections (not shown). (Magnification, 60x).



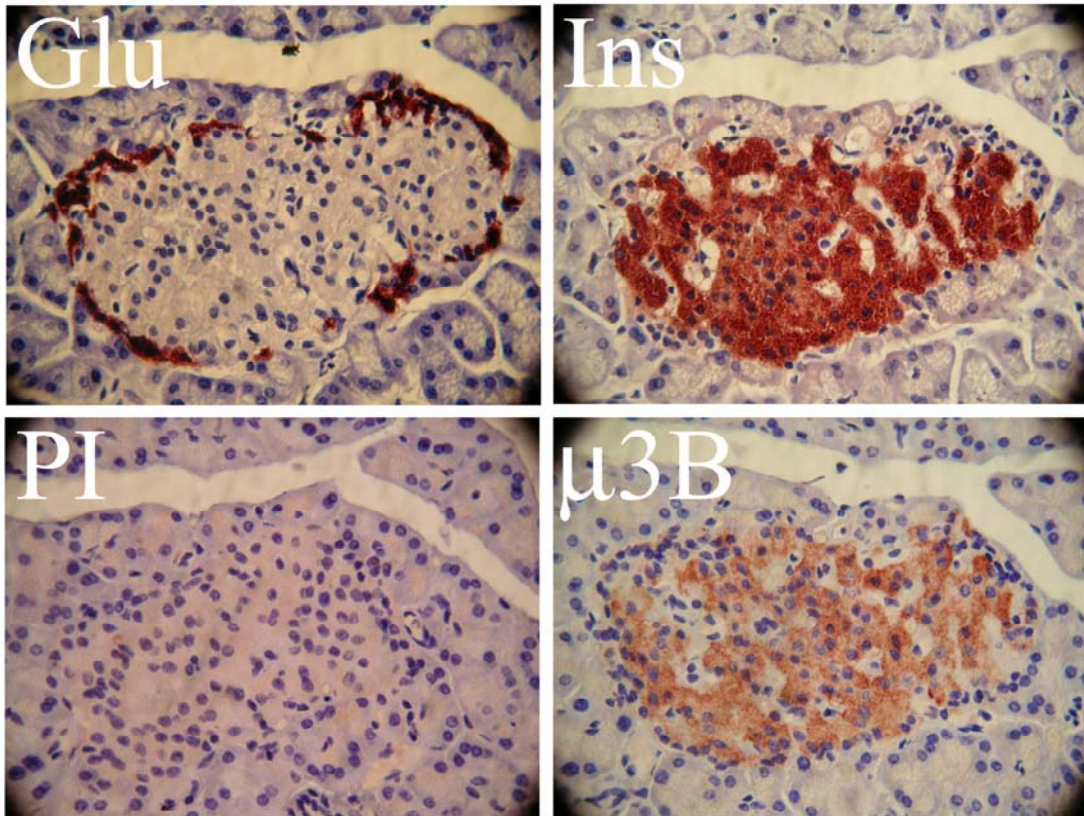


**Figure 3.3.  $\mu 3B$  is detected in pancreatic islet  $\beta$  cells.**

Immunohistochemical localization was performed to determine the localization of  $\mu 3B$  in rat pancreas sections. Serial sections were stained for either insulin (Ins), glucagon (GLU) or, as a control, preimmune serum (PI). Four serial sections containing the same representative islet are shown. As is typical in rodent islets, the glucagon-expressing  $\alpha$ -cells are found in the islet periphery, surrounding the insulin-producing  $\beta$  cells.  $\mu 3B$  was observed in the  $\beta$  cells but not in cells that stained positive for glucagon. As expected,  $\mu 3B$  was also not present in the surrounding pancreatic exocrine tissue. Preimmune serum yielded very little background. (Glu, glucagon; Ins, Insulin; PI, preimmune). (Magnification, 60x).

because the fractionation studies necessary for analyzing SLMV require large numbers of cells [133, 154].

To confirm that INS-1 cells are a suitable model for the study of  $\beta$ -cell SLMV biogenesis, INS-1 cell post nuclear supernatant (S1) was sedimented in a sucrose velocity gradient to resolve both secretory granules and SLMVs. The larger secretory granules and endosomes migrate faster through the gradient than SLMVs [118]. Fractions were collected from the bottom of the gradient and analyzed by immunoblotting with a monoclonal antibody to the synaptic vesicle protein SV2—which, in  $\beta$ -cells, is present in both the microvesicles and secretory granules—or with an antibody to the secretory granule protein carboxypeptidase E (Fig. 3.4) [156, 157].

Two peaks were observed when fractions were stained for SV2: one consistent with the presence of endosomes/secretory granules (centered at fractions 6-7) and one consistent with the presence of SLMVs (centered at fraction 16). The location of the peak resulting from sedimentation of INS-1 SLMVs in the sucrose gradient was identical to the location of the PC-12 cell SLMV peak. This demonstrates that INS-1 SLMVs and PC-12 SLMVs have the same sedimentation properties in sucrose velocity gradients. To confirm that the first peak contained secretory granules, INS-1 fractions were stained for carboxypeptidase E, a marker of secretory granules but not SLMV, and only one peak, which corresponded to the earlier of the two SV2 peaks, was observed (fractions 6-7; Fig. 3.4) [156]. Carboxypeptidase E can be processed from a membrane-bound to a soluble form which is released from broken secretory granules, and the protein was, as expected, also present in the top fractions (fractions 17 and 18) containing the pool of soluble proteins [158].

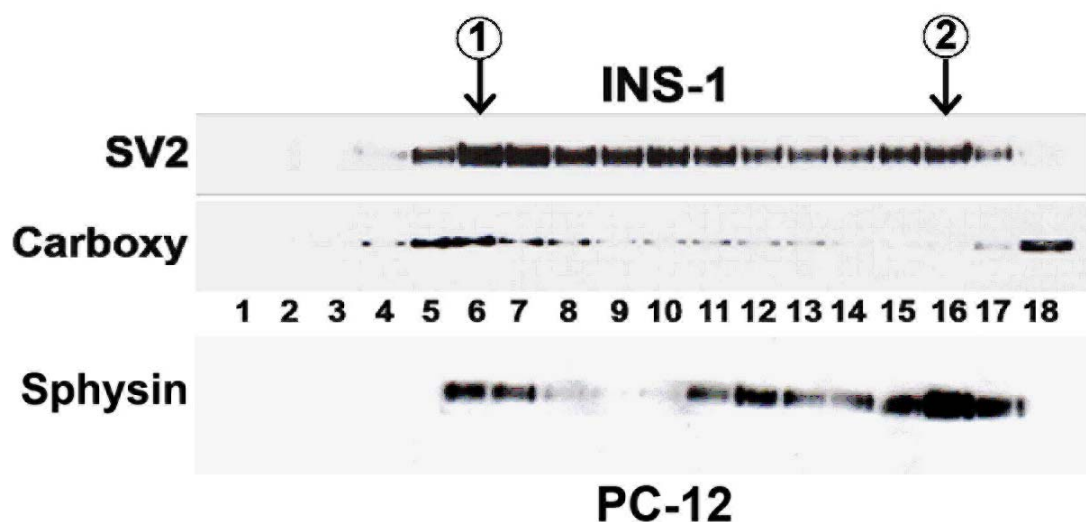


**Figure 3.4. Detection of synaptic-like microvesicles (SLMVs) in INS-1 cell homogenates by sucrose gradient sedimentation.**

Post nuclear supernatant (S1) from INS-1 cells was sedimented in 5-45% sucrose gradients and the resulting fractions analyzed by immunoblotting. When fractions were stained with SV2 antibody, two distinct peaks (labeled “1” and “2”) were observed at fractions 6 and 16. Larger vesicles sediment to the lower-numbered fractions, and peak 1 results from the presence of SV2 in larger endosomes and secretory granules. The presence of secretory granule proteins in peak 1 was confirmed by immunoblotting for a specific marker of the secretory granules: carboxypeptidase E (Carboxy). The presence of a second peak centered at fraction 16 is consistent with the presence of SLMVs in INS-1 cells and with the association of SV2 with the INS-1 cell SLMVs. The absence of carboxypeptidase E from the second peak demonstrates that the population of microvesicles comprising peak 2 was not contaminated with secretory granules. Carboxypeptidase E released from broken secretory granules was, as expected, present in the pool of soluble proteins in fraction 18. An immunoblot from PC-12 cells fractionated in parallel (bottom row) was probed for synaptophysin (sphysin), which localizes primarily to SLMV. Synaptophysin content formed a peak around fraction 16, demonstrating that the pattern of PC-12 SLMV sedimentation in the sucrose gradient matches that of INS-1 SLMV. Lesser amounts of synaptophysin are also present in larger PC-12 cell compartments, including secretory granules, which explains the presence of bands in PC-12 fractions 6 and 7 [159, 160].

#### 4. *INS-1 and PC-12 SLMVs cosediment and share similar synaptic vesicle markers*

A defining feature of SLMV and SV is their distinctive size of ~40 nm [161, 162]. Past studies to determine the size of the  $\beta$  cell SLMVs by electron microscopy have produced conflicting results. This may be due to the difficulty of discriminating sectioned tubules and endosomes from SLMVs in whole cells [134, 163]. A recent study, for example, reported the average size of the  $\beta$ -cell SLMV to be 90 nm with SLMVs ranging up to ~150 nm [25].

Glycerol velocity gradient sedimentation allows discrimination of organelles based on size [118]. In these gradients, brain SVs and P12 SLMVs co-sediment in the middle of the gradient as a symmetric peak. Moreover, the size of these organelles has been confirmed independently by electron microscopy [161, 164, 165]. To corroborate that the SV2 peak observed in Fig. 3.4 corresponded to SLMV, we performed glycerol velocity sedimentation to determine whether INS-1 cell microvesicles co-sediment with PC-12 cell SLMVs [134]. PC-12 cells contain SLMV that are virtually indistinguishable from neuronal SV, and the PC-12 cell line is commonly used for the study of SV/SLMV biogenesis [134].

INS-1 and PC-12 post nuclear supernatants (S1) were spun at 27,000 x g for 35 minutes to generate high speed supernatants (S2) lacking larger membranes such as endosomes and secretory granules. S2 high-speed supernatants from both cell lines were then sedimented in glycerol velocity gradients to resolve SLMV according to size. Fractions were collected from the bottom of the gradients and analyzed by immunoblotting with antibodies to markers of PC-12 cell SLMVs including synaptophysin, SV2 and vacuolar ATPase (Fig. 3.5). PC-12 fractions were analyzed by

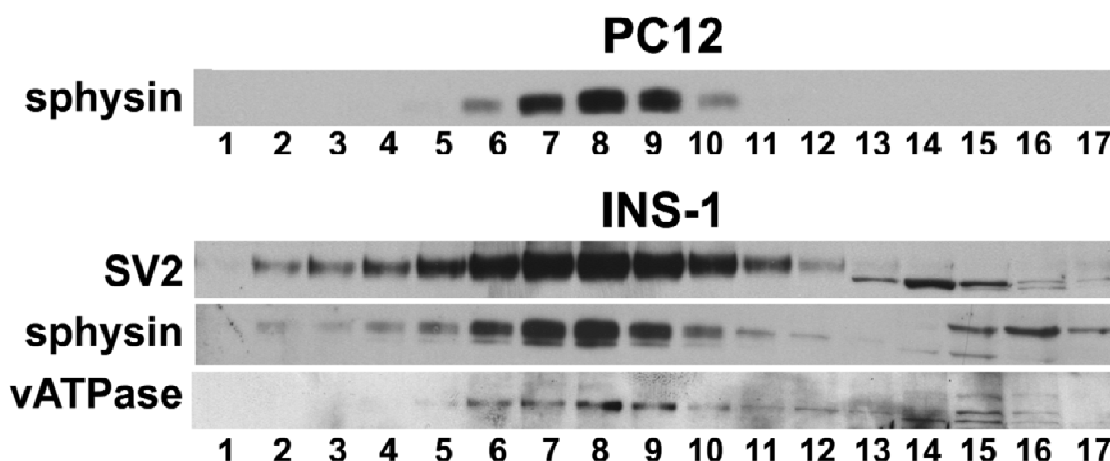


**Figure 3.5.  $\beta$ -cell microvesicles are identical in size to PC-12 SLMVs and have matching cargo protein content.**

PC-12 cells produce SLMVs with biophysical properties indistinguishable from those of neuronal SVs. High speed supernatants (S2) obtained from PC-12 and INS-1 cells were fractionated by glycerol gradient centrifugation, a technique especially well suited for resolving the ~40 nm SVs and SLMVs. Fractions containing SLMVs were identified using antibodies to previously-characterized PC-12 SLMV proteins. Maximal immunoreactivity to the SV marker synaptophysin (sphysin) was observed in fraction 8 in both INS-1 and PC-12 cells, demonstrating that the SLMVs in the two cell types are the same size. Vacuolar ATPase (vATPase), a constituent of SV/SLMV, and SV2 were also detected in the INS-1 SLMV fractions (rows 2 and 4) as was phosphatidylinositol 4-kinase type II alpha (PI4KII $\alpha$ ), an SV protein sorted specifically by an AP-3B dependent mechanism (see Fig. 3.6).

immunoblot with synaptophysin antibodies (Fig. 3.5, top row). Maximal PC-12 cell synaptophysin immunoreactivity was observed in fraction 8. When INS-1 fractions were stained with synaptophysin, maximal immunoreactivity was also observed in fraction 8. This indicates that INS-1 SLMV co-sediment with PC-12 SLMVs, as would be predicted if  $\beta$ -cell SLMVs were ~40 nm (Fig. 3.5). Further, INS-1 fractions enriched in SLMVs were also enriched in other characteristic markers of SV and SLMV such as SV2 and vacuolar ATPase (Fig 3.5). Importantly, INS-1 SLMV also contained an SV/SLMV protein whose sorting to these organelles is regulated by AP-3: phosphatidylinositol-4-kinase type II alpha (PI4KIIa, Fig 3.6) [166-168]. These results indicate that INS-1  $\beta$  cell SLMVs closely resemble PC-12 SLMVs and suggest that neuronal AP-3 subunits may contribute to the biogenesis of INS-1  $\beta$  cell SLMVs.

##### *5. An AP-3 Dependent Pathway Drives SLMV Biogenesis in INS-1 $\beta$ -Cells*

Brefeldin A inhibits AP-3 mediated SV/SLMV biogenesis from endosomes but does not affect AP-2 mediated SV/SLMV biogenesis from the plasma membrane [151, 169]. To determine whether SLMV biogenesis in  $\beta$ -cells is dependent on AP-3, INS-1 cells were incubated in the presence or absence of brefeldin A, and high speed supernatants were sedimented in 5-25% glycerol gradients to resolve SLMV. SLMV content was analyzed using antibodies to proteins known to be associated with rat brain SV and PC-12 SLMV. Equal loading of proteins from untreated (-) and treated (+) cells into the gradients was confirmed using an antibody to tubulin (Fig. 3.6). Relative to control cells (- signs in Fig. 3.6), treatment with brefeldin A (+ signs in Fig. 3.6) markedly reduced the content of SV2, synaptophysin and vacuolar ATPase in INS-1

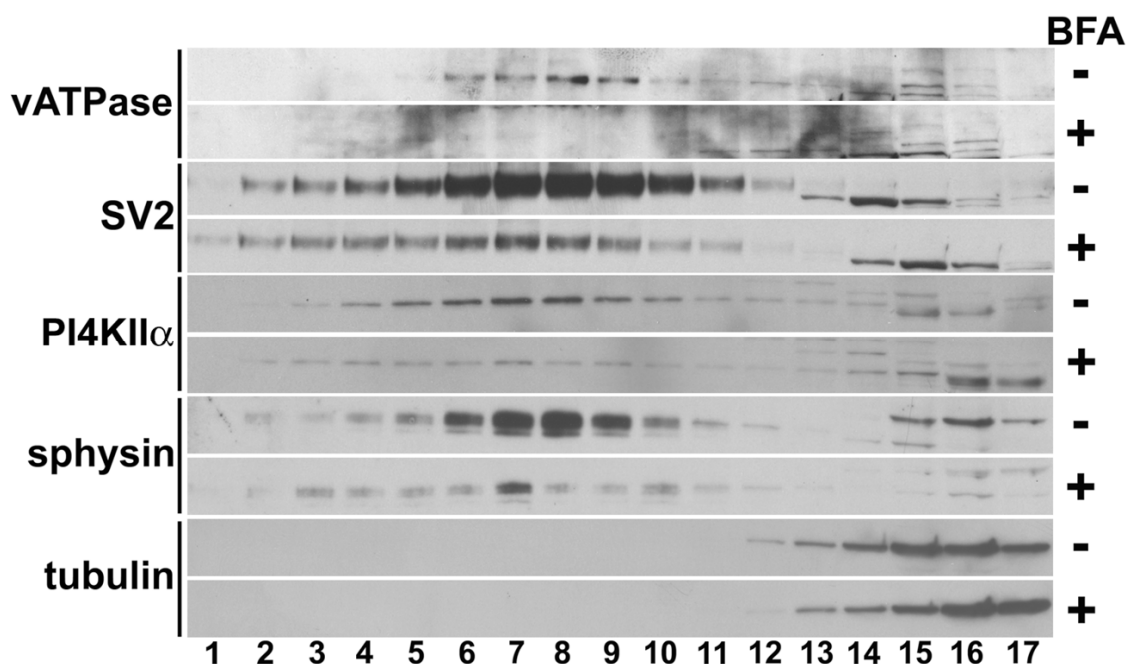


**Figure 3.6. SLMV biogenesis in INS-1  $\beta$  cells is mediated by AP-3.**

High-speed S2 supernatants obtained from INS-1 cells incubated for 2 h in the presence (+ in column on the far right) or absence (-) of brefeldin A (BFA) were sedimented in 5-25% glycerol velocity gradients to resolve SLMV. Fractions (numbered 1- 17) were analyzed by immunoblotting using antibodies to proteins known to be associated with SVs and PC-12 SLMVs. Recovery of SLMVs from the glycerol gradient peaked at Fraction 8. Treatment with BFA markedly reduced the content of vacuolar ATPase (vATPase), SV2, phosphatidylinositol 4-kinase type II alpha (PI4KII $\alpha$ ) and synaptophysin (sphysin) in the INS-1 SLMV fractions (compare fractions 6-9 in the “+” rows with the same fractions in the “-“ rows directly above). The observed depletion of protein content in the INS-1 SLMV fractions during brefeldin A treatment is identical to previous results demonstrating AP-3-mediated SLMV biogenesis using brefeldin A in PC-12 cells [164, 170, 171]. Probing for tubulin (bottom two rows, fractions 14-17) confirmed that the glycerol gradients were loaded with extracts with equal protein content. Cytosolic proteins like tubulin are expected to localize to the upper fractions, as is seen here. “+” and “-“ blots were run, transferred and exposed to film (for equal lengths of time) in parallel.

SLMV (fractions 6-10 in Fig. 3.6). The content of PI4KII $\alpha$ , a protein specifically targeted to AP-3 derived SLMV, was similarly reduced after treatment with BFA (fractions 6-10) [166-168]. These data show that INS-1 SLMV biogenesis is sensitive to brefeldin A. The depletion of SLMV proteins from the INS-1 SLMV fractions by brefeldin A parallels results from earlier studies in which the presence of an AP-3-mediated pathway of SLMV biogenesis in PC-12 cells was demonstrated using brefeldin A in the same manner as depicted here [164, 170, 171]. These results are consistent with a model where AP-3 mediates the bulk of SLMV biogenesis in INS-1  $\beta$ -Cells.

#### E. Discussion

The pancreatic islet  $\beta$ -cells express much of the machinery that is important for the differentiation and maintenance of GABAergic (inhibitory) synapses in the central nervous system (CNS) [149]. Previous studies with mice lacking the neuronal AP-3 subunits  $\beta$ 3B ( $\beta$ -NAP) and  $\mu$ 3B show that these proteins are important for normal synaptic function and play an important role in GABAergic signaling [59, 60]. In  $\mu$ 3B knockout mice, Nakatsu et al (2004) observed impairment of K<sup>+</sup>-evoked release of GABA which they attributed, at least in part, to reductions in synaptic VGAT protein levels [59]. Islet  $\beta$ -cells express VGAT and other components of the neuronal GABAergic signaling machinery [5, 99]. Because of more recent findings also suggesting that  $\beta$ -cells mature in a manner similar to that of GABAergic synapses, we hypothesized that AP-3B would be important for the biogenesis of SLMVs in  $\beta$ -cells [149]. Here, we



demonstrate the expression of  $\beta 3B$  and  $\mu 3B$  in the pancreatic islets. This is the first time that  $\beta 3B$  and  $\mu 3B$  have been shown to be expressed outside of neural tissue.

Our results indicate that rat pancreatic expression of AP-3B is islet  $\beta$ -cell-specific. We show that, as in neurons, AP-3 protein complexes in INS-1  $\beta$ -cells are involved in the biogenesis of SLMVs, as suggested by the strong inhibition of SLMVs after brefeldin A treatment. Because AP-3B-mediated microvesicle formation occurs at endosomes,  $\beta$ -cell SLMVs may primarily originate from endosomal compartments [56]. Our results confirm that the protein content and sedimentation properties of INS-1  $\beta$  cell SLMVs closely resemble that of PC-12 and neuronal SVs/SLMVs.

#### 1. *Expression of AP-3B Subunits in Islets and Beta-Cells*

Transcripts of both adaptin subunits specific to the neuronal AP-3 complex,  $\beta 3B$  ( $\beta$ -NAP) and  $\mu 3B$ , were detected in islets. Immunolocalization studies demonstrated that both AP-3B subunits are expressed exclusively by the islet  $\beta$ -cells in rat pancreas sections.

The expression of  $\beta 3B$  by  $\beta$ -cells, the propensity for  $\beta$ -cell autoantigens to be vesicle-associated and the prior observation that  $\beta 3B$  functions as an autoantigen in cerebellar degeneration suggested that  $\beta 3B$  itself could be a  $\beta$ -cell autoantigen [38, 53, 54]. Alternatively,  $\beta 3B$  and  $\mu 3B$  may contribute to the triggering of anti- $\beta$  cell autoimmunity by mediating the formation of nerve-terminal-like vesicles that carry potential autoantigens in a way that allows them to be discharged outside the cell under certain circumstances [38, 51]. The SLMV-associated enzyme GAD65, for example, is a

major autoantigen in type 1 diabetes and is released into the circulation during  $\beta$ -cell injury [51]. We conducted a preliminary search for evidence of autoreactivity against  $\beta$ 3B and  $\mu$ 3B using radioligand binding assays similar to a proven assay for GAD65 and other autoantibodies [172, 173]. Plasma samples from controls and from 10 children newly diagnosed with type 1 diabetes were tested for  $\beta$ 3B and  $\mu$ 3B antibodies. These 10 well-characterized samples have previously been used by the Immunology of Diabetes Workshops to standardize measurements of diabetes-associated autoantibodies [174, 175]. Results from this pilot study were negative for the presence of autoantibodies against either of the two proteins in the sera of subjects with type 1 diabetes and controls.

## 2. *AP-3-mediated SLMV Biogenesis in $\beta$ Cells*

The biophysical properties of synaptic vesicles and synaptic-like microvesicles are virtually identical [134]. Both are characterized by their homogenous size, the presence of unique markers and the absence of markers of larger endosomes and secretory granules. It was unclear how the biophysical properties of islet  $\beta$  cell SLMVs compare to SVs and PC-12 SLMVs. Previous characterization of these vesicles has yielded conflicting results and suggested that the size of these microvesicles differ from true SVs/SLMVs, which have a remarkably constant diameter of about 40 nm [161, 162]. Using electron microscopy, Braun et al. reported that the  $\beta$ -cell SLMV are on average 90 nm in diameter and can be as large as 150 nm, whereas Christgau et al. reported that these same vesicles are between 30-60 nm [25, 46]. Such electron microscopy-based analysis performed in intact cells cannot discriminate between sectioned tubules and endosomes and SLMVs unless proper markers are used. To circumvent this problem,

SLMVs can be separated from endosomes and larger vesicles with standard cell fractionation techniques followed by sedimentation through glycerol velocity gradients [134, 164]

The INS-1 line is one of the best-characterized  $\beta$  cell lines [133, 154]. Sucrose gradient sedimentation of INS-1  $\beta$ -cell homogenates yielded a peak due to the presence of endosomes/secretory granules and a second peak consistent with the presence of SLMVs that co-sediment with PC-12 SLMVs. Glycerol gradient sedimentation confirmed that the INS-1  $\beta$ -cells contain bona fide SLMVs. Our results show that INS-1 SLMVs carry SV/SLMV markers including SV2, synaptophysin, PI4KII $\alpha$  and vacuolar ATPase. INS-1 SLMVs sedimented in the same glycerol gradient position as PC-12 SLMVs indicating that INS-1 SLMVs are the same size as PC-12 SLMVs and neuronal SVs, with a diameter of around 40 nm. These results validate INS-1 cells as a model for investigations of SLMV biogenesis and SLMV function in  $\beta$ -cells.

Treatment of INS-1  $\beta$ -cells with brefeldin A markedly inhibited the formation of SLMVs, suggesting that neuronal AP-3 mediates the biogenesis of a significant portion of  $\beta$ -cell SLMVs. These studies do not exclude the possibility that there is also a population of SLMVs formed via an AP-2 dependent mechanism. Both pathways are used for the biogenesis of SLMV in PC-12 cells [164].

$\beta$ -cells and testis are the only tissues outside the CNS that express the zinc transporter ZnT3 [176, 177]. In neural tissue, ZnT3 incorporation into SVs/SLMVs is AP-3 dependent [164]. It is possible that, as in neurons,  $\beta$ -cell neuronal AP-3 drives the biogenesis of SLMV containing ZnT3 and these that vesicles are important for zinc

storage. ZnT3 plays a significant role in  $\beta$ -cell function: silencing of ZnT3 expression in  $\beta$ -cells decreases insulin secretion [176]. This may occur because zinc is important for insulin storage in secretory granules [178]. Also, zinc is secreted with insulin after glucose stimulation and has been proposed to act in a paracrine manner on  $\alpha$ -cells [179]. Further characterization of the function of  $\beta$ -cell SLMVs formed as a result of AP-3 action may lead to novel insights into both zinc and GABAergic autocrine/paracrine signaling within the islet.

### 3. *Closing Remarks*

Taken collectively, our data demonstrate expression of the neuronal AP-3 subunits outside of the CNS and the neurosecretory chromaffin cells and suggest that AP-3-mediated SLMV biogenesis occurs in  $\beta$ -cells. Experiments utilizing glycerol velocity gradient confirm that the biophysical properties of  $\beta$ -cell SLMVs match those of the bona fide SLMVs produced by PC-12 cells. Future studies of AP-3-derived SLMV may provide insights into important aspects of pancreatic  $\beta$ -cell biology including the function of GABA within the islet,  $\beta$ -cell zinc metabolism and the mechanisms that render neuronal, vesicle-associated  $\beta$ -cell proteins particularly susceptible to autoimmune targeting.

### F. Acknowledgements

A manuscript including chapter 3 has been submitted to *American Journal of Physiology: Endocrinology and Metabolism*. The dissertation author was the primary investigator in the development and execution of the study, and the principal author of this paper.

I thank Dr. Branch Craige and Dr. Victor Faundez for assistance with synaptic-like microvesicle preparations, and Dr. William Cain for assistance with generating antibodies to AP-3B protein.

CHAPTER 4: THE INHIBITORY PHENOTYPE OF THE ISLET  $\beta$ -CELL:  
EXPRESSION OF NEUREXIN, NEUROLIGIN, AND THEIR CYTOPLASMIC  
BINDING PARTNERS IN THE PANCREATIC BETA-CELLS AND THE  
INVOLVEMENT OF NEUROLIGIN IN INSULIN SECRETION

A. Abstract

The composition of the  $\beta$ -cell exocytic machinery is very similar to that of neuronal synapses, and the developmental pathway of  $\beta$ -cells and neurons substantially overlap.  $\beta$  cells secrete GABA and express proteins that, in the brain, are specific markers of inhibitory synapses. Recently, neuronal coculture experiments have identified three families of synaptic cell-surface molecules--neurexins, neuroligins and SynCAMs--that drive synapse formation in vitro and that control the differentiation of nascent synapses into either excitatory or inhibitory fully mature nerve terminals. The inhibitory-synapse-like character of the  $\beta$  cells led us to hypothesize that members of these families of synapse-inducing adhesion molecules would be expressed in  $\beta$  cells and that the pattern of expression would resemble that associated with neuronal inhibitory synaptogenesis. Here, we describe  $\beta$ -cell expression of the neuroligins, neurexins and SynCAM and show that neuroligin expression affects insulin secretion in INS-1  $\beta$  cells and rat islet cells. Our findings demonstrate that neuroligins and neurexins are expressed outside the central nervous system and help confer an inhibitory-synaptic-like phenotype onto the  $\beta$  cell surface. Analogous to their role in synaptic neurotransmission, neurexin-neuroligin interactions may play a role in the formation of the submembrane insulin secretory apparatus.

## B. Introduction

Insulin-secreting, pancreatic islet  $\beta$ -cells appear to have evolved from a neuronal precursor and to have retained exocytic mechanisms that, in neurons, are important for neurotransmitter release. Evidence linking the  $\beta$ -cells to a neuronal ancestor includes the finding that in some non-vertebrate species, such as *Drosophila*, insulin is exclusively released from neurons in the brain and also the observation that neural progenitor cells can be differentiated into glucose-responsive, insulin-secreting cells [6, 7].  $\beta$ -cells also express many of the scaffolding and synaptic vesicle proteins important for neurotransmitter secretion, and these seem to be key components of the insulin secretory machinery [12-18]. Consistent with their resemblance to neurons,  $\beta$ -cells express high levels of the major inhibitory neurotransmitter GABA and all of the machinery necessary for GABA synthesis, secretion and signaling [1, 5, 180]. The  $\beta$ -cell GABAergic signaling machinery most likely functions to regulate islet hormone secretion via an autocrine or paracrine signaling mechanism [1].

In the central nervous system, the differentiation and maturation of synapses to either a glutamatergic (excitatory) or GABAergic (inhibitory) phenotype is regulated, at least in part, by the synaptic adhesion molecules neurexin and neuroligin [181]. The neurexins are encoded by 3 distinct genes, are subject to a high degree of alternative splicing and, each can be transcribed from two promoters, generating longer  $\alpha$  and shorter  $\beta$  forms [182]. Transcription of  $\alpha$  and  $\beta$  variants of each of the three neurexin genes results in the expression of 6 different neurexin transcripts:  $1\alpha$ ,  $1\beta$ ,  $2\alpha$ , etc. Their expression is restricted to axons (pre-synaptic) and they interact across the synaptic cleft

with the neuroligins, which are localized to dendrites (post-synaptic). The neuroligins are encoded by five genes in humans and four in rodents and are also subject to alternative splicing [183, 184]. SynCAM1, a member of a family of adhesion molecules encoded by 4 distinct genes, also helps drive the functional differentiation of synapses [71].

Co-culture experiments using non-neuronal cell lines expressing members of the neurexin and neuroligin gene families revealed that neurexins specifically induce post-synaptic differentiation and neuroligins specifically induce pre-synaptic differentiation at points of contact between the non-neuronal cells expressing these proteins and hippocampal neurons [65, 66, 185, 186]. SynCAM induces both pre- and post-synaptic differentiation in contacting neurons [187]. Neuroligin-1 and specific  $\beta$ -neurexin splice variants are important for the formation of glutamatergic synapses while the  $\alpha$ -neurexins and neuroligin-2 drive the formation of GABAergic synapses [74, 188]. These results are in accord with differential expression patterns of neuroligins-1 and -2, where neuroligin-1 is detected primarily at excitatory synapses [75] and neuroligin-2 exclusively at inhibitory synapses [76] and with overexpression studies demonstrating that neuroligin-1 exclusively affects excitatory neurotransmission and neuroligin-2 exclusively affects inhibitory neurotransmission [74]. More recent *in vivo* studies with mice lacking the neuroligin genes confirms that these genes are important for determining whether a maturing synaptic connection will be excitatory or inhibitory [74].

Previously, we described the expression of the vesicular GABA transporter VGAT in islet  $\beta$  cells [5, 99]. Because  $\beta$  cells express the protein machinery necessary for GABAergic neurotransmission and because neuroligin-2 is important for driving the functional differentiation of GABAergic (inhibitory) synapses, we hypothesized that



neuroligin-2 and the interacting neuexins are expressed in  $\beta$ -cells. There, they may play a role in the maturation of autocrine or paracrine GABAergic signaling mechanisms. Furthermore, since neuroligin-neurexin interactions induce assembly of the synaptic exocytic machinery in tissue culture and are necessary for its proper functioning *in vivo* [65, 66, 72, 73], we postulated that neuexins and neuroligins may be important for the normal maturation and/or functioning of the highly-similar insulin secretory apparatus.

Here, we demonstrate expression of neuroligin and neuexin family members in  $\beta$ -cells, as well as expression of intracellular, inhibitory-synapse-associated neuroligin and neuexin binding partners and provide evidence that neuroligin family members play a role in the insulin secretory mechanism. Our findings suggest that the functional maturation of the  $\beta$  cell may share common mechanisms with that of the inhibitory synapse.

### C. Materials and Methods

#### *Antibodies*

The following primary antibodies were obtained commercially: mouse anti-gephyrin, mouse anti-PSD-95, mouse anti-CASK (BD Biosciences, San Diego, CA), goat anti-neurexin 1 (P-15), goat anti-neuroligin 2 (D-15) (Santa Cruz Biotechnology, Santa Cruz, CA), rabbit anti-neuroligin-3 (Synaptic Systems), mouse anti-insulin, mouse anti-glucagon, mouse anti-syntaxin-1 (Sigma, St. Louis, MO) and chicken anti-SynCAM (Medical & Biological Laboratories Co., Woburn, MA). Rabbit antibodies against neuroligin-2 were made by Alpha Diagnostic, Inc. (San Antonio, TX) after injection of the extracellular domain, which was generated in HEK293 cells as previously described

[189]. Antiserum was validated for affinity to neuroligin-2 by ELISA and western blotting.

#### *Plasmid Constructs*

cDNAs encoding rat neuroligin-1, -2 and -3 and human neuroligin-4 were subcloned into a vector encoding the FLAG epitope tag (Sigma) downstream of the amino-terminal cleaved signal sequence of preprotrypsin [190, 191]. Neuroligin-4 cDNA was a kind gift of Dr. Sergio Gloor, Swiss Federal Institute of Technology. A previously-described splice variant of acetylcholinesterase that lacks a transmembrane domain but that is anchored to the membrane via a GPI linkage was used in transfection experiments [191].

To generate reference templates for real time quantitative PCR analysis (qPCR), regions of the neurexin-2 and neurexin-3 genes flanking the real-time PCR amplicons were amplified by PCR of rat brain cDNA. The following primers were used: neurexin-2 (5'—gcactgttggggtgatttt—3' and 5'—tggctgtgaagatggtcag—3') and neurexin-3 (5'—agcgggtgtctcatcctcta—3' and 5'—tcgttgacaggggttctctc—3'). These PCR products were ligated into the TOPO TA vector (Invitrogen, Carlsbad, CA), transformed into TOP10 cells (Invitrogen), isolated and then quantified.

#### *PCR/RT-PCR*

Human fetal pancreas RNA was generously donated by Alberto Hayek (University of California, San Diego). Total RNA from INS-1 cells, NIT cells and human islets was isolated using the RNA Easy isolation Kit (Qiagen). RNA was reverse transcribed using random hexamers at 42 °C for 50 minutes with SuperScript II Reverse

Transcriptase (Invitrogen). The gene-specific primers used to amplify cDNA are shown in Table 4.1. For amplification with HotStarTaq enzyme, cDNA was denatured at 92°C, annealed between 58 and 62 °C and extended at 72 °C for 35 cycles. PCR products were analyzed by agarose gel electrophoresis and ethidium bromide staining. Controls with no template were used to ensure that there was no DNA contamination.

### *Quantitative RT-PCR*

Total RNA was isolated from INS-1 cells and rat brain using TriZOL (Invitrogen) and from human and rat islets using the GenElute Total Mammalian RNA miniprep kit (Sigma). It was then treated with Turbo DNase (Ambion) to remove any contaminating genomic DNA. RNA was reverse transcribed with Superscript II reverse transcriptase (Invitrogen) and random hexamers. Using gene-specific primers and TaqMan probes, quantitative PCR analysis was performed with the cDNA product from 50 ng RNA per well on an ABI Prism 7700 (Applied Biosystems). Primers and TaqMan probes are listed in supplemental tables 4.2, 4.3 and 4.4. Each sample was analyzed in duplicate along with a corresponding sample to which no reverse transcriptase was added (no RT control). To generate standard curves, real-time PCR analysis was performed with  $10^1$  to  $10^6$  copies of plasmid DNA encoding either the full-length neuroligin/neurexin genes or the portions of the neurexin genes flanking the qPCR amplicons. The standard curves allowed for calculation of the number of copies of each gene present in the cDNA samples. For analysis of RNA interference studies, neuroligin gene expression was

**Table 4.1. Primers for PCR Analysis.**

	<b>Forward Primer</b>	<b>Reverse Primer</b>
rat neuroligin-1	5'—gatggaccagcgcgagaacatt—3'	5'—atcgatcacaggtccaaagg—3'
rat neuroligin-2	5'—tttctgcgggaatttgtacc—3'	5'—cctgctatgcaaggaggaag—3'
rat neuroligin-3	5'—gacggggatgaagatgaaga—3'	5'—agcccctcagagtgatgaga—3'
rat neurexin-1 $\alpha$	5'—gcagatacccttcgactgga—3'	5'—tcatacattgtgccactga—3'
rat neurexin-1 $\beta$	5'—gcacctcgagaagactgtcc—3'	5'—cggagcatcctctggtacat—3'
rat neurexin-2 $\alpha$	5'—tcaacctgtccctcaagtc—3'	5'—ggtgtaatcctcctgcgtgt—3'
rat neurexin-2 $\beta$	5'—gtctcgtccagcctcagc—3'	5'—gggaggccatgtatataggtga—3'
rat neurexin-3 $\alpha$	5'—cattgtggagccagtgatg—3'	5'—gcccacacatagaggagtgca—3'
rat neurexin-3 $\beta$	5'—tgggagaagtgccatcagtc—3'	5'—gcttctggctgacctacctg—3'
human neuroligin-1	5'—gttgccacaaaaagtgggt—3'	5'—ttgagtgaagatccgctgtg—3'
human neuroligin-2	5'—ggcttaagggacacagtggga—3'	5'—gattgtcgggattgttttgg—3'
human neuroligin-3	5'—cacctgtggttctcagtt—3'	5'—cgtggatgtagaccatgacg—3'
human neurexin-1 $\alpha$	5'—cgacttcctggagctgattc—3'	5'—agcacacacctccgttgag—3'
human neurexin-1 $\beta$	5'—cggctatgtttcggattgtt—3'	5'—tcaatggcgatgtcatctgt—3'
human neurexin-2 $\alpha$	5'—ttgtcatcgagctggcaag—3'	5'—tggcacaggactcttcagt—3'
human neurexin-2 $\beta$	5'—ccggcaggaaactttgataa—3'	5'—catctgtgttctgggtggtg—3'
human neurexin-3 $\alpha$	5'—ctctggcaccatcaaagtga—3'	5'—ttctgcaggggtagctgtc—3'
human neurexin-3 $\beta$	5'—aaactcacctgaaccacttg—3'	5'—cccatcatagcaggaggaag—3'
mouse neuroligin-1	5'—ggggatgaggttccctatgt—3'	5'—ccgtggatggcacttttagtt—3'
mouse neuroligin-2	5'—tagcaggtgggagcagactt—3'	5'—agacacaagtgggaggggtg—3'
mouse neuroligin-3	5'—acatggaaggaaacaggcaac—3'	5'—agagccactttggatgatgg—3'
mouse neurexin-1	5'—agttgtacctgggtggcttg—3'	5'—aaaccgttgcctctctctca—3'
mouse neurexin-2	5'—caccaccagaacacagatg—3'	5'—tgttcttctggccttgctt—3'
mouse neurexin-3	5'—tcctaaccacaacgggctac—3'	5'—ctcagtggcgaaagtcaa—3'

**Table 4.2. Primers and Taqman Probes for Real Time PCR Analysis of INS-1 Cells and Rat Islets.**

<b>Transcript</b>	<b>Forward Primer</b>	<b>Reverse Primer</b>	<b>Probe</b>
Neuroigin-1	tccatattgctgctccaccaa	cggatatcagaccagggagatg	agaacatcgatttcagcctccagaacca
Neuroigin-2	ggcgatgtagtccttgatgac	cgccaatgagcatgttcgtagt'	tgagatcctcatgcaacagggagaattcc
Neuroigin-3	ggaagtagcctgggtccaaataca	gatcacgaacccttggttca	cccgggaccagctctaccttcacatc
Neurexin-1 $\alpha$	ttccgcaacaccactctctaca	ccctgcgcttggacttga	cgctgaggccaagtgggtgga
Neurexin-1 $\beta$	gcgcaccacatccacat	gctggtgacctgtagattgcaat	catggcagcagcaagcatcattcagt
Neurexin-2	cacggatgacattacaattgatga	agcgcaccacgtgatatttg	ccaacgccatctgtagcgacg
Neurexin-3	gacccagcacacgctctga	tgcgtactaagacaccatcctca	tcgccgtgggattcagcacca
18s	cgccgctagaggtgaaattc	ttggcaaatgctttcgctc	tggaccggcgcaagacggac

**Table 4.3. Primers for Real Time PCR Analysis of Human Islets.**

<b>Transcript</b>	<b>Forward Primer</b>	<b>Reverse Primer</b>
Neurologin-1	5'—aatggatgatgtggaccactggt—3'	5'—agatggtggttctggaggctgaaa—3'
Neurologin-2	5'—ccgagcgtatcaccatctt—3'	5'—gcagacactccacagctca—3'
Neurologin-3	5'—tcacctgcctacagcaacgagaat—3'	5'—aggccagaacgttaaggaacagga—3'
Neurexin-1 $\alpha$	5'—caacaatgtggaaggctctgg—3'	5'—atattgtcaccatagcgtgtc—3'
Neurexin-1 $\beta$	5'—cacatccaccatttccatgg—3'	5'—tttcctggtgtatatgcag—3'
Neurexin-2 $\alpha$	5'—gtcaatggcaagttcaacga—3'	5'—cttatagaccacgtccttgag—3'
Neurexin-2 $\beta$	5'—ccaccattccacagcaag—3'	5'—gcgaagttgtgttaagtgtg—3'
Neurexin-3 $\alpha$	5'—gcgaagttgtgttaagtgtg—3'	5'—ctgatatagtacctgatctgcc—3'
Neurexin-3 $\beta$	5'—ttagcttctcctctcca—3'	5'—accaagatgccatccttcac—3'
Beta-Actin	5'—tcatgaagtgtgacgttgacatccgt—3'	5'—cctagaagcatttgcgggtgcacgatg—3'
18s	5'—cgccgctagaggtgaaattc—3'	5'—ttggcaaatgcttgcgtc—3'

**Table 4.4. Primers for Splice Site Analysis of Neurexin and Neuroligin in INS-1 Cells and Human Islets.**

<b>Transcript</b>	<b>Forward Primer</b>	<b>Reverse Primer</b>
rat nl-1 flanking SSA	5'—tgtgcaagaccagagtgaaga—3'	5'—taccgtagcttgccaacaca—3'
human nl-1 flanking SSA	5'—ctcctgtgtgtcccagaat—3'	5'—ccccactgtcccgaatatct—3'
rat nl-1 internal SSA	5'—caccatctccctggctctgat—3'	5'—attttcttgccgggtttct—3'
human nl-1 internal SSA	5'—ctcctgtgtgtcccagaat—3'	5'—atattttcttgccgggcttt—3'
rat nl-1 flanking SSB	5'—gctgactttatccattattctgaa—3'	5'—gctggaagggtgttccactctga—3'
human nl-1 flanking SSB	5'—ctgcaaagggaactatgga—3'	5'—actaacagcccagctggaaa—3'
rat nl-1 internal SSB	5'—ttgggggtacttggcttcttg—3'	5'—ttgctccaacgggtaccttc—3'
human nl-1 internal SSB	5'—ggtaaccgttgagcaattc—3'	5'—tgtggtatcgagctggttga—3'
rat nl-2 flanking SSA	5'—tgtgtggttcaccgacaact—3'	5'—gccgtgtagaacagcatga—3'
human nl-2 flanking SSA	5'—tgtgtggttcaccgacaact—3'	5'—tggagaacagcatcacagg—3'
rat nl-2 internal SSA	5'—tgtgtggttcaccgacaact—3'	5'—tatctgtgtctggcggattg—3'
human nl-2 internal SSA	5'—ccatcatgctgcctgtgtg—3'	5'—gattgagcgtcgcctcgt—3'
rat nl-1 flanking SSA1/2	5'—ttatatccaggagcccaacg—3'	5'—tccgtgatgtagaccatga—3'
human nl-1 flanking SSA1/2	5'—ggttcactgccaacttgat—3'	5'—cgtggatgtagaccatgacg—3'
rat nl-1 internal SSA1	5'—cccagaacatccacacagc—3'	5'—attttctgttgggctttcg—3'
human nl-1 internal SSA1	5'—tgtaaagcggattccaagg—3'	5'—cgtggatgtagaccatgacg—3'
rat nl-1 internal SSA2	5'—aagaaacaggcgaggactt—3'	5'—atgacgatgacgttgccata—3'
human nl-1 internal SSA2	5'—aagaaacaggcgaggactt—3'	5'—ggatgatgacgatgacattgc—3'
rat nrxn-1 flanking SS4	5'—gcctgggtgactaccttgag—3'	5'—tgtggtggtctccatgattg—3'
human nrxn-1 flanking SS4	5'—acagatgacatgccattga—3'	5'—ccgccaattattatggttgc—3'
rat nrxn-1 internal SS4	5'—acagatgacatgccattga—3'	5'—aggcgctcgttatcattgtt—3'
human nrxn-1 internal SS4	5'—acatcgccattgaagaatcc—3'	5'—ccattcatcaactactcgacca—3'

normalized to the expression of 18s rRNA. RNA knockdown was analyzed using the formula:  $2^{((C_T \text{ neuroigin-2 in INS-1 cells treated with RNAi} - C_T \text{ 18s in same cells}) - (C_T \text{ neuroigin-2 in INS-1 cells treated with control RNAi} - C_T \text{ 18s in same cells}))}$ .

### *Cell Culture and Transfection*

INS-1 cells were cultured in RPMI 1640 medium supplemented with 10% fetal bovine serum, 50  $\mu$ M  $\beta$ -mercaptoethanol, 1mM sodium pyruvate, 2 mM L-Glutamine, 100 U/mL penicillin and 100 mg/mL streptomycin in a humidified 37° C incubator with 5% CO<sub>2</sub>. NIT-1 cells were cultured in DMEM supplemented with 10% fetal bovine serum, 2 mM L-Glutamine, 100 U/mL penicillin and 100 mg/mL streptomycin. Rat islets were cultured in RPMI 1640 medium supplemented with 10% fetal bovine serum, 2 mM L-Glutamine, 100 U/mL penicillin and 100 mg/mL streptomycin. 24 hours prior to transfection, rat islets were dispersed using 0.05% trypsin-EDTA and plated onto 24 well plates coated with poly-D-lysine.

For transfections, INS-1 cells were plated on to 12 well plates and allowed to grow to 50% confluency in antibiotic-free media. The cells were then transfected with the gene of interest using Lipofectamine 2000 (Invitrogen) according to the manufacturer's protocol. Cells were incubated in the transfection cocktail for 48 hours prior to conducting insulin secretion experiments and confirmation of gene expression by western blot analysis.



### *RNA Interference*

A pool of siRNA duplexes targeted to neuroligin-2 was purchased from Dharmacon Research. The siRNA duplexes lacked significant homology to other rat genes as confirmed by a BLAST search. The sequences of each of the duplexes is listed in table 4.5. The pool of siRNA duplexes was transfected into INS-1 cells or dissociated rat islets with Lipofectamine 2000 (Invitrogen) according to the manufacturer's protocol. As a control, a pool of non-targeting siRNA duplexes (Dharmacon Research) were used. Insulin secretion assays were performed 48 hours post-transfection and knockdown was analyzed via quantitative PCR analysis. For rat islet experiments, 12 wells were treated with non-targeting siRNA and 12 wells were treated with neuroligin-2 siRNA. Half of each of these samples were used to isolate RNA for analysis of knockdown and half were used to isolate protein for analysis of total insulin content.

### *Insulin Secretion Assays*

Cells were washed twice with Hanks Balanced Salt Solution and then incubated in Krebs–Ringer bicarbonate buffer containing 0.2% BSA and 2.75 mM glucose. After 30 min incubation, this solution was removed and replaced with Krebs–Ringer containing 2.5 mM glucose for one hour. The solution was collected and replaced with Krebs–Ringer containing 15 mM glucose for INS-1 cells or 25 mM glucose for rat islets for an additional hour. The solution was collected and insulin content was measured using a rat insulin RIA (Linco/Millipore, Billerica, MA).

**Table 4.5. Neuroligin-2 SiRNA Pool.**

SiRNA #	Sense	Antisense (5'P on all)
<b>1</b>	5'—gagcuaagcgugacuguaguu—3'	5'—cuacagucacgcuuagcucuu—3'
<b>2</b>	5'—gcacggaagcuguggauguu—3'	5'—cauuccacagcuuccgugcuu—3'
<b>3</b>	5'—gcgcaguagucaugaccuauu—3'	5'—uaggucaugacuacugcgcuu—3'
<b>4</b>	5'—guauaggagcaagucaacauu—3'	5'—uguugaacuugcuccauacuu—3'

### *Immunofluorescence*

Cells were seeded on 4-well chamber slides (BD Biosciences) coated with poly-D-lysine and allowed to grow to confluency. Prior to immunostaining, they were fixed in a 4% paraformaldehyde solution for 10 minutes, washed twice in 1x PBS and permeabilized with 0.2% triton x-100 in PBS for 20 minutes.

16  $\mu\text{m}$  sections of frozen rat pancreas were prepared by the the University of California, San Diego histology core. Before staining, frozen sections were fixed in a 1:1 acetone:methanol solution at  $-20^{\circ}\text{C}$  for 20 minutes. For paraffin sections, the tissue was fixed for 24 hours in Pen-Fix (Richard Allan Scientific), embedded in paraffin and sections were cut at 6  $\mu\text{m}$ . Immunostaining experiments were performed as previously described [5, 192]. Images were captured using either Nikon-TE-200 deconvolution microscope or an Olympus FV1000 spectral confocal microscope configured with an Argon/Krypton laser (488- and 568-nm excitation lines) and either 40 or 60x oil immersion lenses. Controls included tissue stained with either secondary antibody and no primary antibody or preimmune serum followed by secondary antibody.

### *Islet Isolation*

Rat islets were provided by the University of Washington Diabetes and Endocrinology Research Center (DERC) Islet Cell and Functional Analysis Core [5]. Briefly, islets were isolated from the pancreata of Sprague Dawley rats by digestion with Liberase (Roche Molecular Biochemicals) followed by Optiprep (Nycomed) gradient purification as previously described [193]. Isolated islets were hand-picked in Hank's balanced salt solution (Invitrogen).

### *Western Blot Analysis*

Cell extract was made by homogenizing the tissue or cells of interest in RIPA buffer (PBS, 1% NP-40, 0.5% sodium deoxycholate, 0.1% SDS, 45 µg/ml aprotinin, 100 µg/ml PMSF and 1mM sodium orthovanadate). Cell extract was quantified using the Bio-Rad D<sub>c</sub> Protein Assay (Bio-Rad, Hercules, CA). Protein diluted 1:4 with reducing sample buffer was electrophoresed on either 4-12% Bis-Tris NuPage gel or 3-8% Tris-Acetate NuPage Gels (Invitrogen). The protein was then transferred to PVDF membrane and analyzed by immunoblot analysis as previously described [5, 99].

### *Statistical Analysis*

Data are presented as means ± S.E. Differences between quantitative data sets were analyzed by t-test.  $P < 0.05$  was considered significant.

## **D. Results**

### *1. Expression of neurexin and neuroligin transcripts in islets and $\beta$ -cell lines at levels comparable to brain.*

Initial PCR studies revealed the expression of neuroligin-1, -2 and -3 and the neurexin family members 1 $\alpha$ , 1 $\beta$ , 2 $\alpha$  2 $\beta$  and 3 $\beta$  in human islets (Fig. 4.1A). Expression was also observed in the rat-derived INS-1 and mouse-derived NIT  $\beta$ -cell lines and in the developing human pancreas (Fig. 4.1B-D).

To compare the expression levels of individual neuroligin and neurexin family members in islets and to determine how these levels compare with those observed in

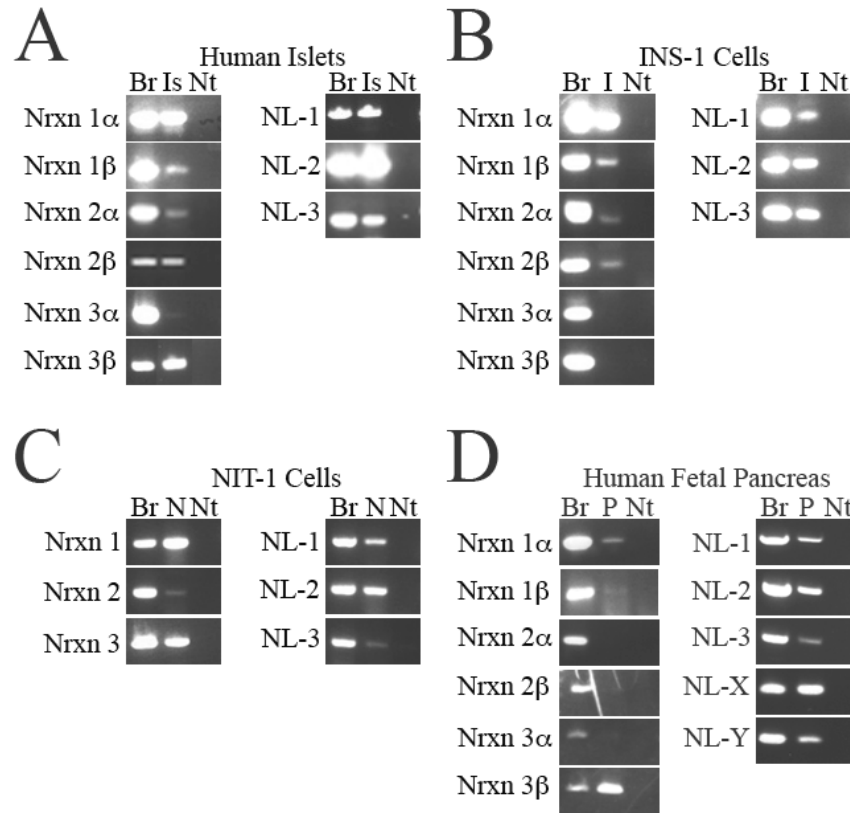


**Figure 4.1. Expression of neurexin and neuroligin mRNA in human pancreatic islets and rat and mouse  $\beta$ -cell lines.**

To determine whether neurexin and neuroligin transcripts are expressed in islets and  $\beta$ -cell lines, cDNA from human islets, INS-1 cells, NIT cells and human fetal pancreas was analyzed by PCR amplification using gene-specific primers to all neurexin and neuroligin family members. Brain cDNA from the appropriate species was used as a positive control. As expected, products of the expected molecular weight were detected in brain for all neurexin and neuroligin family members analyzed. (A) In human islets, products corresponding to transcripts from the neurexin-1 $\alpha$ , -1 $\beta$ , -2 $\alpha$ , -2 $\beta$ , -3 $\beta$  and from the neuroligin-1, -2 and -3 genes were detected. (B) In the rat  $\beta$ -cell line INS-1, products corresponding to transcripts from the neurexin-1 $\alpha$ , -1 $\beta$ , -2 $\alpha$ , -2 $\beta$  and from the neuroligin-1, -2 and -3 genes were detected. (C) In NIT-1 cells, products corresponding to transcripts from the neurexin-1, -3, neuroligin-1 and -2 genes were detected. Faint bands corresponding to neurexin-2 and neuroligin-3 were also observed. (D) In fetal pancreas, products corresponding neurexin-3 $\beta$  and all of the neuroligin genes were detected. Trace amounts of the neurexin-1 $\alpha$  and -1 $\beta$  PCR products were detected but the other neurexin genes were not. The lack of expression of neurexin-3 $\alpha$  in humans islets, fetal pancreas and INS-1 cells distinguishes their neurexin expression from that in brain, from which neurexin-3 $\alpha$  was readily amplified. (Br, brain; Is, human islets; Nt, no template; I, INS-1 cells; N, NIT cells; P, human fetal pancreas; Nrnx, neurexin; NL, neuroligin).

brain, absolute real-time qPCR analysis was performed using cDNA derived from rat islets, INS-1 cells and rat brain. Rat islets were found to express high levels of neuroligin-1, neuroligin-2, neurexin-1 $\alpha$  and neurexin-3 (Fig. 4.2). Transcript copy numbers were comparable to or greater than those observed in brain. Relatively lower levels of neuroligin-3, neurexin-1 $\beta$  and neurexin-2 are detected in rat islets (Fig. 4.2). The total number of copies observed for neurexin 2 and neurexin 3 represent the sum of both the  $\alpha$  and  $\beta$  isoforms. The restricted pattern of expression observed in rat islets is distinct from that observed in brain where neuroligin and neurexin family members are expressed at relatively similar levels. The pattern of expression in human islets is similar to that observed in rat islets (Fig. 4.3).

In the rat  $\beta$ -cell line INS-1, neuroligin-2 was the most abundant transcript detected (Fig. 4.2). Its level of expression was 8-fold greater than neuroligin-1 and 3-fold greater than neuroligin-3. Of the neurexin family members, neurexin-1 $\alpha$  and neurexin-2 were the most abundant transcripts detected. Both of these transcripts were expressed at levels that were at least 10-fold greater than neurexin-1 $\beta$  and neurexin-3. The levels of neuroligin-2, neurexin-1 $\alpha$  and neurexin-2 observed in INS-1 cells did not differ statistically from those observed in brain (Fig. 4.4).

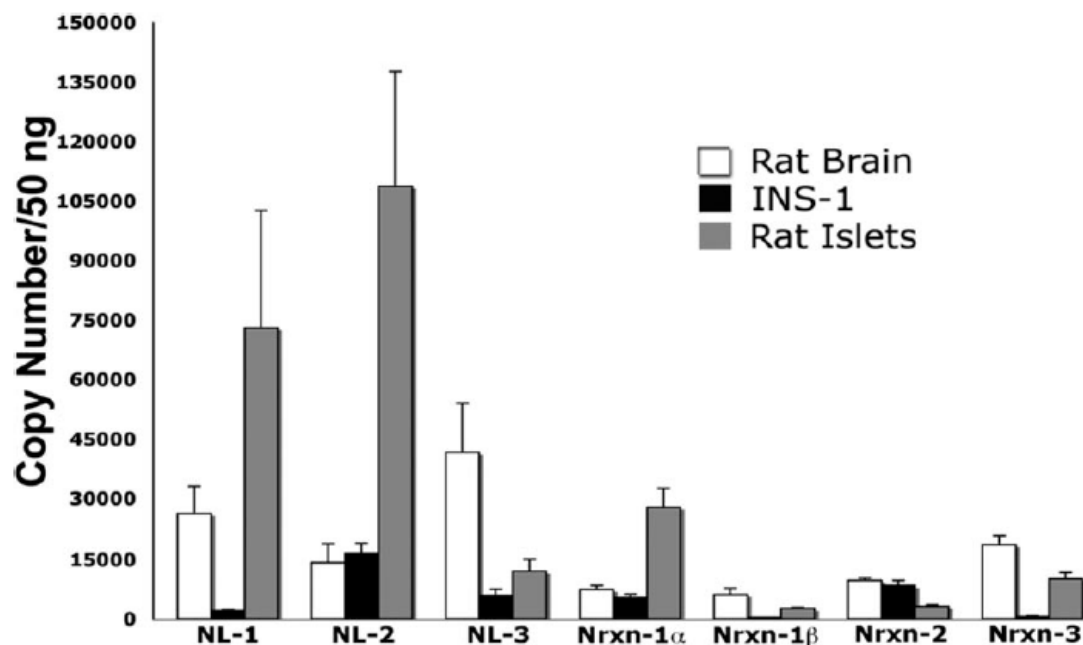


**Figure 4.2. Abundance of neuroigin and neurexin transcripts in INS-1  $\beta$  cells and Rat Islets.**

Absolute real-time qPCR analysis was employed to compare the expression levels of individual neuroigin (NL) and neurexin (Nrnxn) family members within rat-derived INS-1  $\beta$  cells, rat islets and rat brain. Standard curves were generated using plasmids encoding either whole or partial neuroigin/neurexin sequences, and these were used to calculate the number of copies of each transcript per cDNA sample. Samples were prepared in parallel, though rat islet RNA was prepared separately because of the need to utilize an alternative method. Each cDNA sample represents an equal amount (50 ng) of input total RNA. In INS-1 cells, neuroigin-2 ( $16,489 \pm 1,055$  copies/50 ng RNA), neurexin-1 $\alpha$  ( $5,296 \pm 927$  copies/50 ng RNA) and neurexin-2 ( $8,370 \pm 1,302$  copies/50 ng RNA) are expressed at the highest levels relative to other neuroigin and neurexin family members. (The neurexin-2 and -3 primer sets could not distinguish between the  $\alpha$  and  $\beta$  forms.) In rat islets, neuroigin-1 ( $72,914 \pm 14,836$  copies), neuroigin-2 ( $108,683 \pm 14,413$  copies), neurexin-1 $\alpha$  ( $27,668 \pm 2,417$  copies) and neurexin-3 ( $10,115 \pm 769$  copies) are expressed at the highest levels relative to other neuroigin and neurexin family members. In rat brain, expression of neuroigin and neurexin mRNA is more evenly distributed. Values obtained were: neuroigin-1 ( $15,058 \pm 3,987$  copies), neuroigin-2 ( $9,260 \pm 2888$  copies), neuroigin-3 ( $26,156 \pm 8,018$  copies), neurexin-1 $\alpha$  ( $4,412 \pm 1,077$  copies), neurexin-1 $\beta$  ( $3,464 \pm 883$  copies), neurexin-2 ( $6,451 \pm 1,552$  copies) and neurexin-3 ( $11,239 \pm 2,727$  copies). Equal loading of input RNA was verified by parallel qPCR analysis of 18s rRNA. 18s cycle threshold values ( $C_T$ ) in INS-1 cells and rat brain were consistently identical. Rat islet 18s cycle threshold values were higher (slightly less than 2  $C_T$  values), likely the result of differences in the technique used for RNA isolation. (*n* of 3 separately-prepared RNA/ cDNA samples per experiment).

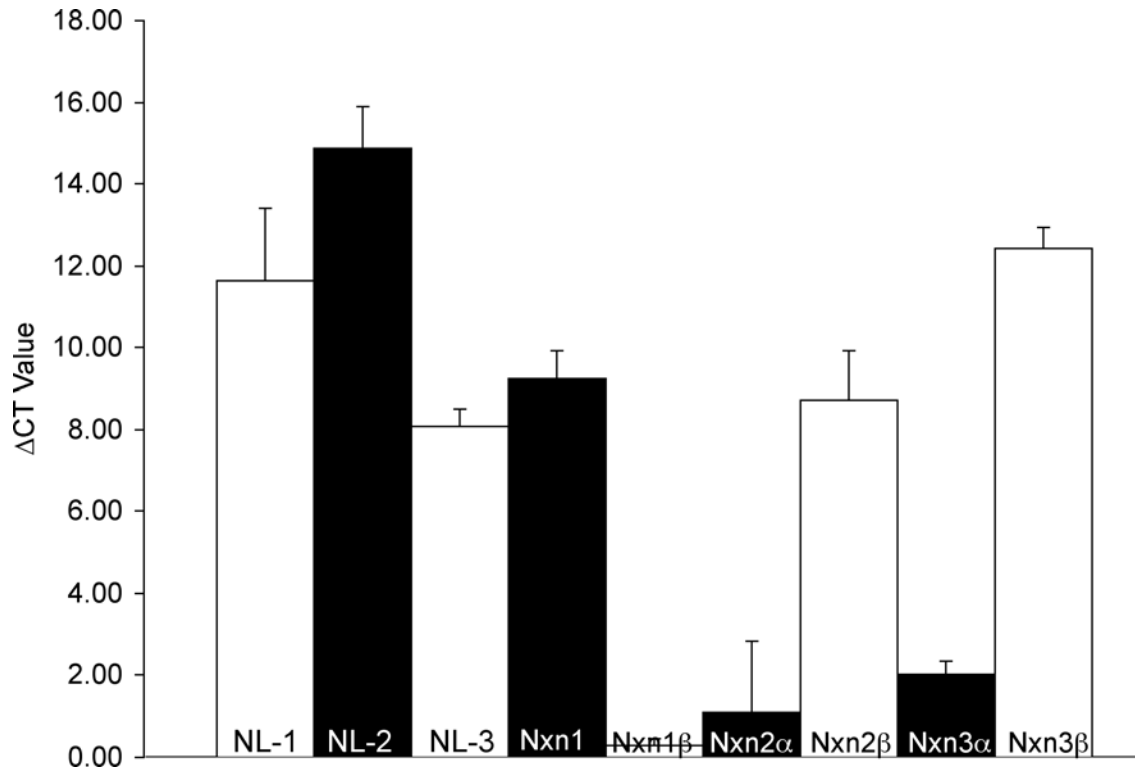


**Figure 4.3. Neuroigin and neurexin mRNA expression in human islets.**

To determine the relative abundance of neuroigin and neurexin transcripts in human islets, RNA was isolated and reverse transcribed to cDNA and analyzed by real time PCR analysis. Neuroigin-1, neuroigin-2, neurexin-1 $\alpha$ , neurexin-2 $\beta$  and neurexin-3 $\beta$  were the most abundant transcripts detected. Lower levels of neuroigin-3, neurexin-2 $\alpha$  and neurexin-3 $\alpha$  transcripts were detected and neurexin-1 $\beta$  was not detected in human islets. Data are expressed as the difference between cycle threshold values for human islet cDNA amplified with either neurexin or neuroigin primers and background signal (RNA not treated with reverse transcriptase).



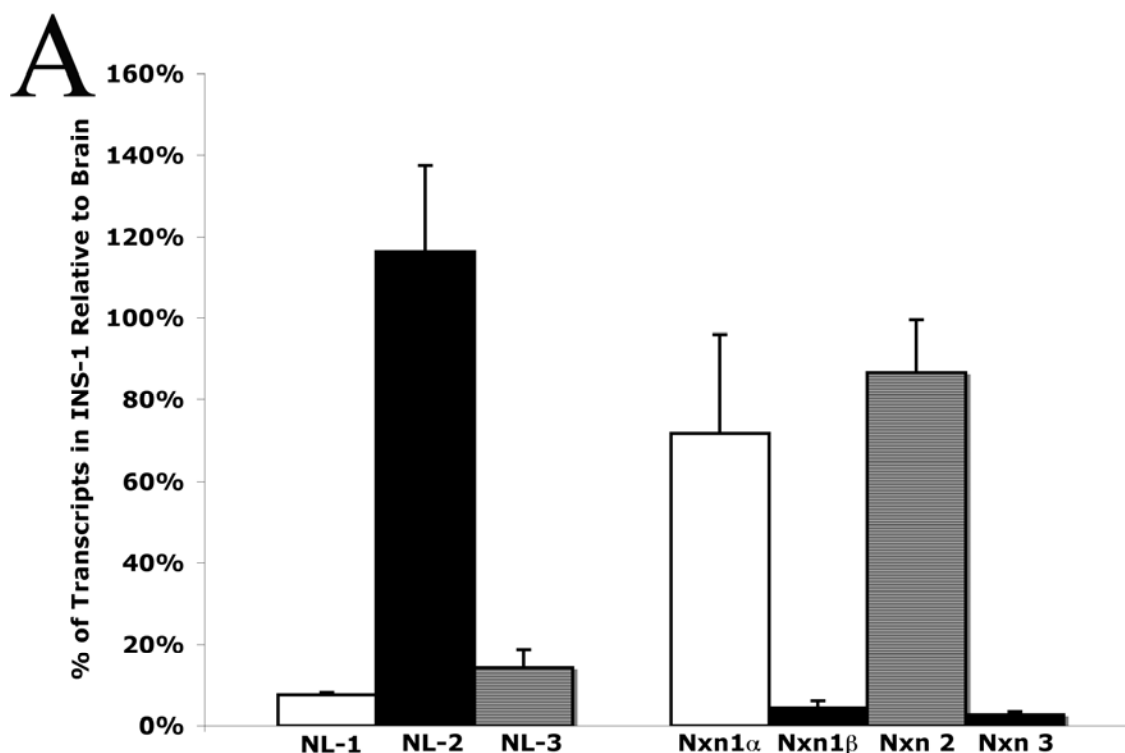


**Figure 4.4. Abundance of Neurexin and Neuroligin transcripts in INS-1 cells relative to rat brain.**

To determine how transcript levels compare in INS-1 cells and the rat brain, the number of transcripts detected in INS-1 cells was expressed as a percentage of the number of transcripts detected in brain. Statistically, no difference was detected between brain and INS-1 mRNA levels for neuroligin-2 (116%), neurexin-1 $\alpha$  (72%) or neurexin-2 (87%). Neuroligin-3 was expressed in INS-1 cells at 14% of brain levels and all other neurexin and neuroligin genes tested were at levels that were at least 10-fold lower than levels detected in brain. Elevated 18s  $C_T$  values in rat islets, possibly as a result of differing RNA isolation methods, made us uncomfortable expressing rat islets as a percentage of brain. (*n* of 3 separately-prepared RNA/ cDNA samples per experiment).

## 2. *Expression of alternatively spliced neuroligin exons in human islets and INS-1 cells*

Alternative splicing within the extracellular domain occurs in all neuroligin family members [68, 184]. For neuroligin-1, two alternative exons, A and B, have been described (Fig. 4.5A) [70]. The other neuroligin family members undergo alternative splicing at site A but not site B (Fig 4.5A) [68]. This alternative splicing helps to determine synapse type (excitatory or inhibitory) and to determine the neurexin isoforms to which neuroligin molecules can bind [184, 194]. To compare alternative splicing of neuroligin transcripts in  $\beta$ -cells to splicing in the brain, primers that either flank or sit within each of the potential inserts (see table 4.4) were used to amplify neuroligin regions from human islet and INS-1 cDNA. In parallel, cDNA samples prepared from rat and human brain RNA were also amplified.

Amplification using primers internal to the alternatively spliced exons yielded products of the expected size in both human islets and INS-1 cells for each of the alternatively spliced exons (Fig. 4.5B-4.5D). This indicates that neuroligin mRNA processing in the  $\beta$ -cells can yield the same pattern of alternative splicing as observed in brain. Sequencing of neuroligin transcripts from human islet and INS-1 cells confirmed that the alternatively spliced exons were identical in islet and brain (data not shown).

In human brain, only primers flanking neuroligin 3 site A yielded a PCR product consistent with the absence of the alternatively spliced exon (Fig. 4.5D). The absence of PCR products lacking inserts at splice sites A and B for neuroligin-1 (Fig. 4.5B) and splice site A for neuroligin 2 (Fig. 4.5C) suggests that, in human brain, neuroligin-1 and -2 transcripts that contain the alternatively spliced exons predominate. In human islets, PCR products consistent with the absence of inserts at splice site A in neuroligin-1 and

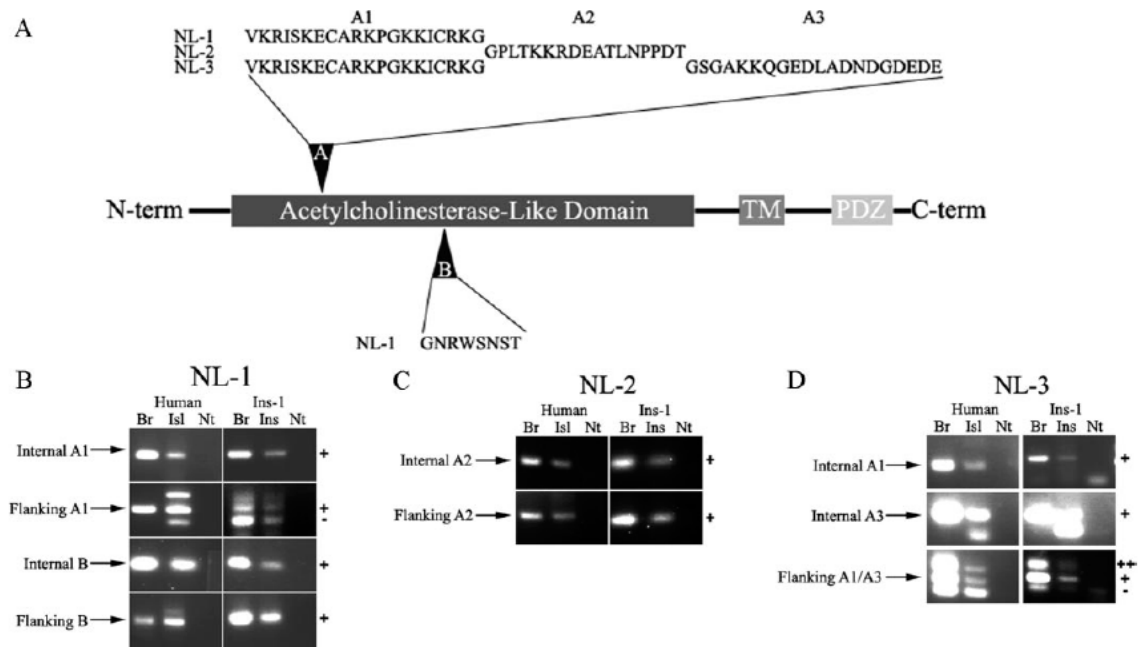


**Figure 4.5. Characterization of neuroligin splice variants in pancreatic  $\beta$  cells.**

(A) Schematic representation of alternative splice inserts in neuroligin (NL) gene family members. Splice site A is present in all neuroligin family members, while splice site B is only present in neuroligin-1. Different alternative exons (A1-A3) can be included at site A. (B-D) To determine which neuroligin splice variants are expressed in islets, primers were designed to either flank or sit on each of the known neuroligin splice inserts. PCR was performed using cDNA from either human islets or INS-1 cells and from either human or rat brain. Each of the known splice inserts in neuroligin-1 (B), neuroligin-2 (C) and neuroligin-3 (D) were detected in both human islets and INS-1 cells. Transcripts lacking inserts at splice site A in neuroligin-1 were detected in human islets, rat brain and INS-1 cells but not in human brain (B, row 2). Neuroligin-1 transcripts lacking inserts at splice site B and neuroligin-2 inserts lacking site A were not detected in brain, INS-1 cells or human islets (bottom two panels of B and C). Neuroligin-3 transcripts lacking an insert at splice site A were detected in all tissues tested. (D, bottom two panels). (Br, brain; Isl, islets; Ins, INS-1; Nt, no template; (+), presence of insert; (-), absence of insert; (++) , presence of both inserts).

neuroligin-3 were detected (Fig. 4.5B, 4.5D). PCR products lacking splice inserts at splice site B in neuroligin-1 and at splice site A in neuroligin-2 were not detected (Fig. 4.5B, 4.5C). Findings concerning the presence or absence of splice variants are summarized in Table 4.6.

Rat brain cDNA, unlike human, yielded a neuroligin-1 PCR product lacking an insert at splice site A (Fig. 4.5B). This transcript appears to be the predominant form. As with human brain, amplification of neuroligin-2 from rat brain cDNA yielded only a PCR product containing a spliced-in exon at site A (Fig. 4.5C). These data are consistent with previous studies of neuroligin-1 and -2 splicing in rat brain [184]. Alternative splicing at neuroligin-1 site A results in inclusion of a different alternative exon than splicing at neuroligin-2 site A (Fig. 4.5A). Splice site A in neuroligin-1 is conserved in neuroligin-3. Additionally, a distinct exon can be used at this site (A3, Fig. 4.5A). Unexpectedly, both of these alternatively spliced exons were utilized at site A in neuroligin-3: neuroligin-3 transcripts containing both alternative exons, one exon or lacking both were detected (Fig. 4.5D and Table 4.6).

### 3. *Expression of an insert at splice site 4 in neurexin-1 transcripts*

Alternative splicing of  $\alpha$ -neurexin can occur at 5 sites; these are numbered 1 through 5 beginning at the site closest to the amino-terminus of the  $\alpha$ -neurexin gene as depicted in Fig. 4.6A. Three sites occur exclusively in  $\alpha$  variants, and two (splice sites 4 and 5) are shared by both  $\alpha$  and  $\beta$  variants (Fig. 4.6A) [67]. A splice insert at splice site 4 favors the formation of inhibitory synapses [77]. Because we hypothesize that the

**Table 4.6. Neuroligin and Neurexin Splice Variants Detected.**

	Human		Rat	
	Brain	Islet	Brain	INS-1 $\beta$ cells
NL-1, site A	[+]	[+, -]	+, -	+, -
NL-1, site B	+	+	+	+
NL-2, site A	+	+	+	+
NL-3, site A	++, +, -	++, +, -	++, +, -	++, +, -
Nx-1, site 4	+	+	[+, -]	[+]

Differences between brain and islet/INS-1 tissue highlighted by brackets: [ ]. At site A in NL-3, the alternative exon used in NL-1 and an exon specific to NL-3 can either be incorporated in tandem (++) or only one of the alternative exons may be spliced in (+).

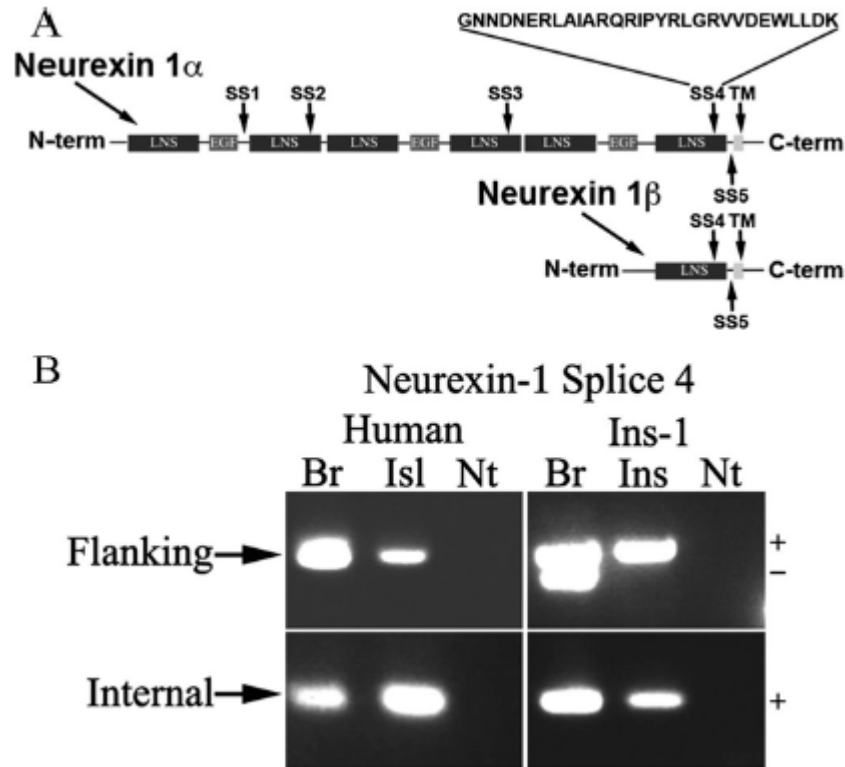


**Figure 4.6. Expression of an insert at splice site 4 in neurexin 1 islet transcripts.**

(A) Schematic representation of splice insertions in neurexin gene family members. A total of 5 alternative exons have been described in the neurexin-1 gene. An insert at splice site 4 is known to promote the formation of inhibitory synapses. LNS domains are the extracellular neurexin domains that resemble repeats of laminin-neurexin-sex hormone-binding globulin. (B) To determine if neurexin transcripts in human islets and rat-derived INS-1  $\beta$  cells contain an insert in splice site 4, primers were designed to either flank or sit on this insert. PCR was performed using cDNA from either human islets or INS-1 cells and either rat or human brain. Transcripts with an insert at splice site 4, but not ones lacking, were detected in both human islets and INS-1 cells. As expected, neurexin-1 transcripts both with and without an insert at site 4 were detected in rat brain. In contrast, in human brain, human islets and INS-1  $\beta$  cells, only transcripts containing an insert at splice site 4 were detected. (Br, brain; Isl, islets; Ins, INS-1; Nt, no template; (+), presence of insert; (-), absence of insert).

functional development of the  $\beta$ -cell may parallel that of the inhibitory synapse, we asked whether  $\beta$ -cell neurexin-1 transcripts contain the alternatively spliced insert at site 4.

As seen in Fig. 4.6B, the splice insert at site 4 was detected in both human islets and INS-1 cells as well as in the brain controls. When PCR was performed with primers flanking the splice site, transcripts both containing and lacking the insert were detected in rat brain (Fig. 4.6B, upper panels). It is unclear why transcripts lacking the insert were not detected in human brain; it is possible that transcripts containing the splice insert represent the predominant form in the human brain. In islets and INS-1 cells, only neurexin transcripts containing the inhibitory synapse-associated insert at site 4 were detected (Fig. 4.6B, Table 4.6).

#### *4. Expression of specific inhibitory and excitatory post-synaptic protein markers in $\beta$ cells*

In coculture experiments, neurexin expression on non-neuronal cells induces the clustering of both inhibitory and excitatory post-synaptic markers in the dendrites of cultured hippocampal neurons [185]. Gephyrin and PSD-95 are examples of specific markers of the inhibitory and excitatory post-synaptic densities, respectively [195, 196]. Because  $\beta$ -cells appear to differentiate along a pathway that results in an inhibitory-synapse-like phenotype (with  $\beta$ -cell expression of both pre- and post-synaptic proteins), we predicted that  $\beta$ -cells would express gephyrin, a cytoplasmic neuroligin binding partner and the central scaffolding protein at the inhibitory synapse, but not the scaffolding protein PSD-95, a central constituent of the excitatory post-synaptic density

[197, 198]. Immunoblot analysis revealed that rat and human islets as well as the  $\beta$ -cell lines INS-1 and NIT express gephyrin but not PSD-95 (Fig. 4.7). As expected, both gephyrin and PSD-95 were detected in extracts from human, mouse and rat brain (Fig. 4.7).

The cytoplasmic protein CASK, along with Mint, directly interacts with neuexins to help initiate the assembly of the presynaptic secretory machinery [92]. Previously, Mint was shown to be expressed in  $\beta$ -cells [18]. If, as in axons, assembly of the  $\beta$ -cell secretory machinery is dependent on neuexin clustering, we hypothesized that CASK would also be expressed in  $\beta$ -cells. As shown in Figure 4.7, CASK was detected in all islet and  $\beta$ -cell extracts tested by immunoblot analysis.

##### *5. Expression of neuroligin-2 protein in pancreatic islets*

Neuroligin-2 was detected by western blot analysis in human brain, human colon and human islets but was not detected in human heart, liver, kidney or whole pancreas (Fig. 4.8A). Due to sequence homology between the neuroligins, it is possible that this antibody, which was raised to the extracellular domain of neuroligin-2, has some level of affinity for other neuroligin proteins. Identification of the neuroligin band detected in human islets rests on the observations that 1) the band comigrates with neuroligin-2 and not neuroligin-1 and 2) that neuroligin-3 is not detected in human islets using an antibody that is specific for this protein and that detects neuroligin-3 in brain (Fig. 4.8B). We were unable to identify a neuroligin-1 antibody that detects the human variant of this protein (data not shown).



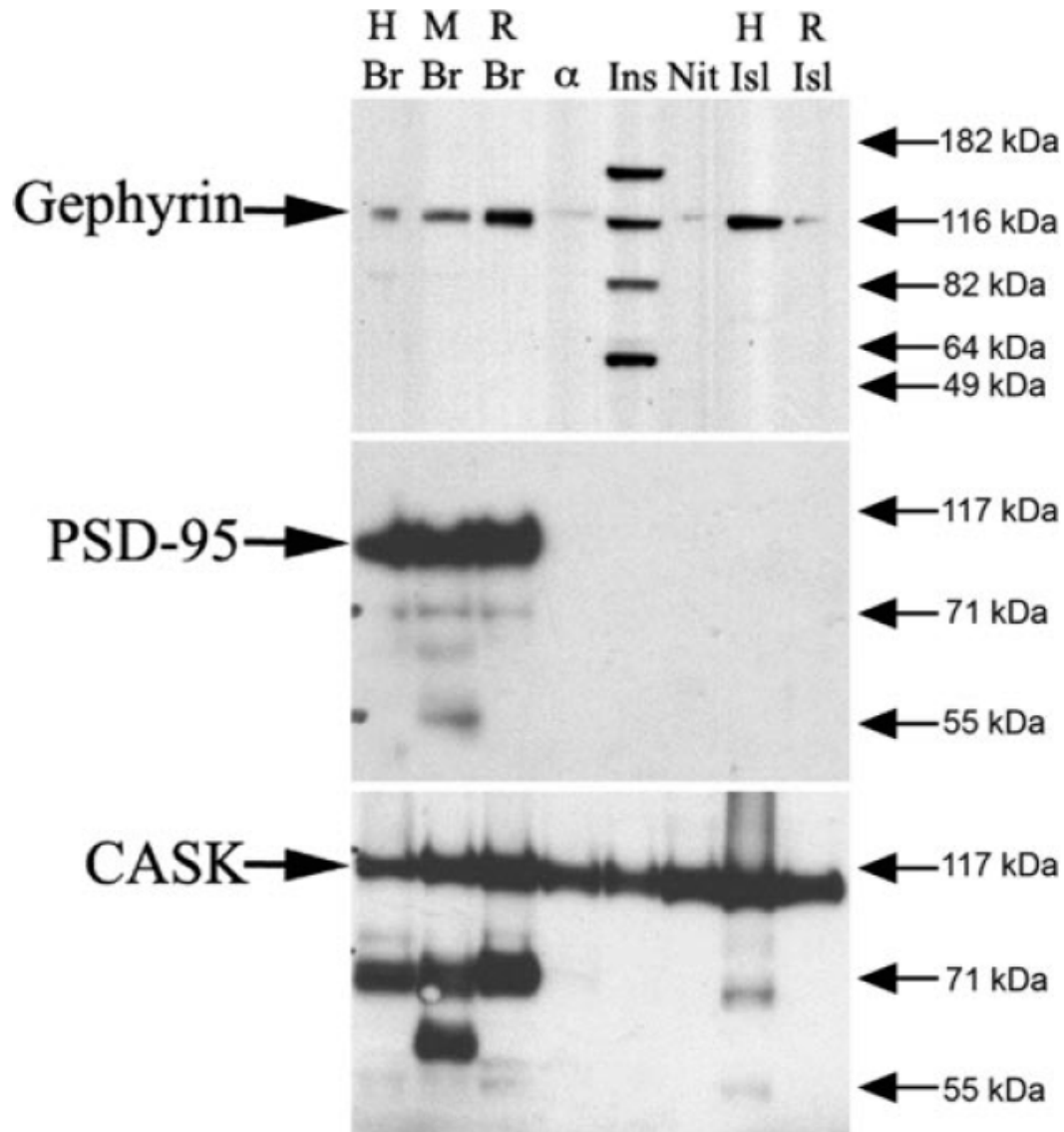


**Figure 4.7. Expression of gephyrin and CASK but not PSD-95 in islets and  $\beta$ -cell lines.**

Western blot analysis was performed on islet and  $\beta$ -cell line extracts using antibodies to gephyrin, PSD-95 and CASK. Brain lysates were used as positive controls. As expected, gephyrin, PSD-95 and CASK were detected in human, mouse and rat brain near their expected molecular weights of 93 kDa, 95 kDa and 120 kDa, respectively. Gephyrin was also detected in human islets, rat islets, INS-1 cells, NIT-1 cells and  $\alpha$ TC-6 cells (with the latter two extracts yielding a weaker band). Alpha-TC6 is a partially dedifferentiated islet  $\alpha$  cell line. PSD-95 was not detected in human islets, rat islets or any of the islet cell-lines tested. CASK was detected in human islets, rat islets and all islet cell lines. (H, human; M, mouse; R, rat; Br, brain;  $\alpha$ ,  $\alpha$ tc-6 cell lysate; Ins, INS-1 cell lysate; Nit, NIT-1 cell lysate; Isl, islet tissue lysate).

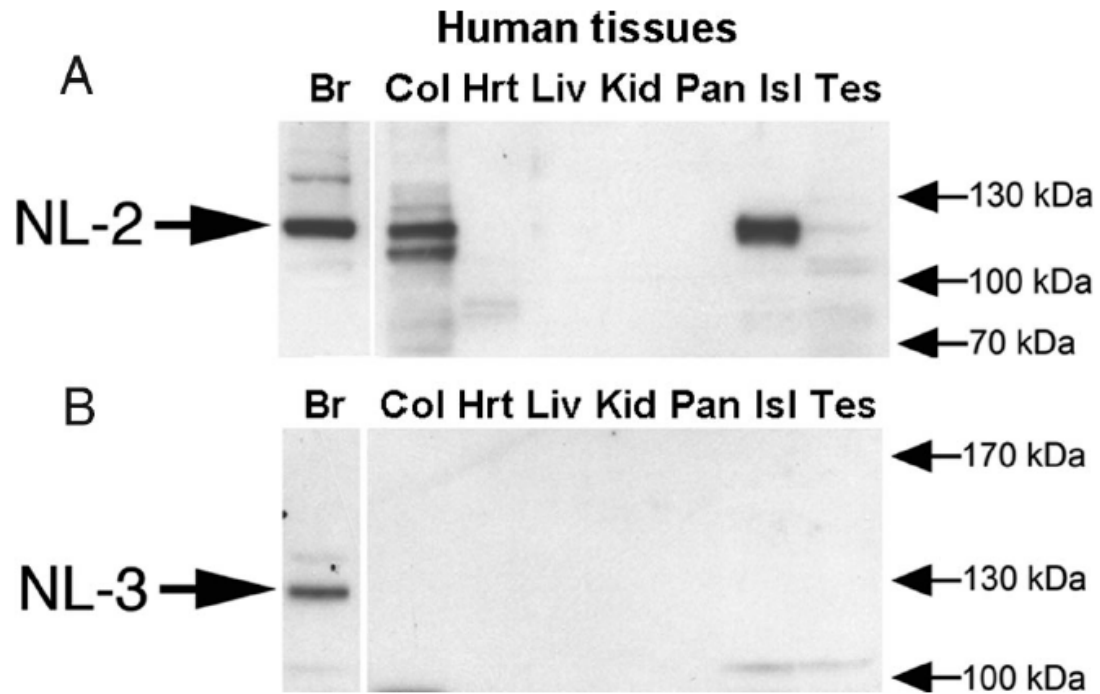


**Figure 4.8. Expression of neuroligin-2 in islets.**

To determine whether neuroligin-2 and neuroligin-3 proteins are expressed in islets, western blot analysis was performed using rabbit polyclonal antibodies to (B) neuroligin-2 and (C) neuroligin-3. (A) Neuroligin-2 was detected in human brain, human colon and human islet cell lysate. Possible low-level expression was also observed in the testes cell lysate. (B) Neuroligin-3 was only detected in human brain. (Isl, Islet extract; Br, brain extract; Col, colon extract; Hrt, heart extract; Liv, liver extract; Kid, kidney extract; Pan, pancreas extract; Tes, testes extract).

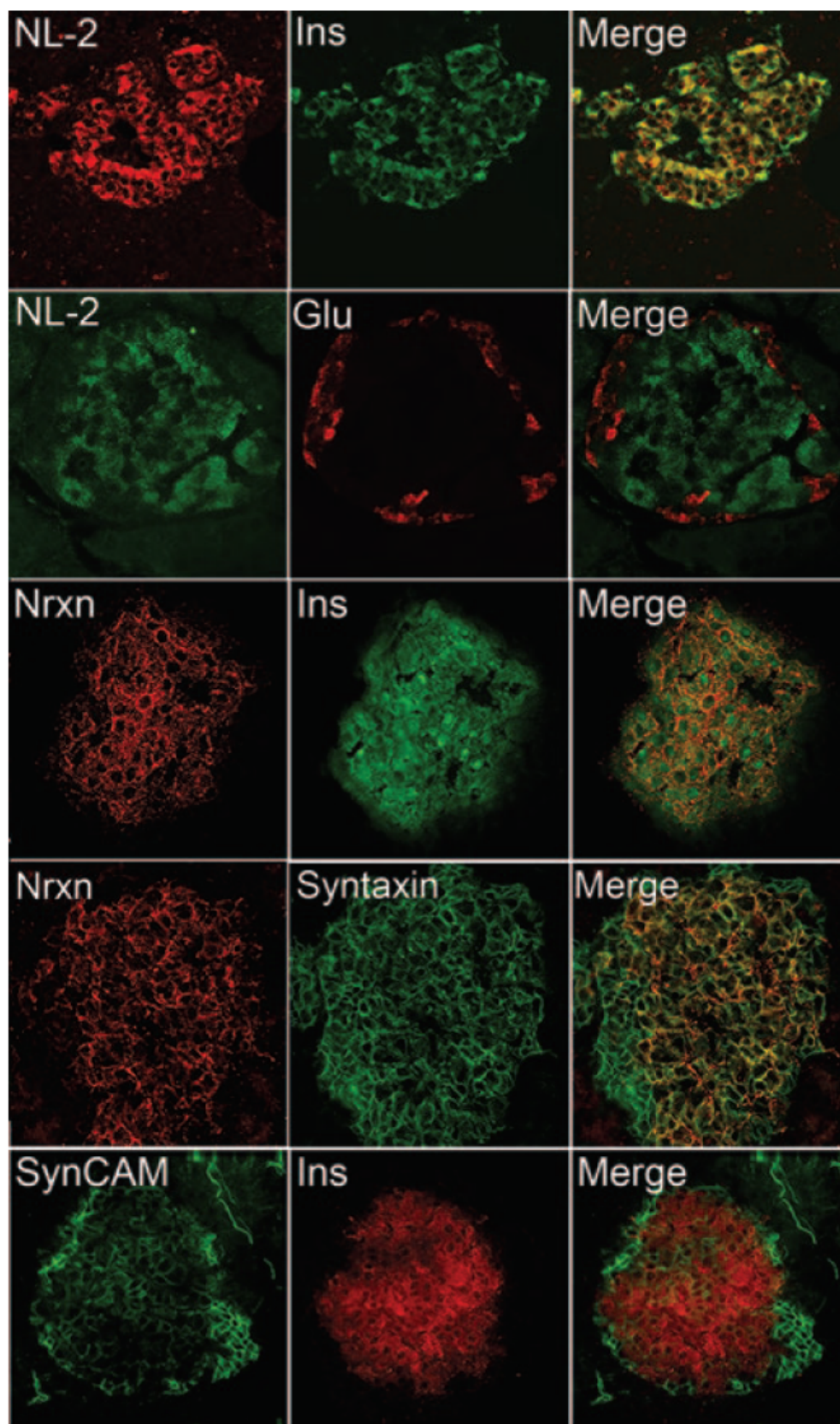
6. *Localization of the synaptogenic adhesion molecules neurexin, neuroligin and SynCAM in pancreatic islets*

To determine the localization of neuroligin and neurexin proteins, immunohistochemistry was performed on rat pancreas sections using antibodies to neurexin and neuroligin. Both neurexin-1 and neuroligin-2 were detected exclusively in cells expressing insulin ( $\beta$ -cells) (Fig. 4.9 rows 1 and 3) but not in cells expressing glucagon ( $\alpha$ -cells) (Fig 4.9 row 2 and Fig. 4.10). Neuroligin-2 staining was not cell-surface specific, indicating that there is a significant cytoplasmic content. This lack of plasma membrane-specific localization of neuroligin is consistent with the pattern of immunostaining previously observed by others in neurons and non-neuronal cell lines: exclusive cell-surface localization of neuroligin proteins is only observed when neuroligins are overexpressed in non-neuronal cell lines such as HEK293 or COS [65, 75, 106]. Neurexin-1 was expressed in a punctate pattern on the surface of the  $\beta$  cells and did not co-localize with insulin (Fig. 4.9 row 3). Neurexin-1 co-localized with syntaxin-1—a SNARE protein expressed on the cytoplasmic face of the  $\beta$ -cell plasma membrane (Fig. 4.9 row 4) [63].

SynCAM, like the neuroligins and neurexins, induces synaptic differentiation in adjacent neurons in coculture experiments [71]. SynCAM's synaptogenic activity is dependent on homophilic SynCAM1 binding interactions or on heterophilic SynCAM1-SynCAM2 binding across the synaptic cleft [71, 187]. If the pattern of expression synapse-inducing adhesion molecules on the  $\beta$ -cell surface resembles that in the synaptic cleft, we reasoned that the  $\beta$  cells would express SynCAM. Immunostaining revealed

**Figure 4.9. Localization of Neuroligin-1, Neuroligin-2 and SynCAM in Pancreatic Islets.**

To determine the localization of neurexin, neuroligin and SynCAM in rat pancreas sections, immunohistochemical localization was performed using antibodies to neurexin-1, neuroligin-2 and SynCAM. Tissues were co-stained for insulin, glucagon or syntaxin-1. Images were captured under either a confocal or deconvolution microscope equipped with a 60x lens. Both neuroligin (row 1) and neurexin (row 3) were exclusively detected in cells that expressed insulin and absent in cells that expressed glucagon (row 2 and supplemental fig. 4), indicating a  $\beta$ -cell specific pattern of expression. Neuroligin-2 displayed some intracellular co-localization with insulin (row 1, yellow in merged image). Neurexin was primarily expressed on the cell-surface and co-localized in  $\beta$ -cells with the plasma-membrane associated SNARE protein syntaxin-1 (row 4). SynCAM was detected both in the islet mantle (the periphery, which primarily consists of non- $\beta$  endocrine cells: mostly  $\alpha$ -cells) and in the insulin positive  $\beta$ -cells (row 5). Staining for SynCAM was consistently stronger in the islet mantle region (NL-2, neuroligin-2; Nrnx, neurexin-1; Ins, insulin; Glu, Glucagon).



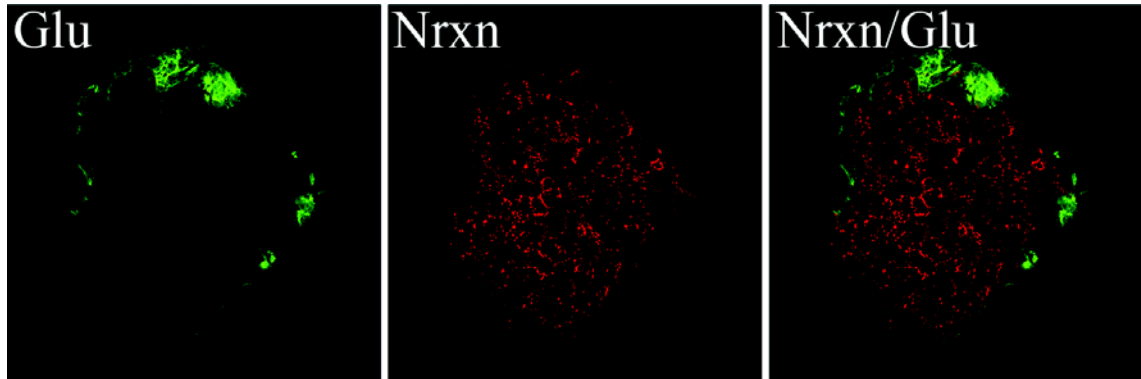


**Figure 4.10. Neurexin-1 is not expressed in  $\alpha$ -cells.**

To determine whether neurexin was expressed in islet  $\alpha$ -cells, immunohistochemical localization was performed using a polyclonal antibody to neurexin-1 and a monoclonal antibody to glucagons. Images were captured with a confocal microscope equipped with a 60x lens. Neurexin was not detected in cells expressing glucagon. (Nrnx, neurexin-1; glu, glucagon).

that SynCAM is expressed on the cell surface of both the  $\alpha$  and  $\beta$ -cells, with higher expression evident in the  $\alpha$ -cells and evident cell-surface localization (Fig. 4.9 row 5). The observed staining pattern was reminiscent of that previously reported for the neural adhesion molecule NCAM [199]. Overall, islet-specific expression of members of each of the three families of synapse-inducing synaptic adhesion molecules—the neuroligins, neuexins and the SynCAMs—was observed.

### *7. Overexpression of neuroligin family members increases insulin secretion*

Since the neuronal neurotransmitter and  $\beta$ -cell insulin secretory apparatuses are highly similar to one another, we asked whether neuroligins are important for insulin secretion [200, 201]. To test this hypothesis, INS-1 cells were transiently transfected with neuroligin-2 and secreted insulin was measured 48 hours post-transfection. Controls included either cells treated with Lipofectamine alone, cells transfected with empty vector or cells transfected with acetylcholinesterase, an  $\alpha$ - $\beta$ -hydrolase-fold protein that shares significant sequence identity with the extracellular domain of the neuroligins [202].

At basal levels of glucose, no significant difference in insulin secretion was observed between mock-transfected cells and cells transfected with acetylcholinesterase. Overexpression of neuroligin-2 resulted in 61% (Fig. 4.11A) and 47% (Fig. 4.11B) increases in secreted insulin relative to mock-transfected cells and cells overexpressing acetylcholinesterase. When insulin secretion was measured in cells transfected with neuroligin-2 at stimulating levels of glucose (15 mM), a 44% increase in insulin secretion was observed relative to mock-transfected controls (Fig. 4.11A). Transfection of the

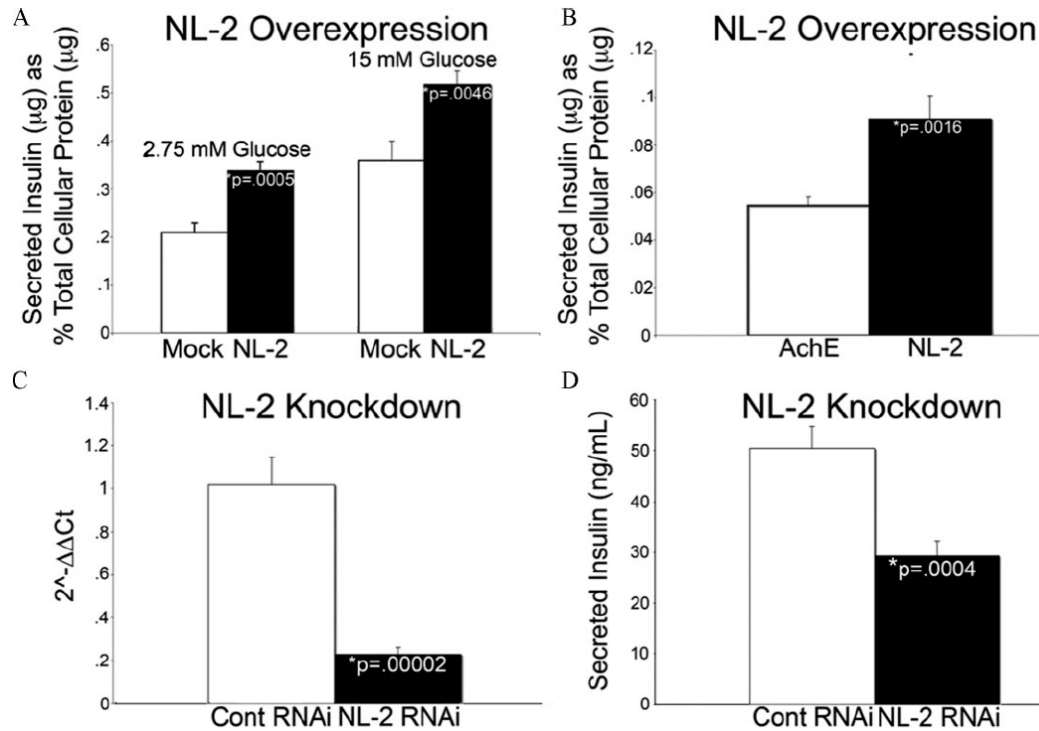


**Figure 4.11. Overexpression and knockdown of neuroligin-2 alters insulin secretion in INS-1 cells.**

INS-1 cells were transfected with a construct encoding full-length neuroligin-2 (NL-2), cultured for 48 hours and then conditioned for 1 hour in a solution containing 2.75 mM glucose. After conditioning, secreted insulin was measured by radioimmunoassay after sequential treatment with low (2.75 mM) and high (15 mM) glucose for 1h each. Secreted insulin was normalized to total cellular protein content. (A) Overexpression of NL-2 increased secreted insulin levels by 61% (n=6, p=.0005) and 44% (n=6, p=.0046) relative to mock-transfected cells when cultured under conditions of low and high glucose. (B) As a control, INS-1 cells were transfected with acetylcholinesterase, a protein which shares significant homology with the extracellular domain of neuroligin. Secreted insulin levels were measured at basal glucose levels and compared to cells transfected in parallel with neuroligin-2. A 66% increase in secreted insulin was observed in NL-2-transfected cells relative to acetylcholinesterase-transfected cells (n=12, p=.0016). Overexpression of NL-1, -3 and -4 similarly increased basal insulin secretion (Fig. 4.12). (C and D) INS-1 cells were transfected with either a pool of non-targeting siRNAs or a pool of siRNAs targeted to NL-2, cultured for 48 hours and then conditioned for 1 hour in a solution containing 2.75 mM glucose. After conditioning, secreted insulin was measured by radioimmunoassay after treatment with 15 mM glucose for 1h. RNA was isolated, reverse transcribed to cDNA and knockdown was analyzed by real time quantitative PCR analysis. (C) NL-2 mRNA was decreased by 77% in cells treated with NL-2 siRNAs relative to those treated with non-targeting siRNAs (n=10, p=.00002). (D) A 42% decrease in secreted insulin was observed in NL-2 siRNA treated cells relative to non-targeting siRNA treated cells (n=10, p=.0004).



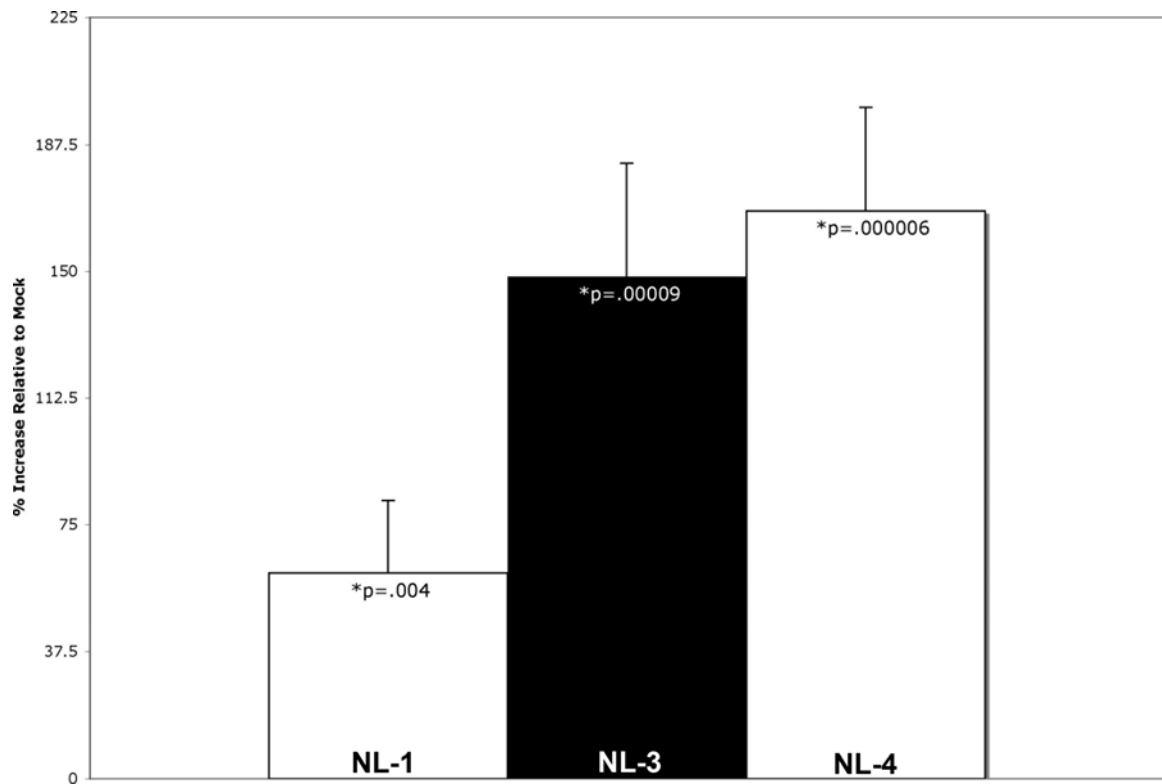


**Figure 4.12. Overexpression of Neuroligin-1, -3 and -4 increase insulin secretion at basal glucose levels.**

INS-1 cells were transfected with a constructs encoding either full-length neuroligin-1, neuroligin-3 or neuroligin-4, cultured for 48 hours and then conditioned for 1 hour in a Krebs-ringer solution containing 2.75 mM glucose. After conditioning, secreted insulin was measured by radioimmunoassay after treatment with low (2.75 mM) glucose for 1h. Overexpression of neuroligin-1, -3 and -4 led to 61% (n=7, p=.004), 149% (n=12, p=.00009) and 168% (n=12, p=.000006) increases in secreted insulin levels relative to mock-transfected controls.

other three major neuroligins into INS-1 cells also increased insulin secretion at basal glucose levels (Fig. 4.12).

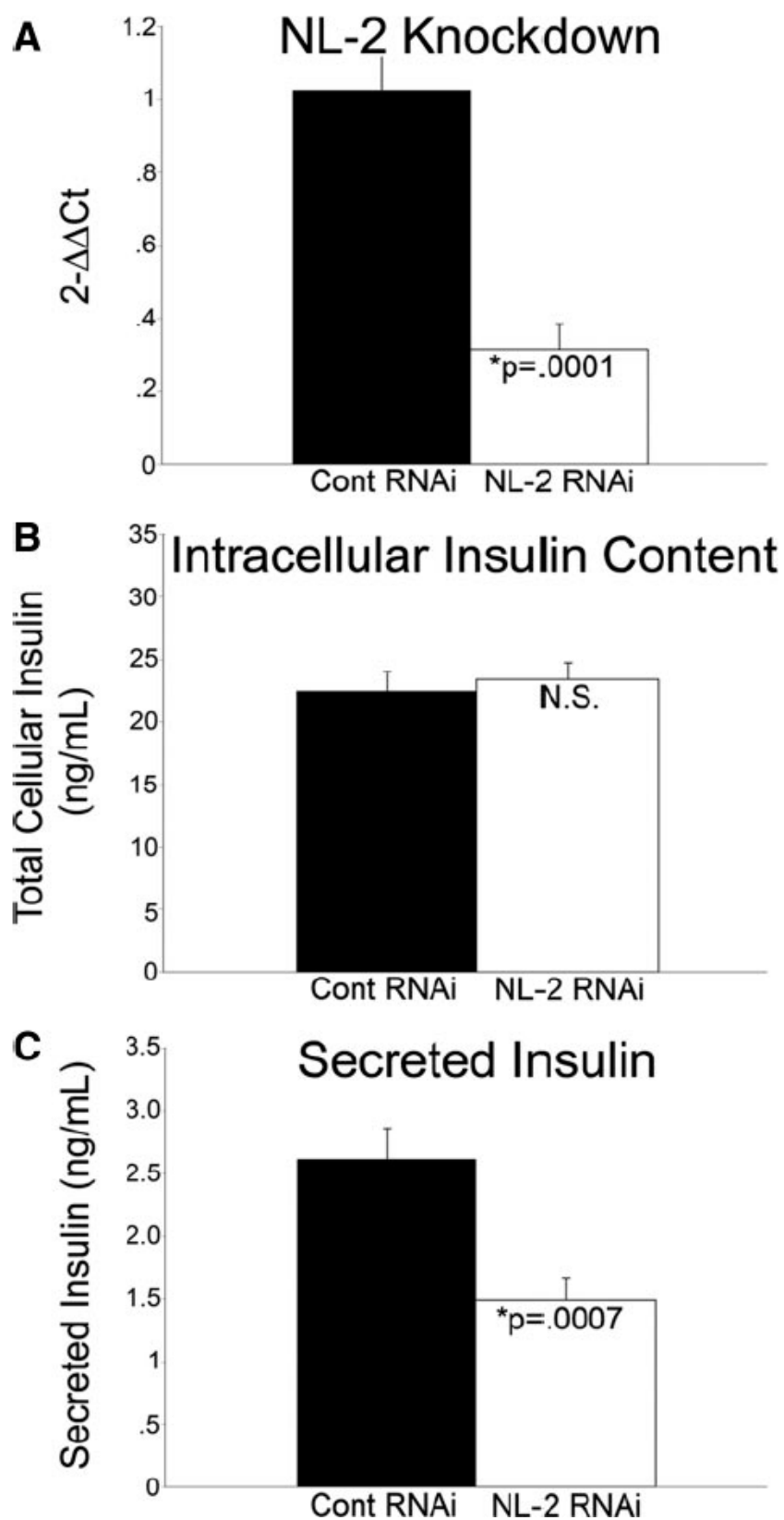
#### 8. *Neuroligin Knockdown Reduces Insulin Secretion in INS-1 Cells and Rat Islet Cells*

INS-1 cells were transiently transfected with either a pool of neuroligin-2 siRNAs or a pool of non-targeting, control siRNAs and secreted insulin was measured 48 hours post-transfection. Knockdown was verified by real time PCR analysis. Neuroligin-2 RNA was decreased by 77% in cells treated with neuroligin-2 siRNAs relative to those treated with non-targeting siRNAs (Fig. 4.11C). After treatment with 15 mM glucose, a 42% decrease in insulin secretion was observed relative to non-targeting siRNA treated control cells (Fig. 4.11D).

Dissociated rat islets were also transfected with either a pool of non-targeting siRNAs or a pool of siRNAs targeted to neuroligin-2 and secreted insulin was measured 48 hours-post-transfection. Neuroligin-2 RNA was decreased by 69% in islet cells treated with neuroligin-2 siRNAs relative to those treated with non-targeting siRNAs (Fig. 4.13A). Total intracellular insulin was virtually identical between cells treated with control siRNAs and neuroligin-2 siRNAs (Fig. 4.13B). Under high glucose conditions (25 mM), a 43% decrease in secreted insulin was observed in neuroligin-2 siRNA treated dispersed islet cells relative to non-targeting siRNA treated dispersed islet cells. Dissociated islet cells treated with high glucose (25 mM) and non-targeting siRNA secreted 40% more insulin than those treated with low glucose (2.75 mM) and non-targeting siRNA (n=6, p=.01; Fig. 4.14). Consistent with previous studies performed on dissociated rat islet cells, robust glucose-stimulated insulin secretion was not observed in

**Figure 4.13. Knockdown of neuroligin-2 in dissociated rat islets inhibits insulin secretion.**

Dissociated rat islets were transfected with a pool of control, non-targeting siRNAs or a pool of siRNAs targeted to neuroligin-2, cultured for 48 hours and then conditioned for 1 hour in a solution containing 2.75 mM glucose. After conditioning, secreted insulin was measured by radioimmunoassay after treatment with high (25 mM) glucose for 1h. (A) RNA was isolated from half of the samples, reverse transcribed to cDNA and knockdown was analyzed by real time quantitative PCR analysis. Neuroligin-2 was decreased by 69% in dispersed islet cells treated with neuroligin-2 siRNAs relative to those treated with control siRNAs (n=6, p=.0001). (B) Protein was isolated from the other half of the samples and total cellular insulin content was measured in the cell lysate. No difference in insulin content was detected between cells treated with control siRNAs and neuroligin-2 siRNAs. An equal amount of lysis buffer was used to prepare each sample. (C) Under high glucose conditions (25 mM), a 43% decrease in secreted insulin was observed in neuroligin-2 siRNA treated dispersed islet cells relative to control siRNA treated cells (n=12, p=.0007). At 2.75 mM glucose, there was no significant change in insulin secretion between cells treated with control siRNA and those treated with neuroligin-2 siRNA.



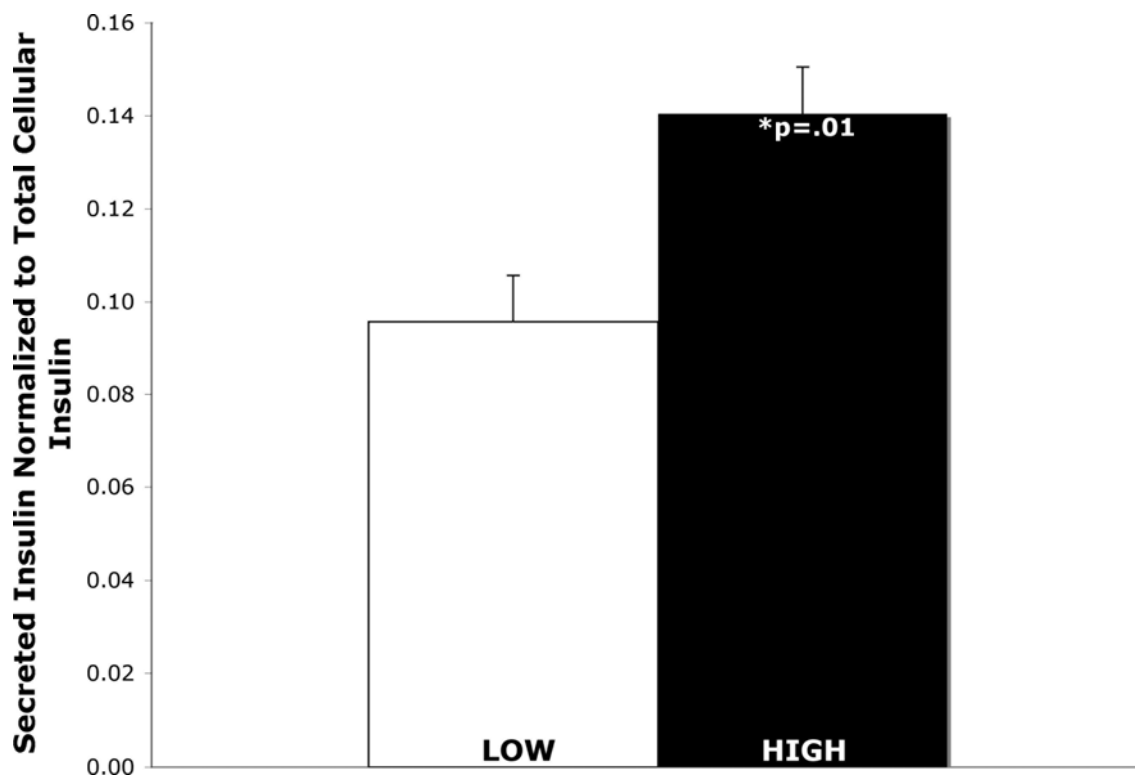


**Figure 4.14. Insulin secretion from dispersed islet cells treated with low and high glucose.**

Dispersed islets were transfected with a pool of non-targeting siRNA, cultured for 48 hours and then conditioned for 1 hour in Krebs-ringer solution containing 2.75 mM glucose. After conditioning, basal insulin secretion was measured by radioimmunoassay after treatment with low (2.75 mM) glucose for 1h. Dispersed islets were then treated with high glucose (25 mM) for 1 hour to measure stimulated insulin secretion. Dispersed islet cells treated with high glucose (25 mM) and non-targeting siRNA secreted 40% more insulin than those treated with low glucose (2.75 mM) and non-targeting siRNA (n=6, p=.01). Secreted insulin was normalized to total insulin in the cell layer.

these studies [203]. Under low glucose conditions, a significant difference in secreted insulin was not observed between dispersed islet cells treated with neuroligin-2 siRNA and cells treated with non-targeting siRNA.

## E. Discussion

The great resemblance at the molecular level between the  $\beta$  cells of the endocrine pancreas and inhibitory (GABAergic) synapses suggests that key insights into the final functional maturation of  $\beta$ -cells can be derived from knowledge of synapse formation and differentiation [1, 2, 5, 22]. A similar resemblance has been observed between the  $\alpha$ -cells of the endocrine pancreas and excitatory (glutamatergic) synapses [204]. During synaptogenesis, the synaptogenic adhesion molecules neurexin and neuroligin appear to be important for instructing a developing synaptic density to become either glutamatergic (excitatory) or GABAergic (inhibitory) [74, 181, 188]. Here, we demonstrate that islets express several neurexin and neuroligin family members and reveal a pattern of expression in  $\beta$  cells that resembles the pattern observed in inhibitory synapses. Overall, these results indicate that knowledge of the pathways that guide inhibitory synapse formation will aid in our understanding of  $\beta$ -cell development and functional differentiation.

### 1. *Neuroligin and neurexin gene expression in rat and human islets and INS-1 $\beta$ cells*

In the CNS, neuroligin-2 is specifically expressed by and important for the differentiation of inhibitory synaptic densities [74, 76], and neuroligin-1 is primarily

expressed by and implicated in the differentiation of excitatory synapses [74, 75]. Alpha-neurexins, like neuroligin-2, specifically promote the formation of inhibitory synaptic densities in co-culture studies [188]. Rat and human islets and the  $\beta$  cell line INS-1 all express high levels of both neuroligin-2 and neurexin-1 $\alpha$ , a finding consistent with published microarray results identifying these genes as having high level expression in human islets [205]. In marked contrast to the brain, in which neurexin-1 $\alpha$  and neurexin-1 $\beta$  are expressed at similar levels, islet and INS-1 neurexin-1 expression consists almost exclusively of the  $\alpha$  form. Neuroligin-1 is also expressed at high levels by rat and human islets but is only detected at low levels in INS-1 cells. The expression of high levels of neuroligin-2 and neurexin-1 $\alpha$  in these cells, and relatively low levels of neuroligin-1 in INS-1  $\beta$  cells, along with immunolocalization studies demonstrating that expression of neuroligin-2 and neurexin-1 is restricted to  $\beta$  cells are consistent with the idea that the functional differentiation of the  $\beta$ -cells parallels that of the inhibitory synapse.

Expression by  $\beta$  cells of the inhibitory synaptic marker gephyrin but not the excitatory synaptic marker PSD-95, is further evidence of their parallel development. Interestingly, neuroligin-1 promotes the formation of inhibitory synapses in the absence of PSD-95 [106]. Although an effect on inhibitory synapses is not observed in the CNS of mice lacking the neuroligin-1 gene [74], the high level expression of neuroligin-1 in islets along with the absence of PSD-95 might favor the development of an inhibitory phenotype by  $\beta$  cells. Alternatively, neuroligin-1 might, as it does in the CNS, promote the development of the excitatory phenotype observed in  $\alpha$  cells.

## 2. *Alternative splicing of neurexin and neuroligin in islets*

Because alternative splicing of neuroligin and neurexin transcripts helps to determine the ability of specific pairs of neurexin and neuroligin proteins to interact, the pattern of expression of alternative splicing contributes towards the specification of nascent synapses as either excitatory or inhibitory [77, 184, 188, 194]. We found that human islet and INS-1  $\beta$ -cell neurexin-1 transcripts uniformly contain an insert at splice site 4. This clearly differentiates the pattern of INS-1  $\beta$ -cell neurexin-1 splicing from that observed in the rat brain, in which both insert-positive and insert-negative forms are expressed [188]. This splicing pattern, along with the predominance of the  $\alpha$  form of neurexin-1, would be expected to strongly favor development of an inhibitory synaptic phenotype [77, 188].

Neuroligin-1 transcripts with an insert at splice site B (neuroligin-1B+) are predominant in islets, matching the pattern observed in brain [184]. The splice insert at site B introduces a site of N-glycosylation that impedes the binding of neuroligin-1B+ to splice site 4-positive neurexin-1 $\beta$  molecules. In neurons, inclusion of the insert at neuroligin-1 site B favors excitatory synapse formation. In islets, neuroligin-1B+ molecules might be important for promoting the development of glutamatergic signaling within  $\alpha$  cells—an autocrine signaling mechanism important in the regulation of glucagon secretion from these cells [204]. As in brain,  $\beta$ -cell neuroligin-1 and -2 transcripts containing an insert at splice site A are predominant. A report by Chih et al. suggests an association between inclusion of the alternatively spliced exon at this site and the formation of GABAergic synapses [184].



In neuroligin-3, two splice inserts can be alternatively spliced into splice site A. Neuroligin-3 has been less well studied than neuroligins-1 and -2, and the effects of alternative splicing on interactions with neurexins is unknown. We found that in both islets and brain, neuroligin-3 transcripts are produced containing none, one, or both of the alternative site A inserts. Further work will be required to unravel the function of neuroligin 3 and the role of alternative splicing at neuroligin-3 site A in both neurons and  $\beta$  cells.

### *3. Expression of gephyrin, but not PSD-95, in $\beta$ cells*

Gephyrin is a post-synaptic cytoplasmic protein that clusters near GABA<sub>A</sub> receptors and binds the intracellular domain of neuroligin-2 [195].  $\beta$ -cell expression of gephyrin is consistent with an inhibitory synapse-like character. The presence of GABA<sub>A</sub> receptors on the surface of human  $\beta$  cells further enhances this similarity [206]. In contrast, PSD-95--a protein that clusters exclusively at excitatory synapses--was not detected in islets or in  $\beta$ -cell lines [207].

### *4. $\beta$ cell-specific expression of neurexin and neuroligin*

Immunolocalization studies demonstrated that  $\beta$  cells express members of each of the three synaptic adhesion protein families that are capable of inducing synaptogenesis in cultured neurons: the neuroligins, the neurexins and the SynCAMs. The ability of these proteins to initiate assembly of the presynaptic exocytic machinery points to their potential importance in  $\beta$ -cell secretory function. The expression of these proteins

suggests that the  $\beta$  cell surface displays synaptic adhesion proteins capable of heterophilic or (in the case of SynCAM) homophilic extracellular binding interactions [71, 187, 208]. Since  $\beta$  cells lack an equivalent of the axon/dendrite polarization of synaptic protein expression in neurons, neuroligin-neurexin interactions can potentially occur in trans (between molecules on different  $\beta$  cells) and/or in cis (between molecules on the surface of the same  $\beta$  cell). Structural characterization of neurexin-neuroligin interactions in neurons indicates that a trans interaction is likely [189, 194, 209]. The possibility of trans-cellular interactions between heterophilic binding partners co-expressed on the  $\beta$  cell surface is exemplified by Ephrin A and EphA, which were recently shown to be co-expressed on the  $\beta$  cell surface, to localize to different micro-domains and to engage in trans interactions that help regulate insulin secretion [85].

It has been observed that mature nerve terminals develop in neuronal processes at sites of contact with cultured islet endocrine cells [210]. The presence on the  $\beta$  cell surface of neuroligins, neurexins and SynCAM available for interaction with their neuronal binding partners would readily explain how cultured islet cells induce synaptic differentiation in neurons.

Unlike neuroligin-2 or neurexin, SynCAM is present on both the  $\alpha$  and  $\beta$  cell surface, and SynCAM binding interactions could potentially bridge the two different cell types. The neural adhesion protein NCAM shares with SynCAM a pattern of  $\alpha$ -cell predominant islet expression [199, 211]. NCAM is neither synapse-specific nor synapse-inducing, so it is unclear whether, despite their similar intra-islet distribution, NCAM's function in mediating islet cell organization provides clues as to the role of SynCAM.

### 5. *Involvement of neurexin and neuroligins in exocytosis and conclusion*

During synaptogenesis, transcellular neurexin-neuroligin interactions initiate the assembly of a complex presynaptic scaffolding assembly around Mint and CASK proteins bound to neurexin PDZ domains [212]. Mint is expressed in  $\beta$ -cells [18]. Consistent with the idea that  $\beta$ -cell and synaptic secretory function develop along parallel pathways, we have found that CASK is also expressed. It is possible that neuroligin-neurexin interactions similarly enable GABA secretion by  $\beta$  cells. However, it is also conceivable that the GABAergic and insulin secretory assemblies are separate, perhaps being formed at sites seeded by a distinct combination of neurexin-neuroligin interactions.

There is a very high degree of overlap between the proteins known to mediate neurotransmitter secretion and those known to mediate insulin secretion, and it is highly likely that assembly of the apparatus necessary for insulin release is, like assembly of the presynaptic active site, dependent on neuroligin-neurexin interactions. Our finding that neuroligin overexpression increases insulin secretion and that neuroligin knockdown decreases insulin secretion in both INS-1 cells and rat islet cells supports the hypothesis that the neuroligins are involved in insulin secretion. This is consistent with the recent observation that the neuroligin-1 gene is one of two genetic loci linked to fasting insulin levels [213]. Preliminary evidence that neurexin knockout mice exhibit impaired insulin secretion and hyperglycemia also implicates the neurexins as participating in the insulin secretory mechanism [214]. The involvement of transcellular neurexin-neuroligin interactions in insulin exocytosis may, like Ephrin-Eph A interactions, contribute to the decreased glucose-stimulated insulin secretion by individual  $\beta$  cells that is observed after

islet dissociation [82, 84, 86, 203]. Extracellular interactions involving SynCAM may similarly function to help establish normal  $\beta$  cell secretory function.

In the future, it will be important to identify the specific roles in  $\beta$ -cell functional maturation and exocytic function of each of the individual neuroligins, neurexins and SynCAMs expressed within the islet. This may lead to new means by which to coax  $\beta$ -cells generated in vitro into behaving more like true  $\beta$  cells—for example, by inducing expression of inhibitory-synapse-associated proteins—and to new therapies for modulating islet function and thereby treating diabetes.

#### G. Acknowledgements

Chapter 4 is a reprint of the material as it appears in Suckow, A. T., Comoletti, D., Waldrop, M., Mosedale, M., Egodage, S., Taylor, P. and Chessler, S. D. (2008). *Endocrinology*. The dissertation author was the primary investigator in the development and execution of the study, and the principal author of this paper.

CHAPTER 5: UTILIZATION OF THE INHIBITORY SYNAPTIC MACHINERY FOR  
REGULATION OF INSULIN SECRETION: IDENTIFICATION OF A NEUROLIGIN-  
DEPENDENT BUT NEUREXIN-INDEPENDENT MECHANISM FOR  
REGULATION OF INSULIN SECRETION FROM PANCREATIC BETA-CELLS.

A. Introduction

The architecture of the pancreatic islet  $\beta$ -cell secretory apparatus is remarkably similar to the machinery used by neurons for neurotransmitter release. Many of the scaffolding and synaptic vesicle proteins important for neurotransmitter secretion are expressed by  $\beta$ -cells and seem to be key components of the insulin secretory machinery [12-18]. In  $\beta$ -cells and neurons, the proper differentiation, assembly and functioning of this machinery is dependent on interactions between opposing cell membranes [82, 87, 215].

In neurons, synaptic adhesion molecules (SAM) on dendrites interact through both homophilic or heterophilic mechanisms with SAM family members on axons to recruit the machinery necessary for neurotransmitter release to the synapse (pre-synaptic differentiation) [216]. SAM families that can induce the assembly of the synaptic exocytic machinery on neurons include neuroligin, SynCAM, netrin G ligands and EphB. Co-culture experiments using non-neuronal cell lines expressing each of these proteins demonstrated that they can induce presynaptic differentiation at points of contact between the non-neuronal cells expressing these proteins and hippocampal neurons [71, 72, 217, 218]. These findings have been validated *in vivo* as mice lacking the genes for several of these SAMs have significant synaptic dysfunction [72, 217, 219, 220].

Interactions are also important between islet  $\beta$ -cells, providing for maintenance of a differentiated state and a robust secretory response to glucose [82, 87]. Unlike  $\beta$ -cells embedded in islets, dissociated  $\beta$ -cells fail to secrete insulin in response to glucose. Reaggregation of these cells restores normal stimulus-secretion coupling [87]. Analysis of secretion from individual  $\beta$  cells relative to contacting  $\beta$ -cell pairs, triplets and so on reveals increased glucose-stimulated insulin secretion on a per cell basis as the number of contacting cells increases. This effect is not observed when the contacting cell is another islet cell type [82]. Contact enhanced stimulus-secretion coupling has been replicated in the  $\beta$ -cell line MIN-6, thereby validating it as a satisfactory model for studying cell-cell interactions in  $\beta$ -cells [84, 86]. The molecular basis for this phenomenon in MIN-6 cells and islets has been attributed, at least in part, to homophilic cadherin and heterophilic ephrin A/ephrin A interactions [83, 85].

The neuroligin family of SAMs, and in particular neuroligin-2, is of particular interest because neuroligin-2 is expressed specifically by  $\beta$  cells and has been implicated by our group in the regulation of glucose-stimulated insulin secretion in INS-1  $\beta$ -cells and rat islets [149]. In neurons, interaction of post-synaptic neuroligin with either neurexin or another protein is thought to drive the recruitment of the neurotransmitter release machinery to the axonal membrane [66, 185]. Evidence that neuroligin regulates pre-synaptic differentiation through another protein comes from the finding that non-synaptogenic neuroligin point mutants can still interact with neurexin as effectively as wildtype neuroligin and from studies where overexpression of non-neurexin binding neuroligin mutants in neurons enhances synaptic density equally as well as wildtype

neurons [66, 221]. *In vivo* studies confirm the role of neuroligin in presynaptic differentiation as significantly higher expression levels of several key components of the exocytic machinery are observed in transgenic mice overexpressing neuroligin-2, and significant deficits and dysfunction in several key components of the exocytic machinery are observed in mice lacking all three neuroligin genes [72, 80]. The clear role of neuroligin-2 in the maintenance and differentiation of the neurotransmitter release machinery, along with the importance of cell-cell contacts in the regulation of stimulus secretion in  $\beta$  cells, led us to hypothesize that neuroligin drives the assembly of the  $\beta$  cell secretory apparatus through *trans*-cellular interactions and that this interaction facilitates glucose-stimulated insulin secretion in contacting cells.

Here, we demonstrate cell-surface expression of neuroligin-2 in  $\beta$  cells and the presence of a neuroligin-2 binding partner on the surface of these cells. Further, we provide evidence that neuroligin-2 is important for contact enhanced stimulus-secretion coupling through co-culture assays in MIN-6 cells and through use of a soluble neuroligin-2 protein to disrupt endogenous *trans*-interactions in rat islets. Evidence that the ability of neuroligin-2 to drive GSIS occurs through a neurexin-independent mechanism is also presented. Combined, these data suggest that neuroligin may promote the development, maturation and maintenance of stimulus-secretion coupling in  $\beta$  cells through *trans*-cellular interactions.

## B. Materials and Methods

### *Antibodies*

The following antibodies were obtained commercially: mouse anti-FLAG (Sigma-Aldrich Corp., St. Louis, MO), goat anti-mouse HRP, goat anti-rabbit HRP (Santa Cruz Biotechnology, Inc., Santa Cruz, CA) and Alexa Fluor 488 goat anti-mouse IgG (Invitrogen, Carlsbad, CA). Rabbit antibodies against neuroligin-2 were made by Lampire Biological Laboratories after injection of the soluble extracellular domain. Antiserum was validated for affinity to neuroligin-2 by ELISA and Western blotting. Incubation of the antibodies with soluble NL-2 prior to primary antibody incubation abolished binding to transfected NL-2 and the co-migrating bands in rat brain (Fig. 5.1). Rabbit antibodies against  $\alpha$ -neurexin were made by after injection of the KLH conjugated cytoplasmic peptide CAKSANKNKKNKDKEYV. Antiserum was validated for affinity to  $\alpha$ -neurexin by ELISA and Western Blotting, and specificity confirmed by knockdown of endogenous  $\alpha$ -neurexin via RNA interference and Western Blotting (Merrie Mosedale, Unpublished Data).

### *Cell Culture*

INS-1 cells were obtained from the University of Washington Diabetes and Endocrinology Research Center Virus, Molecular Biology and Cell Core. INS-1E cells were generously provided by Dr. Pierre Maechler at the Universite De Genève. MIN-6 cells were generously provided by Dr. R. Paul Robertson at the University of Washington, Dr. Fred Levine at the University of California, San Diego and Dr. Kathryn Haskins at the University of Colorado Denver.



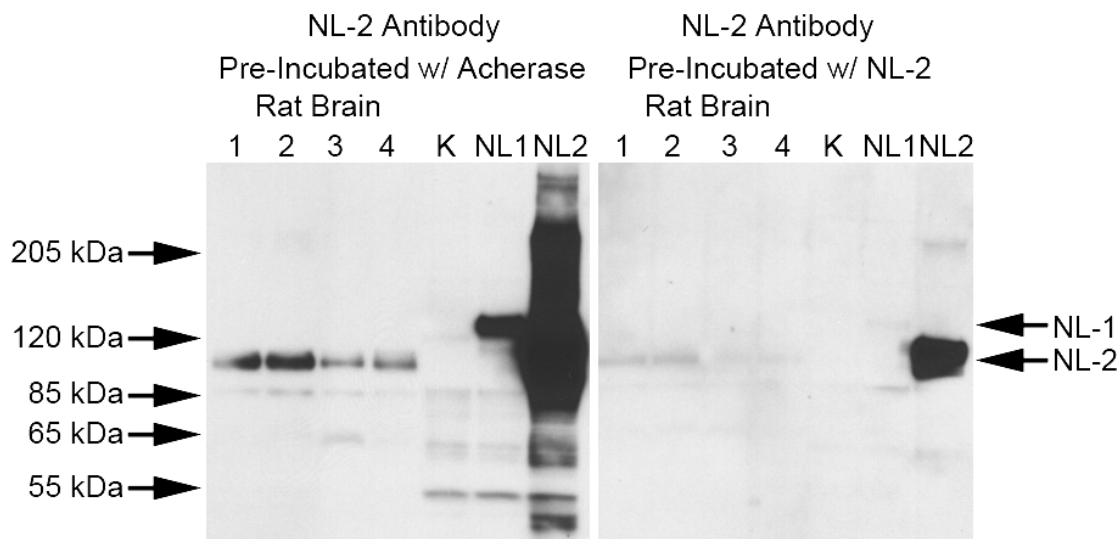


**Figure 5.1. Immunoblotting Analysis with Neuroligin-2 Antibodies Pre-incubated with Soluble Acetylcholinesterase or Soluble Neuroligin-2.**

To validate antibodies generated against the extracellular domain of neuroligin-2, Western blot analysis was performed after pre-incubation of the antibodies with a 200-fold molar excess of soluble acetylcholinesterase (left blot) or neuroligin-2 (right blot). On blots treated with antibody pre-incubated with acetylcholinesterase, neuroligin-2 was detected at its expected molecular weight in rat brain lysates. These bands co-migrated with a band in HEK cells transfected with full-length neuroligin-2 that is absent in untransfected HEK cells. A band was also detected in cells transfected with neuroligin-1, indicating some affinity for this close family member. On blots treated with antibody pre-incubated with neuroligin-2, the neuroligin-2 bands were greatly diminished in rat brain lysates and HEK cells transfected with neuroligin-1 and neuroligin-2. (Acherase, acetylcholinesterase; NL-2, neuroligin-2; 1, rat brain lysate; 2, rat brain lysate; 3, rat brain lysate; 4, rat brain lysate; K, untransfected HEK cells; NL1, HEK cells transfected with full-length NL-1; NL2, HEK cells transfected with full-length NL-2).

INS-1 and INS-1E cells were cultured in RPMI 1640 medium supplemented with 10% fetal bovine serum, 50  $\mu$ M  $\beta$ -mercaptoethanol, 1 mM sodium pyruvate, 2 mM L-glutamine, 100 U/mL penicillin, and 100 mg/mL streptomycin. MIN-6 cells were cultured in DMEM supplemented with 20% fetal bovine serum, 2 mM L-glutamine, 50  $\mu$ M  $\beta$ -mercaptoethanol, 100 U/mL penicillin, and 100 mg/mL streptomycin. HEK cells were cultured in DMEM supplemented with 10% fetal bovine serum, 2 mM L-glutamine, 100 U/mL penicillin, and 100 mg/mL streptomycin. Rat Islets were cultured in 2.75 mM glucose RPMI 1640 medium supplemented with 10% fetal bovine serum, 2 mM L-glutamine 100 U/mL penicillin, 100 mg/mL streptomycin and 250  $\mu$ g amphoterecin B. All cells were cultured in a humidified 37° C incubator with 5% CO<sub>2</sub>.

For transfections, HEK cells were plated onto 12-well plates and allowed to grow to 100% confluency in antibiotic-free media. The cells were then transfected with the gene of interest using Lipofectamine 2000 (invitrogen) according to the manufacturer's protocol. Unless otherwise noted, cells were incubated in the transfection cocktail for 48 h before insulin secretion studies and confirmation of gene expression.

### *Protein Purification*

A soluble NL-2 cDNA was generated by introducing a stop codon at phenylalanine 616 of the FLAG-tagged full-length cDNA [189]. The soluble NL-2 was then stably transfected into HEK cells by G418 selection (Sigma-Aldrich Corp). After 3-4 weeks, surviving cells formed colonies suitable for clonal selection. The best producing clones were identified by Western Blotting and expanded in triple layer flasks. After the cells reached 100% confluency, the medium was collected daily and passed over an M2 anti-

FLAG affinity column (Sigma-Aldrich Corp.). The column was washed twice with a 10 mM Hepes/150 mM NaCl buffer and protein was eluted in this Hepes/NaCl buffer containing 100 µg/mL FLAG Peptide. The soluble NL-2 protein was then concentrated in a 30,000 MW Amicon concentrator (Millipore, Billerica, MA) and analyzed on an SDS-PAGE gel by coomassie staining (Invitrogen).

To make NL-2 Fc (NL-2-hIgG), the cDNA encoding for the soluble extracellular domain of neuroligin-2, from AA P42 to L615, was cloned into a PCMV6-XL4 using NOT/Xba restriction enzymes. The original vector, pCMVIGN1a-1, was a kind gift of Dr. Thomas Südhof (Stanford, CA) and it was described in Ushkaryov et al. 1994 [222]. We adapted this construct with the introduction of a 3C protease cleavage site between residue L615 of NLGN2 and the first residue of the hIgG sequence. HEK cells were stably transfected with this construct and selected as described above. The best producing clones were identified by Western Blotting and expanded in triple layer flasks. After the cells reached 100% confluency, the medium was collected daily and passed over a protein A column (Invitrogen). The column was washed twice with Protein A IgG binding buffer (pH 8; Pierce) and then NL-2 Fc protein was eluted with Protein A IgG elution buffer (pH 2.8; Pierce). The soluble NL-2 protein was then concentrated and analyzed as described above.

Soluble acetylcholinesterase was prepared as described previously [223]. Soluble neuroligin-1 was generated by introducing a stop codon at isoleucine 639 of the FLAG-tagged full-length cDNA [189]. To generate non-neurexin binding neuroligin mutant (G500A), site-directed mutagenesis was performed to substitute alanine (GCC) for glycine (GGC).

### *Flow Cytometry*

After MIN-6, INS-1 and INS-1E cells reached 100% confluency in 75 cm<sup>2</sup> flasks, suspensions of cells were prepared by removing the cells with Cellstripper (Cellgro, Manassas, VA), washing the cells with complete media and then equilibrating the cells in Kreb's ringer bicarbonate buffer (KRBB). Cells were then incubated for 45 minutes at 37° C with 700 nM FLAG peptide or 700 nM FLAG-NL-2 pre-incubated with monoclonal FLAG antibody, washed three times with ice cold KRBB and then incubated with AlexaFluor 488 goat anti-mouse IgG for 30 minutes at 4° C. They were washed three more times with KRBB and analyzed by flow cytometry using a FACSCalibur (BD Biosciences, San Jose, CA).

For experiments to determine whether NL-2 is present on the surface of INS-1, suspensions of cells were incubated for 45 minutes at 4° C with either pre-immune serum or NL-2 antibodies, washed three times with ice cold KRBB and then incubated with AlexaFluor 488 goat anti-rabbit IgG for 30 minutes at 4° C. They were washed three more times with KRBB and analyzed as described above.

### *Islet Isolation*

Islets were isolated from Sprague-Dauley or Wistar rats (240-260 grams; Charles River, Wilmington, MA) euthanized with an intra-peritoneal injection of 150 mg/kg nembutol as previously described [99]. Briefly, pancreata were digested with collagenase P (Roche, Indianapolis, IN) and islets were isolated from acinar tissue on a Histopaque gradient (Sigma-Aldrich). Islets were handpicked under a dissecting microscope and 10 islets were plated per well on a 96-well plate. Prior to experimental analysis, they were

cultured in RPMI 1640 containing 2.75 mM glucose for 18 hours to allow for recovery from the isolation process. All animal procedures were approved by the University of California, San Diego Internal Animal Care and Use Committee. For some experiments, islets were provided by the University of Washington Diabetes and Endocrinology Research Center Islet Cell and Functional Analysis Core.

### *Competitive Binding Assays*

Soluble neuroligin-2 was labeled with  $^{125}\text{I}$  by Dr. Robert Speth by the Iodogen method according to the manufacturer's protocol (Pierce, Rockford, IL). The specific activity of  $^{125}\text{I}$ -labeled soluble neuroligin-2 was  $113.7 \mu\text{Ci}/\mu\text{g}$ .

After iodination, polypropylene test tubes containing INS-1E cells ( $2.5 \times 10^5$ ) in 170  $\mu\text{L}$  of media were placed in a shaking water bath at 37 degrees Celsius for 30 minutes. Using an Eppendorf Repeater pipet, varying concentrations of unlabeled neuroligin-2 were added to the test tubes just prior to adding  $^{125}\text{I}$ -labeled soluble neuroligin-2. The cells were further incubated for 30 minutes. The concentration of  $^{125}\text{I}$ -labeled soluble neuroligin-2 in the media was approximately 50 pM. Accumulation of radiolabel was determined by separating the cell associated radioactivity (CAR) from the free radioactivity by transferring the cell suspension to a 0.4 mL centrifuge tube containing a layer of oil consisting of 1:37.5 volume to volume ratio of n-dodecane: bromo-dodecane (Sigma-Aldrich) and spinning for 8 seconds at  $12,535 \times g$ . Tubes were placed briefly in liquid nitrogen, cut through the radioactive-free oil layer with a razor blade, and the bottom portion of the tube containing the pellet was placed into a borosilicate glass scintillation vial (7mL). Radioactivity was counted on a gamma

counter (Packard 5500 Augogamma gamma counter, Meriden, CT). The CAR relative to the CAR<sub>w</sub> of water was calculated as the ratio of CAR for soluble neuroligin-2 to the CAR of [3H]-water (Amersham Life Science, Buckingham, England) that was determined by counting on a Packard Tri-Carb liquid scintillation counter (Model 1900CA, Packard, Meriden, CT).

#### *Soluble NL-2 Insulin Secretion Studies*

Suspensions of small clusters of MIN-6 cells were prepared as described above. Cells were then washed twice with KRBB containing 2.75 mM glucose, aliquoted to wells on a 96 well plate and allowed to equilibrate in this KRBB for 45 minutes. Cells were then incubated in a 30 mM glucose KRBB containing either FLAG peptide, soluble acetylcholinesterase, soluble NL-1 or soluble NL-2. The KRBB for each condition was then collected and the cells were lysed in RIPA buffer. Secreted insulin and total cellular insulin content were analyzed by radioimmunoassay (Linco/Millipore, Billerica, MA). In experiments where islets were incubated with the soluble proteins, conditions were identical with the exception that islets were not treated and dissociated with Cellstripper.

#### *Co-Culture Assays*

HEK cells were transiently transfected with full-length NL-2 as described above. 24 hours post-transfection, trypsinized MIN-6 cells were seeded onto confluent monolayers of untransfected HEK cells or HEK cells transfected with NL-2 and were incubated overnight in MIN-6 media. Co-cultured cells were then washed twice with KRBB containing 2.75 mM glucose and then equilibrated in this solution for 45 minutes.

They were then treated with KRBB containing either 2.75 mM glucose or 16.75 mM glucose for one hour.

For short-term co-culture assays, HEK cells were transfected as described above. 48 hours post-transfection, confluent HEK cells, HEK cells transfected with NL-2 and MIN-6 cells were prepared as suspensions by removal with Cellstripper. Cells were then separately washed twice with complete MIN-6 media, washed twice with KRBB containing 2.75 mM glucose and then equilibrated in this KRBB for 45 minutes. MIN-6 cells were then combined in 96 well plates with either HEK cells or HEK cells transfected with NL-2 and incubated with KRBB containing 30 mM glucose for one hour.

For each condition in the co-culture assays described above, the KRBB was collected and total protein was isolated from co-cultured cells by lysis with RIPA buffer containing protease inhibitors (Sigma-Aldrich). Secreted insulin and total insulin content were analyzed by radioimmunoassay.

#### *Immunoprecipitation/Western Blot*

Suspensions of MIN-6 cells were prepared as described above and incubated with soluble neuroligin-2 Fc for 45 minutes at 37° C. Cells were washed twice with Kreb's Ringer, twice with D-PBS and then incubated for 2 hours on ice with the membrane-impermeable, reversible cross-linker DTSSP at 2 mM. The crosslinking reaction was stopped with by incubating cells with 20 mM Tris, pH 7.5 for 15 minutes, protein was isolated in RIPA lysis buffer and neuroligin-2 Fc complexes were immunoprecipitated with protein A beads. DTSSP crosslinks were cleaved (reversed) by incubating

immunoprecipitated complexes in 5%  $\beta$ -mercaptoethanol in SDS-PAGE sample buffer at 100° C for 5 minutes and then the dissociated complexes were analyzed by Western blotting using polyclonal neurexin and neuroligin-2 antibodies as previously described [149].

### *Statistical Analysis*

Data are presented as means  $\pm$  S.E. Differences between quantitative data sets were analyzed by the *t* test.  $P < .05$  was considered significant.

## C. Results

### *1. Neuroligin-2 is Expressed on the Surface of $\beta$ -Cells.*

The expression of neuroligin on the cell surface of neurons enables this protein to interact in trans with neurexin and other receptors on the axons of opposing neurons to facilitate presynaptic differentiation and the assembly of the secretory apparatus at synapses [65, 66, 221]. For neuroligin to drive the assembly of the secretory apparatus through interaction with receptors on contacting  $\beta$  cells, at least some of the protein would need to be present on the cell surface. Our previous immunostaining experiments did not clearly demonstrate the expression of neuroligin-2 on the surface of  $\beta$  cells and suggested there might be a significant portion of the protein in intracellular compartments (See Fig. 4.9 and [149]). To determine whether neuroligin-2 is expressed on the surface of  $\beta$  cells, flow cytometry was performed after incubating INS-1E  $\beta$  cells with antibodies generated against the extracellular domain of neuroligin-2 (Fig. 5.2A). An overall increase in the fluorescent signal in INS-1E cells treated with neuroligin-2 antibody



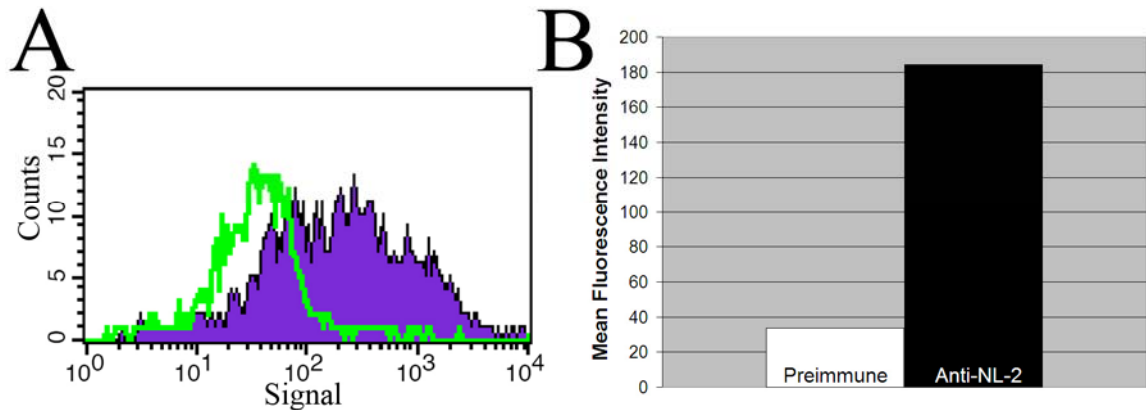


**Figure 5.2. Endogenous Neuroligin-2 is Expressed on the Surface of INS-1E Cells.**

(A) To determine whether neuroligin-2 is expressed on the surface of  $\beta$  cells, flow cytometry was performed on INS-1E cells using an antibody generated against the extracellular domain of neuroligin-2. The x-axis depicts the intensity of fluorescence exhibited by an individual INS-1E cell and the y-axis depicts the number of INS-1E cells with that intensity of fluorescence. Consistent with neuroligin-2 expression on the surface of  $\beta$  cells, the intensity of fluorescence was greater on average on cells treated with neuroligin-2 antibody (purple curve) relative to cells treated with preimmune serum (green curve). (B) Quantification of the mean fluorescent intensity observed in (A).

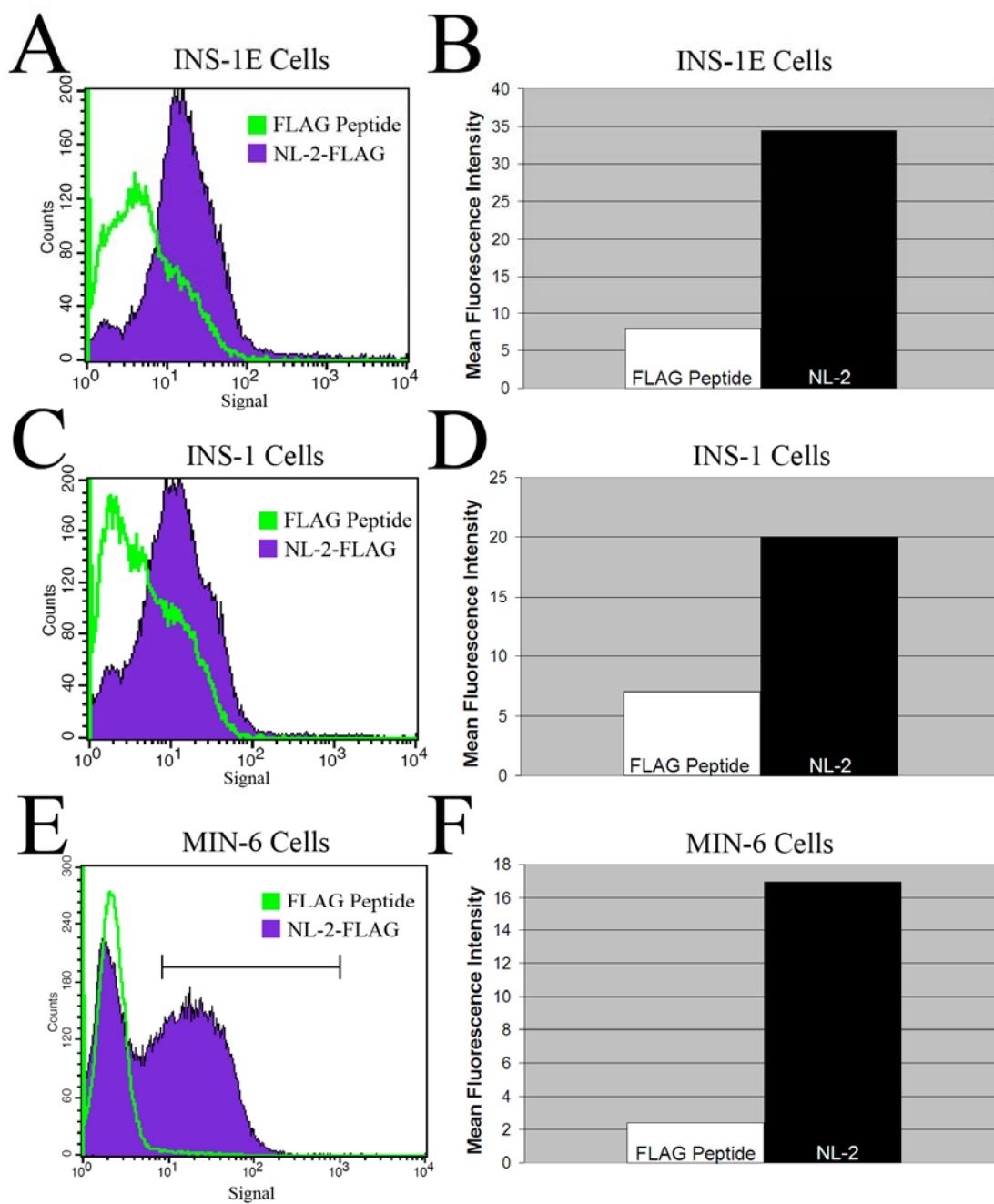
(purple in Fig. 5.2A) is observed as a right shift relative to cells treated with preimmune serum (green in Fig. 5.2A) on the coordinate in Fig. 5.2. Consistent with neuroligin-2 expression on the surface of  $\beta$  Cells, the mean fluorescence intensity of cells treated with neuroligin-2 antibody was 5.47-fold greater than in cells treated with preimmune serum (Fig. 5.2B).

## *2. The Extracellular Domain of Neuroligin-2 Binds to the Surface of $\beta$ -Cells.*

To determine if a neuroligin-2 binding partner is present on the surface of  $\beta$ -Cells, flow cytometry was performed after incubating either clonal INS-1E  $\beta$  cells, INS-1  $\beta$  cells or MIN-6  $\beta$  cells with the purified extracellular domain of neuroligin-2 (soluble neuroligin-2). Consistent with the presence of a neuroligin-2 receptor on the surface of  $\beta$  cells, an overall increase in the fluorescent signal in all three cell lines treated with soluble neuroligin-2 protein (purple) was observed as a right shift relative to cells treated with 3x FLAG peptide (green) on the coordinates in Fig 5.3A, C and E. The mean fluorescent intensity of INS-1E, INS-1 and MIN-6 cells treated with soluble NL-2 protein was 4.33-fold, 2.84-fold and 6.97-fold greater than these cells treated with 3x FLAG peptide (Fig. 5.3B, D and F). Unlike in INS-1 and INS-1E cells, there are two discrete peaks observed in MIN-6 cells treated with soluble neuroligin-2 protein. The peak on the left (Fig. 5.3E, purple) represents cells that do not interact with neuroligin-2 as it aligns exactly with the peak observed in cells treated with 3x FLAG peptide (Fig. 5.3E, green) and the peak on the right, highlighted by the black line above it, represents cells that

**Figure 5.3. Binding of Soluble Neuroligin-2 to the Surface of INS-1E, INS-1 and MIN-6 Cells.**

To determine whether a receptor for neuroligin-2 was present on the surface of  $\beta$  cells, soluble FLAG-neuroligin-2 was incubated with (A) INS-1E cells, (C) INS-1 cells or (E) MIN-6 cells and binding was assessed by flow cytometry. As a control, 3x FLAG peptide was used. Consistent with a neuroligin-2 binding partner being present on the surface of  $\beta$  cells, an increase in fluorescent signal (right shift) was observed in INS-1E, INS-1 and MIN-6 cells treated with soluble neuroligin-2 (purple) relative to cells treated with 3x FLAG peptide (green). (B), (D), (F) Quantification of the mean fluorescent intensity observed for FLAG peptide and soluble neuroligin-2 in (A), (C) and (E). The mean fluorescence intensity was greater in INS-1E, INS-1 and MIN-6 cells treated with soluble neuroligin-2 relative to those cells treated with 3x FLAG peptide.



interact with the soluble neuroligin-2 protein. Each population includes about 50% of the cells.

To determine the affinity of neuroligin-2 for its receptor on  $\beta$  cells, a trace amount of  $^{125}\text{I}$ -labeled soluble neuroligin-2 was incubated with INS-1E cells and competed away with increasing concentrations of unlabeled soluble neuroligin-2. A clear decrease in the cell associated reactivity (CAR) relative to the CAR of [ $^3\text{H}$ ]-water is observed with increasing concentrations of soluble neuroligin-2 (Fig. 5.4). Neuroligin-2 binding is detected at concentrations as low as 2 nM and saturates at about 100 nM. From this plot, the dissociation constant ( $K_D$ ) of soluble neuroligin-2 for its receptor on INS-1E cells was determined to be 15 nM.

### *3. Co-Culture of $\beta$ -Cells with HEK Cells Expressing Full-Length Neuroligin-2 Markedly Enhances Glucose Stimulated Insulin Secretion*

In the CNS, trans-synaptic interaction of neuroligin on dendrites with neurexin and possibly other proteins on axons is important for presynaptic differentiation [66, 72, 80, 221]. The high degree of overlap between the synaptic exocytic machinery and the  $\beta$  cell secretory machinery, along with the observation that  $\beta$  cell- $\beta$  cell interactions are essential for robust glucose-stimulated insulin secretion (GSIS) [84, 85, 87, 224], led us to hypothesize that neuroligin drives the assembly of the  $\beta$  cell secretory apparatus, similar to the way it drives the assembly of the synaptic exocytic machinery *in vitro*, through trans-cellular interactions with neurexin and/or other cell surface receptors and that this interaction facilitates glucose-stimulated insulin secretion in contacting cells.

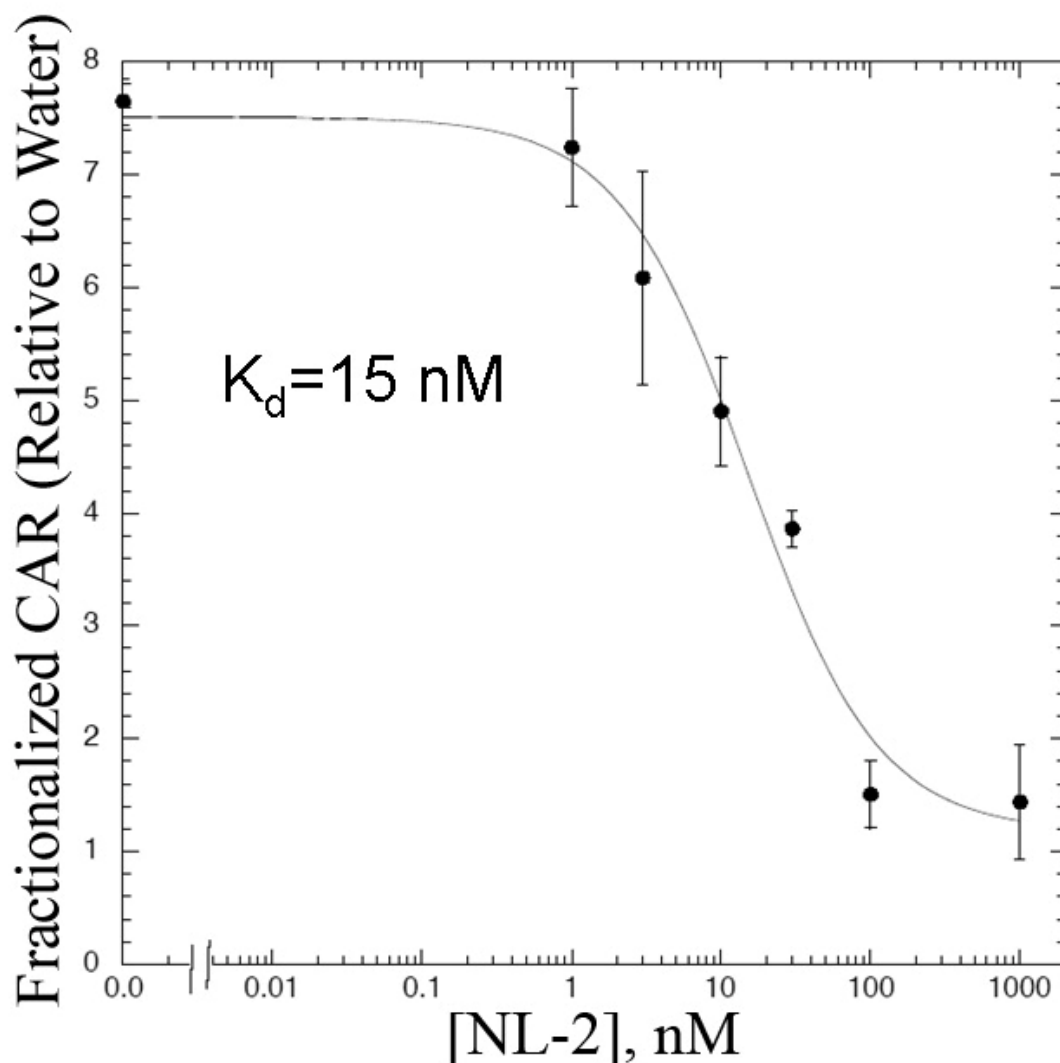


**Figure 5.4. Neurotrophin-2 Binds to the Surface of INS-1E Cells with a Dissociation Constant of 15 nM.**

To determine the affinity of neurotrophin-2 for its receptor on  $\beta$  cells, a trace amount of  $^{125}\text{I}$ -labeled soluble neurotrophin-2 was incubated with INS-1E cells and competed away with increasing concentrations of unlabeled soluble neurotrophin-2. A clear decrease in the cell associated reactivity (CAR) relative to  $^3\text{H}$ -water is observed with increasing concentrations of soluble neurotrophin-2. From this plot, the dissociation constant ( $K_D$ ) of soluble neurotrophin-2 for its receptor on INS-1E cells was determined to be 15 nM.

To provide evidence for this hypothesis, HEK cells were transiently transfected with full-length neuroligin-2 and co-cultured overnight with MIN-6  $\beta$  cells. Secreted insulin was then measured by RIA after incubation for 1 hour in Kreb's Ringer containing either basal (2.75 mM) or stimulatory (15 mM) levels of glucose. The ability of MIN-6 cells to secrete insulin in response to glucose was not affected by co-culturing as MIN-6 cells cultured on untransfected HEK cells secreted 3.49-fold more insulin under stimulatory conditions than MIN-6 cells treated with basal levels of glucose (Fig. 5.5). Consistent with neuroligin-2 playing a role in the assembly and organization of the  $\beta$  cell secretory apparatus, MIN-6 cells cultured on HEK neuroligin-2 expressing cells secreted 2.87-fold more insulin under basal glucose conditions and 3.26-fold more insulin under stimulatory glucose conditions than MIN-6 cells cultured on untransfected HEK cells (Fig. 5.5). Secreted insulin was not detected from untransfected HEK cells or HEK cells expressing full-length neuroligin-2 (data not shown).

#### 4. *Soluble NL-2 Markedly Inhibits Glucose-Stimulated Insulin Secretion*

To provide further support for a role for neuroligin-2 in the assembly of the  $\beta$  cell secretory apparatus, a soluble neuroligin-2 protein lacking the transmembrane and cytoplasmic domains was incubated with clusters of MIN-6 cells and intact rat islets in order to disrupt existing trans interactions between endogenous neuroligin and its  $\beta$  cell receptor (Fig. 5.6 and 5.7). MIN-6 cells treated with soluble neuroligin-2 and high glucose secreted 70.9% less insulin than cells treated with high glucose and 3x FLAG peptide (Fig. 5.6A). As a control, MIN-6 cells were treated with identically prepared soluble acetylcholinesterase--a protein that shares significant sequence identity with the

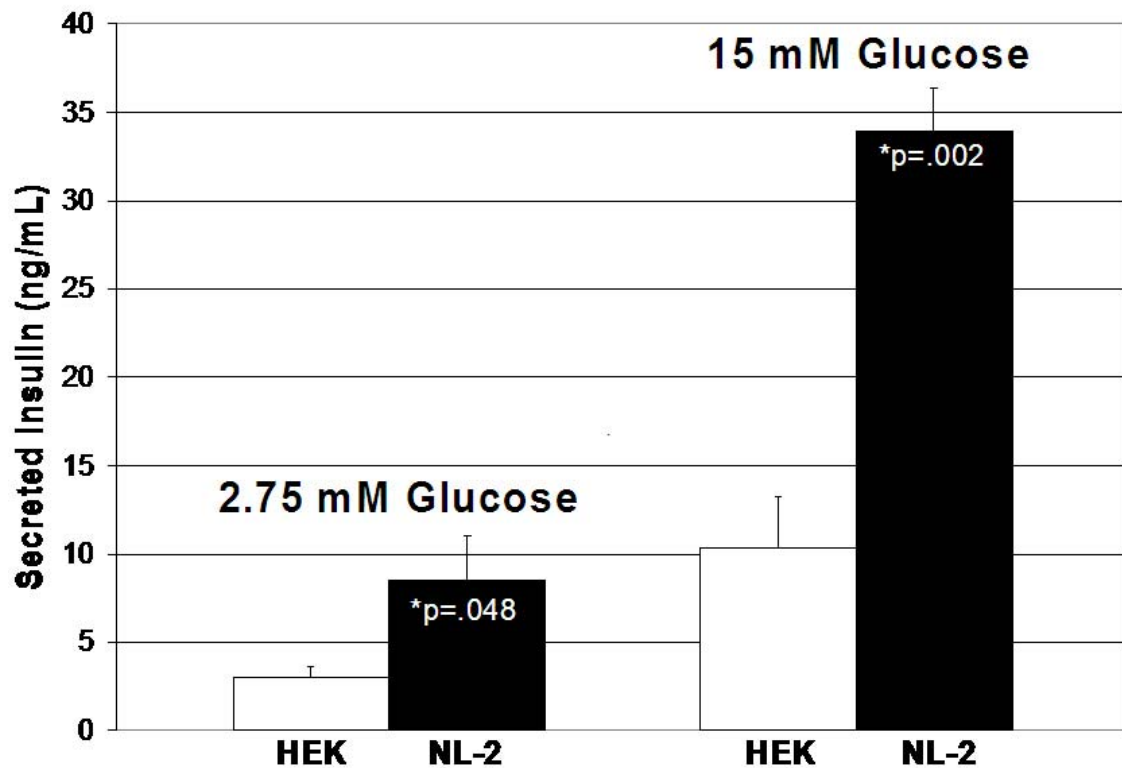


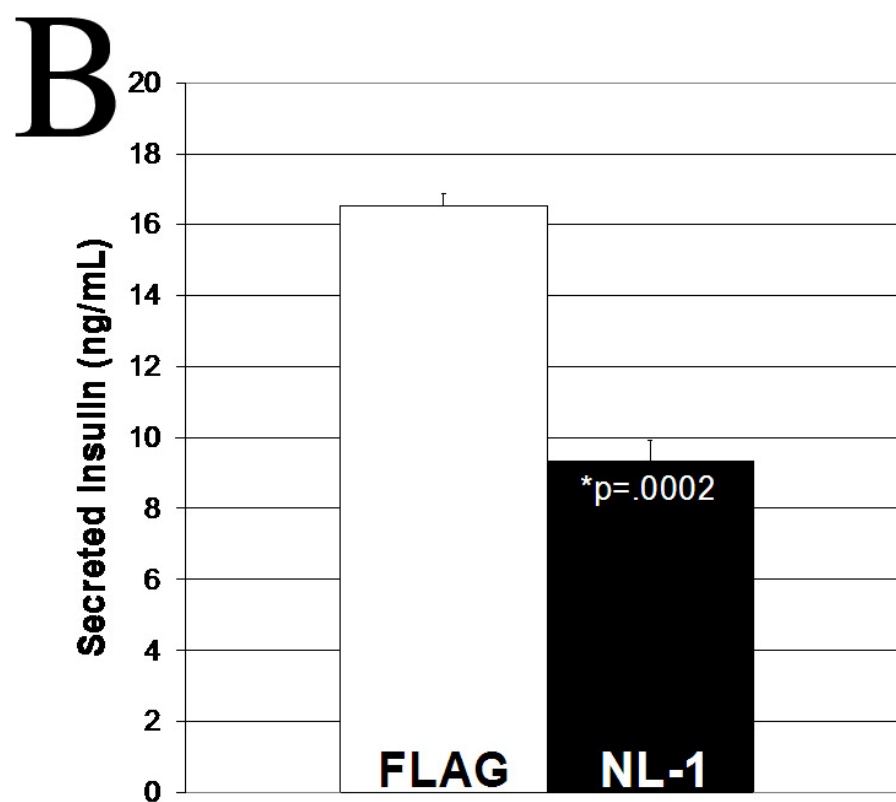
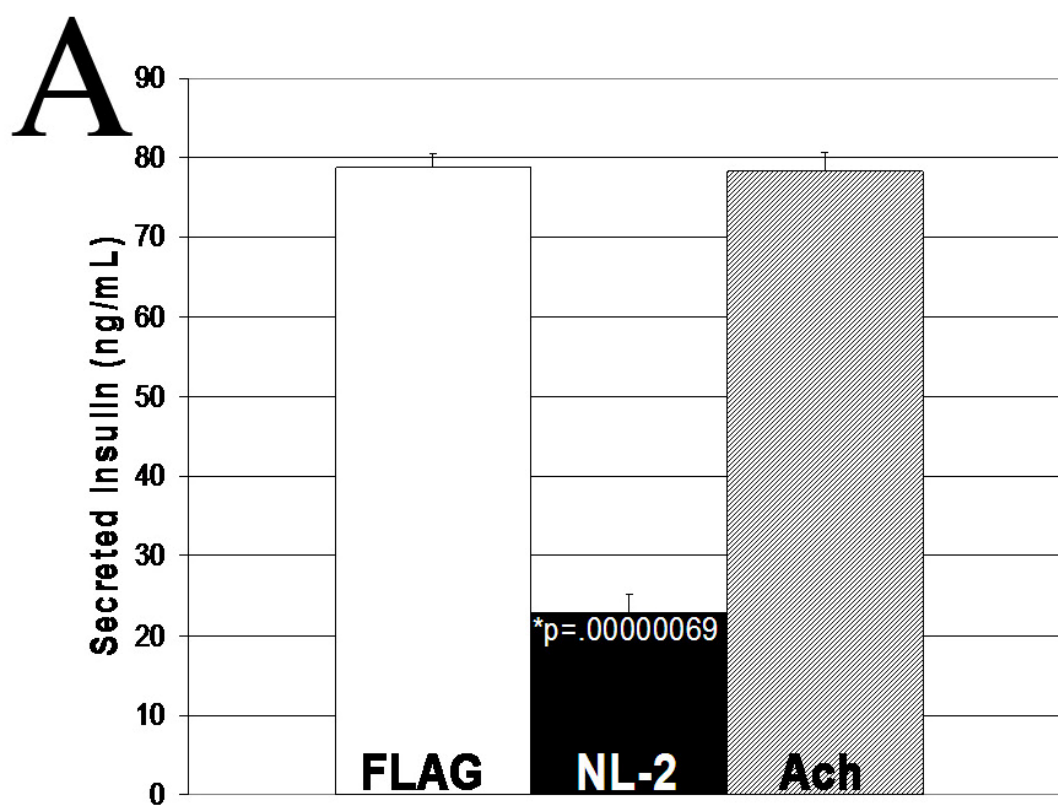
**Figure 5.5. Co-culture of MIN-6 Cells with HEK Cells Expressing Full-length Neuroligin-2 Markedly Enhances Insulin Secretion.**

MIN-6 cells were cultured for 24 hours on monolayers of HEK cells transfected with Neuroligin-2. After conditioning of co-cultured cells in 2.75 mM glucose for 1 hour, secreted insulin was measured by RIA after a 1 hour treatment with low (2.75 mM) or high (16.75 mM) glucose. Consistent with functional stimulus-secretion coupling in co-cultured cells, MIN-6 cells cultured on untransfected HEK cells secreted 3.49-fold more insulin under high glucose conditions relative to low glucose conditions. MIN-6 cells cultured on HEK neuroligin-2 expressing cells secreted 2.87-fold more insulin under low glucose conditions relative MIN-6 cells cultured on untransfected HEK cells (n=3; P=.048). Under high glucose conditions, MIN-6 cells cultured on HEK neuroligin-2 expressing cells secreted 3.26-fold more insulin relative to MIN-6 cells cultured on untransfected HEK cells (n=3; P=.002).



**Figure 5.6. Soluble Neuroligin-2 Inhibits Insulin Secretion from MIN-6 Cells.**

Suspended MIN-6 cells were conditioned in a 2.75 mM glucose Kreb's ringer buffer for 1 hour. Cells were then incubated for 1 hour in a 30 mM glucose Kreb's ringer solution with either 10 uM 3x FLAG peptide, 10 uM soluble neuroligin-2, 10 uM soluble acetylcholinesterase or 10 uM soluble neuroligin-1. Secreted insulin was then measured by radioimmunoassay. (A) MIN-6 cells treated with soluble neuroligin-2 secreted 70.9% less insulin than cells treated with 3x FLAG peptide (n=4; p=.00000069) and 70.8% less insulin than cells treated with acetylcholinesterase (n=4; p=.00000141). (B) MIN-6 cells treated with soluble neuroligin-1 secreted 43.4% less insulin than MIN-6 cells treated with 3x FLAG peptide (n=3; p=.0002). In this experiment, a similar response was observed for MIN-6 cells treated with soluble neuroligin-2.



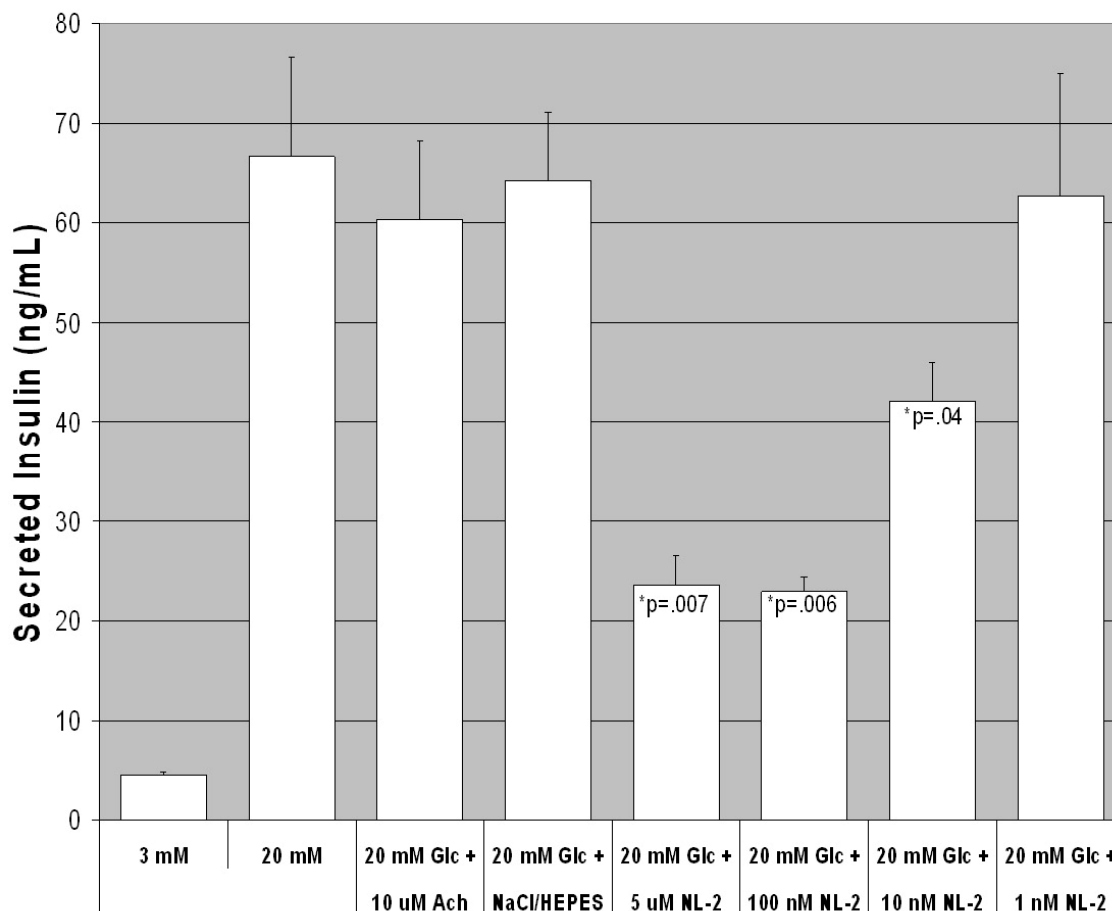


**Figure 5.7. Soluble NL-2 Inhibits Glucose Stimulated Insulin Secretion from Rat Islets in a dose dependent fashion.**

To determine whether soluble NL-2 can inhibit insulin secretion in islets, intact islets were conditioned for 1 hour in 3 mM glucose Kreb's ringer buffer and were then treated for 1 hour with 20 mM glucose containing soluble NL-2 at varying concentrations. As controls, islets were separately incubated with 3 mM glucose, 20 mM glucose, 20 mM glucose and 10 uM acetylcholinesterase, and 20 mM glucose and NaCl HEPES (the buffer the protein is stored in). Relative to 3 mM glucose, robust and similar glucose-stimulated insulin secretion was observed in all controls. There was not any significant difference in secreted insulin between islets treated with 20 mM glucose only, islets treated with 20 mM glucose and either 10 uM soluble acetylcholinesterase or NaCl/HEPES. Islets treated with 20 mM glucose and either 5 uM NL-2, 100 nM NL-2 or 10 nM NL-2 secreted 64.6% (n=3; p=.007), 65.6% (n=3; p=.006) and 36.9% (n=3; p=.04) less insulin than islets treated with 20 mM glucose alone. Islets treated with 20 mM glucose and 1 nM NL-2 secreted insulin at control levels.

extracellular domain of neuroligin but lacks synaptogenic and neuroligin binding activity (Fig. 5.6A) [65, 191]. No decrease in GSIS was observed when MIN-6 cells treated with soluble acetylcholinesterase were compared with cells treated with 3x FLAG peptide (Fig. 5.6A). When neuroligin-2 treated cells were compared to acetylcholinesterase treated cells, a 70.8% decrease in GSIS was observed (Fig. 5.6A). MIN-6 cells were also treated with high glucose and soluble neuroligin-1 lacking the transmembrane and intracellular domains to determine whether the effect on GSIS was specific within the neuroligin protein family to neuroligin-2. Consistent with the effect not being specific to neuroligin-2, a 43.4% decrease in GSIS was observed in MIN-6 cells treated with soluble neuroligin-1 relative to cells treated with 3x FLAG peptide (Fig. 5.6B).

In rat islets incubated with high glucose and soluble neuroligin-2, GSIS was significantly inhibited at neuroligin-2 concentrations of 10 nM and above (Fig. 5.7). Relative to islets treated with 20 mM glucose only, GSIS was inhibited by 36.9% when islets were treated with 10 nM soluble neuroligin-2, 65.6% when islets were treated with 100 nM neuroligin-2 and 64.6% when islets were treated with 1  $\mu$ M neuroligin-2. Decreased GSIS was not observed at 1 nM (Fig. 5.7). As controls, islets were separately incubated with 3 mM glucose, 20 mM glucose, 20 mM glucose and NaCl/HEPES (the buffer the protein is stored in), and 20 mM glucose and 10  $\mu$ M acetylcholinesterase. Robust GSIS was observed relative to 3 mM glucose in all controls incubated with high glucose (Fig. 5.7) and no differences in GSIS were observed between islets treated with 20 mM glucose alone or with either NaCl/HEPES or 10  $\mu$ M acetylcholinesterase (Fig. 5.7). To determine whether the inhibitory effects of neuroligin-2 on GSIS in rat islets correlates with the soluble neuroligin-2 dissociation constant, a dose response curve was

generated (Fig 5.8). Inhibition is dose-dependent and is maximal at concentrations greater than 100 nM. The concentration at which soluble neuroligin-2 causes 50% inhibition ( $IC_{50}$ ) of its maximal effect on GSIS is 9 nM (Fig. 5.8), a value that is strikingly similar to the 15 nM dissociation constant observed for neuroligin-2 binding to the cell surface of INS-1E  $\beta$  cells (Fig. 5.4).

#### *5. Neuroligin-2 Interacts with $\alpha$ -Neurexin in $\beta$ -Cells.*

To determine whether neuroligin-2 associates with  $\alpha$ -neurexin in MIN-6  $\beta$ -Cells, soluble neuroligin-2-Fc bound to the surface of MIN-6 cells was cross-linked with DTSSP. Neuroligin-2-Fc complexes were then immunoprecipitated, dissociated and analyzed by Western blot using rabbit polyclonal antibodies to neurexin. As a control, cells were treated identically with soluble acetylcholinesterase. Western blot analysis revealed that  $\alpha$ -neurexin was immunoprecipitated from cells treated with soluble neuroligin-2-Fc but not from cells treated with acetylcholinesterase (Fig. 5.9A). To confirm that neuroligin-2-Fc was successfully immunoprecipitated, Western blot analysis was performed on immunoprecipitated proteins using rabbit polyclonal antibodies to neuroligin-2. A band at the expected molecular weight of neuroligin-2-Fc was detected in cells treated with soluble NL-2 but not with cells treated with acetylcholinesterase (Fig. 5.9B).

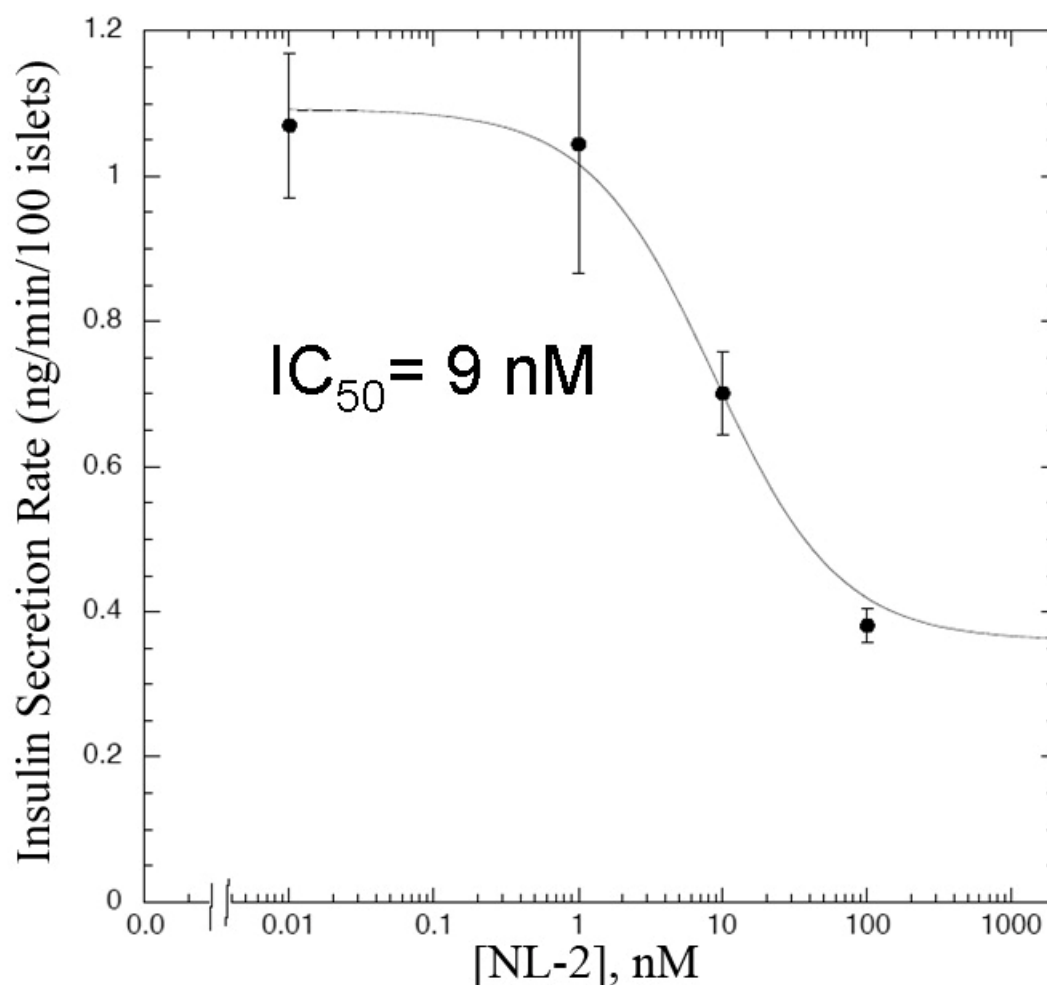
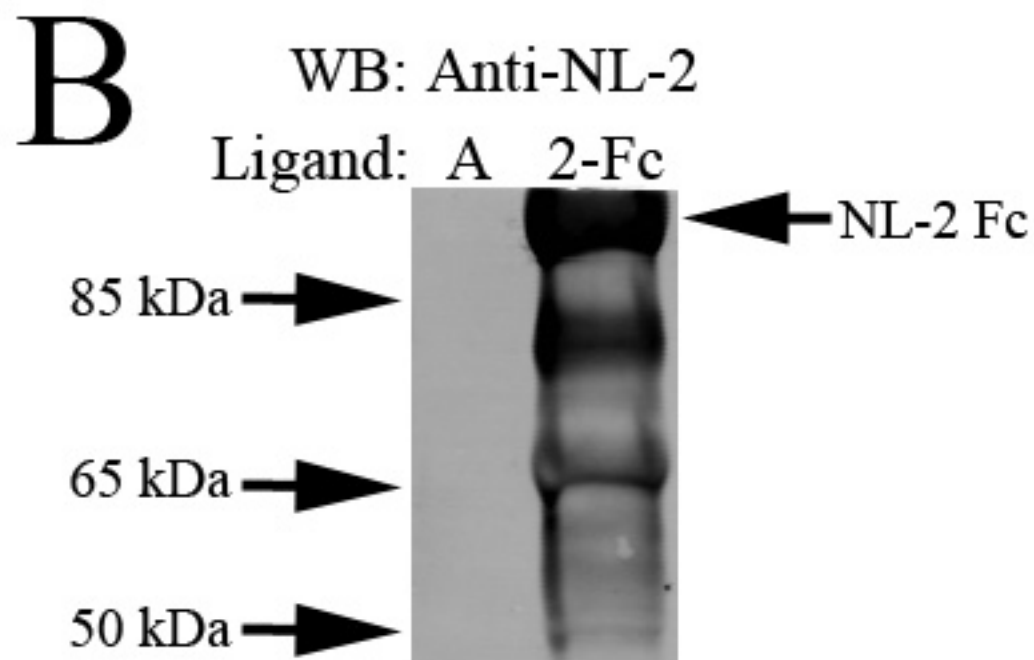
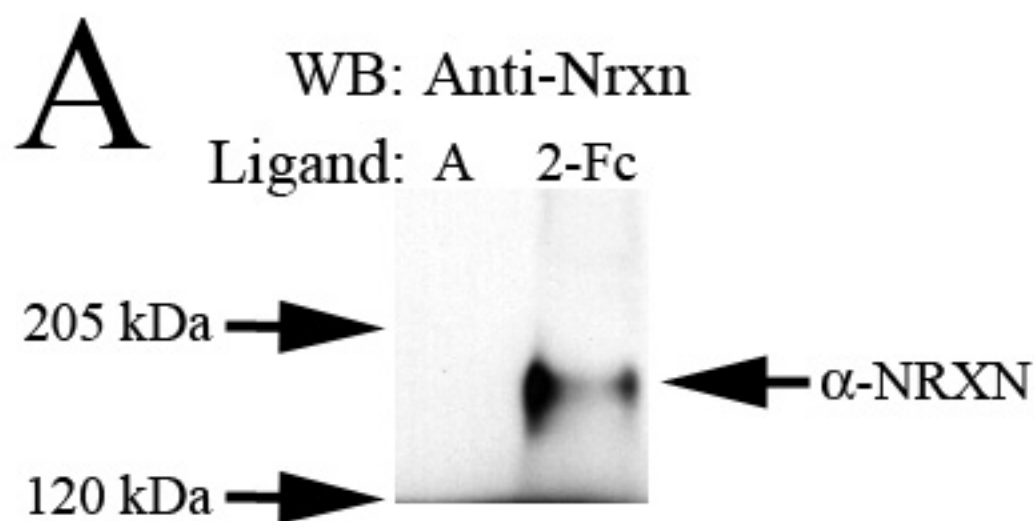


**Figure 5.8. Dose-Response Curve for NL-2 Inhibition of Glucose-Stimulated Insulin Secretion from Rat Islets.**

To determine whether the soluble NL-2 binding dissociation constant correlates with the inhibitory effects of NL-2 on glucose-stimulated insulin secretion in rat islets, rat islets were conditioned in 3 mM glucose and then incubated for one hour in 20 nM glucose and varying concentrations of soluble NL-2. Secreted insulin was measured by RIA and a dose-response curve was generated. Inhibition is maximal at concentrations greater than 100 nM. The concentration at which soluble NL-2 causes 50% inhibition of its maximal effect on GSIS was calculated to be 9 nM.

**Figure 5.9. NL-2 is Associated with  $\alpha$ -Neurexin in MIN-6  $\beta$  Cells.**

To determine whether NL-2 interacts with  $\alpha$ -neurexin, soluble NL-2-Fc was incubated with suspended MIN-6 cells for 45 minutes, unbound NL-2 was washed away and a reversible membrane impermeable crosslinker was applied. Complexed NL-2-Fc was immunoprecipitated with protein A, the crosslink reversed and the immunoprecipitated proteins were analyzed by Western blot. As a control, cells were treated identically with soluble acetylcholinesterase. (A) Consistent with an association between NL-2 and  $\alpha$ -neurexin, Western blot analysis using affinity purified rabbit polyclonal antibodies to neurexin revealed that  $\alpha$ -neurexin was immunoprecipitated with cells treated with soluble NL-2 but not with cells treated with acetylcholinesterase. (B) To confirm that NL-2 was successfully immunoprecipitated, Western blot analysis was performed on immunoprecipitated proteins using rabbit polyclonal antibodies to NL-2. A band at the expected molecular weight of NL-2-Fc was detected in cells treated with soluble NL-2 but not with cells treated with acetylcholinesterase. (A, soluble acetylcholinesterase; 2-Fc, soluble neuroligin-2 Fc).





## *6. Neuroligin Regulates Glucose-Stimulated Insulin Secretion Via a Neurexin-Independent Mechanism*

In neurons, neuroligin can enhance synapse formation via a neurexin-independent mechanism [66, 221]. To determine whether the affect of neuroligin on GSIS was dependent on neurexin binding, intact rat islets were treated with a soluble neuroligin that cannot bind to neurexin (Davide Comoletti, Unpublished Data). This protein contains a glycine to alanine substitution, at position 500 of neuroligin-1, which is at the neuroligin-neurexin binding interface and is calculated based on analysis of binding energies to destabilize the neuroligin-neurexin complex [225, 226]. Treatment of rat islets with 20 mM glucose and 10 uM neuroligin mutant decreased insulin secretion by 42% relative to islets treated with 20 mM glucose and HEPES/NaCl buffer. A 5.1-fold increase in GSIS was observed in islets treated with 20 mM glucose relative to islets treated with 2.75 mM glucose.

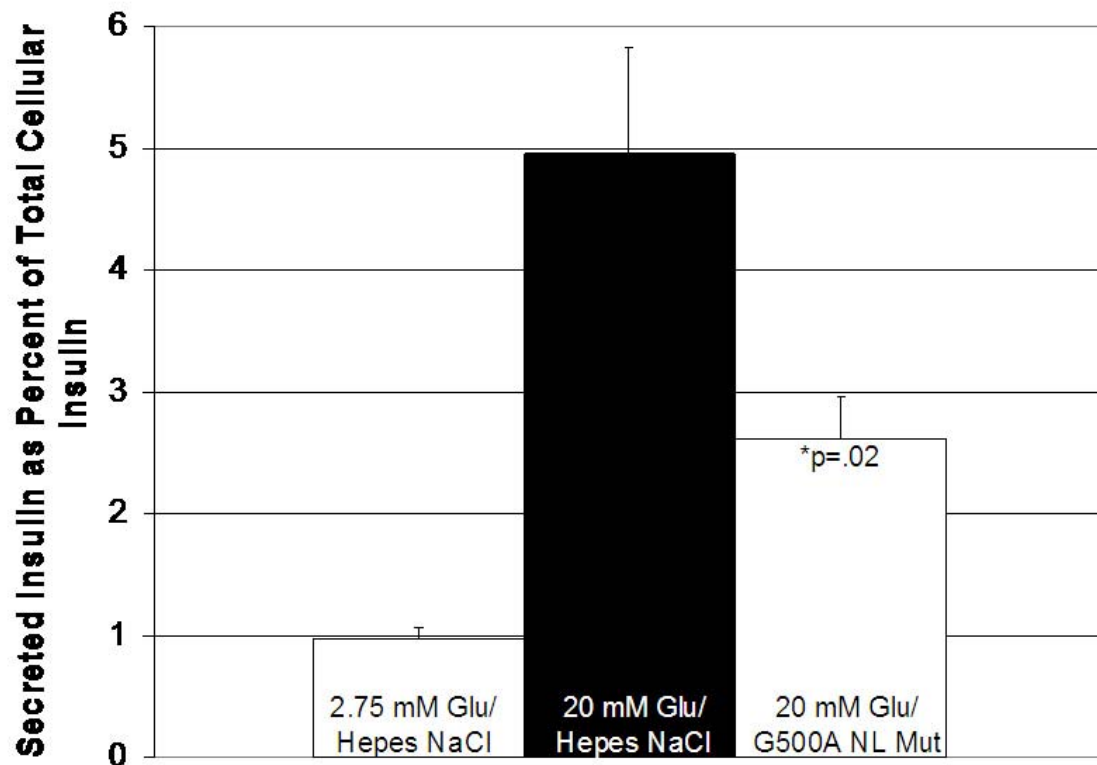


**Figure 5.10. Neuroligin Inhibits Glucose Stimulated Insulin Secretion via a Neurexin-Independent Mechanism.**

To determine whether neuroligin inhibition of insulin secretion is dependent on interaction with neurexin, intact islets were treated with a soluble neuroligin containing a single amino acid substitution (Glycine to Alanine at position 500 of NL-1) that prevents interaction with neurexin. Treatment with 20 mM glucose and 10 uM neuroligin-1 mutant decreased insulin secretion by 42% (n=4; p=.02) relative to islets treated with 20 mM glucose and HEPES/NaCl buffer (the buffer the protein is stored in).

## D. Discussion

Previously, we demonstrated the expression of the synaptogenic adhesion molecules neuroligin and neuroligin in  $\beta$  cells and provided evidence that neuroligin is important for glucose-stimulated insulin secretion [149]. These studies and the abundance of *in vitro* and *in vivo* evidence implicating neuroligin in the functioning and differentiation of the presynaptic active zone in neurons led us to hypothesize that neuroligin may play a role in the formation of the submembrane insulin secretory apparatus [65, 72, 80, 185]. In the present study, we demonstrate that neuroligin-2 can potentiate glucose stimulated insulin secretion through a *trans*-interaction with a receptor on the  $\beta$  cell surface. Disruption of this interaction significantly diminishes the ability  $\beta$  cells to secrete insulin in response to glucose. These studies suggest that neuroligin is important for the maintenance and possibly the proper differentiation of the  $\beta$ -cell stimulus-secretion coupling machinery.

### 1. *Cell-Surface Expression of Neuroligin-2 and a Receptor on the Surface of $\beta$ -Cells*

Pancreatic  $\beta$  cells express high levels of neuroligin-2 and its *trans*-synaptic binding partner  $\alpha$ -neuroligin [149]. The striking polarity of these proteins observed in neurons, where neuroligins are postsynaptic (on dendrites) and neuroligins are presynaptic (on axons), and the lack of an obvious equivalent to the axo-dendritic axis in  $\beta$  cells leaves open several questions regarding the localization, organization and role of these proteins within  $\beta$  cells. Our previous immunofluorescence studies clearly demonstrated the expression of  $\alpha$ -neuroligin on the surface of  $\beta$  cells but suggested that a significant

proportion of neuroligin-2 was localized to intracellular compartments (See Fig. 4.9 and [149]). For neuroligin to drive the assembly of the secretory apparatus through *trans*-interaction with neurexin or other receptors on contacting  $\beta$  cells, as it does in neurons, at least some of the protein needs to be present on the cell surface. The finding that endogenous neuroligin-2 is present on the surface of  $\beta$  cells and that the exogenous soluble extracellular domain of neuroligin-2 interacts with a protein on the surface of  $\beta$  cells demonstrates the potential for neuroligin-2 on one  $\beta$  cell to interact in *trans*- with a receptor on a contacting  $\beta$  cell. Because in the present study, the soluble neuroligin-2 orientation and presentation is not controlled as it would normally be in the plasma membrane it is impossible to determine whether this protein is interacting in *cis*- or *trans*- with its receptor on the  $\beta$  cell surface. Evidence that neuroligin-2 acts via a *trans*-interaction with its receptor on contacting  $\beta$  cells is supported by the finding that full-length neuroligin-2 expressed on the surface of non-neuronal HEK cells leads to increased glucose-stimulated insulin secretion from contacting MIN-6 cells.

In MIN-6 cells treated with soluble neuroligin-2, a population of cells that interacts with neuroligin-2 and a population of cells that does not interact with neuroligin-2 are observed. This particular cell line, along with most  $\beta$  cell lines, is known to dedifferentiate and lose the ability to secrete insulin in response to stimuli [227, 228]. In our hands, several of the MIN-6 cell lines initially obtained for this study stop responding to glucose and eventually to IBMX several passages after thawing, and it has been observed that those cells that are unresponsive to glucose and IBMX do not bind to neuroligin-2. Although outside the scope and purpose of this study, these observations

suggest that the cells that bind neuroligin-2 might represent differentiated MIN-6 cells and the cells that do not represent dedifferentiated cells. Further studies are necessary to validate and formally test this hypothesis.

## *2. The Involvement of Neuroligin-2 in the Regulation of Glucose-Stimulated Insulin Secretion*

Synapses are highly specialized regions of the membrane where neurotransmitter is released. Neuroligin was initially implicated in the formation of synapses and presynaptic differentiation after co-culture studies of non-neuronal cells with hippocampal neurons revealed the ability of this protein to recruit the active zone proteins necessary for neurotransmitter exocytosis to sites of contact between the neuroligin expressing cells and neurons [65]. Neuroligin and these same presynaptic active zone proteins are expressed by  $\beta$  cells and are implicated in the regulation of glucose-stimulated insulin secretion [12-18, 149]. As in axo-dendritic neuronal contacts,  $\beta$  cell- $\beta$  cell interactions are important for the proper functioning of the  $\beta$  cell stimulus-secretion coupling machinery [82, 87]. It is possible that the interaction of neuroligin on one  $\beta$  cell with neurexin or another receptor on a contacting  $\beta$  cell drives the assembly of the stimulus-secretion coupling machinery and facilitates the enhanced glucose-stimulated insulin secretion observed in contacting  $\beta$  cells.

Co-culture of MIN-6  $\beta$ -cells with non-neuronal cells expressing full-length neuroligin-2 markedly enhances glucose-stimulated insulin secretion from MIN-6 cells, suggesting that neuroligin-2 can act in *trans* with a  $\beta$  cell receptor to regulate glucose-

stimulated insulin secretion from  $\beta$  cells. The clustering of neuroligin-2 through its cytoplasmic tail is important for its localization and its ability to drive presynaptic differentiation. Treatment of contacting MIN-6  $\beta$  cells and intact islets with a soluble neuroligin-2 lacking the transmembrane and cytoplasmic domains of the molecule significantly disrupts glucose-stimulated insulin secretion, as might be expected if the soluble neuroligin-2 displaced endogenous neuroligin-2 and disrupted existing neuroligin-receptor interactions around which the secretory machinery was already assembled. Strikingly, the concentration at which soluble neuroligin-2 causes 50% inhibition of glucose-stimulated insulin secretion is almost identical to the binding constant ( $K_D$ ) determined for the interaction of soluble neuroligin-2 with the surface of  $\beta$  cells. Taken together, these data demonstrate that neuroligin acts to regulate stimulus-secretion coupling by a mechanism similar to the one used by neurons to regulate pre-synaptic differentiation and the proper functioning of the neurotransmitter release machinery.

In the central nervous system, neuroligin expressed on dendrites interacts with neurexin on axons of an opposing neuron [185]. Cross-linking studies demonstrate that neuroligin-2 can interact with neurexin on the surface of  $\beta$  cells. Because contacting  $\beta$  cells lack an obvious equivalent to the axonal and dendritic membrane regions, the possible organization of neuroligin and neurexin within islet  $\beta$  cells is not very clear. One attractive possibility is that the interaction of neuroligin with neurexin on contacting  $\beta$  cells leads to the formation of microdomains where the stimulus-secretion coupling machinery assembles. The existence of specialized  $Ca^{2+}$  rich regions (microdomains) on

the  $\beta$  cell membrane has previously been proposed [229]. Further support for the existence of these domains comes from total internal reflection fluorescence microscopy studies where discrete clusters of syntaxin were observed at regions of the  $\beta$  cell membrane where insulin exocytosis was occurring [230]. Interestingly, syntaxin has been shown to interact with neurexin [94]. The development of reagents or animal models to help assess the spatial organization of these proteins within contacting  $\beta$  cells may help to provide more insight into the mechanism by which these proteins interact to regulate insulin secretion and may shed light on the possible existence of microdomains and the organization of the secretory apparatus at these domains.

### *3. Neuroligin-2 Regulates Glucose-Stimulated Insulin Secretion Through a Neurexin-Independent Pathway*

In the central nervous system, evidence is mounting that at least some of the synaptogenic effects of neuroligin on neurons can occur through a neurexin-independent pathway. The observations that non-synaptogenic neuroligin mutants can interact with neurexin as effectively as wildtype neuroligin (synaptogenic) and that overexpression of non-neurexin binding neuroligin point mutants in neurons increases synaptic density to levels identical to levels seen with wildtype neuroligin suggest that neuroligin can mediate at least some aspects of pre-synaptic differentiation through another protein [66, 221]. Treatment of islets with a soluble non-neurexin binding neuroligin mutant inhibits glucose-stimulated insulin secretion nearly as effectively as treatment with soluble neuroligin-1 or -2, suggesting that neuroligin can regulate stimulus-secretion coupling in  $\beta$  cells through a protein other than neurexin. Identification of the receptor through

which neuroligin is acting to mediate both glucose-stimulated insulin secretion may provide insight into the signaling pathways through which it is acting in both  $\beta$  cells and neurons.

#### 4. *Closing Remarks*

In summary, these findings implicate neuroligin in the regulation of contact enhanced glucose-stimulated insulin secretion in islets and suggest that it acts to mediate the assembly of the secretory machinery through *trans*-interactions with an as yet unidentified receptor on a contacting  $\beta$  cell. Future studies will attempt to elucidate whether neuroligin is critical for the development and differentiation of  $\beta$  cells and whether neuroligin or downstream molecules might be useful targets for alleviating the dysfunction in glucose-stimulated insulin secretion observed in diabetic patients.

#### E. Acknowledgements.

Chapter 5 represents a manuscript that I intend to submit for publication in early The dissertation author was the primary investigator in the development and execution of the study, and the principal author of this manuscript. I thank Dr. Davide Comoletti for assistance with protein purification, Dr. Ian Sweet for assistance with radioligand binding assays and Dr. Joseph Cantor for assistance with flow cytometry.



## CHAPTER 6: CONCLUSIONS, OPEN QUESTIONS AND FUTURE STUDIES

The major goal of this dissertation was to test the hypothesis that key insights into the functional maturation of  $\beta$  cells could be derived from existing knowledge of the development, differentiation and maintenance of GABAergic synapses in the CNS. The work that resulted from testing this hypothesis has demonstrated that at least one of the GABAergic trafficking pathways thought to be exclusive to neurons is used by  $\beta$  cells to generate synaptic-like microvesicles and revealed that the proteins that drive the assembly of the GABAergic neurotransmitter release machinery in neurons are expressed and used by  $\beta$  cells for maintenance of glucose-stimulated insulin secretion. A novel variant of a key GABAergic transporter protein is also described. Because an extensive discussion of these findings is provided at the end of each chapter, this final chapter will be devoted to addressing the open questions that remain as a result of this work. Along the way, the future work that might help to resolve some of these open questions and the potential use of these molecules as targets for diabetes diagnosis and therapy are discussed.

### A. Does GAD-65 Associate with AP-3 Generated Synaptic-Like Microvesicles in Islet $\beta$ Cells?

The interest in understanding the biogenesis of the synaptic-like microvesicles in  $\beta$  cells stemmed from the finding that the synaptic-like microvesicle associated protein GAD-65, a major autoantigen in type 1 diabetes, is released into the circulation in a rat model of autoimmune diabetes [51, 231]. Because a key characteristic of autoantigens

in diabetes and autoimmune diseases of the central nervous system is their tendency to be vesicle-associated proteins, the questions of whether the association of GAD-65 with the synaptic-like microvesicle makes it more susceptible to discharge from the  $\beta$  cell under certain conditions and whether the discharge of GAD is the primary trigger for autoimmune attack of the  $\beta$  cell during the pathogenesis of type 1 diabetes were of particular interest[38].

In chapter 3 of this dissertation, the biogenesis of  $\beta$  cell synaptic-like microvesicles is demonstrated to be mediated by the neuronal AP-3 complex. While it is likely that the vesicles generated by AP-3 are the GAD-65 containing vesicles, it is not unequivocally demonstrated in this dissertation. Because mouse islets do not express GAD-65 and as a result autoimmunity to GAD-65 is not observed in the NOD mouse model of autoimmune diabetes, the questions of whether GAD-65 associates with AP-3 generated vesicles in  $\beta$  cells and whether this association triggers autoimmune attack can not be addressed by investigating the various mouse lines lacking AP-3 subunits or by crossing these lines onto a NOD background [232]. The analysis of GAD-65 expression is further complicated because  $\beta$  cell lines do not express endogenous GAD-65 and isolated islets lose expression after 24 hours in culture, making perturbations in AP-3 gene expression in these models fruitless [233]. Although not ideal, the question of whether AP-3 mediated vesicles carry GAD-65 might best be addressed by introducing GAD-65 cDNA into islets isolated from mice lacking AP-3 subunits and assessing the trafficking patterns of GAD-65 protein relative to wildtype islets. The increased knowledge of the trafficking of GAD-65 and the mechanism of its association with the  $\beta$ -cell synaptic-like microvesicles that might be yielded by this type of analysis will likely

provide new insights into its release from  $\beta$  cells and additional opportunities to analyze its role in the pathogenesis of islet autoimmunity.

#### B. The Localization of Neuroligin and Neurexin in Islet $\beta$ Cells?

The expression of neuroligin and neurexin on distinct regions of the neuronal membrane, where neuroligins are expressed on dendrites and neurexins are expressed on axons, and the lack of an obvious equivalent to the axo-dendritic axis in  $\beta$  cells leaves open several questions regarding their localization and organization within  $\beta$  cells. While evidence is presented throughout this dissertation that the pancreatic  $\beta$  cells express high levels of neuroligin-2 and its *trans*-synaptic binding partner  $\alpha$ -neurexin, and that these proteins can interact, it is left unresolved how  $\beta$  cells might regulate the trafficking of these proteins [149].

One attractive possibility is that  $\beta$  cell neuroligin and neurexin are segregated by distinct membrane trafficking pathways into discrete regions of the plasma membrane. In neurons, the cytoplasmic tails of neuroligin and neurexin regulate their trafficking into discrete vesicles destined for the dendrite in the case of neuroligin and the axon in the case of neurexin [234, 235]. Because  $\beta$  cells share several membrane trafficking pathways with neurons (See Chapter 1 and 3 for in depth analysis), it seems reasonable to propose that neuroligin and neurexin are similarly trafficked to different regions of the  $\beta$  cell membrane, hereafter referred to as microdomains, via the pathways that regulate their trafficking in neurons. In this scenario, the neurexin-containing microdomains in one cell interact with the neuroligin-containing microdomains on another cell to drive the

assembly of the stimulus-secretion coupling machinery on the neurexin-containing microdomain and the recruitment of GABAergic receptors important for autocrine regulation of insulin secretion on the neuroligin-containing microdomain. The possible existence of “pre-synaptic” microdomains is supported by the presence of specialized  $\text{Ca}^{2+}$  rich regions on the  $\beta$  cell membrane and the finding by total internal reflection fluorescence microscopy that there are discrete clusters of syntaxin, a protein important for vesicle fusion, at regions of the  $\beta$  cell membrane where insulin exocytosis is occurring [230]. Although hypothetical, this model representing the  $\beta$ -cell equivalent of a synapse makes sense in light of the strikingly polarity of these proteins in both neuronal function and localization, the ability of neuroligin to drive the assembly of the secretory machinery on axons and to cluster neurotransmitter receptors at dendrites, and in light of the importance of autocrine feedback mechanisms through GABAergic signaling mechanisms within  $\beta$  cells. The future development of constructs or animal models that result in the expression of tagged versions of these genes in  $\beta$ -cell lines or islets combined with high-resolution microscopy, such as TIRF, might help to assess the spatial organization of these proteins within contacting  $\beta$  cells and will likely provide more insight into the possible existence of microdomains, into the organization of the secretory apparatus at these domains and into the mechanism by which these proteins interact to regulate insulin secretion.

### C. What is the Receptor through which Neuroligin Acts to Potentiate Insulin Secretion in the $\beta$ Cells?

The finding, here, that a non-neurexin binding neuroligin mutant can alter glucose-stimulated insulin secretion as well as wildtype neuroligin suggests that neuroligin regulates stimulus-secretion coupling in  $\beta$  cells through a neurexin-independent pathway. This is consistent with the recent finding that the ability of neuroligin to alter at least some synaptic activities occurs through a binding partner that is yet to be identified [66, 221]. The identification of the receptor through which neuroligin is acting to mediate glucose-stimulated insulin secretion will likely provide great insight into the signaling pathways through which it is acting in both  $\beta$  cells and neurons.

During the early stages of this dissertation work, studies were conducted to identify proteins other than neurexins that might interact with neuroligin-2 as a result of a hypothesis that is no longer supported by compelling data. The pull-down studies that were performed to test this hypothesis identified several candidate proteins as a neuroligin-2 receptor. A close family member of the most interesting candidate, eph receptor A2, was demonstrated to interact in *trans* on contacting  $\beta$  cells to potentiate insulin secretion through ephrin-A—a protein that associates with the membrane through a GPI-linkage. The transmembrane protein that allows ephrin-A to traverse signals into the cell and ultimately to the secretory machinery has not yet been identified [85]. Cross-linking in combination with immunoprecipitation analyses are currently being conducted to confirm an association between the eph receptor A2-ephrin-A complex and neuroligin-2, and to identify other proteins that might interact with neuroligin-2 to potentiate insulin

secretion. Because eph receptor A2-ephrin-A signaling pathways have been identified in  $\beta$  cells, efforts are also under way to determine if these signaling proteins are activated after the *trans*-presentation of neuroligin-2 to  $\beta$ -cell lines or dissociated  $\beta$  cells.

Elucidating the receptor and/or signaling pathways through which neuroligin-2 acts to regulate insulin secretion  $\beta$  cells will likely provide insight into its ability to regulate synaptic function and yield targets for remedying some of the  $\beta$ -cell dysfunction that occurs during the pathogenesis of diabetes.

#### D. Are $\beta$ cell Neuroligin and Neurexin Important for Both Regulated GABA and Insulin Secretion?

In the central nervous system, neuroligin-2 is exclusively expressed by and essential for the normal differentiation and functioning of GABAergic synapses [74, 76]. It has been stressed throughout this dissertation that  $\beta$  cells resemble GABAergic synapses and may use GABAergic signaling to regulate hormone secretion via autocrine and paracrine mechanisms from  $\beta$  cells and other islet cell types, yet the role of neuroligin-2 in the regulation of GABA secretion from  $\beta$  cells has not been addressed experimentally in this dissertation [32, 35]. The failure to study GABA secretion was primarily due to the lack of a robust assay to directly measure its release from islets over meaningful time periods (< 1 hour). Although it has been demonstrated here that neuroligin-2 potentiates insulin secretion from the  $\beta$  cell, it is conceivable given its role in the central nervous system that its interaction with  $\alpha$ -neurexin and/or another receptor might also drive the assembly of the in  $\beta$ -cell GABAergic exocytic machinery.

How, then, might neuroligin-2 simultaneously regulate the exocytosis of GABA from synaptic-like microvesicles and insulin from secretory granules in  $\beta$  cells? Both the exocytosis of insulin and GABA are stimulated by glucose and are dependent on depolarization via  $\text{Ca}^{2+}$  entry through L-type voltage-gated  $\text{Ca}^{2+}$ -channels [25, 27, 34]. This suggests that both GABA and insulin are released in parallel from the  $\beta$  cell. These two distinct vesicles also share proteins that are important for their docking and fusion during exocytosis [15]. One scenario to help explain how neuroligin-2 might regulate both GABAergic and insulin exocytosis from distinct vesicles is that sites of neuroligin-2-neurexin interaction on the  $\beta$  cells represent sites where exocytosis of both GABA and insulin might occur simultaneously. In another scenario that might result from the extensive splicing that both neuroligin and neurexin family members undergo, the GABAergic and insulin secretory machinery are regulated similarly but assemble on separate regions of the  $\beta$ -cell membrane around differentially spliced combinations of neuroligin-2 and neurexin [67, 184, 189, 194]. Future studies to attempt to distinguish between these two possibilities will be difficult because most  $\beta$ -cell lines lack (unpublished observations) and isolated islets lose expression of some key components of the GABAergic machinery after 24 hours in culture [233]. The analysis of perfused pancreases from mice lacking the neuroligin-2 gene with newly developed GABA immunoassays, along with measurements to determine if paracrine inhibition of glucagon secretion is perturbed in these mice, might help to determine whether neuroligin-2 is also important for the assembly of the GABAergic secretory apparatus.

#### E. Are $\beta$ -cell Neuroligin and Neurexin Necessary for the Differentiation and Maturation of the Stimulus-Coupling Machinery in $\beta$ cells?

The identification of proteins that promote the development, maturation and maintenance of stimulus-secretion coupling in  $\beta$ -cells might be useful for the development of new therapies for both forms of diabetes. The work presented throughout this dissertation clearly implicates neuroligin-2 as a key player in the regulation of glucose-stimulated insulin secretion from  $\beta$ -cells. Additionally, the finding here that  $\beta$  cells express high levels of  $\alpha$ -neurexin and the unpublished observation by a close collaborator that mice lacking the  $\alpha$ -neurexin gene are hyperglycemic, their  $\beta$  cells are hypomorph and they exhibit defects in stimulus-secretion coupling suggests that  $\alpha$ -neurexin may be important for the differentiation and maturation of the  $\beta$ -cell stimulus-secretion coupling machinery. In order to establish that neuroligin-2, and confirm that  $\alpha$ -neurexin, are necessary for the functional differentiation of  $\beta$  cells, future studies will need to determine whether the onset of neurexin/neuroligin gene expression coincides with the appearance of stimulus-secretion coupling in developing  $\beta$ -cells and whether perturbations in neurexin/neuroligin gene expression affect the normal development of glucose-stimulated insulin secretion in  $\beta$ -cells.

Along with a time course investigating neuroligin and neurexin gene expression at various time points throughout islet development, an already established *in vitro* model might be useful for determining whether the onset of neurexin/neuroligin gene expression coincides with the appearance of stimulus-secretion coupling in developing  $\beta$ -cells. It has been well-documented that fetal and neonatal islets do not secrete insulin in response



to changes in glucose concentration and that isolation and culturing of these developing islets under hyperglycemic conditions induces the development/maturation of stimulus-secretion coupling [236, 237]. If fetal/neonatal islets are cultured under hypoglycemic conditions then the islets fail to secrete insulin in response to changes in glucose concentration, suggesting that hyperglycemic conditions induce the expression of genes important for normal stimulus-secretion coupling. Using this model, it seems reasonable to propose that differences in the expression of neurexin and neuroligin would be observed between fetal/neonatal islets treated with hyperglycemic conditions relative to those treated with hypoglycemic conditions if these genes are important for the development/maturation of stimulus-secretion coupling in  $\beta$ -cells [236, 237].

Although the analysis of mice lacking the neuroligin-2 or  $\alpha$ -neurexin gene would be ideal for determining whether perturbations in neurexin/neuroligin gene expression affect the normal development of glucose-stimulated insulin secretion in  $\beta$ -cells, this *in vitro* model might be useful as an alternative or interim approach given the complexities and time involved in obtaining and breeding these mice. The role of neurexin and neuroligin in the development of stimulus-secretion coupling in this *in vitro* model could be further investigated through the use of adenoviruses designed to express either neuroligin-2 or  $\alpha$ -neurexin cDNA or alternatively, neuroligin-2 or  $\alpha$ -neurexin shRNA. Increasing the expression of either the neurexin and/or the neuroligin genes through the introduction of their cDNA might be expected to speed up the development/maturation of stimulus-secretion coupling whereas decreasing the expression through the introduction of shRNA might be expected to slow down the development/maturation of stimulus-secretion coupling in fetal islets exposed to hyperglycemic conditions if these genes are

important for the functional differentiation and maturation of stimulus-secretion coupling in developing  $\beta$ -cells. Whether these approaches are used, or alternative approaches are employed, it will be important to further understand the role of neuroligin and neurexin in the development and/or maintenance of glucose-stimulated insulin secretion in islet  $\beta$  cells as these genes might be useful targets for future therapies or represent markers for identifying differentiated  $\beta$  cells in the pursuit to generate a  $\beta$  cell replacement therapy from stem cells.

#### F. Where is Neuroligin-1?

Endogenous neuroligin-1 exclusively localizes to glutamatergic (excitatory) synapses in the central nervous system and is essential for their proper differentiation [74, 75]. Interestingly, the glucagon-secreting  $\alpha$ -cells of the endocrine pancreas express much of the machinery necessary for glutamatergic signaling including ionotropic glutamate receptors and the vesicular glutamate transporter [100, 147, 204, 238]. Under hypoglycemic conditions, glutamate is co-secreted from secretory granules with glucagon and thought to act in an autocrine manner to potentiate glucagon secretion [147, 204]. These observations, along with the established association of neuroligin with ionotropic glutamate receptors at synapses and my work in chapter 4 demonstrating high level expression of neuroligin-1 in rat and human islets but not in the  $\beta$ -cell line INS-1, suggest that islet neuroligin-1 is expressed by  $\alpha$ -cells and is important for the co-secretion of glucagon and glutamate and the ability of the  $\alpha$ -cell to potentiate glucagon secretion through glutamate receptors [149, 239].

Because of the distinct and opposite roles of neuroligin-1 and neuroligin-2 in synaptic neurotransmission, an intense effort was put forth as part of this dissertation work to determine the localization of neuroligin-1 within islets. The lack of available commercial antibodies and the inability to generate antibodies that are both specific for neuroligin-1 and useful for immunostaining during this dissertation work hindered this effort. Future *in situ* hybridization analyses on pancreatic sections or single-cell RT-PCR analyses on dissociated islet cells may be necessary to determine the localization of neuroligin-1 within islets.

#### G. The Synaptogenic Adhesion Molecules as Targets for $\beta$ Cell Imaging?

Type 1 diabetes results from autoimmune attack and destruction of islet  $\beta$  cells. Autoantibodies to  $\beta$ -cell antigens are present years before clinical onset and their presence is predictive of the eventual manifestation of disease [240-242]. Most patients do not present with clinical symptoms until 90% of their  $\beta$  cells have been destroyed [243]. There is also a significant loss of  $\beta$ -cell mass in Type 2 diabetics [244]. Because the goal of most therapies is to prevent/slow the destruction of  $\beta$  cells or alternatively, to induce the regeneration of  $\beta$  cells, a method of tracking  $\beta$ -cell mass *in vivo* has been a highly sought after but elusive goal. Such a method would allow for tracking the progression of  $\beta$ -cell destruction during the etiology of Type 1 diabetes, and could be used to evaluate the efficacy of therapies aimed at slowing or preventing the disease. Down the road, quantification of  $\beta$  cell mass might be useful as an endpoint to measure the success of clinical trials.

Thus far, the major hurdle in tracking  $\beta$ -cell mass using imaging technologies such as position emission tomography (PET) is identification of agents that bind to beta cells with high enough specificity to overcome the low ratio of  $\beta$  cells to exocrine tissue [117]. The finding here that the cell surface proteins, neuroligin-2 and  $\alpha$ -neurexin, are expressed at high levels specifically by  $\beta$  cells and the finding by another group whose microarray study demonstrated that these genes are the 10<sup>th</sup> and 11<sup>th</sup> most abundant membrane-associated transcripts in human islets suggests that these proteins are ideal candidate targets for tracking  $\beta$ -cell mass [205].

One approach to the design of high affinity binding reagents to neuroligin-2 and  $\alpha$ -neurexin might be to generate antibodies, and eventually antibody fragments that reduce non-specific binding and blood clearance time, to the extracellular domains of these proteins [117, 245]. After extensive characterization and testing, the antibody fragments could then be labeled with positron-emitting iodine using standard methods, injected into patients, where  $\beta$  cell mass would be proportional to the radioactive decay measured by PET.

An alternative approach might involve taking advantage of the growing list of proteins known to interact with any one of the six distinct extracellular lamin-neurexin-sex hormone binding domains (LNS) of  $\alpha$ -neurexin. Some binding partners with similarly restricted expression patterns include: neuroligins,  $\alpha$ -dystroglycan, neurexophilin and  $\alpha$ -latrotoxin [68, 246-248]. With the recent publication of several neurexin-neuroligin crystal structures and the advancement of peptide array technologies, peptides at the interface of  $\alpha$ -neurexin interaction with any one of its binding partners

could be identified that might eventually be useful for tracking  $\beta$ -cell mass [208, 225, 249-252]. Briefly,  $\alpha$ -neurexin peptides from the LNS domain of interest could be synthesized by a peptide synthesizer and arrayed onto a membrane. The membrane containing the peptides could then be incubated with the extracellular domains of binding partners and interacting peptides detected by immunoblotting for bound extracellular domain. Identified peptides might then be modified to enhance affinity, tagged with an appropriate positron-emitting label and after extensive characterization and testing used for tracking  $\beta$ -cell mass.

#### H. Therapeutic Applications?

Although the necessary proof of principle studies for the application of this dissertation research for the treatment of disease are probably several years away, a brief discussion on the potential therapeutic applications of this work seems warranted given this dissertation will result in a degree in biomedical sciences from a medical school. The demonstration here that soluble neuroligin-2 potently inhibits insulin secretion from islet  $\beta$  cells, as a result of its ability to disrupt endogenous neuroligin-2-receptor interactions around which the insulin secretory machinery is thought to be assembled, may have implications for insulinoma treatment. Insulinomas are rare tumors that originate from  $\beta$  cells and eventually lose the ability to regulate insulin secretion in response to changes in the concentration of serum glucose. As a result, they continuously secrete insulin, leading to increased uptake of serum glucose by peripheral tissues and eventually to hypoglycemia [253]. It is possible that insulin secretion and glucose homeostasis might be better controlled in patients with insulinomas by treatment with either soluble

neuroligin-2 or a molecule that is similarly capable of interfering with endogenous neuroligin-2-receptor interactions. Because most insulinomas are benign and normal glucose homeostasis generally returns after surgical removal of the tumor, this type of treatment may only be warranted in patients prior to surgical removal, in patients with metastatic insulinomas or in patients that are not healthy enough to undergo surgery.

Type 2 diabetes is another indication that this work may have implications for. During the pathogenesis of Type 2 diabetes, peripheral insulin resistance develops, leads to increased hepatic glucose production and decreased uptake of glucose by peripheral tissues, and as a result hyperglycemia occurs. There are also significant deficits in the ability of  $\beta$  cells to secrete insulin in response to glucose [254]. One of the two major methods of treatment involves the use of secretagogues that aim to increase the secretion of endogenous insulin from  $\beta$  cells. The hope with this treatment is that the increased insulin will help to overcome resistance, lead to suppression of glucose production from the liver and increased glucose uptake in peripheral tissues, and alleviate at least some of the hyperglycemia associated with Type 2 diabetes [255]. Through co-culture studies, it has been demonstrated that it is likely that endogenous neuroligin-2 acts to drive the assembly of the insulin secretory apparatus and this results in a marked enhancement in glucose-stimulated insulin secretion. Combined with data from neurons demonstrating that the clustering of neuroligin is necessary for its function, these data suggest that the development of agents that act to enhance the clustering of neuroligin-2 might potentiate insulin secretion from  $\beta$  cells and ultimately be useful as secretagogues for the treatment of Type 2 diabetes [256].

## REFERENCES

1. Franklin, I.K. and C.B. Wollheim, *GABA in the endocrine pancreas: its putative role as an islet cell paracrine-signalling molecule*. J Gen Physiol, 2004. **123**(3): p. 185-90.
2. Gammelsaeter, R., et al., *Glycine, GABA and their transporters in pancreatic islets of Langerhans: evidence for a paracrine transmitter interplay*. J Cell Sci, 2004. **117**(Pt 17): p. 3749-58.
3. Garry, D.J., et al., *Immunoreactive GABA transaminase within the pancreatic islet is localized in mitochondria of the B-cell*. J Histochem Cytochem, 1987. **35**(8): p. 831-6.
4. Okada, Y., H. Taniguchi, and C. Shimada, *High concentration of GABA and high glutamate decarboxylase activity in rat pancreatic islets and human insulinoma*. Science, 1976. **194**(4265): p. 620-2.
5. Suckow, A.T., et al., *Identification and characterization of a novel isoform of the vesicular gamma-aminobutyric acid transporter with glucose-regulated expression in rat islets*. J Mol Endocrinol, 2006. **36**(1): p. 187-99.
6. Rulifson, E.J., S.K. Kim, and R. Nusse, *Ablation of insulin-producing neurons in flies: growth and diabetic phenotypes*. Science, 2002. **296**(5570): p. 1118-20.
7. Hori, Y., et al., *Differentiation of insulin-producing cells from human neural progenitor cells*. PLoS Med, 2005. **2**(4): p. e103.
8. Atouf, F., P. Czernichow, and R. Scharfmann, *Expression of neuronal traits in pancreatic beta cells. Implication of neuron-restrictive silencing factor/repressor element silencing transcription factor, a neuron-restrictive silencer*. J Biol Chem, 1997. **272**(3): p. 1929-34.
9. Bruce, A.W., et al., *The transcriptional repressor REST is a critical regulator of the neurosecretory phenotype*. J Neurochem, 2006. **98**(6): p. 1828-40.
10. D'Alessandro, R., A. Klajn, and J. Meldolesi, *Expression of dense-core vesicles and of their exocytosis are governed by the repressive transcription factor NRSE/REST*. Ann N Y Acad Sci, 2009. **1152**: p. 194-200.
11. D'Alessandro, R., et al., *Expression of the neurosecretory process in PC12 cells is governed by REST*. J Neurochem, 2008. **105**(4): p. 1369-83.
12. Dresbach, T., et al., *The presynaptic cytomatrix of brain synapses*. Cell Mol Life Sci, 2001. **58**(1): p. 94-116.

13. Fujimoto, K., et al., *Piccolo, a Ca<sup>2+</sup> sensor in pancreatic beta-cells. Involvement of cAMP-GEFII.Rim2.Piccolo complex in cAMP-dependent exocytosis.* J Biol Chem, 2002. **277**(52): p. 50497-502.
14. Ohara-Imaizumi, M., et al., *ELKS, a protein structurally related to the active zone-associated protein CAST, is expressed in pancreatic beta cells and functions in insulin exocytosis: interaction of ELKS with exocytotic machinery analyzed by total internal reflection fluorescence microscopy.* Mol Biol Cell, 2005. **16**(7): p. 3289-300.
15. Regazzi, R., et al., *VAMP-2 and cellubrevin are expressed in pancreatic beta-cells and are essential for Ca(2+)-but not for GTP gamma S-induced insulin secretion.* Embo J, 1995. **14**(12): p. 2723-30.
16. Sadoul, K., et al., *SNAP-25 is expressed in islets of Langerhans and is involved in insulin release.* J Cell Biol, 1995. **128**(6): p. 1019-28.
17. Zhang, W., et al., *Munc-18 associates with syntaxin and serves as a negative regulator of exocytosis in the pancreatic beta -cell.* J Biol Chem, 2000. **275**(52): p. 41521-7.
18. Zhang, W., et al., *Mint1, a Munc-18-interacting protein, is expressed in insulin-secreting beta-cells.* Biochem Biophys Res Commun, 2004. **320**(3): p. 717-21.
19. Abderrahmani, A., et al., *Neuronal traits are required for glucose-induced insulin secretion.* FEBS Lett, 2004. **565**(1-3): p. 133-8.
20. Martin, D., et al., *Functional significance of repressor element 1 silencing transcription factor (REST) target genes in pancreatic beta cells.* Diabetologia, 2008.
21. Baekkeskov, S., et al., *Identification of the 64K autoantigen in insulin-dependent diabetes as the GABA-synthesizing enzyme glutamic acid decarboxylase.* Nature, 1990. **347**(6289): p. 151-6.
22. Chessler, S.D. and A. Lernmark, *The role of glutamic acid decarboxylase and GABA in the pancreas and diabetes*, in *GABA in the nervous system: the view at fifty years*, D.L. Martin and R.W. Olson, Editors. 2000, Lippincott Williams & Wilkins: Philadelphia. p. 471-484.
23. Mally, M.I., et al., *Ontogeny and tissue distribution of human GAD expression.* Diabetes, 1996. **45**(4): p. 496-501.
24. Thomas-Reetz, A., et al., *A gamma-aminobutyric acid transporter driven by a proton pump is present in synaptic-like microvesicles of pancreatic beta cells.* Proc Natl Acad Sci U S A, 1993. **90**(11): p. 5317-21.



25. Braun, M., et al., *Regulated exocytosis of GABA-containing synaptic-like microvesicles in pancreatic beta-cells*. J Gen Physiol, 2004. **123**(3): p. 191-204.
26. Garry, D.J., et al., *Cellular and subcellular immunolocalization of L-glutamate decarboxylase in rat pancreatic islets*. J Histochem Cytochem, 1988. **36**(6): p. 573-80.
27. MacDonald, P.E., et al., *Regulated exocytosis and kiss-and-run of synaptic-like microvesicles in INS-1 and primary rat beta-cells*. Diabetes, 2005. **54**(3): p. 736-43.
28. Reetz, A., et al., *GABA and pancreatic beta-cells: colocalization of glutamic acid decarboxylase (GAD) and GABA with synaptic-like microvesicles suggests their role in GABA storage and secretion*. Embo J, 1991. **10**(5): p. 1275-84.
29. Braun, M., et al., *GABAB receptor activation inhibits exocytosis in rat pancreatic beta-cells by G-protein-dependent activation of calcineurin*. J Physiol, 2004. **559**(Pt 2): p. 397-409.
30. Brice, N.L., et al., *Metabotropic glutamate and GABA(B) receptors contribute to the modulation of glucose-stimulated insulin secretion in pancreatic beta cells*. Diabetologia, 2002. **45**(2): p. 242-52.
31. Gu, X.H., et al., *Suppressive effect of GABA on insulin secretion from the pancreatic beta-cells in the rat*. Life Sci, 1993. **52**(8): p. 687-94.
32. Bonaventura, M.M., et al., *GABAB receptors and glucose homeostasis: evaluation in GABAB receptor knockout mice*. Am J Physiol Endocrinol Metab, 2008. **294**(1): p. E157-67.
33. Rorsman, P., et al., *Glucose-inhibition of glucagon secretion involves activation of GABAA-receptor chloride channels*. Nature, 1989. **341**(6239): p. 233-6.
34. Wendt, A., et al., *Glucose inhibition of glucagon secretion from rat alpha-cells is mediated by GABA released from neighboring beta-cells*. Diabetes, 2004. **53**(4): p. 1038-45.
35. Xu, E., et al., *Intra-islet insulin suppresses glucagon release via GABA-GABAA receptor system*. Cell Metab, 2006. **3**(1): p. 47-58.
36. Carrillo, J., et al., *Islet-infiltrating B-cells in nonobese diabetic mice predominantly target nervous system elements*. Diabetes, 2005. **54**(1): p. 69-77.
37. Winer, S., et al., *Autoimmune islet destruction in spontaneous type 1 diabetes is not beta-cell exclusive*. Nat Med, 2003. **9**(2): p. 198-205.

38. Solimena, M., *Vesicular autoantigens of type 1 diabetes*. Diabetes Metab Rev, 1998. **14**(3): p. 227-40.
39. Lernmark, A., *Glutamic acid decarboxylase--gene to antigen to disease*. J Intern Med, 1996. **240**(5): p. 259-77.
40. Baekkeskov, S., et al., *Does GAD have a unique role in triggering IDDM?* J Autoimmun, 2000. **15**(3): p. 279-86.
41. von Boehmer, H. and Sarukhan, *GAD, a single autoantigen for diabetes*. Science, 1999. **284**: p. 1135-1137.
42. Yoon, J.W., et al., *Control of autoimmune diabetes in NOD mice by GAD expression or suppression in beta cells*. Science, 1999. **284**(5417): p. 1183-7.
43. Chen, Q.Y., et al., *Antibodies to glutamic acid decarboxylase in Australian children with insulin-dependent diabetes mellitus and their first-degree relatives*. Pediatr Res, 1993. **34**(6): p. 785-90.
44. Rowley, M.J., et al., *Antibodies to glutamic acid decarboxylase discriminate major types of diabetes mellitus*. Diabetes, 1992. **41**(4): p. 548-51.
45. Verge, C.F., et al., *Anti-glutamate decarboxylase and other antibodies at the onset of childhood IDDM: a population-based study*. Diabetologia, 1994. **37**(11): p. 1113-20.
46. Christgau, S., et al., *Membrane anchoring of the autoantigen GAD65 to microvesicles in pancreatic beta-cells by palmitoylation in the NH2-terminal domain*. J Cell Biol, 1992. **118**(2): p. 309-20.
47. Kanaani, J., et al., *Palmitoylation controls trafficking of GAD65 from Golgi membranes to axon-specific endosomes and a Rab5a-dependent pathway to presynaptic clusters*. J Cell Sci, 2004. **117**(Pt 10): p. 2001-13.
48. Shi, Y., B. Veit, and S. Baekkeskov, *Amino acid residues 24-31 but not palmitoylation of cysteines 30 and 45 are required for membrane anchoring of glutamic acid decarboxylase, GAD65*. J Cell Biol, 1994. **124**(6): p. 927-34.
49. Ziegler, B., et al., *Glutamate decarboxylase (GAD) is not detectable on the surface of rat islet cells examined by cytofluorometry and complement-dependent antibody-mediated cytotoxicity of monoclonal GAD antibodies*. Horm Metab Res, 1996. **28**(1): p. 11-5.
50. Waldrop, M.A., et al., *A Highly Sensitive Immunoassay Resistant to Autoantibody Interference for Detection of the Diabetes-Associated Autoantigen Glutamic Acid Decarboxylase 65 in Blood and Other Biological Samples*. Diabetes Technol Ther, 2006. **8**(2): p. 207-218.

51. Waldrop, M.A., et al., *Release of glutamate decarboxylase-65 into the circulation by injured pancreatic islet beta-cells*. Endocrinology, 2007. **148**(10): p. 4572-8.
52. De Camilli, P., et al., *The synaptic vesicle-associated protein amphiphysin is the 128-kD autoantigen of Stiff-Man syndrome with breast cancer*. J Exp Med, 1993. **178**(6): p. 2219-23.
53. Newman, L.S., et al., *Beta-NAP, a cerebellar degeneration antigen, is a neuron-specific vesicle coat protein*. Cell, 1995. **82**(5): p. 773-83.
54. Hirai, H., et al., *Selective screening of secretory vesicle-associated proteins for autoantigens in type 1 diabetes: VAMP2 and NPY are new minor autoantigens*. Clin Immunol, 2008. **127**(3): p. 366-74.
55. Boehm, M. and J.S. Bonifacino, *Adaptins: the final recount*. Mol Biol Cell, 2001. **12**(10): p. 2907-20.
56. Blumstein, J., et al., *The neuronal form of adaptor protein-3 is required for synaptic vesicle formation from endosomes*. J Neurosci, 2001. **21**(20): p. 8034-42.
57. Newell-Litwa, K., et al., *Neuronal and non-neuronal functions of the AP-3 sorting machinery*. J Cell Sci, 2007. **120**(Pt 4): p. 531-41.
58. Jin, H., et al., *Demonstration of functional coupling between gamma - aminobutyric acid (GABA) synthesis and vesicular GABA transport into synaptic vesicles*. Proc Natl Acad Sci U S A, 2003. **100**(7): p. 4293-8.
59. Nakatsu, F., et al., *Defective function of GABA-containing synaptic vesicles in mice lacking the AP-3B clathrin adaptor*. J Cell Biol, 2004. **167**(2): p. 293-302.
60. Seong, E., et al., *Genetic analysis of the neuronal and ubiquitous AP-3 adaptor complexes reveals divergent functions in brain*. Mol Biol Cell, 2005. **16**(1): p. 128-40.
61. Kang, L., et al., *Munc13-1 is required for the sustained release of insulin from pancreatic beta cells*. Cell Metab, 2006.
62. Kwan, E.P., et al., *Munc13-1 deficiency reduces insulin secretion and causes abnormal glucose tolerance*. Diabetes, 2006. **55**(5): p. 1421-9.
63. Ohara-Imaizumi, M., et al., *Correlation of syntaxin-1 and SNAP-25 clusters with docking and fusion of insulin granules analysed by total internal reflection fluorescence microscopy*. Diabetologia, 2004. **47**(12): p. 2200-7.
64. Piechotta, K., I. Dudanova, and M. Missler, *The resilient synapse: insights from genetic interference of synaptic cell adhesion molecules*. Cell Tissue Res, 2006. **326**(2): p. 617-42.

65. Scheiffele, P., et al., *Neuroigin expressed in nonneuronal cells triggers presynaptic development in contacting axons*. Cell, 2000. **101**(6): p. 657-69.
66. Dean, C., et al., *Neurexin mediates the assembly of presynaptic terminals*. Nat Neurosci, 2003. **6**(7): p. 708-16.
67. Missler, M., R. Fernandez-Chacon, and T.C. Sudhof, *The making of neurexins*. J Neurochem, 1998. **71**(4): p. 1339-47.
68. Ichtchenko, K., T. Nguyen, and T.C. Sudhof, *Structures, alternative splicing, and neurexin binding of multiple neuroligins*. J Biol Chem, 1996. **271**(5): p. 2676-82.
69. Ushkaryov, Y.A., et al., *Neurexins: synaptic cell surface proteins related to the alpha-latrotoxin receptor and laminin*. Science, 1992. **257**(5066): p. 50-6.
70. Ichtchenko, K., et al., *Neuroigin 1: a splice site-specific ligand for beta-neurexins*. Cell, 1995. **81**(3): p. 435-43.
71. Biederer, T., et al., *SynCAM, a synaptic adhesion molecule that drives synapse assembly*. Science, 2002. **297**(5586): p. 1525-31.
72. Varoqueaux, F., et al., *Neuroligins determine synapse maturation and function*. Neuron, 2006. **51**(6): p. 741-54.
73. Missler, M., et al., *Alpha-neurexins couple Ca<sup>2+</sup> channels to synaptic vesicle exocytosis*. Nature, 2003. **423**(6943): p. 939-48.
74. Chubykin, A.A., et al., *Activity-dependent validation of excitatory versus inhibitory synapses by neuroligin-1 versus neuroligin-2*. Neuron, 2007. **54**(6): p. 919-31.
75. Song, J.Y., et al., *Neuroigin 1 is a postsynaptic cell-adhesion molecule of excitatory synapses*. Proc Natl Acad Sci U S A, 1999. **96**(3): p. 1100-5.
76. Varoqueaux, F., S. Jamain, and N. Brose, *Neuroigin 2 is exclusively localized to inhibitory synapses*. Eur J Cell Biol, 2004. **83**(9): p. 449-56.
77. Graf, E.R., et al., *Structure function and splice site analysis of the synaptogenic activity of the neurexin-1 beta LNS domain*. J Neurosci, 2006. **26**(16): p. 4256-65.
78. Dudanova, I., et al., *Important contribution of alpha-neurexins to Ca<sup>2+</sup>-triggered exocytosis of secretory granules*. J Neurosci, 2006. **26**(41): p. 10599-613.
79. Zhang, W., et al., *Extracellular domains of alpha-neurexins participate in regulating synaptic transmission by selectively affecting N- and P/Q-type Ca<sup>2+</sup> channels*. J Neurosci, 2005. **25**(17): p. 4330-42.

80. Hines, R.M., et al., *Synaptic imbalance, stereotypies, and impaired social interactions in mice with altered neuroligin 2 expression*. J Neurosci, 2008. **28**(24): p. 6055-67.
81. Wittenmayer, N., et al., *Postsynaptic Neuroligin1 regulates presynaptic maturation*. Proc Natl Acad Sci U S A, 2009. **106**(32): p. 13564-9.
82. Bosco, D., L. Orci, and P. Meda, *Homologous but not heterologous contact increases the insulin secretion of individual pancreatic B-cells*. Exp Cell Res, 1989. **184**(1): p. 72-80.
83. Dahl, U., A. Sjodin, and H. Semb, *Cadherins regulate aggregation of pancreatic beta-cells in vivo*. Development, 1996. **122**(9): p. 2895-902.
84. Hauge-Evans, A.C., et al., *Pancreatic beta-cell-to-beta-cell interactions are required for integrated responses to nutrient stimuli: enhanced Ca<sup>2+</sup> and insulin secretory responses of MIN6 pseudoislets*. Diabetes, 1999. **48**(7): p. 1402-8.
85. Konstantinova, I., et al., *EphA-Ephrin-A-mediated beta cell communication regulates insulin secretion from pancreatic islets*. Cell, 2007. **129**(2): p. 359-70.
86. Luther, M.J., et al., *MIN6 beta-cell-beta-cell interactions influence insulin secretory responses to nutrients and non-nutrients*. Biochem Biophys Res Commun, 2006. **343**(1): p. 99-104.
87. Pipeleers, D., et al., *Glucose-induced insulin release depends on functional cooperation between islet cells*. Proc Natl Acad Sci U S A, 1982. **79**(23): p. 7322-5.
88. Mears, D., *Regulation of insulin secretion in islets of Langerhans by Ca(2+)channels*. J Membr Biol, 2004. **200**(2): p. 57-66.
89. Biederer, T. and T.C. Sudhof, *Mints as adaptors. Direct binding to neuroligins and recruitment of munc18*. J Biol Chem, 2000. **275**(51): p. 39803-6.
90. Biederer, T. and T.C. Sudhof, *CASK and protein 4.1 support F-actin nucleation on neuroligins*. J Biol Chem, 2001. **276**(51): p. 47869-76.
91. Hata, Y., S. Butz, and T.C. Sudhof, *CASK: a novel dlg/PSD95 homolog with an N-terminal calmodulin-dependent protein kinase domain identified by interaction with neuroligins*. J Neurosci, 1996. **16**(8): p. 2488-94.
92. Tabuchi, K., et al., *CASK participates in alternative tripartite complexes in which Mint 1 competes for binding with caskin 1, a novel CASK-binding protein*. J Neurosci, 2002. **22**(11): p. 4264-73.

93. Zhang, Y., et al., *The scaffolding protein CASK mediates the interaction between rabphilin3a and beta-neurexins*. FEBS Lett, 2001. **497**(2-3): p. 99-102.
94. O'Connor, V.M., et al., *On the structure of the 'synaptosecretosome'. Evidence for a neurexin/synaptotagmin/syntaxin/Ca<sup>2+</sup> channel complex*. FEBS Lett, 1993. **326**(1-3): p. 255-60.
95. Perin, M.S., *The COOH terminus of synaptotagmin mediates interaction with the neurexins*. J Biol Chem, 1994. **269**(11): p. 8576-81.
96. Satin, L.S. and T.A. Kinard, *Neurotransmitters and their receptors in the islets of Langerhans of the pancreas: what messages do acetylcholine, glutamate, and GABA transmit?* Endocrine, 1998. **8**(3): p. 213-23.
97. Elliott, J.F., et al., *Immunization with the larger isoform of mouse glutamic acid decarboxylase (GAD67) prevents autoimmune diabetes in NOD mice*. Diabetes, 1994. **43**(12): p. 1494-9.
98. Gasnier, B., *The SLC32 transporter, a key protein for the synaptic release of inhibitory amino acids*. Pflugers Arch, 2004. **447**(5): p. 756-9.
99. Chessler, S.D., et al., *Expression of the vesicular inhibitory amino acid transporter in pancreatic islet cells: distribution of the transporter within rat islets*. Diabetes, 2002. **51**(6): p. 1763-71.
100. Hayashi, M., et al., *Vesicular Inhibitory Amino Acid Transporter Is Present in Glucagon-Containing Secretory Granules in alphaTC6 Cells, Mouse Clonal alpha-Cells, and alpha-Cells of Islets of Langerhans*. Diabetes, 2003. **52**(8): p. 2066-74.
101. Bedet, C., et al., *Constitutive phosphorylation of the vesicular inhibitory amino acid transporter in rat central nervous system*. J Neurochem, 2000. **75**(4): p. 1654-63.
102. Takamori, S., D. Riedel, and R. Jahn, *Immunoisolation of GABA-specific synaptic vesicles defines a functionally distinct subset of synaptic vesicles*. J Neurosci, 2000. **20**(13): p. 4904-11.
103. Echigo, N. and Y. Moriyama, *Vesicular inhibitory amino acid transporter is expressed in gamma-aminobutyric acid (GABA)-containing astrocytes in rat pineal glands*. Neurosci Lett, 2004. **367**(1): p. 79-84.
104. Dumoulin, A., et al., *Presence of the vesicular inhibitory amino acid transporter in GABAergic and glycinergic synaptic terminal boutons*. J Cell Sci, 1999. **112**(Pt 6): p. 811-23.

105. Chih, B., H. Engelman, and P. Scheiffele, *Control of excitatory and inhibitory synapse formation by neuroligins*. Science, 2005. **307**(5713): p. 1324-8.
106. Prange, O., et al., *A balance between excitatory and inhibitory synapses is controlled by PSD-95 and neuroligin*. Proc Natl Acad Sci U S A, 2004. **101**(38): p. 13915-20.
107. Geigerseder, C., et al., *Evidence for a GABAergic system in rodent and human testis: local GABA production and GABA receptors*. Neuroendocrinology, 2003. **77**(5): p. 314-23.
108. Saito, T., et al., *Somatostatin regulates brain amyloid beta peptide Abeta42 through modulation of proteolytic degradation*. Nat Med, 2005. **11**(4): p. 434-9.
109. McIntire, S.L., et al., *Identification and characterization of the vesicular GABA transporter*. Nature, 1997. **389**(6653): p. 870-6.
110. Hampe, C.S., et al., *A novel monoclonal antibody specific for the N-terminal end of GAD65*. J Neuroimmunol, 2001. **113**(1): p. 63-71.
111. Bieg, S., et al., *Genetic isolation of iddm 1 on chromosome 4 in the biobreeding (BB) rat*. Mamm Genome, 1998. **9**(4): p. 324-6.
112. Lingohr, M.K., et al., *Decreasing IRS-2 expression in pancreatic beta-cells (INS-1) promotes apoptosis, which can be compensated for by introduction of IRS-4 expression*. Mol Cell Endocrinol, 2003. **209**(1-2): p. 17-31.
113. Wrede, C.E., et al., *Fatty acid and phorbol ester-mediated interference of mitogenic signaling via novel protein kinase C isoforms in pancreatic beta-cells (INS-1)*. J Mol Endocrinol, 2003. **30**(3): p. 271-86.
114. Wrede, C.E., et al., *Protein kinase B/Akt prevents fatty acid-induced apoptosis in pancreatic beta-cells (INS-1)*. J Biol Chem, 2002. **277**(51): p. 49676-84.
115. Dickson, L.M., et al., *Differential activation of protein kinase B and p70(S6)K by glucose and insulin-like growth factor 1 in pancreatic beta-cells (INS-1)*. J Biol Chem, 2001. **276**(24): p. 21110-20.
116. Sweet, I.R., et al., *Dynamic perfusion to maintain and assess isolated pancreatic islets*. Diabetes Technol Ther, 2002. **4**(1): p. 67-76.
117. Sweet, I.R., et al., *Systematic screening of potential beta-cell imaging agents*. Biochem Biophys Res Commun, 2004. **314**(4): p. 976-83.
118. Clift-O'Grady, L., et al., *Reconstitution of synaptic vesicle biogenesis from PC12 cell membranes*. Methods, 1998. **16**(2): p. 150-9.

119. O'Farrell, P.H., *High resolution two-dimensional electrophoresis of proteins*. J Biol Chem, 1975. **250**(10): p. 4007-21.
120. Ames, G.F. and K. Nikaido, *Two-dimensional gel electrophoresis of membrane proteins*. Biochemistry, 1976. **15**(3): p. 616-23.
121. McCarthy, J., et al., *Carbamylation of proteins in 2-D electrophoresis--myth or reality?* J Proteome Res, 2003. **2**(3): p. 239-42.
122. Kozak, M., *Initiation of translation in prokaryotes and eukaryotes*. Gene, 1999. **234**(2): p. 187-208.
123. Brown, J.L. and W.K. Roberts, *Evidence that approximately eighty per cent of the soluble proteins from Ehrlich ascites cells are Nalpha-acetylated*. J Biol Chem, 1976. **251**(4): p. 1009-14.
124. Persson, B., et al., *Structures of N-terminally acetylated proteins*. Eur J Biochem, 1985. **152**(3): p. 523-7.
125. Chevallet, M., et al., *New zwitterionic detergents improve the analysis of membrane proteins by two-dimensional electrophoresis*. Electrophoresis, 1998. **19**(11): p. 1901-9.
126. Santoni, V., M. Molloy, and T. Rabilloud, *Membrane proteins and proteomics: un amour impossible?* Electrophoresis, 2000. **21**(6): p. 1054-70.
127. Zink, M. and R. Spanagel, *Ethanol induces GAD67 and VGAT in slice cultures of newborn rat cerebral cortex*. Neuroreport, 2005. **16**(4): p. 377-80.
128. Zink, M., et al., *Differential effects of long-term treatment with clozapine or haloperidol on GABA transporter expression*. Pharmacopsychiatry, 2004. **37**(4): p. 171-4.
129. Kang, T.C., et al., *Presynaptic gamma-aminobutyric acid type B receptor-mediated regulation of vesicular gamma-aminobutyric acid transporter expression in the gerbil hippocampus*. Neurosci Lett, 2003. **346**(1-2): p. 49-52.
130. Petersen, J.S., et al., *Regulation of GAD expression in rat pancreatic islets and brain by gamma-vinyl-GABA and glucose*. Diabetologia, 1998. **41**(5): p. 530-5.
131. Smismans, A., F. Schuit, and D. Pipeleers, *Nutrient regulation of gamma-aminobutyric acid release from islet beta cells*. Diabetologia, 1997. **40**(12): p. 1411-5.
132. Hao, W., et al., *Functional state of the beta cell affects expression of both forms of glutamic acid decarboxylase*. Pancreas, 1994. **9**(5): p. 558-62.



133. Poitout, V., L.K. Olson, and R.P. Robertson, *Insulin-secreting cell lines: classification, characteristics and potential applications*. Diabetes Metab, 1996. **22**(1): p. 7-14.
134. Clift-O'Grady, L., et al., *Biogenesis of synaptic vesicle-like structures in a pheochromocytoma cell line PC-12*. J Cell Biol, 1990. **110**(5): p. 1693-703.
135. Wieczorek, R., R. Stover, and M. Sebenik, *Nonspecific nuclear immunoreactivity after antigen retrieval using acidic or basic solutions..* J Histotechnol, 1997. **20**(2): p. 139-143.
136. Miller, R.T., *Technical Immunohistochemistry: Achieving Reliability and Reproducibility of Immunostains*. 2001, Society for Applied Immunohistochemistry: Dallas. p. 1-53.
137. Chang, K.L., D.A. Arber, and L.M. Weiss, *CD20: A review*. Applied Immunohistochemistry, 1996. **4**(1): p. 1-15.
138. Donev, S.R., *Ultrastructural evidence for the presence of a glial sheath investing the islets of Langerhans in the pancreas of mammals*. Cell Tissue Res, 1984. **237**(2): p. 343-8.
139. Regoli, M., et al., *Glial fibrillary acidic protein (GFAP)-like immunoreactivity in rat endocrine pancreas*. J Histochem Cytochem, 2000. **48**(2): p. 259-66.
140. O'Donovan, K.J. and J.M. Baraban, *Major Egr3 isoforms are generated via alternate translation start sites and differ in their abilities to activate transcription*. Mol Cell Biol, 1999. **19**(7): p. 4711-8.
141. Liu, J., et al., *Initiation of translation from a downstream in-frame AUG codon on BRCA1 can generate the novel isoform protein DeltaBRCA1(17aa)*. Oncogene, 2000. **19**(23): p. 2767-73.
142. Barraille, P., et al., *Alternative initiation of translation accounts for a 67/45 kDa dimorphism of the human estrogen receptor ERalpha*. Biochem Biophys Res Commun, 1999. **257**(1): p. 84-8.
143. Byrd, M.P., M. Zamora, and R.E. Lloyd, *Generation of multiple isoforms of eukaryotic translation initiation factor 4GI by use of alternate translation initiation codons*. Mol Cell Biol, 2002. **22**(13): p. 4499-511.
144. Ebihara, S., K. Obata, and Y. Yanagawa, *Mouse vesicular GABA transporter gene: genomic organization, transcriptional regulation and chromosomal localization*. Brain Res Mol Brain Res, 2003. **110**(1): p. 126-39.

145. Battaglioli, G., H. Liu, and D.L. Martin, *Kinetic differences between the isoforms of glutamate decarboxylase: implications for the regulation of GABA synthesis*. J Neurochem, 2003. **86**(4): p. 879-87.
146. Bai, L., X. Zhang, and F.K. Ghishan, *Characterization of vesicular glutamate transporter in pancreatic alpha - and beta -cells and its regulation by glucose*. Am J Physiol Gastrointest Liver Physiol, 2003. **284**(5): p. G808-14.
147. Hayashi, M., et al., *Secretory granule-mediated co-secretion of L-glutamate and glucagon triggers glutamatergic signal transmission in islets of Langerhans*. J Biol Chem, 2003. **278**(3): p. 1966-74.
148. Thomas-Reetz, A.C. and P. De Camilli, *A role for synaptic vesicles in non-neuronal cells: clues from pancreatic beta cells and from chromaffin cells*. Faseb J, 1994. **8**(2): p. 209-16.
149. Suckow, A.T., et al., *Expression of neurexin, neuroligin, and their cytoplasmic binding partners in the pancreatic beta-cells and the involvement of neuroligin in insulin secretion*. Endocrinology, 2008. **149**(12): p. 6006-17.
150. Wang, S., et al., *The origin of islet-like cells in Drosophila identifies parallels to the vertebrate endocrine axis*. Proc Natl Acad Sci U S A, 2007. **104**(50): p. 19873-8.
151. Shi, G., et al., *Neuroendocrine synaptic vesicles are formed in vitro by both clathrin-dependent and clathrin-independent pathways*. J Cell Biol, 1998. **143**(4): p. 947-55.
152. Feany, M.B., et al., *The synaptic vesicle protein SV2 is a novel type of transmembrane transporter*. Cell, 1992. **70**(5): p. 861-7.
153. Guo, J., et al., *Phosphatidylinositol 4-kinase type IIalpha is responsible for the phosphatidylinositol 4-kinase activity associated with synaptic vesicles*. Proc Natl Acad Sci U S A, 2003. **100**(7): p. 3995-4000.
154. Hohmeier, H.E. and C.B. Newgard, *Cell lines derived from pancreatic islets*. Mol Cell Endocrinol, 2004. **228**(1-2): p. 121-8.
155. Weaver, C.D., et al., *Differential expression of glutamate receptor subtypes in rat pancreatic islets*. J Biol Chem, 1996. **271**(22): p. 12977-84.
156. Guest, P.C., et al., *Co-secretion of carboxypeptidase H and insulin from isolated rat islets of Langerhans*. Biochem J, 1989. **264**(2): p. 503-8.
157. Iezzi, M., et al., *SV2A and SV2C are not vesicular Ca<sup>2+</sup> transporters but control glucose-evoked granule recruitment*. J Cell Sci, 2005. **118**(Pt 23): p. 5647-60.

158. Fricker, L.D., *Carboxypeptidase E*. Annu Rev Physiol, 1988. **50**: p. 309-21.
159. Schilling, K. and M. Gratzl, *Quantification of p38/synaptophysin in highly purified adrenal medullary chromaffin vesicles*. FEBS Lett, 1988. **233**(1): p. 22-4.
160. Schmidle, T., et al., *Synaptin/synaptophysin, p65 and SV2: their presence in adrenal chromaffin granules and sympathetic large dense core vesicles*. Biochim Biophys Acta, 1991. **1060**(3): p. 251-6.
161. Craige, B., G. Salazar, and V. Faundez, *Isolation of Synaptic Vesicles*, in *Current protocols in cell biology*, J. Bonifacino, Editor. 2004, John Wiley: New York. p. 12.1-12.17.
162. Takamori, S., et al., *Molecular anatomy of a trafficking organelle*. Cell, 2006. **127**(4): p. 831-46.
163. Cooney, J.R., et al., *Endosomal compartments serve multiple hippocampal dendritic spines from a widespread rather than a local store of recycling membrane*. J Neurosci, 2002. **22**(6): p. 2215-24.
164. Salazar, G., et al., *The zinc transporter ZnT3 interacts with AP-3 and it is preferentially targeted to a distinct synaptic vesicle subpopulation*. Mol Biol Cell, 2004. **15**(2): p. 575-87.
165. Schmidt, A., M.J. Hannah, and W.B. Huttner, *Synaptic-like microvesicles of neuroendocrine cells originate from a novel compartment that is continuous with the plasma membrane and devoid of transferrin receptor*. J Cell Biol, 1997. **137**(2): p. 445-58.
166. Newell-Litwa, K., et al., *Roles of BLOC-1 and adaptor protein-3 complexes in cargo sorting to synaptic vesicles*. Mol Biol Cell, 2009. **20**(5): p. 1441-53.
167. Salazar, G., et al., *Hermansky-Pudlak syndrome protein complexes associate with phosphatidylinositol 4-kinase type II alpha in neuronal and non-neuronal cells*. J Biol Chem, 2009. **284**(3): p. 1790-802.
168. Craige, B., G. Salazar, and V. Faundez, *Phosphatidylinositol-4-kinase type II alpha contains an AP-3-sorting motif and a kinase domain that are both required for endosome traffic*. Mol Biol Cell, 2008. **19**(4): p. 1415-26.
169. Ooi, C.E., E.C. Dell'Angelica, and J.S. Bonifacino, *ADP-Ribosylation factor 1 (ARF1) regulates recruitment of the AP-3 adaptor complex to membranes*. J Cell Biol, 1998. **142**(2): p. 391-402.
170. Faundez, V., J.T. Horng, and R.B. Kelly, *ADP ribosylation factor 1 is required for synaptic vesicle budding in PC12 cells*. J Cell Biol, 1997. **138**(3): p. 505-15.

171. Salazar, G., et al., *Phosphatidylinositol-4-Kinase Type II Alpha Is a Component of AP-3-derived Vesicles*. Mol Biol Cell, 2005.
172. Falorni, A., et al., *Radioimmunoassays for glutamic acid decarboxylase (GAD65) and GAD65 autoantibodies using 35S or 3H recombinant human ligands*. J Immunol Methods, 1995. **186**(1): p. 89-99.
173. Chessler, S.D., et al., *Immune reactivity to GAD25 in type 1 diabetes mellitus*. Autoimmunity, 2002. **35**(5): p. 335-41.
174. Bonifacio, E., A. Lernmark, and R.L. Dawkins, *Serum exchange and use of dilutions have improved precision of measurement of islet cell antibodies*. J Immunol Methods, 1988. **106**(1): p. 83-8.
175. Mire-Sluis, A.R., R.G. Das, and Lernmark, *The development of a World Health Organisation international standard for islet cell antibodies: the aims and design of an international collaborative study*. Diabetes Metab Res Rev, 1999. **15**(1): p. 72-77.
176. Smidt, K., et al., *SLC30A3 responds to glucose- and zinc variations in beta-cells and is critical for insulin production and in vivo glucose-metabolism during beta-cell stress*. PLoS One, 2009. **4**(5): p. e5684.
177. Palmiter, R.D., et al., *ZnT-3, a putative transporter of zinc into synaptic vesicles*. Proc Natl Acad Sci U S A, 1996. **93**(25): p. 14934-9.
178. Chausmer, A.B., *Zinc, insulin and diabetes*. J Am Coll Nutr, 1998. **17**(2): p. 109-15.
179. Ishihara, H., et al., *Islet beta-cell secretion determines glucagon release from neighbouring alpha-cells*. Nat Cell Biol, 2003. **5**(4): p. 330-5.
180. Baekkeskov, S., et al., *Identification of the 64K autoantigen in insulin-dependent diabetes as the GABA-synthesizing enzyme glutamic acid decarboxylase*. Nature, 1990. **347**(6289): p. 151-6.
181. Craig, A.M. and Y. Kang, *Neurexin-neuroligin signaling in synapse development*. Curr Opin Neurobiol, 2007. **17**(1): p. 43-52.
182. Missler, M. and T.C. Sudhof, *Neurexins: three genes and 1001 products*. Trends Genet, 1998. **14**(1): p. 20-6.
183. Bolliger, M.F., et al., *Unusually rapid evolution of Neuroligin-4 in mice*. Proc Natl Acad Sci U S A, 2008. **105**(17): p. 6421-6.

184. Chih, B., L. Gollan, and P. Scheiffele, *Alternative splicing controls selective trans-synaptic interactions of the neuroligin-neurexin complex*. Neuron, 2006. **51**(2): p. 171-8.
185. Graf, E.R., et al., *Neurexins induce differentiation of GABA and glutamate postsynaptic specializations via neuroligins*. Cell, 2004. **119**(7): p. 1013-26.
186. Sara, Y., et al., *Selective capability of SynCAM and neuroligin for functional synapse assembly*. J Neurosci, 2005. **25**(1): p. 260-70.
187. Fogel, A.I., et al., *SynCAMs organize synapses through heterophilic adhesion*. J Neurosci, 2007. **27**(46): p. 12516-30.
188. Kang, Y., et al., *Induction of GABAergic postsynaptic differentiation by alpha-neurexins*. J Biol Chem, 2008. **283**(4): p. 2323-34.
189. Comoletti, D., et al., *Gene selection, alternative splicing, and post-translational processing regulate neuroligin selectivity for beta-neurexins*. Biochemistry, 2006. **45**(42): p. 12816-27.
190. Comoletti, D., et al., *The Arg451Cys-neuroligin-3 mutation associated with autism reveals a defect in protein processing*. J Neurosci, 2004. **24**(20): p. 4889-93.
191. Comoletti, D., et al., *Characterization of the interaction of a recombinant soluble neuroligin-1 with neurexin-1beta*. J Biol Chem, 2003. **278**(50): p. 50497-505.
192. Reed, N.A., et al., *An immunohistochemical method for the detection of proteins in the vertebrate lens*. J Immunol Methods, 2001. **253**(1-2): p. 243-52.
193. Sweet, I.R., et al., *Regulation of ATP/ADP in pancreatic islets*. Diabetes, 2004. **53**(2): p. 401-9.
194. Boucard, A.A., et al., *A splice code for trans-synaptic cell adhesion mediated by binding of neuroligin 1 to alpha- and beta-neurexins*. Neuron, 2005. **48**(2): p. 229-36.
195. Sassoe-Pognetto, M. and J.M. Fritschy, *Mini-review: gephyrin, a major postsynaptic protein of GABAergic synapses*. Eur J Neurosci, 2000. **12**(7): p. 2205-10.
196. O'Brien, R.J., L.F. Lau, and R.L. Huganir, *Molecular mechanisms of glutamate receptor clustering at excitatory synapses*. Curr Opin Neurobiol, 1998. **8**(3): p. 364-9.
197. Irie, M., et al., *Binding of neuroligins to PSD-95*. Science, 1997. **277**(5331): p. 1511-5.

198. Pouloupoulos, A., et al., *Interaction of neuroligins with gephyrin is a critical link in inhibitory postsynaptic organization*. 2007 Neuroscience Meeting Planner. San Diego, CA: Society for Neuroscience, 2007. Online., 2007: p. 35.7/E16.
199. Cirulli, V., et al., *Expression of neural cell adhesion molecule (N-CAM) in rat islets and its role in islet cell type segregation*. J Cell Sci, 1994. **107 ( Pt 6)**: p. 1429-36.
200. Craig, A.M., E.R. Graf, and M.W. Linhoff, *How to build a central synapse: clues from cell culture*. Trends Neurosci, 2006. **29**(1): p. 8-20.
201. Easom, R.A., *Beta-granule transport and exocytosis*. Semin Cell Dev Biol, 2000. **11**(4): p. 253-66.
202. De Jaco, A., et al., *A single mutation near the C-terminus in alpha/beta hydrolase fold protein family causes a defect in protein processing*. Chem Biol Interact, 2005. **157-158**: p. 371-2.
203. Weir, G.C., et al., *Dispersed adult rat pancreatic islet cells in culture: A, B, and D cell function*. Metabolism, 1984. **33**(5): p. 447-53.
204. Cabrera, O., et al., *Glutamate is a positive autocrine signal for glucagon release*. Cell Metab, 2008. **7**(6): p. 545-54.
205. Maffei, A., et al., *Identification of tissue-restricted transcripts in human islets*. Endocrinology, 2004. **145**(10): p. 4513-21.
206. von Blankenfeld, G., et al., *Expression of functional GABAA receptors in neuroendocrine gastropancreatic cells*. Pflugers Arch, 1995. **430**(3): p. 381-8.
207. Kennedy, M.B., *The postsynaptic density at glutamatergic synapses*. Trends Neurosci, 1997. **20**(6): p. 264-8.
208. Fabrichny, I.P., et al., *Structural analysis of the synaptic protein neuroligin and its beta-neurexin complex: determinants for folding and cell adhesion*. Neuron, 2007. **56**(6): p. 979-91.
209. Comoletti, D., et al., *Synaptic arrangement of the neuroligin/beta-neurexin complex revealed by X-ray and neutron scattering*. Structure, 2007. **15**(6): p. 693-705.
210. Hooghe-Peters, E.L., P. Meda, and L. Orci, *Co-culture of nerve cells and pancreatic islets*. Brain Res, 1981. **227**(2): p. 287-92.
211. Moller, C.J., et al., *Differential expression of neural cell adhesion molecule and cadherins in pancreatic islets, glucagonomas, and insulinomas*. Mol Endocrinol, 1992. **6**(8): p. 1332-42.

212. Lise, M.F. and A. El-Husseini, *The neuroligin and neurexin families: from structure to function at the synapse*. Cell Mol Life Sci, 2006. **63**(16): p. 1833-49.
213. Watanabe, R.C., W.; Erdos, M.; Saxena, R.; Jackson, A; Lyssenko, V.; Uda, M.; Buchanan, T.; Schlessinger, D.; Groop, L.; Collins, F.; Altshuler, D.; Abecasis, G.; Boehnke, M.; Scuteri, A.;, *Novel Genetic Loci for Fasting Glucose and Insulin Identified by Genome-wide Association in Caucasians*. 2008 American Diabetes Association Annual Meeting, 2008. **137-OR**.
214. Sons, M.S., et al., *alpha-Neurexins are required for efficient transmitter release and synaptic homeostasis at the mouse neuromuscular junction*. Neuroscience, 2006. **138**(2): p. 433-46.
215. Yamagata, M., J.R. Sanes, and J.A. Weiner, *Synaptic adhesion molecules*. Curr Opin Cell Biol, 2003. **15**(5): p. 621-32.
216. Brose, N., *Synaptic cell adhesion proteins and synaptogenesis in the mammalian central nervous system*. Naturwissenschaften, 1999. **86**(11): p. 516-24.
217. Kayser, M.S., et al., *Intracellular and trans-synaptic regulation of glutamatergic synaptogenesis by EphB receptors*. J Neurosci, 2006. **26**(47): p. 12152-64.
218. Kim, S., et al., *NGL family PSD-95-interacting adhesion molecules regulate excitatory synapse formation*. Nat Neurosci, 2006. **9**(10): p. 1294-301.
219. Aoto, J., et al., *Postsynaptic ephrinB3 promotes shaft glutamatergic synapse formation*. J Neurosci, 2007. **27**(28): p. 7508-19.
220. Zhang, W., et al., *Netrin-G2 and netrin-G2 ligand are both required for normal auditory responsiveness*. Genes Brain Behav, 2008. **7**(4): p. 385-92.
221. Ko, J., et al., *Neuroligin-1 performs neurexin-dependent and neurexin-independent functions in synapse validation*. Embo J, 2009. **28**(20): p. 3244-55.
222. Ushkaryov, Y.A., et al., *Conserved domain structure of beta-neurexins. Unusual cleaved signal sequences in receptor-like neuronal cell-surface proteins*. J Biol Chem, 1994. **269**(16): p. 11987-92.
223. De Jaco, A., et al., *A mutation linked with autism reveals a common mechanism of endoplasmic reticulum retention for the alpha,beta-hydrolase fold protein family*. J Biol Chem, 2006. **281**(14): p. 9667-76.
224. Brereton, H.C., et al., *Homotypic cell contact enhances insulin but not glucagon secretion*. Biochem Biophys Res Commun, 2006. **344**(3): p. 995-1000.

225. Arac, D., et al., *Structures of neuroligin-1 and the neuroligin-1/neurexin-1 beta complex reveal specific protein-protein and protein-Ca<sup>2+</sup> interactions*. Neuron, 2007. **56**(6): p. 992-1003.
226. Reissner, C., et al., *Mutational analysis of the neurexin/neuroligin complex reveals essential and regulatory components*. Proc Natl Acad Sci U S A, 2008. **105**(39): p. 15124-9.
227. Dowling, P., et al., *Proteomic screening of glucose-responsive and glucose non-responsive MIN-6 beta cells reveals differential expression of proteins involved in protein folding, secretion and oxidative stress*. Proteomics, 2006. **6**(24): p. 6578-87.
228. O'Driscoll, L., et al., *Phenotypic and global gene expression profile changes between low passage and high passage MIN-6 cells*. J Endocrinol, 2006. **191**(3): p. 665-76.
229. Rutter, G.A., T. Tsuboi, and M.A. Ravier, *Ca<sup>2+</sup> microdomains and the control of insulin secretion*. Cell Calcium, 2006. **40**(5-6): p. 539-51.
230. Ohara-Imaizumi, M., et al., *Site of docking and fusion of insulin secretory granules in live MIN6 beta cells analyzed by TAT-conjugated anti-syntaxin 1 antibody and total internal reflection fluorescence microscopy*. J Biol Chem, 2004. **279**(9): p. 8403-8.
231. Clare-Salzler, M.J., A.J. Tobin, and D.L. Kaufman, *Glutamate decarboxylase: an autoantigen in IDDM*. Diabetes Care, 1992. **15**(1): p. 132-5.
232. Velloso, L.A., et al., *Absence of autoantibodies against glutamate decarboxylase (GAD) in the non-obese diabetic (NOD) mouse and low expression of the enzyme in mouse islets*. Clin Exp Immunol, 1994. **96**(1): p. 129-37.
233. Winnock, F., et al., *Correlation between GABA release from rat islet beta-cells and their metabolic state*. Am J Physiol Endocrinol Metab, 2002. **282**(4): p. E937-42.
234. Fairless, R., et al., *Polarized targeting of neurexins to synapses is regulated by their C-terminal sequences*. J Neurosci, 2008. **28**(48): p. 12969-81.
235. Rosales, C.R., et al., *A cytoplasmic motif targets neuroligin-1 exclusively to dendrites of cultured hippocampal neurons*. Eur J Neurosci, 2005. **22**(9): p. 2381-6.
236. Freinkel, N., et al., *Differential effects of age versus glycemic stimulation on the maturation of insulin stimulus-secretion coupling during culture of fetal rat islets*. Diabetes, 1984. **33**(11): p. 1028-38.



237. Hellerstrom, C. and I. Swenne, *Functional maturation and proliferation of fetal pancreatic beta-cells*. Diabetes, 1991. **40 Suppl 2**: p. 89-93.
238. Hayashi, M., et al., *Expression and localization of vesicular glutamate transporters in pancreatic islets, upper gastrointestinal tract, and testis*. J Histochem Cytochem, 2003. **51**(10): p. 1375-90.
239. Heine, M., et al., *Activity-independent and subunit-specific recruitment of functional AMPA receptors at neurexin/neuroligin contacts*. Proc Natl Acad Sci U S A, 2008. **105**(52): p. 20947-52.
240. Bekris, L.M., T.J. Kavanagh, and A. Lernmark, *Targeting type 1 diabetes before and at the clinical onset of disease*. Endocr Metab Immune Disord Drug Targets, 2006. **6**(1): p. 103-24.
241. Lernmark, A., *Type 1 diabetes as a model for prediction and diagnosis*. Autoimmunity, 2004. **37**(4): p. 341-5.
242. Knip, M., *Prediction and prevention of type 1 diabetes*. Acta Paediatr Suppl, 1998. **425**: p. 54-62.
243. Gepts, W. and J. De Mey, *Islet cell survival determined by morphology. An immunocytochemical study of the islets of Langerhans in juvenile diabetes mellitus*. Diabetes, 1978. **27 Suppl 1**: p. 251-61.
244. Butler, A.E., et al., *Beta-cell deficit and increased beta-cell apoptosis in humans with type 2 diabetes*. Diabetes, 2003. **52**(1): p. 102-10.
245. Hampe, C.S., et al., *Quantitative evaluation of a monoclonal antibody and its fragment as potential markers for pancreatic beta cell mass*. Exp Clin Endocrinol Diabetes, 2005. **113**(7): p. 381-7.
246. Davletov, B.A., et al., *High affinity binding of alpha-latrotoxin to recombinant neurexin I alpha*. J Biol Chem, 1995. **270**(41): p. 23903-5.
247. Missler, M., R.E. Hammer, and T.C. Sudhof, *Neurexophilin binding to alpha-neurexins. A single LNS domain functions as an independently folding ligand-binding unit*. J Biol Chem, 1998. **273**(52): p. 34716-23.
248. Sugita, S., et al., *A stoichiometric complex of neurexins and dystroglycan in brain*. J Cell Biol, 2001. **154**(2): p. 435-45.
249. Chen, X., et al., *Structural basis for synaptic adhesion mediated by neuroligin-neurexin interactions*. Nat Struct Mol Biol, 2008. **15**(1): p. 50-6.
250. Koehnke, J., et al., *Crystal structure of the extracellular cholinesterase-like domain from neuroligin-2*. Proc Natl Acad Sci U S A, 2008. **105**(6): p. 1873-8.

- 251. Min, D.H. and M. Mrksich, *Peptide arrays: towards routine implementation*. Curr Opin Chem Biol, 2004. **8**(5): p. 554-8.
- 252. Gould, C.M., et al., *The chaperones Hsp90 and Cdc37 mediate the maturation and stabilization of protein kinase C through a conserved PXXP motif in the C-terminal tail*. J Biol Chem, 2009. **284**(8): p. 4921-35.
- 253. Grant, C.S., *Gastrointestinal endocrine tumours. Insulinoma*. Baillieres Clin Gastroenterol, 1996. **10**(4): p. 645-71.
- 254. Porte, D., Jr., *Clinical importance of insulin secretion and its interaction with insulin resistance in the treatment of type 2 diabetes mellitus and its complications*. Diabetes Metab Res Rev, 2001. **17**(3): p. 181-8.
- 255. DeFronzo, R.A., *Pharmacologic therapy for type 2 diabetes mellitus*. Ann Intern Med, 1999. **131**(4): p. 281-303.
- 256. Levinson, J.N., et al., *Postsynaptic scaffolding molecules modulate the localization of neuroligins*. Neuroscience, 2009.